Fortschritt-Berichte VDI

Reihe 3

Verfahrenstechnik

Prof. Dr.-Ing. Lothar R. Oellrich, Karlsruhe
Dr.-Ing. Klaus Althaus, Mannheim

Nr. 679

# GERG – Water Correlation (GERG Technical Monograph TM 14)

## Relationship Between Water Content and Water Dew Point Keeping in Consideration the Gas Composition in the Field of Natural Gas

VDI Verlag

Oellrich, Lothar R.; Althaus, Klaus
**GERG – Water Correlation**
**(GERG Technical Monograph TM 14)**
**Relationship Between Water Content and Water Dew Point Keeping in Consideration the Gas Composition in the Field of Natural Gas**
Fortschr.-Ber. VDI Reihe 3 Nr. 679. Düsseldorf: VDI Verlag 2001.
180 Seiten, 62 Bilder, 37 Tabellen.
ISBN 3-18-367903-5, ISSN 0178-9503, DM 106,00, € 54,20.

**Für die Dokumentation:** Phase Equilibria – High Pressure – Water Content – Dew Point – Coulometric Karl-Fischer Titration – Dew Point Mirror – Natural Gas – Methane – Ethane – Cubic Equation of State

Water dew points and water content data were determined by means of a continuous flow phase equilibrium apparatus for pressures in the range from 5 bar up to 100 bar and temperatures between −25°C and +20°C. The water dew points were set by careful operation of a saturator and two condensers and checked with a dew point mirror. For the water content determination, the coulometric Karl-Fischer titration was applied (according to ISO 10101-3:1993). Four binary systems (methane-, ethane-, nitrogen-, argon-water), one ternary (methane-ethane-water) and seven multi-component-water (natural gas-water) mixtures were investigated. The phase situation, present during the respective experiments, is discussed in detail. For an accurate reproduction of the experimental data, an optimised calculation method (GERG-WATER) is presented, based on the Peng-Robinson equation of state. Finally, the results of this method, as well as results from calculation- and conversion methods for water contents and dew points, available in literature and natural gas industries, are compared with experimental data.

**Die Reihen der FORTSCHRITT-BERICHTE VDI:**

**1** Konstruktionstechnik/Maschinenelemente
**2** Fertigungstechnik
**3** Verfahrenstechnik
**4** Bauingenieurwesen
**5** Grund- und Werkstoffe/Kunststoffe
**6** Energietechnik
**7** Strömungstechnik
**8** Meß-, Steuerungs- und Regelungstechnik
**9** Elektronik/Mikro- und Nanotechnik
**10** Informatik/Kommunikation
**11** Schwingungstechnik
**12** Verkehrstechnik/Fahrzeugtechnik
**13** Fördertechnik/Logistik
**14** Landtechnik/Lebensmitteltechnik
**15** Umwelttechnik
**16** Technik und Wirtschaft
**17** Biotechnik/Medizintechnik
**18** Mechanik/Bruchmechanik
**19** Wärmetechnik/Kältetechnik
**20** Rechnerunterstützte Verfahren (CAD, CAM, CAE, CAP, CAQ, CIM, . . .)
**21** Elektrotechnik
**22** Mensch-Maschine-Systeme



ISSN 0178-9503
ISBN 3-18-367903-5



**Disclaimer:**

**GERG, the companies participating in the GERG Project PC1 WG 1.6, ITTK and VDI shall not be liable for any damage of any kind incurred in connection with the usage of this GERG Monograph.**

# Acknowledgements

Klaus Althaus and Lothar Oellrich would like to express their thanks to GERGWATER group for supporting this project and for the numerous valuable discussions and contributions to the successful finalisation of the work.

We also would like to express our gratitude to Dr.-Ing. Thorsten Engler for his help in translating large parts of the thesis [249, where the GERGWATER calculation procedure is called BWT] and for performing the lay out. Without his help the completion of this report would not have been possible in due time.

Thyssengas (Germany) sponsored measurements and parts of the project.

A windows compatible program containing the GERGWATER-method is available from Ruhrgas AG, D-54138 Essen (Germany).



# Contents

# Annex

# Abstract

The water content of natural gases often poses problems during the production, transmission and distribution of natural gas. These problems have increased due to the fact that the transportation pressure of the pipeline system has risen over the year to maximum pressures of presently about 10 MPa. The problems with the water content also can be traced back to inadequate description with currently available methods. The temperature and pressure range of interest in pipeline transmission poses additional problems due to the possible formation of solid precipitation in form of gas hydrates or ice.

In order to solve these problems GERG founded a task group GERGWATER and decided to set up a detailed project incorporating experimental investigations as well as the development of a calculation procedure.

It is the aim of this monograph to present a sound method for calculating the water dew point and the water content of natural gases that will be used as the GERG standard method. In order to achieve this goal first measurements of water dew point and water content of key binary systems methane - water, ethane - water and nitrogen - water were carried out. In addition also data for the binary argon - water were assembled. Then of the water dew point and the water content of seven natural gases typical for being distributed in the European pipeline grid were determined. The majority of the data were collected in the pressure range of 5 to 100 bar (5, 15, 40, 60, 80, 100 bar) and for temperatures between - 15 °C and + 15 °C. Some data also were taken down to -25 °C and at + 20 °C.

To develop a reliable method for calculation of the water dew point and the water content of natural gases the Peng Robinson (PR) equation of state was chosen as the basis. It turned out that a prerequisite for a good description of the water dew point and water content is a precise representation of the saturation vapour pressure and sublimation pressure of water. To achieve this goal, parameter a in the PR equation had to be made substance dependent. For all other natural gas components the generalised form of the parameters could be retained. As a result of the substance specific parameter a for water all binary parameters for binary systems containing water had to be re-estimated. When investigating the influence of natural gas components on the representation of the water dew point and on the water content it turned out that natural gas compositions according to the standard analysis following ISO6974-4 are sufficient for a accurate calculation.

Within the temperature and pressure range under consideration the water dew point is represented by the new method GERGWATER to within ± 2 K. The new proposed GERG calculation method is superior to the methods currently used in natural gas practice, such as Bukacek et al [155], ASTM 1142-95 [59] or the diagrams according to McKetta et al [150], also in the version of Wichert [157] or that of GASUNIE [149].

The GERGWATER method was developed at the Institut für Technische Thermodynamik und Kältetechnik of the Universität Karlsruhe (TH) (ITTK)[1] under contract to the Groupe Europeen de Recherche Gazieres (GERG).

A windows compatible program containing the GERGWATER-method is available from Ruhrgas AG, D-54138 Essen (Germany).

[1] In [249] the GERGWATER calculation method is called BWT (Berechnungsprogramm Wassergehalt Taupunkt)



# Zusammenfassung

Bis in die Gegenwart treten Probleme im Betrieb von Gasförder-, Transport- und Verteilungseinrichtungen bedingt durch den Wassergehalt von Erdgasen auf. Auch durch die Tatsache, daß der Betriebsdruck in den letzten Jahrzehnten stetig anstieg auf derzeit maximal etwa 10 MPa, haben sich diese Probleme noch verstärkt. Eine der Ursachen des Auftretens dieser Probleme liegt in der ungenügenden Beschreibung des Wassergehaltes von Erdgasen mit den gegenwärtig in der Praxis eingesetzten Bestimmungsmethoden. Der Temperatur- und Druckbereich des Pipelinetransports wirft zusätzliche Probleme durch die mögliche Ausscheidung fester Ablagerungen in Form von Gashydraten oder Eis auf.

Um diese Probleme zu lösen, bildeten europäische Gasgesellschaften in der Groupe Europeene de Recherche Gaziere (GERG) ein Programm GERGWATER und beschlossen, ein ausführliches Projekt durchzuführen, das sowohl die experimentelle Untersuchung als auch die Entwicklung einer Berechnungsmethode zur Bestimmung der Wassertaupunkte und des Wassergehalts in Gasgemischen beinhaltete.

Es ist das Ziel dieses Monographs, eine verläßliche Methode zur Berechnung des Wassertaupunktes und des Wassergehaltes vorzulegen, die als GERG Standardmethode eingesetzt werden kann. Um dieses Ziel zu erreichen, wurden zunächst Messungen des Wassertaupunktes und des Wassergehaltes der binären Schlüsselsysteme Methan-, Ethan- und Stickstoff-Wasser durchgeführt. Zusätzlich wurde auch das System Argon - Wasser vermessen. Anschließend erfolgten die entsprechenden Messungen für sieben Erdgase, die typisch für die im europäischen Erdgaspipelinenetz verteilten Erdgase sind. Der Hauptanteil der Daten wurde im Druckbereich 5 bis 100 bar (5, 15, 40, 60, 80, 100 bar) und bei Temperaturen zwischen -15 und +15 °C gemessen; einige Daten wurden auch bis -25 °C und bei +20 °C gemessen.

Die Peng Robinson (PR) Zustandsgleichung wurde als Basis für die Berechnungsmethode zur Bestimmung des Wassertaupunktes und des Wassergehaltes von Erdgasen gewählt. Es stellte sich heraus, daß eine Grundvoraussetzung für eine gute Beschreibung des Wassertaupunktes und des Wassergehalts die exakte Wiedergabe des Sättigungsdampfdruckes und des Sublimationsdruckes von Wasser ist. Um dieses Ziel zu erreichen, mußte der Parameter a der PR-Gleichung stoffspezifisch angepaßt werden. Für alle anderen Erdgaskomponenten wurde die generalisierte Form der Parameter beibehalten. Wegen der stoffspezifischen Anpassung für Wasser mußten alle Binärparameter für die wasserhaltigen binären Systeme neu angepaßt werden. Bei der Untersuchung des Einflusses von Erdgaskomponenten auf die Wiedergabe des Wassertaupunktes und des Wassergehaltes stellte sich heraus, daß zur Charakterisierung eines Erdgases die Standardanalyse nach ISO 6974-4 ausreichend für eine zuverlässige Berechnung ist.

Innerhalb des betrachteten Temperatur- und Druckbereiches kann der Wassertaupunkt mit der neuen Methode GERGWATER (Berechnungsprogramm Wassergehalt Taupunkt) innerhalb von ±2 K wiedergegeben werden. Die neue vorgeschlagene GERG Berechnungsmethode ist damit den gegenwärtig in der Praxis eingesetzten Methoden nach Bukacek [155], ASTM 1142-95 [59] oder den Diagrammen nach McKetta et al [150], auch in der Version von Wichert [157] und dem Diagramm der GASUNIE [149] überlegen.

Die GERGWATER Methode wurde am Institut für Technische Thermodynamik und Kältetechnik (ITTK)[2] der Universität Karlsruhe (TH) im Auftrag der GERG entwickelt.

Ein mit Windows kompatibles Programm, das die Berechnungsmethode GERGWATER enthält, ist von der Ruhrgas AG, D-54138 Essen, erhältlich.

[2] In [249] wird die GERGWATER Methode mit BWT (Berechnungsprogramm Wassergehalt Taupunkt) bezeichnet.

# Symbols

**Important Symbols:**

| | | |
|---|---|---|
| $\alpha$ | temperature dependency of the attraction parameter | [-] |
| $\delta,\varepsilon,\Theta,\eta$ | parameter in the general cubic equation of state | |
| $\Delta$ | difference | |
| $\varphi$ | fugacity coefficient | [-] |
| $\vartheta$ | temperature | [°C] |
| $\mu$ | chemical potential | [J/mole] |
| $\kappa$ | coefficient | [-] |
| $\omega$ | acentric factor | [-] |
| n | number of moles | [mol] |
| $A_i$ | coefficient in eq. (4.2) | [-] |
| $a_i$ | coefficient | [-] |
| $b_i$ | coefficient | [-] |
| b | parameter in the general cubic equation of state | [m³/mole] |
| c | parameter in the general cubic equation of state | [m³/mole] |
| f | fugacity | [Pa] |
| *F* | degree of freedom | [-] |
| F | Faraday´s-constant | [(A·s)/mole] |
| $k_{ij}$ | binary interaction parameter | [-] |
| $k_p$ | enhancement factor | [-] |
| m | mass | [kg] |
| M | molecular weight | [kg/mol] |
| p | pressure | [Pa] |
| PIR4 | pressure at measuring point 4 (see annex D) | [Pa] |
| R | universal gas constant | [J/(mole·K)] |
| r | repeatability limit | [mg/Nm³] |
| R | reproducibility limit | [mg/Nm³] |
| S | entropy | [J/K] |
| s | standard deviation | |



| | | |
|---|---|---|
| T | temperature | [K] |
| TIR4 | temperature at measuring point 4 | [K] |
| U | internal energy | [J] |
| U | uncertainty | |
| x | mole fraction in the liquid phase | [-] |
| y | mole fraction in the gaseous phase | [-] |
| N | number of components | [-] |
| I | ice | [-] |
| L | liquid phase | [-] |
| H | hydrate phase | [-] |
| V | gaseous (vapour) phase | [-] |
| V | volume | [m³] |
| v | molar volume | [m³/mole] |
| Q | quadruple point | [-] |
| Q | charge | [A·s] |
| Z | compressibility factor | [-] |

**Superscripts:**

$\alpha, \beta, \gamma$

| | |
|---|---|
| $\pi$ | phases |
| L | liquid phase |
| V | gaseous (vapour) phase |

**Subscripts:**

| | |
|---|---|
| b | reference state |
| calc. | Calculated |
| C | combined |
| exp. | experimentally determined |
| tot. | Total |
| $H_2O$ | water |
| HC | hydrocarbon |
| i, j, k | integer index |
| KF | Karl-Fischer |
| crit. | critical |

| | |
|---|---|
| M | mixture |
| MeOH | methanol |
| N | physical standard condition (101325 Pa, 273.15 K) |
| NGZ | gas meter (wet type) |
| o | pure compound |
| R | reduced |
| SFK | sealing liquid |
| STP | standard reference state (101325 Pa, 60°F) |
| dew | dew point condition |
| Gas,dry | referred to dry gas composition |
| amb | ambient |
| Ü | above atmospheric pressure |
| w | water |
| WC | water content |

**Frequently Used Abbreviations:**

| | |
|---|---|
| OP | operation point |
| VPC | vapour pressure curve |
| CA02 | Karl-Fischer Coulometer Mitsubishi CA-02 |
| CA06 | Karl-Fischer Coulometer Mitsubishi CA-06 |
| KF684 | Karl-Fischer Coulometer Metrohm KF-684 |
| KF | Karl Fischer |
| CP | critical point |
| SM | series of measurements |
| MV | mean value |
| NB | physical standard condition |
| NGZ | wet type gas meter |
| PR | equation of Peng and Robinson |
| SPC | sublimation pressure curve |
| SFK | sealing liquid |
| DP | dew point |
| WC | water content |
| EOS | equation of state |



# 1 Introduction

## 1.1 Objective of this Work

Natural gas is mainly being transmitted by means of pipelines. The huge natural gas fields in Siberia, in Algeria and in the North Sea are interconnected with the consumer countries by pipeline systems [1]. Due to economic reasons the international transport is being realised at high pressures (up to PN 100 in onshore applications [2]). The gas is fed from the high pressure network into the regional distribution grid. To be able to cover the large seasonal and daily variations in delivery, gas is being stored in intermediate high pressure facilities and released to cover the peak loads. In Germany in recent years several leached salt caverns have been introduced for this purpose [3].

From a thermodynamic point of view natural gas is a multicomponent mixture, composed mainly of methane. The water content results from natural fields, from saturation of the gas in caverns and aquifer storages or from water remainders after pressure testing of the transport lines. Even though present in small amounts only, a multitude of problems in production and transport of natural gas may be traced back to the component water. Among others, the formation of corrosive media from sour gas constituents or the mechanical destruction of control systems by droplet erosion may be attributed to the water content, too. The occurence of ice and hydrate formation is responsible for problems in operation up to interruption of gas supply. Natural gas hydrates are counted to the class of clathrates, which remain stable under pressure even above 0°C, unlike ice. Hydrate formation leads to a reduction in the pipeline cross-section and in extreme cases the gas transmission may be blocked completely.

To avoid these problems and the incurred high additional cost caused by the component water, natural gas is dried prior to feeding into the pipeline system. In order to obtain an efficient design of the drying plants, the exact knowledge of water dew point and water content as a function of pressure, temperature and gas composition is a pre-requisite.

In this work the water content and water dew points of selected binary, one ternary and seven multicomponent mixtures (natural gases) were measured at temperatures ranging from -25°C up to +25 C and pressures between 5 and 100 bar. The compositions of the natural gases cover the range of gases being distributed in the European network. The dew point mirror device and the coulometric Karl-Fischer titration are discussed in detail in this monograph, with respect to their possibilities and limitations. In the section "data reduction", emphasis is put on the discussion of phase equilibrium conditions prevailing during the measurements.

Using experimental and literature data of the binary systems, a new calculation method is developed, which allows to estimate water contents as well as water dew points with a good accuracy. For validation of the new method, experimental data from seven natural gases are used.

## 1.2 Dew Point and Condensation Point

In this work the definitions of DIN 51871 [5] are being used for the water dew point and the hydrocarbon dew point. According to DIN 51871 the water dew point of a gas is the temperature, at which the gas is saturated with water at a given pressure. According to [5], the water dew point will be briefly called "dew point". A gas is saturated with water vapour if the water vapour in the gaseous phase is in equilibrium with a liquid aqueous phase. The water dew point is called "frost point", in case water vapour coexists with a solid ice phase. The hydrocarbon dew point is called as "condensation point" [5].

For a complete specification of the dew point and the condensation point, temperature, pressure and gas composition must be known.

## 1.3 The Water Content

The concentration of the water vapour in the gaseous phase is called "water content". Usually the water content is given in one of the following concentration units [6]:

- as mole fraction (mass or volume fraction[3], respectively) independent of a reference state
- as water content dependent on a reference state
  (mass of water referred to a reference amount of gas) in "mg/m³" or "µg/l"

The water content, in dimensionless concentration quantities mass or mole fraction, is independent of a reference state (reference pressure or temperature). In the region of very low water contents, concentration usually is given in a dimenionless form as "ppm" (parts per million). In the case of water this is equivalent to one mole of water in $10^6$ moles of gas mixture.

$$ppm = 10^{-6}\frac{n_W}{n_{tot}} = 10^{-6}\frac{n_W}{n_W + n_{gas,dry}} \qquad (1.1)$$

$n_W$ : number of moles of water
$n_{tot}$ : total number of moles (humid)
$n_{gas,dry}$ : number of moles of the dry gas, i.e. without water

In the region of low concentrations, the dimensions "ppb" (part per billion) and "ppt" (part per trillion) are used. Table 1.1 contains a list of the different additional state information used as concentration variables[4], at the example "ppm".

[3] The volume fraction usually is based on the assumption of ideal gas behaviour. For ideal gases, the volume fraction is equal to the mole fraction.
[4] When using experimental literature values with these concentration variables one has to observe whether the reference unit (whole mass, whole volume, whole moles) is referred to the gas on a humid or dry basis.



Table 1.1: Concentration specifications, example "ppm" [6]

| | |
|---|---|
| mole fraction | "ppm" |
| mass fraction | "ppm(m)" |
| volume fraction | "ppm(v)" or "ppmv" |

In addition of giving the water contents in "ppm", the units "mg/Nm³" or "mg/m³($V_N$)" (milligram per cubic meter at standard conditions) are often used in practice. Here, the mass of water is referred to one standard cubic meter, which is the amount of gas contained in one m³ at 0°C and 101325 Pa [4]. The letter *N* added to the cubic meter (Nm³ or $V_N$, respectively) indicates the physical standard conditions as reference state.

Physical standard condition $V_N$: $P_N = 101325$ Pa
$T_N = 273.15$ K (1.2)

The water content at standard conditions (*WC*) may be calculated by referring mole fractions of water to the composition of the dry gas mixture as follows:

$$WC = \frac{y_W}{1-y_W}\cdot\frac{M_W\,P_N}{Z_N\,R\,T_N}\quad\left[\frac{mg}{Nm^3}\right] \qquad (1.3)$$

$y_W$ : mole fraction of water in the gaseous phase
(number of moles of water in relation to the total number of moles)
$M_W$ : molecular weight of water, ($M_W$ = 18.0152 g/mole [7] )
$T_N, P_N$ : temperature and pressure at standard conditions (see eq. 1.2)
$Z_N$ : compressibility factor of the dry gas at physical standard conditions
$R$ : universal gas constant (R = 8.3145 J/(mol·K) [8])

With $Z_N$=1 it follows: $WC = \frac{y_W}{1-y_W}\cdot 803745\,\frac{mg}{Nm^3}$

Besides the physical standard state also other reference states are used in practise. In English literature the reference state for 1 m³ gas at a temperature of +15.56°C (60°F) and 101325 Pa (14.7 psia) is preferably used. The following reference state is called "standard reference state". The corresponding term for water content is "mg/m³ (STP)" [247].

Standard state $V_{STP}$: $P_{STP}$ = 101325 Pa ( 14.7 psia ) (1.4)
$T_{STP}$ = 288.71 K ( 60°F )

For a complete specification of the water content in "mg/m³", therefore the reference state has to be given as well as the information, if it is referred to humid or dry gas conditions. In this work all figures in "mg/m³" are referred to the dry gas mixture conditions.



# 2 Experimental Part

This chapter is dedicated to the design of the experimental set up as well as to the description of its main parts including the applied measuring techniques. A detailed discussion of the experimental methods, the uncertainty estimation and the sensitivity analysis is contained in annex C and D.

Figure 2.1 shows a simplified block flow sheet of the set up. The set up is designed according to the continuous flow principle. A multistage procedure is applied, to obtain a fully saturated gas flow. First, the gas is saturated with water in a saturator near room temperature[5]. Thereafter, the gas is cooled down in two successive steps (condensers) to the required dew point temperature and the excess water is removed. The experimental set up can be divided into four main parts, following the gas flow routing:

- gas supply with pressure control,
- saturation unit,
- condenser unit, and
- analytical unit.

A detailed flow sheet of the experimental set up is given in figure 2.2.

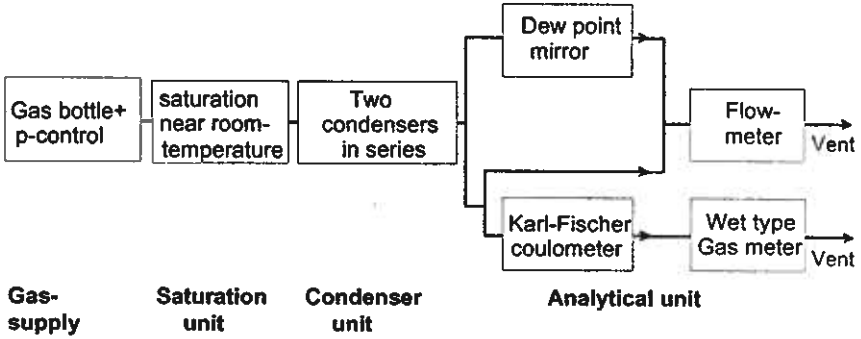


Figure 2.1: Block flow sheet of the experimental set up (according to [248])

The gas supply is assured via commercially available gas bottles, which are connected to the pressure reduction station by a flexible high pressure coil. After passing a sinter metal filter, the gas pressure is being reduced in a one stage pressure reducer to the inlet pressure of the following pressure control valve V2. The electronically controlled valve V2 adjusts the plant pressure to the set-value.

[5] The operability of the saturation unit has been verified during the commissioning tests with a dew point mirror.

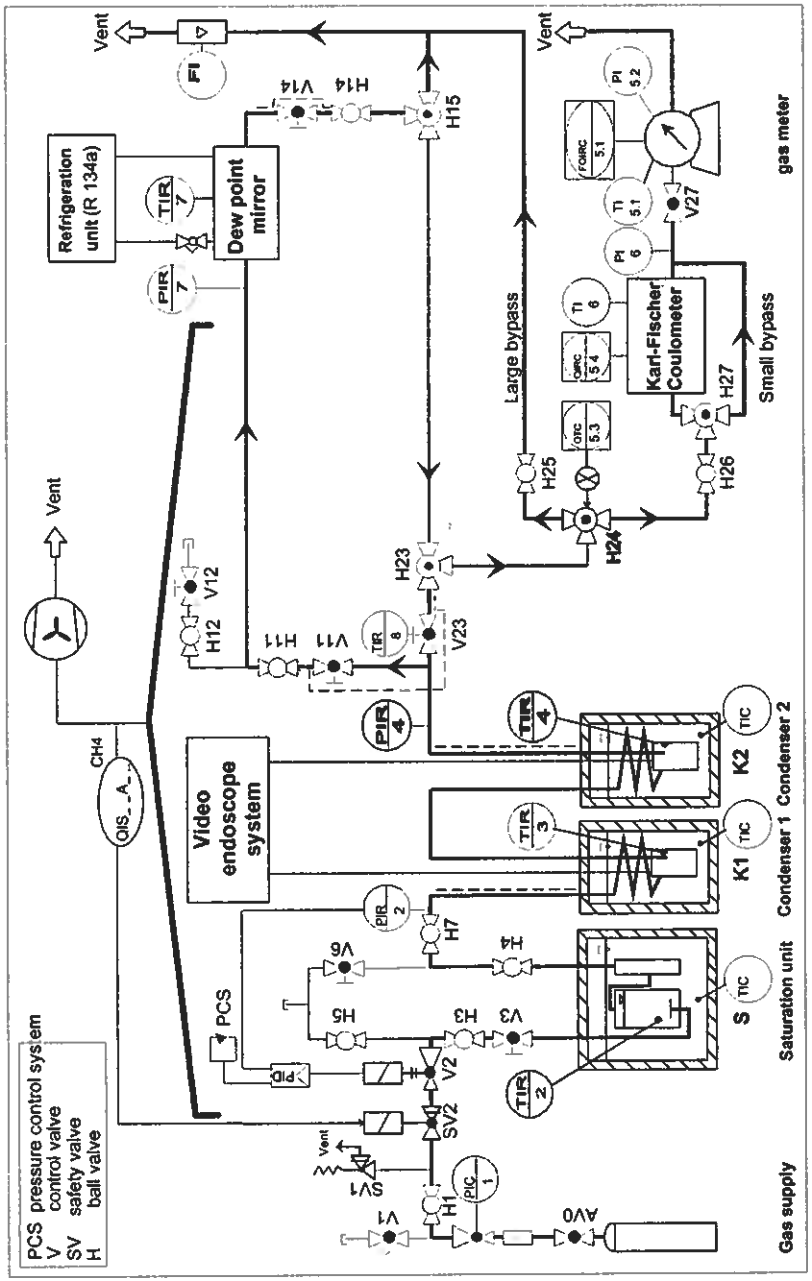


Figure 2.2: Flow scheme of the experimental set up



The gas is then saturated in the saturator S with bidestilled water. The gas flows through a stainless steel sinter metal frit (pore size 0.5-2 µm) and then flows through a water column of approximately 150 mm in height. At the top of the saturator, a first removal of possibly entrained water droplets is secured by two metal sheets (figure C.2a in annex C). Then, the gas passes through a pressure bottle (figure C.2b) which acts as a second droplet separator, in normal operation. The saturator and the pressure bottle are immersed in a thermostat. By operating the ball valves H3 to H5, the saturator can be bypassed, to obtain a dry (unsaturated) gas flow. The design of the saturator was realised according to Mersmann [114].

After passing the saturator unit, the gas flows through two identical condensers K1 and K2 connected in series (figure C.3), and which are located in two separate thermostat baths. The water is stepwise condensed in both condensers. The temperature of the second condenser is controlled to the desired equilibrium temperature. The gas leaves the condenser unit (from condenser K2) fully saturated at plant pressure (PIR4) and temperature (TIR4).

A two stage analytical unit follows the condensation unit. The gas is either led via a dew point mirror to estimate the dew point, or through a Karl-Fischer unit and a wet gas meter to estimate the water content. It is also possible, to pass the gas through both units in series, with respective positions of valves H15 and H23. The different variants possible, are shown in detail in annex C.6. The flow is adjusted in a needle valve, present in both paths (V14 an V23, respectively). Finally the flow is measured in a rotameter or in the wet type gas meter. In valves V14 and V23, the gas pressure is reduced near to ambient pressure, since both, the Karl-Fischer unit and the wet gas meter, operate at a slight overpressure above the ambient. To avoid cooling, caused by the Joule-Thomson effect and consequent condensation of water and higher hydrocarbons, the lines up- and downstream of the valves as well as the valves themselves are equipped with heat tracing [115] [116] [117]. After flowing through the wet type gas meter or the rotameter, respectively, the gas is led to atmosphere.

After opening the blockings (after V1 and V2 or in the saturation line near H5), gas probes can be taken or purging lines can be connected.

All parts in contact with gas are made of stainless steel except a part of the Karl-Fischer analytical path. The connecting lines are made of chemically cleaned 1/8" stainless steel lines (inner diameter 1 mm). For the coils connecting the condensers as well as the lines up- and downstream of the dew point mirror 6x1.5 mm stainless steel lines are used. The routing of the pipes was executed as short as possible, to minimise the surface available for adsorption and to reach equilibrium fast. Except of the pressure reduction unit near the gas supply bottle and the control valve near the dew point mirror all valves and ball valves are located on a single operation board.

The high pressure vessels are designed for an operation pressure of at least 150 bar by taking into account the respective standards. However, due to the allowable operational range of the control units the maximum experimental pressure is limited to 100 bar (see also the descriptions in annex C.1.1 "pressure measurement and control"). The experimental set up therefore is suited for saturated water content measurements between 1 and 100 bar and temperatures between -25°C and +20°C.

# 3 Experimental Results and Discussion

Dew point and water content measurements according to the procedure described in chapter 2 were carried out and evaluated for twelve systems. The following systems were investigated:

- the four binary mixtures methane-, ethane-, nitrogen-, and argon- water
- the ternary system methane-ethane-water and
- seven multicomponent-water mixtures (natural gas-water systems).

The operating points were within a pressure range of 5 and 100 bar, the temperature was varied between -25°C and +20°C. The major part of the measurements were carried out at

- the six pressures 5, 15, 40, 60, 80 and 100 bar and
- the seven temperatures -15°, -10°, -5°, 0°, 5°, 10°, 15°C.

For some gases measurements were taken at selected pressures and at temperatures of -25°, -20° and +20°C.

## 3.1 Experimental Results of the Dew Point Measurements

As discussed in annex D.1.2, cool down velocities of the dew point mirror of only 3-5 K/min could be realised by using an external refrigeration cycle and a hand-controlled valve[7]. This resulted in a larger uncertainty of the measured dew point temperatures than would be obtained when applying the DIN recommendations. For this reason, the results of the dew point mirror measurements are not presented separately.

It should be noted as a result of the measurements, that in most cases, the dew point, given by the equilibrium apparatus, could be determined within an accuracy of ±2 K, though a higher cooling

Table 3.1: Operating points with occurrence of (retrograde) hydrocarbon condensation for natural gases NG2, NG4 and NG5. (not meas.= operating point not measured)

| | -25°C | -20°C | -15°C | -10°C | -5°C |
|---|---|---|---|---|---|
| 60 bar | [6] | [6] | NG5 | NG5 | NG5 |
| 40 bar | NG5 | NG5 | NG2, NG4, NG5 | NG2, NG4, NG5 | NG2, NG4, NG5 |
| 15 bar | not meas.[6] | not meas.[6] | NG4, NG5 | NG4, NG5 | NG5 |

[6] For the natural gas NG4, at 60 and 80 bar and temperatures of -20°C and -25°C, only water contents have been measured. Due to a technical defect of the dew point mirror, no dew points were measured at these operating points. The occurrence of hydrocarbon condensation at these points is not proved. At the operating points -25°C and -20°C at the 15 bar isobar, no measurements have been carried out (neither water content, nor dew point).

[7] It should be noted that commercially available dew point mirrors in general only give the mirror temperature. The devices do not include a indication of the cooling down velocity. It can therefore questioned, whether the cooling down velocity of max.1 K/min recommendations of DIN 51871 [5] can be kept with manual control without the information on cooling velocity.



down velocity was applied and a partly lower water content occurred. For the natural gases NG2, NG4 and NG5, some operating points were located within the retrograde region (see Table 3.1). At these operation points, a water dew point measurement was considerably hindered by the occurrence of a liquid hydrocarbon phase. Water dew points could not be determined, or only with a large shift towards low temperatures (compared to the expected dew point temperature = temperature T1R4 of condenser K2), because of the overlay by hydrocarbon condensation points. The observed deviations amount up to 10 K.

## 3.2 Experimental Results of the Water Content Measurements

In the following, experimental results of the water content measurements obtained within this work, are presented and discussed by means of selected and representative diagrams. The plotted measuring points represent a total mean value of all measurements, carried out at a operating point (see eq. D.5 in annex D.2.4). This means that measuring points plotted in the diagrams, are the result of at least two independently determined Karl-Fischer measuring series, with an extent of at least 20 singular measurements, respectively. All together, more than 13,000 single determinations of water contents have been carried out within this work, where the Mitsubishi Karl-Fischer coulometer CA-06 has been applied nearly exclusively, due to its low uncertainty. The isobaric plot of water contents versus temperature has been selected as a suitable representation of the data. To highlight the membership of several experimental points to one isobar, they were connected by a line. In the case if literature data were available within the range investigated, these data were compared to the own experimental data. The uncertainty range was not included into the graphs to keep clarity. In the range of small water contents the uncertainty sums up to 20% of the value measured. For the water contents greater than 100 mg/Nm³ the uncertainty of the measuring points lies within the size of the symbols in the logarithmic scale (uncertainty ≤2.5 % of the measured value). Figure D.4 (in annex D.3) shows the course of the uncertainty of the water content over the measured water content. For the 80 bar isobar of the binary system methane-water the uncertainties were added as an example (see figure 3.1).

In annex G.1 additional diagrams can be found. Figures G.2 and G.3 for instance allow to allocate the location of the values measured in respect to the course of the hydrate equilibrium curve. Those numerical values which have passed the statistical test are summarised in annex G.2 in tabular form. All water content values in "mg/Nm³ refer to the dry gas mixture.

### 3.2.1 Binary Mixtures

The water content of the four saturated pure gases methane, ethane, nitrogen and argon were measured. With the exception of argon all the gases are major components of natural gas. The noble gas argon is favoured as a thermodynamic model fluid as the one atomic molecule is

Table 3.2: Purity and selected properties of the pure gases used

| Gas | Nitrogen | Argon | Methane | Ethane |
|---|---|---|---|---|
| purity, % | >99.999 | >99.999 | >99.9995 | >99.95 |
| molecular-Ø, nm [30] | 0.41 | 0.38 | 0.436 | 0.55 |
| $T_{crit.}$, K [228] | 126.26 | 150.69 | 190.55 | 305.33 |
| $P_{crit}$, bar [228] | 33.99 | 48.65 | 45.99 | 48.72 |

spherical and is chemical and electrical inert [142]. The respective purities of the pure gases used can be taken from table 3.2. The main impurity in methane, ethane and argon is nitrogen. In order to give a hint to the relative size of the molecules also the (largest) molecular diameter [30] is included in the table. Among the gases argon possesses the smallest and ethane the largest molecular diameter. The list of critical temperatures clarifies that, with the exception ethane, the experimental temperature range lies far above the respective critical temperatures. All four gases are hydrate formers. The respective hydrate structure formed and the quadruple points can be taken from table B.2 (annex B).

The gases ethane, nitrogen and argon were obtained from Messer Griesheim GmbH, Krefeld, methane was obtained from AGA Edelgas GmbH, Bottrop. The gases were used without any further purification. Figures 3.1 and 3.2 represent the result of the water content measurements of this work for the four binary systems investigated, which are plotted in logarithmic scale over temperature [248]. Again it should be pointed out that the values shown are the original

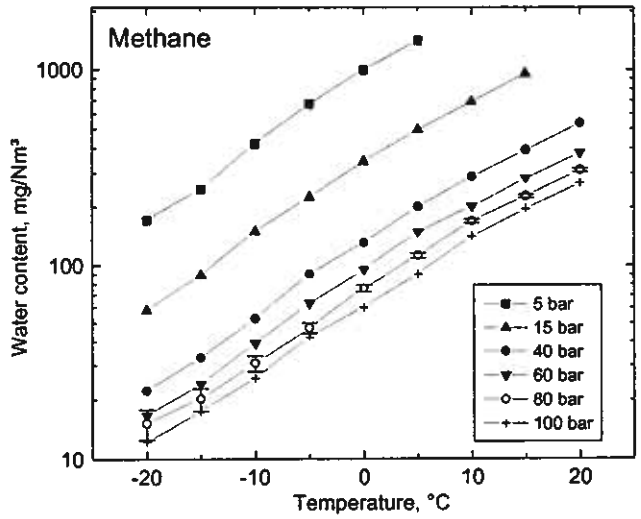


Figure 3.1: Measured water contents of the methane-water binary system. Values at the 80 bar-isobar including uncertainty range.



unprocessed experimental values. The lines connecting the points in the diagrams are mere linear connections between two neighbouring measuring points of a isobar. For the ethane-water binary system, only points below the vapour pressure of ethane could be measured (see figure G.3), since the gas inlet pressure is limited by the pressure of the gas bottle. This led to a relatively small temperature and pressure range covered, compared to the standard measuring plan.

Even though only measuring points were taken into consideration, which satisfied the evaluation criteria according to annex D, individual measuring points show a deviation from the trend (for example in figure 3.1 for methane: 100 bar, -5°C and 80 bar, -20°C). As these points are within the trend of the isobars, however when taking into consideration the uncertainties, these points were not excluded from the data.

Figures 3.1 and 3.2 manifest that the equilibrium water content is a direct function of temperature and an inverse function of pressure, that is, the water content decreases with increasing pressure and decreasing temperature. The water contents of one isobar in logarithmic scale change nearly linearly with temperature. The isobars are nearly parallel to each other. The isobars correspond to the vapour pressure of water over the corresponding condensed phase. Corresponding to the change of the course of the vapour pressure curve at the triple point of pure water (see figure A.1) the temperature dependence of the water content changes with a change of the condensed phase. A change in slope of the isobar (= change in temperature dependence of the water content) therefore is a hint to a probable change of condensed phase. At a stable phase equilibrium, the point of solid-liquid phase change lies on the respective triple point line I-$L_W$-V or $L_W$-H-V (see also figure A.2).

It follows from the slope of the triple point lines that a change in slope is expected near the melting point of pure water (0°C) for a mixture not forming hydrates or in a hydrate free property range, respectively (phase change from aqueous phase to solid ice phase). The phase change from a aqueous phase to a hydrate phase occurs at temperatures well above 0°C (and high pressures). For instance, a hydrate forming temperature of +13.3°C (and 100 bar) is calculated for the binary system methane-water by Sloan [29][8]. For 15 bar, Sloan [29] calculates the change of a solid ice phase to a solid hydrate phase at -18.5°C. According to this, the measuring point at 15 bar, -15°C lies within the ice region, the point at -20°C lies in the hydrate region. For the binary systems ethane- and argon-water part of the investigated measured points also fall within the hydrate region. According to [29] except of the measuring point at 100 bar, -20°C no hydrate formation is possible for the binary system nitrogen-water.

Analysing the slope of the isobars in figure 3.2 reveals that the phase change solid-liquid for the systems nitrogen-and ethane-water occur at about the melting point of ice (at 0°C). For the argon-water mixture, the comparatively large temperature differences between the measuring points of one isobar complicates assessment of the data. The courses of the isobars indicate that the point at 80 bar, -15°C lies a bit too low or the one at 100 bar, -15°C lies a bit too high, respectively. Both operating points lie within the hydrate forming region. No indication of a meta-

[8] Nixdorf [31] has measured a hydrate forming temperature of +12.8 °C at p = 98.7 bar for this mixture.

stable liquid phase could be detected for the 100 bar, -15°C point via the endoscope system (see annex C.3) during the running-in time and during the measuring period. The inner chamber of the condenser was "optically dry" and free of any deposits during the measurements. A possible explanation for the higher value of the 100 bar, -15°C point could be that the measurements were mostly carried out over a metastable ice phase as the water content would be higher here than over a stable hydrate phase. A significant change of slope can be detected for the system methane-water (see figure 3.1 and 3.3) well above 0°C for the high pressures (60, 80, 100 bar). According to the above statements, this could be a hint that a hydrate phase could have been present during the measurements. The change of slope of the isobars can be seen when comparing the water contents of the systems methane-water (hydrate forming) and nitrogen-water (except of the measuring point 100 bar/ -20°C, all points in the investigated area are located outside the hydrate forming region) which is shown in figure 3.3. The location of the kinks of the isobars of the

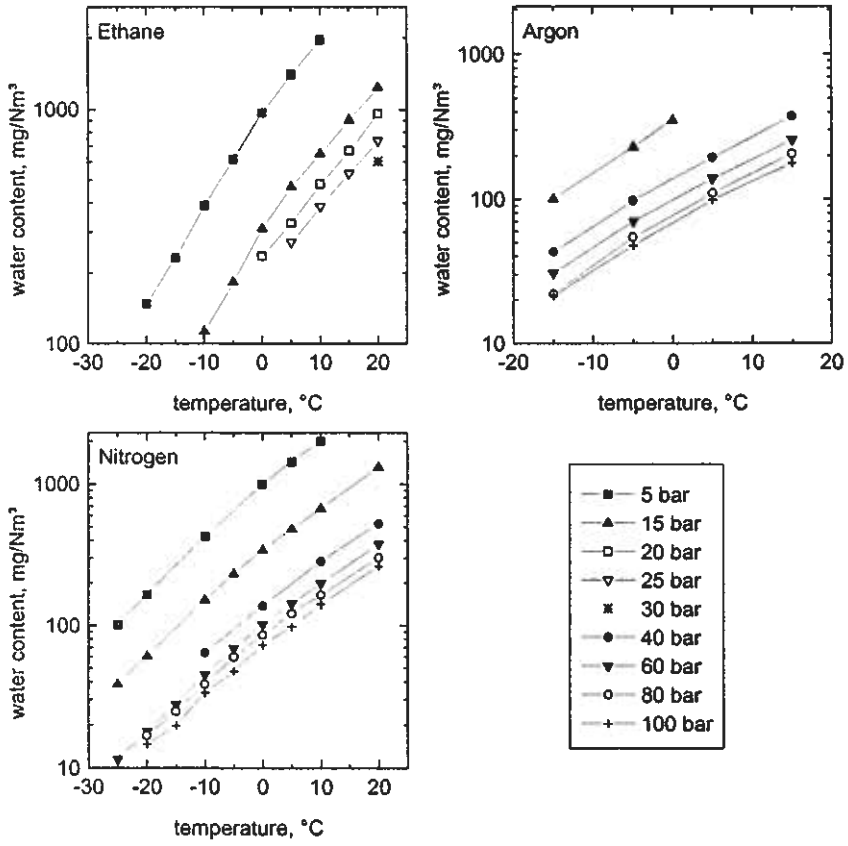


Figure 3.2: Measured water contents of the binary systems: ethane-water, argon-water and nitrogen-water.



methane system at 60, 80 and 100 bar coincide with the hydrate equilibrium line for pure methane calculated according to Sloan [29].

Comparing the water contents for the methane- and nitrogen-water systems, figure 3.3 shows that the measured water contents for the lower pressures (5 and 15 bar) as well as those for the higher pressures (outside the hydrate region) are nearly identical. Inside the hydrate region, the water contents of methane are lower than those of nitrogen. The differences between the water contents of both gases increase with decreasing temperatures, when the distance to the hydrate boundary of methane becomes larger. The statement of Campbell [148], that nitrogen shows lower values of water content than methane, in general cannot be confirmed even when limiting to the measuring points outside the hydrate region of methane. A direct comparison of the figures of the measured water contents (table G.1) shows that only for temperatures of and above +10°C always higher water contents were measured for methane. The deviations of 6-9% for pressures up to 70 bar as indicated by Campbell could not be noted during the own measurements outside the hydrate region.

Figure 3.4 gives a comparison of the water contents measured for nitrogen- and argon-water (numerical values se table F.1). Figure 3.4 verifies that measured water contents of both mixtures, except of the isobar 80 bar, barely can be distinguished from one another. The diagram indicates that for higher temperatures (see the +15°C points), the water contents for the argon-water system are slightly lower than the ones for the nitrogen-water system. However, a direct numerical comparison is not possible as no measurements have been taken at this temperature for nitrogen. Smaller water contents have been measured for argon compared to nitrogen at 80 bar. No unambiguous cause for these systematic deviations of the measured values at this pressure could be found. The point of 80 bar and -15°C for argon had already been classified in the

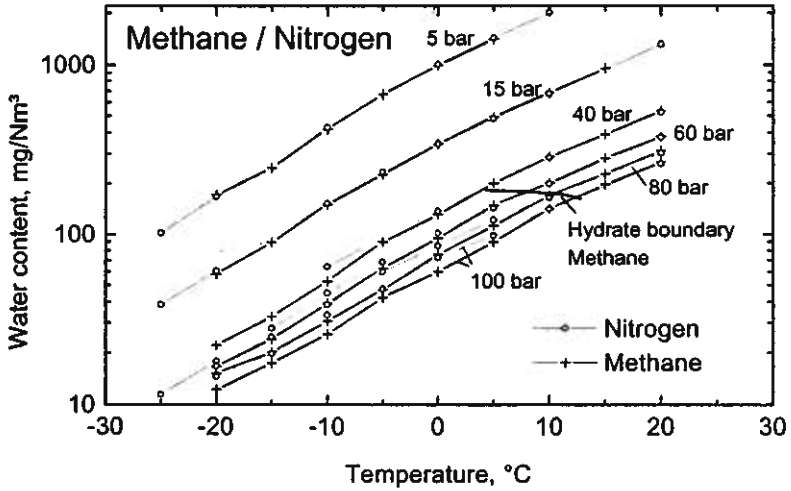


Figure 3.3: Comparison of water contents of the methane-water and nitrogen-water binary systems. Boundary of the hydrate range calculated with CSMHYD [29].

discussion of figure 3.3 as a point of possibly too low water content measured. The difference between the argon and nitrogen measured values are about 10% of the absolute value of the value of argon. A consideration of the uncertainty shows that only at +5 and +15°C the nitrogen values are outside the upper uncertainty limit of the argon values measured due to the high uncertainty at low (high pressure) water contents. The upper uncertainty limit of the water content results from the water content after adding the uncertainty $U_{95,tot}$ (see annex D.2 and figure D.3).

It should be noted that the water contents measured for argon at 100 bar/ -15 and -5°C, even though lying within the hydrate formation area, do not show lower water contents compared to nitrogen as the methane-water mixture does. There are two possible conclusions possible. With argon there were no hydrates yet (not yet or too few, respectively) due to kinetic hindrance but (mainly) metastable ice, or the water content of argon is not much different compared to the one of nitrogen over ice as the condensed phase. The assumption of a metastable ice phase during the measurements is the more likely as the measured points lie near the hydrate equilibrium curve and prior to the measurements the time within the hydrate area was comparatively low as the water content was estimated only for a few points within the hydrate area (see also the remarks in annex D.1).

Figure G.4 (in annex G.1) allows a comparison of the experimental data for the methane-, ethane- and argon-water mixtures. The data for the 20, 25 and 30 bar isobar for ethane were not included as only measurements for ethane-water mixtures were carried out at these pressures; so no further data for comparison were available from own measurements here. Again the location of the experimental data with respect to the hydrate formation region have to be taken into account when evaluating the results. For the ethane-water systems the measured points at +5°C and +10°C at 5 bar and +10°C and +15°C at 15 bar lie outside the hydrate region. At both pressures for methane only the point -20°C at 15 bar lies within the hydrate region. It can be noted that in total at 5 and 15 bar slightly smaller values of the water content have been measured for ethane.

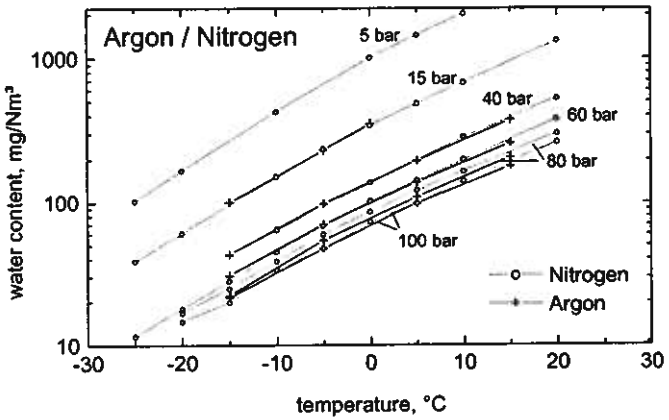


Figure 3.4: Comparison of water contents of the argon-water and nitrogen-water binary systems.



For +5°C and 5 bar both gases (methane and ethane) show nearly identical water content values (no comparison is possible at +10°C as no values have been obtained here with methane); inside the hydrate region the experimental values for ethane at 5 bar are lower by 14 to 31 mg/Nm³ than the respective values for methane. For the 15 bar isobar the three data for ethane outside the hydrate region also lie below those for methane. The deviations for the whole isobar are between 28 and 44 mg/Nm³. A comparison of the numerical values (see table G.1) reveals that with the exception of the -10°C point the deviation between the experimental data of methane and ethane increases with increasing distance to the ethane hydrate equilibrium curve.

On the 15 bar isobar the measured water contents for argon-water are slightly higher than those for the methane-water system (6-11 mg/Nm³). At the higher pressures one can see that argon behaves nearly as nitrogen compared with methane as the water contents of argon- and nitrogen-water nearly coincide. At 40, 60, 80 and 100 bar at +15°C lower water contents were measuring point 100 bar/ -20°C, all points in the investigated area are located outside the hydrate for argon-water than for methane-water.

When evaluating the measured data and the courses of the isobars, the uncertainties of the water contents have to be considered, too. Especially when evaluating the diagrams with respect to the kind of the condensed phase, this fact is of importance. Due to the uncertainties of the water contents measured, due also to the relatively large temperature intervals between the measured points the respective temperatures of the phase change cannot be taken from the slope of the isobars. Only a temperature range of a few Kelvin for a probable phase change can be deduced from the diagrams. This uncertainty in estimating the phase change temperature indicates that one cannot attribute the existence of a (liquid/ice) metastable condensed phase to the individual experimental points. In chapter 3.3, the estimation of the condensed phase, which was present during the measurements, is treated in detail.

The experimental results of this work will be compared to literature data for the binary systems. A listing of the literature data in annex E.2 reveals that only very few data are available for a direct comparison in the pressure and temperature range considered (see also figure 4.2). For three of the four binary systems (with exception of ethane-water) literature data for comparison were found, in the range same covered by the own measurements. All literature data however, were from one source only (Kosyakov [200] [201]).

Figures 3.5 and 3.6 (and figure G.5) show the comparison of the own results with those data of Kosyakov [200] [201], lying within the investigated region of this work. Different from the above procedure the water contents are shown as isotherms over pressure as Kosyakov took his own values at slightly higher pressures (10, 20, 40, 60, 80, 100 atm).The uncertainties shown correspond to the values of the enlarged overall uncertainty ($U_{95,tot}$) of annex D.2[9]. Within the range of properties shown, the values of the uncertainties nearly coincide with the size of the symbols.

[9] The measuring uncertainties given by Kosyakov correspond to those of this work. Not all input figures are available to carry out a uncertainty calculation corresponding to the one described in annex D.3 (according to the DIN-guide [139]), they would have to be guessed for a calculation according to the standard. As a first approximation the estimated uncertainties of B.3.1 were applied to the experimental values of Kosyakov, too.

When discussing the results of different calculation procedures (chapter 6), we will also come back to the values calculated with Raoult's law, with the programs CSMHYD in the 1990- [29] and 1998-version [28] and those calculated with the GERGWATER-method, developed within this work

which are also shown in figures 3.5 and 3.6. For now the courses of the GERGWATER method merely serves for allocating the measured points to a isotherm. The comparison for the system methane-water in figure 3.5 shows that the values measured in this work for the isotherms -10 and 0°C are below those of Kosyakov. With the exception of the points at 0°C at 40 and 100 bar and 40-bar, -10°C the deviations between the measured points are within the uncertainty limits of the water content measurements. This is verified by the overlap of the respective uncertainty limits. For the -20°C isotherm the values are in very good agreement.

Also for the nitrogen-water system the overall agreement can be seen from figure 3.6. Only for two measured points on the 0°C (40 and 60 bar) the deviations are larger than the uncertainties.

Kosyakov indicates that he took the water contents over ice phase[10] even though the major part of his measured data for the binary systems methane-, nitrogen-, and argon-water lie within the hydrate formation region, ice only being a metastable condensed phase here. The possibility that the hydrate phase is the stable phase in the hydrate formation region was not considered by Kosyakov. A possible cause of the deviations found for the system methane-water could be the existence of different condensed phases during the measurements. When measuring the water content above a hydrate phase smaller water contents result compared to those obtained above an ice phase (see annex A.4.2). Following this for the isotherms, shown for the measurements of this work, a condensed hydrate phase could have been present, for those of Kosyakov a metastable ice phase, respectively. At -20°C Kosyakov would have measured the water content above a hydrate phase due to the very good agreement of the data. This assumption is, however, weakened by the fact that Kosyakov's data also has measured slightly higher values for the system nitrogen-water where only the point 100 bar, -20°C is within the hydrate formation region. This seems to indicate that the deviations are not due to different condensed phases but are due to the measuring procedure or the measuring apparatus. Unfortunately, the publications of Kosyakov only contains very scarce information on the measuring apparatus used and the measuring procedure. When considering the uncertainties of the water contents the data therefore cannot be taken as an indication for systematic deviations between the measured values due to different condensed phases.

[10] The gas flowed over a bed of ice for saturation in the experimental set up of Kosyakov.



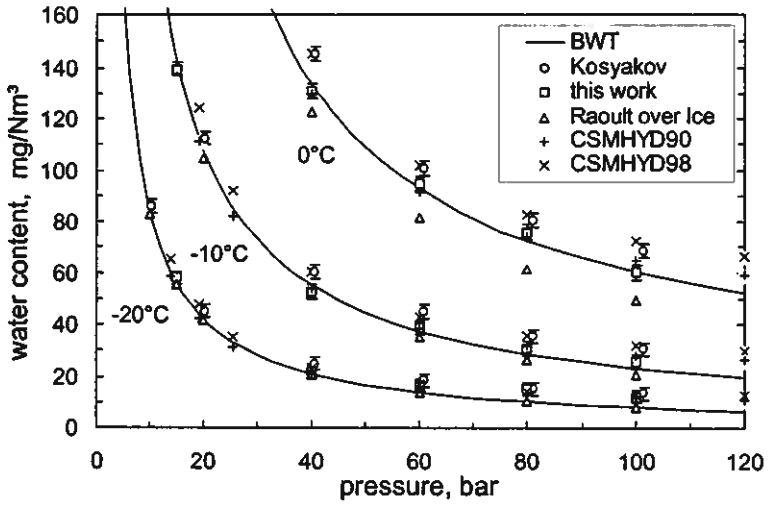


Figure 3.5: Comparison of measured water content data (this work) for **methane-water** mixtures with experimental data by Kosyakov [200], as well with calculated values using Raoult's law (eq. (E.3) over ice), the CSMHYD90-program [29], the CSMHYD98-program [28], and the GERGWATER-method by this work (see chapter 4), respectively.

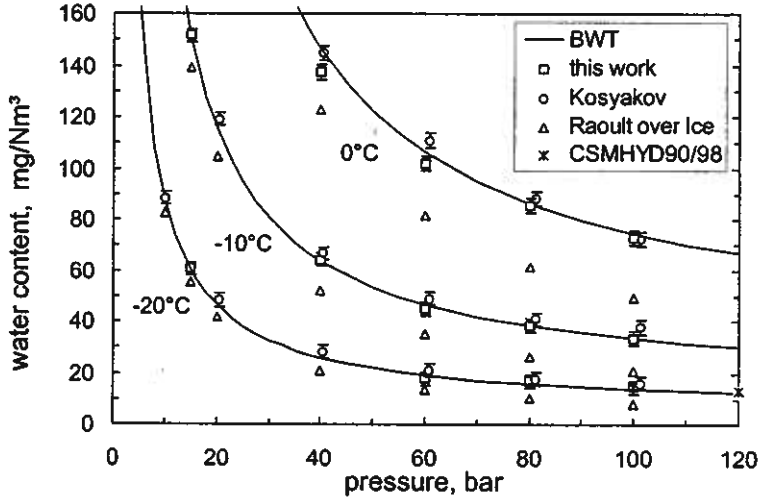


Figure 3.6: Comparison of measured water content data (this work) for **nitrogen-water** with experimental data by Kosyakov [201], as well with calculated values using Raoult's law (eq. (E.3) over ice), CSMHYD-programs [29] [28], and the GERGWATER-method by this work (see chapter 4), respectively

No data in open literature were available within the pressure and temperature range for the system ethane-water. For the system argon-water again data of Kosyakov were available, however at different temperatures and pressures. A direct comparison of the measured points therefore is not possible. On an isothermal plot the data for argon show consistent behaviour with those of Kosyakov (see figure G.5).

### 3.2.2 Ternary Mixture (Methane-Ethane-Water)

A methane-ethane -water mixture was used as the ternary system. The dry gas mixture according to the analysis certificate consisted of 96.96 mole-% methane (quality 3.5) and 3.06 mole-% ethane (quality 3.5). In the following tables and diagrams this mixture will be called "T1-97/3". The ternary methane-ethane-water system forms hydrates of structure I. The gas mixture was received from Messer Griesheim GmbH, Krefeld and was used without further treatment.

In order to isolate effects created by possible different condensed phases (liquid water, ice, hydrate) the measurements with the ternary mixture methane-ethane-water were carried out in a modified way compared to the standard procedure (see annex D.1, "experimental procedure").The measuring points were approached in a defined way via the ice and via the hydrate free liquid water region, respectively. By doing so it was intended if unambiguous results on the prevailing condensed phase in condenser K2 are reached when knowing the (defined) history of the measuring point. Also metastable phases (dependent on the location of the operating point ice, liquid water or subcooled liquid water, see also remarks in annex A.3) can occur instead of the thermodynamic stable phase due to kinetic hindrance. When approaching via ice it is expected that first a metastable ice phase will prevail in the hydrate region. In case of approaching the operating point via the liquid water region, first a metastable liquid water phase is expected due to kinetic hindrance. (A more detailed presentation of the ways to approach the operating points and a thorough discussion of the experimental results with respect of the prevailing phases during the measurements is contained in annex D.9.2 "water content measurements with a well defined history"). As a result one can state that except of the +5°C measuring points in case of the measurements with "defined history" only differences in water contents at the respective operating points could be detected which were within the uncertainty limits. Significant differences in water content which would give a hint to different condensed phases during the measurements were not observed. Based on observations with the video endoscope system a probable reason for the higher deviations between the +5°C measuring points[11] can be that for the water content measurements of the first row a hydrate phase (approach via the ice region) prevailed and during the second row a metastable aqueous phase (approach via the ice region) was the condensed phase. A detailed listing of the measuring results is contained in table D.10.

The results of the water content measurements were summarised for presentation in figure 3.7 (as well as in table G.4), according to the standard evaluation scheme (see annex D.2). Due to the different kinds of condensed phases (as assumed) at +5°C, a summarising of these individual measuring series into one mean value leads to a higher uncertainty, because of a high standard

[11] The differences were between 5.6 and 13.4 mg/Nm³ (see table D.10)



deviation. The plotted measuring points for +5°C possibly are located in between the values of a hydrate and of a metastable aqueous phase, due to the formation of the mean value.

Figure 3.7a gives the results of the water content measurements for the ternary mixture. Figure 3.7b allows a comparison of the experimental data for the ternary system under investigation with the binary mixture methane-water of this work. As had done when comparing the data for the methane- and nitrogen-water systems in figure 3.3 the hydrate equilibrium line (hydrate boundary) for pure methane calculated according to Sloan [29] was also included in figure 3.7b. According to the shifting of the hydrate equilibrium curve to higher temperatures due to admixing ethane the hydrate limit for the methane-ethane mixture is located at slightly higher water contents compared to that of pure methane.

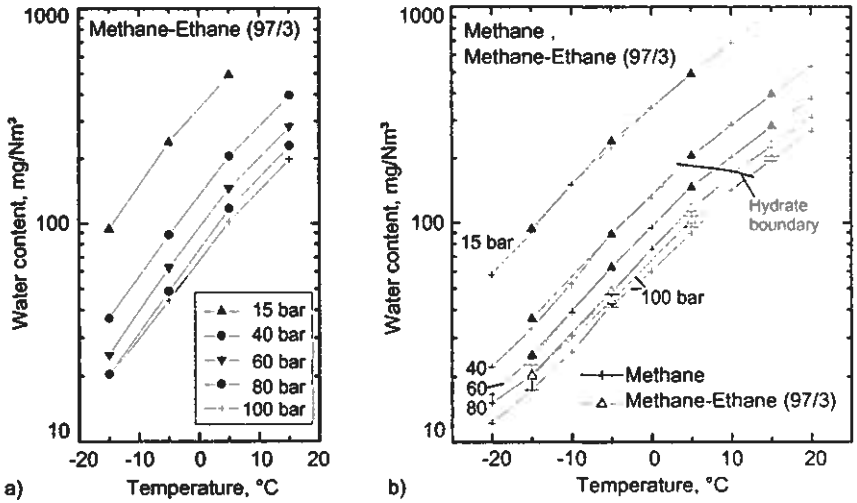


Figure 3.7: a) Measured water contents of the ternary mixture T1-97/3 (methane-ethane-water, dry gas composition 97/ 3 mole-%)
b) Comparison of water contents of the ternary mixture T1-97/3 with data for the methane-water binary system at five pressures (15, 40, 60, 80 and 100 bar).

The measuring point -15°C/ 100 bar exhibits higher water content compared to the trend in figure 3.7a. For this point, a water content corresponding to that at 80 bar was measured. A subcooled liquid phase, as condensed phase, can be excluded as the reason for the higher water content (see also remarks in annex D.9.2). A comparison of the respective measuring value of the first and of the second measuring series (see table 3.3) indicates that the too high value measured cannot be traced back to a metastable ice phase without doubt as well. The measured value at

Table 3.3: Experimental water content data including information about the most likely kind of condensed phase (see chapter 3.3 and annex D.9.2)

| Pressure, bar | Water content, mg/Nm³ | | Most likely kind of condensed phase |
|---|---|---|---|
| | -15°C | -5°C | |
| 100 | 20.21 | 44.20 | Hydrate (+ metastable ice) |
| 100 | 19.92 | 44.06 | Hydrate |
| 80 | 19.94 | 47.97 | Hydrate (+ metastable ice) |
| 80 | 20.96 | 49.24 | Hydrate |

100 bar with approach via ice region probably was measured above a high content of metastable ice phase (20.21 mg/Nm³) and is slightly higher (ΔWC= 0.29 mg/Nm³) than the one reached with approach over probable pure hydrate phase (19.92 mg/Nm³).

Both values, however, do not deviate much from the water contents measured at 80 bar, -15°C. In addition, a contradiction between the water contents measured and the assumed condensed phase occurred at 80 bar, -15°C as well as 100 bar and 80 bar, -5°C measuring points. At these points a higher water content was measured above the condensed phase, being to a high probability hydrate, than in the case where the condensed phase could have to be assumed as a metastable ice phase. Due to the high measuring uncertainties at these very low water contents, however, neither individual experimental values can be excluded nor the assumptions of the respective kinds of condensed phases can be assumed to be wrong. A thorough discussion of the possible kinds of phases existing, is given in chapter 3.3.

A direct comparison of the values measured leads to the result that the values for the ternary mixture methane-ethane-water scatter around the respective values for the binary methane-water system with the exception of the -15°C isotherm and the 100 bar isobar. The result is that adding 3 mole-% to methane has no significant influence on the water content measured. Compared to the binary mixture always slightly higher water contents for the ternary mixture were measured for the 100 bar isobar with the exception of the excluded +5°C point which, due to the special approach, was measured above a metastable liquid phase (see table D.10 and table G.1). The problem of evaluating the measured result taking into account the measuring uncertainties here becomes especially obvious. In spite of the clearly detectable deviations the differences between the measured water contents are still within the uncertainties of the values measured as is shown for the system methane-ethane-water for the 80 bar isobar where the uncertainties are included.



### 3.2.3 Multicomponent Mixtures (Natural Gases)

The investigated multicomponent mixtures are natural gases, which have been filled into pre-conditioned 50 dm³ gas bottles directly at respective compressor stations in Europe[12]. The natural gases chosen, cover the main gas compositions of the European natural gas pipeline network.

Gas chromatographic analyses of the multicomponent mixtures[13] were carried out with different scope. Table 3.4 contains a summary of the molar concentrations of the natural gases investigated.

Table 3.4: Compositions of the natural gases NG1 to NG7 in mole-%, based on a standard gas analysis. Components printed in italic, were determined by a ISO 6974-3 detailed gas analysis. Compound numbers correspond to table 4.2.

| Component | No. | NG1 | NG2 | NG3 | NG4 | NG5 | NG6 | NG7 |
|---|---|---|---|---|---|---|---|---|
| *Helium* | *23* | *0.015* | *0.028* | | *0.152* | *0.004* | *0.043* | *0.038* |
| *Hydrogen* | *24* | | | | | *< 0.001* | | |
| *Oxygen* | *25* | | | | | *< 0.01* | | |
| Nitrogen | 4 | 0.840 | 1.938 | 0.912 | 4.863 | 0.800 | 10.351 | 1.499 |
| Carbon dioxide | 5 | 0.109 | 0.851 | | 0.167 | 1.732 | 1.291 | 25.124 |
| **Methane** | **2** | **98.197** | **93.216** | **88.205** | **86.345** | **84.339** | **83.847** | **70.144** |
| Ethane | 3 | 0.564 | 2.915 | 8.360 | 6.193 | 8.724 | 3.460 | 2.520 |
| Propane | 6 | 0.189 | 0.715 | 1.763 | 1.550 | 3.286 | 0.657 | 0.394 |
| 2-Methylpropane | 7 | 0.029 | 0.093 | 0.293 | 0.214 | 0.311 | 0.093 | 0.067 |
| n-Butane | 8 | 0.038 | 0.135 | 0.441 | 0.314 | 0.584 | 0.126 | 0.074 |
| 2,2-Dimethylpropane | 9 | 0.001 | 0.002 | 0.003 | 0.002 | 0.001 | 0.006 | 0.003 |
| 2-Methylbutane | 10 | 0.007 | 0.029 | 0.020 | 0.061 | 0.080 | 0.031 | 0.029 |
| n-Pentane | 11 | 0.006 | 0.027 | 0.004 | 0.067 | 0.082 | 0.03 | 0.022 |
| $C_{6+}$ | | 0.007 | 0.049 | | 0.064 | 0.049 | 0.069 | 0.118 |
| Σ | | 99.995 | 99.949 | 100.01 | 99.928 | 99.954 | 99.935 | 99.914 |

With the exception of the components helium, hydrogen and oxygen the range of the listed components corresponds to the gas constituents which are analysed as a standard according to ISO 6974-4 [147]. N-Hexane, other hexanes and higher hydrocarbons are summarised in the pseudo component $C_{6+}$. The methane content was used as criterion for sorting the dry gas concentrations. The natural gases show a decreasing methane content with increasing numbering. Due to possible side reactions with the chemicals at water content measurements, special care was

[12] The gas bottles required were specially cleaned by Messer Griesheim, Bottrop and delivered with a slight nitrogen (quality 4.6) over pressure. The gas bottles including the pre-heated connections first were evacuated after connecting them in parallel to the pipeline. Prior to filling the gas bottles were purged a few times with the gas from the pipelines and again evacuated in between.

[13] We would like to thank N.V. Nederlandse Gasunie, Groningen for carrying out the extended gas analyses.

taken on estimating the sulphur components during the analyses. The sulphur analysis resulted in a hydrogen sulphur content of <0.4 mg/Nm³ for all mixtures[14], the total sulphur content was below 1 mg/Nm³. As these numerical values correspond to the sensitivity of the analysis method the gas mixtures were regarded as sulphur free within the frame of this work. At the begin and at the end of each measuring campaign a gas analysis was carried out for each gas. A comparison of these analyses results showed no significant deviations from the input analysis shown in table 3.4.

For the seven natural gases the molar mass and the compression factors at standard conditions are given in table F.10 calculated from the gas analyses from table 3.4. In addition table G.10 gives the specific gravity for the gases as well as the respective Wobbe-number. Natural gases NG1 to NG6 are counted to Group H gases[15] according to German guideline G260/1 [93] considering the combustion characteristics. Natural gas NG5 is located in the transition to group-L gas. The natural gas NG7 being rich of carbon dioxide does not fulfil the specifications of group-H or group-L gases as it shows a too low Wobbe-number and a too high specific gravity. Prior to delivery to the end user this gas has to be conditioned by mixing with other gases.

In order to document that the hydrogen, oxygen and helium contents of the natural gases under consideration are below the analytic sensitivity limit or can be neglected, these components were taken into consideration in the listing of the analytical results, too. Table 3.4 indicates that the content of carbon dioxide which has to be considered with respect to corrosion aspects does not exceed 2 mole-% for the gases NG1 to NG6. For the gases NG1 and NG4 the carbon dioxide content is below 0.2 mole-%; no carbon dioxide could be analysed for gas NG3.

Natural gas NG1 is the gas richest in methane with more than 98 mole-%, natural gas NG7, with 70.1 mole-% methane, has the lowest methane content of all natural gases investigated. Natural gas NG6 has the highest nitrogen content with more than 10 mole-%. With the exception of gas NG4 with 4.9 mole-% nitrogen all other gases have a nitrogen content below 2 mole-%. Due to the high methane content natural gas NG1 only contains small amounts of ethane and propane. The ethane content of all other gases exceeds 2.5 mole-%. Natural gas NG5 shows the highest ethane content with 8.7 mole-%. It also contains the highest propane content of all gases with 3.3 mole-%. The propane content of the remaining gases lies between 0.19 and 1.76 mole-%[16].

The major part of the measuring points for the natural gas therefore lies within the hydrate region as with methane (see figure G.1). At the higher pressures (p≥60 bar) all measuring points with a temperature below +5°C are within the hydrate formation region. Of all natural gases the highest hydrate formation temperatures at constant pressures are calculated for gas NG5. The higher

[14] According to Kaesler [88] an increase in water content by 0.212 mg/Nm³ is to be expected with the KF-titration when the gas investigated has a sulphur content of 0.4 mg/Nm³.

[15] Wobbe-number $W_{o,n}$: group L = 37.8 - 46.8 MJ/m³; group H = 46.1 - 56.5 MJ/m³; specific gravity: 0.55 - 0.7

[16] The gas components are of special importance with respect to hydrate formation. Already small amounts of these gases result in an accelerated hydrate formation and a shifting of the hydrate formation curve to higher temperatures. Together with ethane methane only forms structure I hydrates. As propane (same as iso-butane) only fits into the large cage of structure II, natural gas in general forms structure II hydrates [28] (see annex A.3.2). If these components are admixed to a methane- ethane mixture a change from structure I to structure II can be observed [31].



hydrocarbons are of importance with respect of a possible hydrocarbon condensation. The content of the $C_{6+}$-fraction in natural gases NG1 to NG6 amounts to max. 0.07 mole-%. Natural gas NG3 shows a unique gas composition. Due to a special treatment the higher hydrocarbons including n-hexane ($C_{6+}$-fraction) are missing completely. In addition gas NG3 neither contains carbon dioxide nor helium.

Figure 3.8 shows the measured water contents for the natural gases NG1 to NG7.As expected the courses of the water contents of the multicomponent systems do not deviate much from that of their subsystems discussed in the previous chapter. The natural gases NG2, NG4 and NG5 showed a (retrograde) hydrocarbon condensation behaviour at intermediate pressures and low temperatures which was detected during the measurements with the dew point mirror. The evaluation of the experimental data revealed that only partly the water content data were influenced due to small amounts of hydrocarbons. Only from the results of the water content measurements taken outside the retrograde region at ambient pressure one cannot conclude unambiguously on the occurrence. Only the measured water contents of the -15°C isotherm of natural gas NG5 show significant deviations from the expected course, which however, do not show a trend (see figure 3.8). The measuring point 60 bar, -15°C lies within the retrograde region, the high $C_3$- to $C_5$- contents result in a wide retrograde region for this gas (see table 3.1). No condensation point could be detected for 80 bar, -15°C.

In the hydrate free region a change of the slope of the isobars in the region of 0°C can be detected (for instance 15 bar isobar for natural gas NG2 and NG5) also for the multicomponent mixtures which indicates a change of the condensed phase from liquid water to ice. When considering the isobars over a large temperature range a slight curvature of the isobars can be detected. Compared to the binary methane-water a significant change of the slope of the isobars due to formation of hydrates can only be detected in few cases for the natural gases (for instance natural gas NG2: 40 and 60 bar; natural gas NG5: 60 bar; possibly also natural gas NG4: 80 bar). Due to the fact that only a few measured values are located outside the hydrate region, an evaluation of the isobars with respect to a significant change of slope is quite problematic.

Natural gas NG7 takes a special place because of its high carbon dioxide content. Due to the high solubility of carbon dioxide one has to take into consideration that compared to the hydrocarbons higher contents of carbon dioxide are solved in the bubble column of the saturator, in the condensed liquid on the bottom of the condensers and in the wet gas meter. Therefore the purging times for natural gas NG7 prior to the measurements were prolonged. When changing the operating conditions in the experimental set up fast pressure reductions were not allowed to avoid gassing out of the carbon dioxide dissolved in the aqueous phase. As shown in figure 3.8 the water contents measured for natural gas NG7 correspond to those measured for the natural gases with lower contents of carbon dioxide.

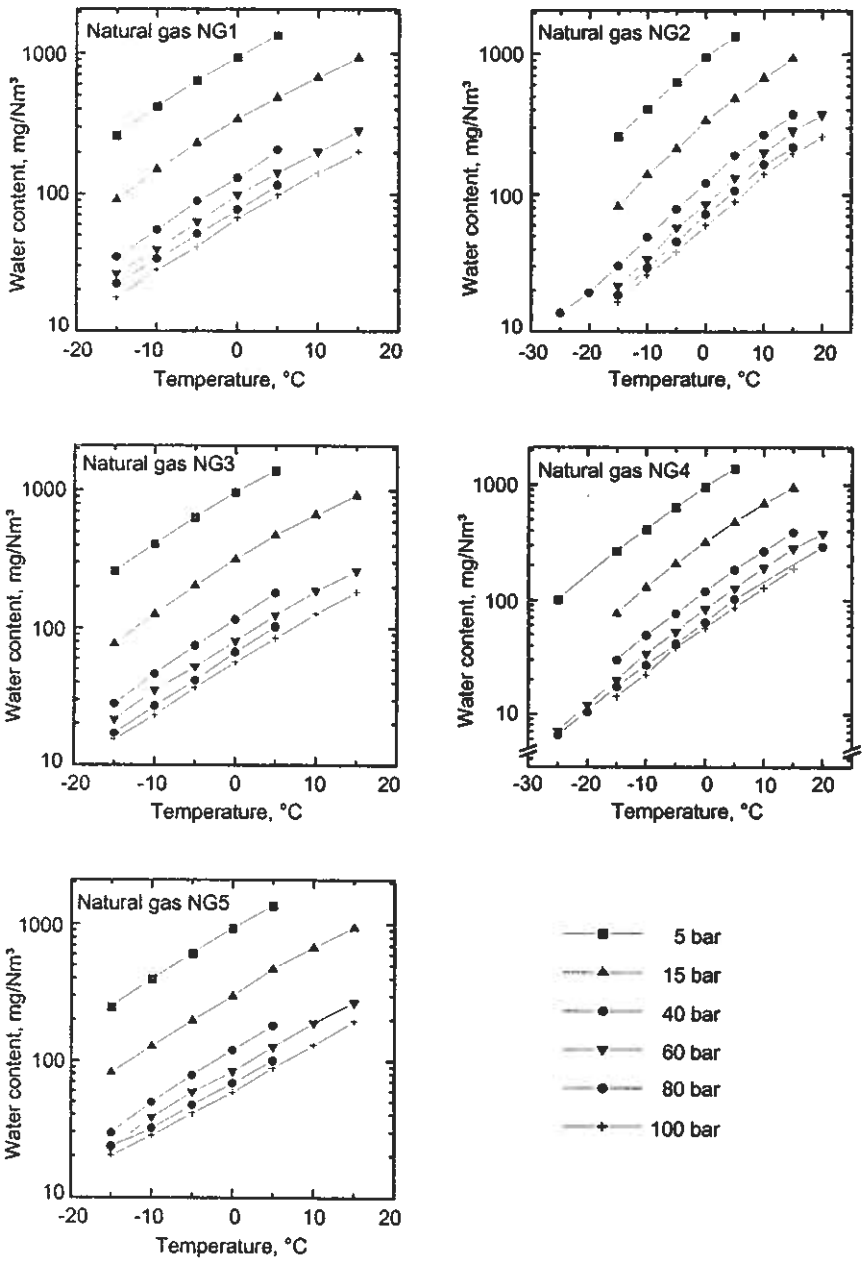


Figure 3.8: Measured water contents for the natural gases NG1 to NG7



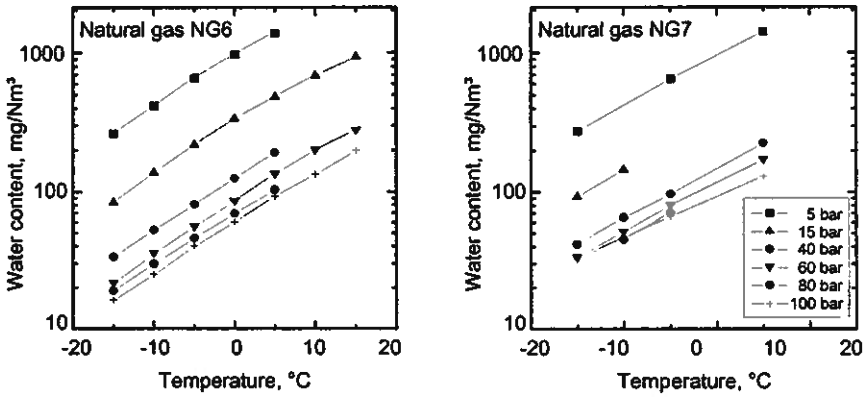


Continued: Figure 3.8: Measured water contents for the natural gases NG6 and NG7

Figure 3.9 allows a comparison of the water contents for the 60 bar isobar for natural gases NG1 to NG7 and for the binaries methane-and nitrogen -water. The corresponding diagrams for the pressures 5, 15, 40, 80 and 100 bar are shown in figure G.6 in annex G.1.2. It can be seen that for the pressures 40 to 100 bar the measured water contents were highest for the carbon dioxide rich gas NG7. For 15 and 5 bar the courses of the water contents for all gases nearly coincide. No influence of gas composition can be detected at these pressures. At the higher pressures the gases NG1 to NG7 also show nearly the same values at temperatures higher than +10°C. Gas NG2 is an exception at 100 bar. In the temperature range of +5 to +15°C it shows slightly higher water contents. During the measurements a "humid" condenser chamber, that is formation of droplets on the sapphire window, could be detected with the video endoscope system. This could be taken as a hint that a metastable aqueous phase could have prevailed during the measurements. The figures indicate that the courses of the water content diverge with increasing pressure to lower temperatures. At water contents below 100 mg/Nm³ deviations of the dew points of 5 K and more result between the different mixtures at a given water content. At constant p and T, the differences in water content (even when excluding natural gas NG7) amount up to 30% (100 bar, -15°C, natural gas NG4= 14.2 mg/Nm³, natural gas NG5= 20.3 mg/Nm³).

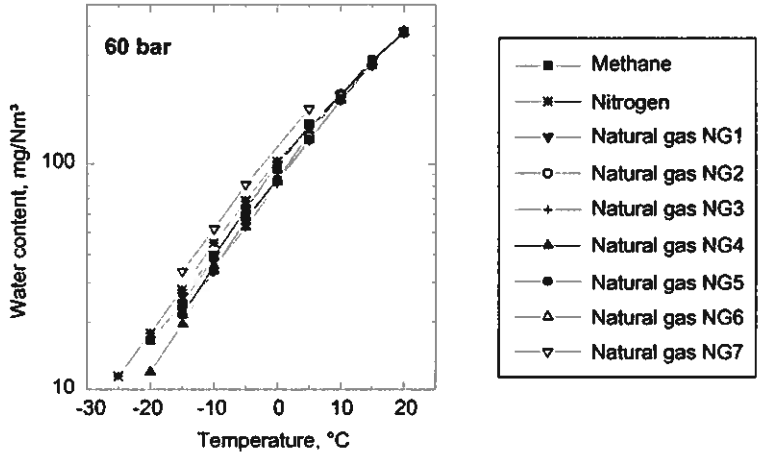


Figure 3.9: Comparison of the courses of measured water contents of the natural gases NG1 to NG7, as well as the binary systems methane-water and nitrogen-water at the example of the 60 bar-isobar.

## 3.3 Discussion of the Phase Situation During the Measurements

The measured gas is cooled to the temperature of the cryostat in the lines to the condensers. Due to the prior saturation of the gas at a higher temperature water condenses on the inner walls of the lines because of the cooling down. Depending on the pressure set and the prevailing temperature in the line different condensed phases can be formed as an equilibrium phase for the vapour phase (liquid water, subcooled liquid water, ice or possibly hydrate). In annex A.4.2 the consequences of a temperature decrease at constant pressure on the phase as well as on the water content in the vapour phase were already described in detail when discussing the schematic pressure-temperature- (figure A.2) and temperature-concentration-phase-diagrams (figure A.3). In this basic discussion it was pointed out that a formation of metastable phases may be a result of kinetic hindrance. The different kinds of condensed phases are related to different equilibrium water contents in the vapour phase. At isobaric and isothermal conditions the water content (WC) above a hydrate phase is lower than the one above a metastable liquid phase or a solid ice phase (see also figure A.3c):

$$(WC_{Hydrate} \leq WC_{Ice} \leq WC_{liq.water})_{T,P}$$

In spite of a broad literature recherche only one source could be found in open literature which gives water contents for all three condensed phases at identical operating points. Makogon [30] gives water contents above the different condensed phases for one natural gas (see table 3.5). It cannot be traced back, however, if the values given are experimental or calculated water contents.



With the data a first guess of the influence of the prevailing condensed phase on the water content can be made. The data listed indicate that significant differences between the water contents above liquid water and above hydrate exist for temperatures above the melting point of ice. For temperatures below 0°C the differences in water content above ice and hydrate are first greater then those above ice and above subcooled liquid. The small differences between the water

content above subcooled liquid and above ice for small values of subcooling correspond to the behaviour which one expects from extrapolation of the vapour pressure to subcooled liquid and of the sublimation curve for pure water (see also figure A.1). Further it can be seen from table 3.5 that the differences between ice and hydrate decrease with increasing distance from the melting temperature, the differences between subcooled liquid and ice increase, however. At 100bar, -10°C the differences between the water content above a hydrate phase and a ice phase amounts to 20% from the upper water content value. The differences of the water content between a ice and a metastable liquid water phase here are about 10% of the upper value.

These data point out that it is of special interest to know the condensed phase inside the potential hydrate formation region for evaluating the data measured. However, the unambiguous determination of the type of condensed phase within the hydrate formation region posed big problems within this work.

In the set up of this work the adjustment of the phase equilibrium for the water content measurements was achieved in the circular line leading to the second condenser. A visual observation of the inside of the lines was not possible as only the big condenser chambers could be monitored with the optical video endoscope system. Even in the seldom cases where deposits formed within the visible area of the endoscope system the type of solid phase (ice/hydrate) could not be distinguished below 0°C merely from the video pictures. Preferably point like or thin layer like deposits formed which did not grow also over longer periods (see figure 3.10)[17]. The only possibility to obtain the type of solid phase with confidence was to heat the condenser. In cases the deposits were still visible above the melting temperature of ice it was hydrate.

Table 3.5: Water contents of a natural gas, measured in equilibrium with different kinds of condensed phases, according to Makogon [30]. (standard state and gas composition were not given in the literature source)

| *Natural gas, mg/m³: liq. Water ($L_w$), Ice (I), Hydrate (H)* | | | | | | | | | |
|---|---|---|---|---|---|---|---|---|---|
| | P= 100 bar | | | P= 75 bar | | | P=50 bar | | |
| T, K | $L_w$ | I | H | $L_w$ | I | H | $L_w$ | I | H |
| 283 | 165,1 | | 127,0 | 196,7 | | 170,0 | 259,9 | | 220,0 |
| 273 | 88,5 | 88,5 | 68,0 | 104,1 | 104,1 | 84,3 | 135,2 | 135,2 | 117,8 |
| 263 | 45,7 | 41,8 | 31,7 | 52,9 | 48,5 | 38,6 | 67,5 | 61,8 | 52,9 |
| 253 | 22,7 | 18,5 | 14,0 | 26,0 | 21,2 | 16,8 | 32,4 | 26,4 | 22,5 |
| 243 | 11,0 | 7,7 | 5,9 | 12,3 | 8,7 | 6,9 | 15,0 | 10,6 | 9,0 |
| 233 | 5,1 | 3,1 | 2,3 | 5,6 | 3,4 | 2,7 | 6,7 | 4,0 | 3,4 |

[17] Chapter F.1.3 contains further pictures of the video endoscope system as well as a explanation of the visible area.

No direct investigation of the condensed phase in the stainless steel lines, for instance by means of spectroscopic measuring methods, were possible, as no instruments were available and the experimental set up did not allow to install the highly sensitive measuring devices in the area of the condensers. It should be noted that the condensers including the lines were fully immersed in the cryostat bath.

Figure 3.10: Dot like hydrate precipitation at the gas outlet pipe (see arrow).

The following hypothesis can be made for the processes, occurring in the pipe: When approaching the operating point via ice region a thin ice layer is formed on the inner walls of the lines at cryostat temperatures below the melting temperature of ice which forms the stable equilibrium phase in the ice region (see figure 3.11 and A.3). When crossing the phase equilibrium line between the ice and the hydrate region ice is a kinetic hindered metastable phase at temperatures below the melting temperature. In an undisturbed state (no energy ingress for instance by stirring or turbulent flow, etc.) a direct change of ice into the stable hydrate phase only occurs very limited and with large time delay [28] [144]. According to Makogon [30] this can be traced back to the fact that the change from ice to hydrate below 0°C only shows a very slow kinetic as the gas molecules first have to diffuse into the ice. The very limited freedom to move in the solid ice crystal hinders the necessary reordering for hydrate formation. For the experiments carried out it follows with a high probability that a metastable ice phase was present over a long time inside the hydrate region, as long as the temperature inside the line was not raised above the melting temperature of the ice. In case of crossing the melting pressure curve of the ice a increased hydrate growth starts on the melting ice surface [145]. As the hydrate phase forms a stable equilibrium phase within the hydrate region, a hydrate phase will grow on the surface of the ice layer. With increasing time inside the hydrate region more and more ice surface is covered with hydrate and even though still a metastable ice phase exists inside the line, the vapour phase no longer is in direct contact with ice. At complete coverage of the ice surface the equilibrium exclusively would be influenced by the hydrate phase.

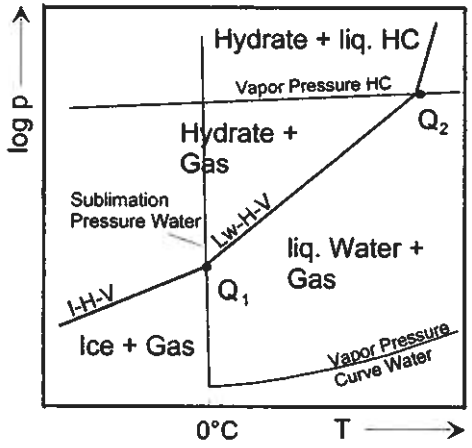


Figure 3.11: Schematic p,T-phase diagram for a hydrate forming gas mixture, according to [31] (see also figure B.2).

The condensed phase within the hydrate region could not be detected exactly with the means available in this work. In dedicated experiments it therefore was tried to reach dedicated conditions in the line and inside the large chamber of condenser K2 by keeping special defined experimental conditions and by doing so to recognise the influence of different condensed phases on the water content. To isolate the phase effects comparative measurements were carried out with a methane-ethane -water mixture (see chapters 3.2.2 and D.9.2) at identical operating points with differing history and detailed fixed approaches for the operating points measured. Main emphasis was laid on operating points inside the hydrate area which were approached in a defined way as well from the ice and form the hydrate free liquid water region. A detailed description of the experimental procedure, a tabular summary of the numerical results as well as a detailed discussion of the experimental data are given in annex D.9.2.



Summarising, it can be noted as a result of measurements[18] with a "well defined history", that the deviations between water contents determined in equilibrium with a hydrate-phase and a ice-hydrate mixed phase were in between the uncertainty of the experimental set up. According to Makogon (see table 3.5), who points out that significant differences in water contents above ice and hydrate phases occur at low temperatures, it can be assumed that the phase equilibrium was influenced mainly by the stable hydrate phase, even during the experiments with an (assumed) ice-hydrate mixed phase, due to the small differences in water content measured.

For those measuring points which were approached via the liquid water region and which are located inside the hydrate region with temperatures above the melting temperature of water (+5°C measuring points and table D.10), larger differences in water content were observed. For these points the pictures taken from the video endoscope system (formation of droplets on the sapphire window, see figure 3.12) indicate that the water content measurements with the higher content (with approach via liquid water) were measured above a metastable liquid phase. Compared to the differences between the water contents above the different condensed phases given by Makogon [30] here, however, smaller differences in water content were measured.

For the measurements carried out according to the standard measuring program (see annex D.1) the higher pressures were approached via the ice region, as has been done for part of the experiments with the methane-ethane-water system, in order to avoid too high water ingress into condenser K2. As a rule the cryostat bath of condenser K2 was kept at a temperature of -10°C (K1 = +2°C) and the pressure was slowly increased to the set pressure. By following this procedure in most cases a deposit free and according to the monitor picture of the video endoscope


Figure 3.12: Sapphire window, almost completely covered by small water droplets. The gas outlet pipe is only shadowy recognisable.

[18] These measurements have been carried out for operating points, located in the hydrate region, and for temperatures below the melting temperature of ice (see figure 3.11). Because of the routing over the liquid water region in the second run of the measurements, ice could be precluded as condensed phase. Ice only could have existed, if a metastable liquid water phase would not have formed hydrate, but a metastable ice phase. No literature information on such a possible phase change has been found.

system inside the visible area also a optic dry chamber of condenser K2 could be obtained.

For a few measuring points in the ice region (nearly exclusively -5°C measuring points) water droplets were observed on the sapphire window (see figure 3.12) which indicate that the condensed phase could have been a subcooled liquid phase.

For the operating points with high humidity in condenser K2, visible via a fog like dimness or heavy droplet formation on the sapphire window (in the following this condition will be called "optical humid"), in general disturbances of the measurements were experienced after a short time due to ice formation forcing to interrupt the experiments. Because of this only very few measuring points are available for which a metastable liquid phase can be assumed having prevailed during the estimation of the water content (for instance natural gas NG2 ,100 bar, +10 to +20°C). With respect to a possible subcooled liquid phase in the ice region a comparison of water content measurements with a long residence time in the ice region (2-3 days) and a optical dry condenser chamber at the start of the measurements with those results when the measuring points were approached via the liquid water region with an optical humid condenser chamber only very little deviations in the water content were observed (a few µg, see for instance the 15 bar points of the ternary methane-ethane -water mixture in table D.10).

When a optical humid condenser chamber K1 was present during a operation point inside the hydrate region the operation was disturbed repeatedly. Due to the higher humidity ingress hydrate formation occurred mainly in the area of condenser K1 with throttling effect. Only in a few cases a optical humid condenser chamber K2 was observed inside the hydrate region at temperatures above the melting temperature of ice. The main reason for having observed a humid condenser chamber K2 only in the few cases is due to the approach of the operating points because of the experimental program and due to the high hydrate formation temperatures of the mixtures investigated (see figure G.2). Only in the first run the possibility of approaching the measuring points within one isobar directly from the hydrate free liquid water region was given because of the random temperatures. In the second run the temperatures as a standard were changed from low to high temperatures within one isobar.

For those measuring points which were approached from the hydrate free region and for which a humid atmosphere was observed in condenser K2 during temperature reduction or pressure increase, in most cases after a short period (a few minutes to max. 1-2 hours, which means within the running-in time), a disturbance of the gas stream (pressure drop) near the condenser K2 was observed, which probably was caused by fast hydrate growth. This may be explained by the fact, that the hydrate free measuring points outside the hydrate region were (in most cases) approached from measuring points inside the hydrate region. When crossing the hydrate equilibrium line the hydrates dissociate. But ordering effects between water molecules in the liquid condensed phase remain, due to the small distance to the hydrate boundary. It is known [22] [28] that these effects shorten the (normally long) induction time considerably and may lead to an accelerated hydrate re-formation. Due to these reasons water content measurements with an "optical humid" condenser K2 at constant operating conditions could not be carried out in practice. The few measuring series that could be carried out with a humid condenser K2 without a disturbance, in general



showed a (sometimes strong) decrease of water content. This is a hint, that the equilibrium had not yet been reached[19] during the measurements. The decrease of the measured values probably can be traced back to a hydrate formation, which first was not detectable by measuring tools (pressure transducer, and video system), due to its small amount. According to experience, a pressure difference between K1 (PIR2) and K2 (PIR4) was an unambiguous indicator for the formation of deposits in the line to condenser K2.

Based on the results of the analysis of the course of the slopes of the isobars for the mixtures investigated in the preceding chapters 3.2.1 to 3.2.3 as well based on the thorough evaluation of all points measured including the uncertainties the following statements can be derived with respect to the prevailing condensed phases:

- During the measurements outside the hydrate region and at temperatures above the melting temperature of ice exclusively liquid water formed the condensed phase.
- Ice was the condensed phase determining the equilibrium below the I-H-V phase equilibrium line inside the ice region.
- According to the hypothesis on the occurrences in the lines no unambiguous secured statement with respect to the condensed phase for measurements inside the hydrate region is possible. It can be assumed that in the majority of the measurements hydrate and metastable ice formed the condensed phase. With increasing residence time inside the hydrate region below the melting temperature of ice, one has to assume that the phase equilibrium nearly exclusively was governed by the hydrate phase. For those measurements taken into consideration for evaluation within the hydrate region above the melting pressure temperature of ice a stable hydrate phase prevailed to a high probability.

With respect to reaching the aims of this work, to develop a new calculation procedure with respect to an accurate dew point calculation, the own data set is optimally suited as at a given water content the stable hydrate shows the highest dew point at constant pressure compared to a metastable ice and water phase (see also figure A.3c). To exclude condensate formation (especially hydrate formation) in a system at given boundary conditions (p,T, dry gas composition) the water content has to be lower than that measured in this work at the respective operating points.

[19] These measuring runs were excluded from evaluation, as a common mean value is senseless.

# 4 Development of the Model

The objective of this chapter is the development or the modification of an equation of state (EOS), which is able to reproduce the measured water contents and dew points with highest accuracy possible. The core region of the pressure and temperature range to be coverd is identical to the region of the experimental data available. The desired application range of the model reaches from -50° up to +40°C in temperature and 1 up to 300 bar in pressure. It contains a large range, which is not covered by experimental data yet.

The binary interaction parameters (BIP) of the model were fitted against binary data only. The results of the multicomponent systems, which were measured within this work, have been used to fix the required extent of the analysis (see chapter 4.5), as well as for the validation of the model (see chapter 5).

## 4.1 Selection of the Model

An extensive literature survey and own investigations have been carried out at the beginning of the model development. It turned out that the systems considered, can be described by relatively simple cubic equations of state (CEOS), if the predictions of water contents and dew point temperatures are regarded [166] [168] [169] [178] [181]. The more complex or theoretical based equations are not expected to give better results than cubic equations of state [176] [177] [180] (see annex E.3).

Therefore the choice of the models was restricted to CEOS. Moreover, these equations have advantages in a clear and simple structure, an analytical solvability and a reliable extrapolation behaviour. For the phase equilibria calculation the homogeneous method has been choosen, which means that components of all phases are calculated with the same equation of state. So one has no difficulty to fix a reference state for the supercritical components methane and nitrogen.

Among the numerous CEOS available, the equation by Peng and Robinson (PR) was selected as a base for an optimised calculation method, because of several reasons: The PR-EOS was especially developed to describe properties of non polar substances such as hydrocarbons [16]. Its suitability to describe the behaviour of complex hydrocarbon systems was proved in several publications in literature (e.g. [177] [182]). Therefore, the PR-EOS proceeded as a standard tool for vapour liquid equlibria (VLE) calculation in natural gas industries [171]. Besides this application the PR-EOS found broad acceptance in many other fields of phase equilibria [164]. Based on this equation parameter optimisations have been carried out successfully in several studies[20] [183] [184] [185].

[20] Some previous investigations (see [117] [190] [178]) may lead to the conclusion, that other CEOS are suitable for a problem specific optimisation as well.



The disadvantages of the PR-EOS in its original version are known as the inaccurate reproduction of the liquid densities and the critical region, as well as the limited applicability for electrolytes and high polar fluids, exhibiting hydrogen bondings [171]. This disadvantages either do not touch the objectives of this work or have been considered as correctable using adequate modifications.

A high accurate description of liquid liquid equilibria (LLE) or the gas solubility of hydrocarbons in the liquid aqueous phase is not required. So the application of density dependent mixing rules (e.g. [186]), asymmetric mixing rules (e.g. [23] [187] [188]), or mixing rules based on excess free energy models (e.g. [189]) is not necessary.

Regarding the description of the gaseous phase, complex mixing rules often are not superior to the simple mixing rules. In this case the number of free parameters is more crucial than the structure of the mixing rules used. For that reason complex terms have not been considered. The symmetric mixing rules by Van der Waals have been applied, to calculate the parameters $a$ and $b$ of the modified PR-EOS (see equations (A.26) to (A.30)).

## 4.2 A New Alpha-Function for Water

A preliminary study showed, that the reproduction of the vapour pressure of pure water is a fundamental condition for the prediction of the phase behaviour of wet natural gases.

The equation parameter $a$ therefore has a significant influence on the vapour pressures of pure substances. The calculation results substantially depend on the temperature function of the $a$-Parameter, i.e. the alpha-function.

As shown in annex B, the generalised alpha-function of the PR-EOS is correlated using the critical temperature $T_c$ and the acentric factor $\omega$. Anderko [12] points out, that the acentric factor is no characteristic parameter for polar substances. This fact may lead to unsatisfying results, if $\omega$ is used in a correlation for those substances. For that reason it is not surprising, that vapour pressures of water are reproduced only with a poor quality, if the PR-EOS is used in its original version. The relative deviation of the triple point pressure, for example, is larger than 20% .

To remedy this deficiency, many solutions have been proposed in literature. Most of them improve the reproduction of vapour pressures of pure substances by a modified alpha-function (see [167] [190]-[196]). Peng and Robinson themselves published a new alpha approach for water already in 1980 [166].

$$\alpha_{H2O,PR80}(T_R)^{1/2} = 1.008568 + 0.8215\,(1 - T_R^{1/2}) \qquad (4.1)$$

The recommended temperature range for equation (4.1) is $0.44 < T_R < 0.72$ (+12 to +193°C).

The PR modifications for water, which are available in literature, frequently were fitted to vapour pressures in a large temperature range (e.g. from the triple point up to the critical point). This leads (in many cases) to larger deviations at the edges of the temperature range considered. In figure 4.1 this behaviour is demonstrated at the example of the alpha-function according to equation (4.1).

The objective of this work was to achieve a good reproduction of the vapour pressures of water in a comparatively small temperature range ($0.34 \leq T_R \leq 0.48$; -50 to +40°C). An acceptable reproduction of the vapour pressure curve beyond this range (e.g. near the critical point) was not considered as necessary.

For the calculation of vapour pressures above a solid phase (sublimation pressures), generally the vapour pressure curve may be extrapolated into the region below the triple point, if the subcooling remains small. The solid phase is treated as a kind of subcooled liquid in this procedure. For small subcooling, the error in the sublimation pressure calculation is negligible. This is caused by the slight difference between the extrapolated curve and sublimation pressure curve near the triple point (see figure A.1). But the error rises strongly with an increasing distance from the triple point. In this case, the sublimation pressure curve should not be approximated by an extrapolated vapour pressure curve. This will be demonstrated at the example of the PR-EOS with modified alpha-functions for water by Peng and Robinson (PR 1980, see eq. (4.1)) and Stryjek and Vera (PRSV-EOS, eq.(F.1)) [191]. For the design of both alpha modifications, no sublimation pressures were used. From this follows, that the sublimation pressures calculated with these alpha-functions correspond to an extrapolation into the ice region. As figure 4.1 shows, vapour pressures are well described by the PRSV-EOS[21]. But it becomes obvious, that the reproduction of the sublimation pressure is not satisfying.

In this work a new polynomial alpha-function for water has been developed (see eq. (4.2)). Two different sets of coefficients were determined for the calculation of vapour pressures above liquid water and solid ice. For the parameter fit sublimation pressures were used in the temperature range from 223.15 K up to 273.16 K (-50 to 0.01°C) [129] and vapour pressures in the range from 273.16 K up to 313.15 K (0.01 to +40°C) [130][22]. Table 4.1 contains the recommended coefficients.

$$\alpha_{H2O}(T_R)^{1/2} = 1 + A_1(1 - T_R^{1/2}) + A_2(1 - T_R^{1/2})^2 + A_3(1 - T_R^{1/2})^4 \qquad (4.2)$$

Table 4.1: Coefficients of the proposed alpha-function according to eq. (4.2)

| | Sublimation pressure curve (SPC) | Vapour pressure curve (VPC) |
|---|---|---|
| | 223.15 K ≤ T < 273.16 K | 273.16 K ≤ T ≤ 313.15 K |
| $A_1$ | 0.106025 | 0.905436 |
| $A_2$ | 2.683845 | -0.213781 |
| $A_3$ | -4.75638 | 0.26005 |

[21] It should be mentioned, that the alpha-function by Stryjek and Vera contains one more parameter and a higher degree in the temperature dependence (exponent) as the alpha-function given by eq. (4.1).

[22] Many thanks to Prof. Dr.-Ing. W. Wagner, Lehrstuhl Thermodynamik II, at Ruhr-Universität Bochum for the donation of the "International Standard Equation of water" calculation program.



The coefficients of both partial functions are connected at the triple point condition (SPC equals VPC).

$$\alpha_{H2O,SPC}(T_{tr}) = \alpha_{H2O,VPC}(T_{tr}) \qquad (4.3)$$

The boundary condition at the critical point: $\alpha(T_R=1)=1$ is fulfilled by the alpha partial function for liquid water ($\alpha_{H2O,VPC}$), though this constraint is not absolutely necessary in the temperature range considered.

The first temperature derivatives of the alpha partial functions $\alpha_{H2O,SPC}$ and $\alpha_{H2O,VPC}$ at the triple point do not match, which leads to a point of discontinuity in the function course. From this follows, that the VPC and the SPC calculated with these alpha-functions at the triple point will exhibit a discontinuity, as well as it is observed in reality (see fig. A.1). For the calculation of caloric properties, where temperature derivatives of the alpha-function are required, this procedure may cause problems [117]. But it does not affect the calculation of water contents and dew points, however, which is the major objective of this work.

In figure 4.1 relative deviations are plotted between vapour pressures (above ice, or liquid water respectively) calculated with the PR-EOS using the new alpha-function and reference data from literature [129] [130].

Figure 4.1 shows clearly, that an extrapolation of the vapour pressure curve far away from the triple point does not give sufficiently accurate sublimation pressures. The own approach and the alpha-function by Stryjek and Vera are equally good, with respect to the reproduction of vapour

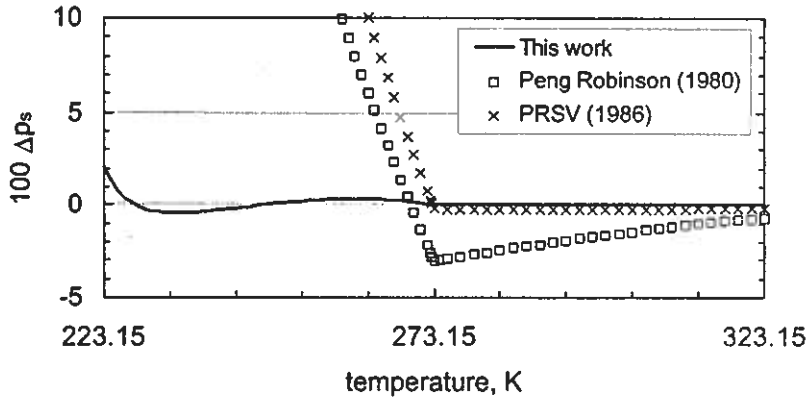


Figure 4.1: Relative deviations $\Delta p_s = (p_{s,ber}/p_{s,ref} - 1)$ between vapour pressures (above ice, or liquid water respectively), calculated with the PR-EOS using the new alpha-function and reference data from literature [129] [130]. For comparison the deviations are included, if the alpha-functions by Peng Robinson [166] or Stryjek Vera (PRSV) [191] (which are already optimized for water) are applied.

pressures. The maximum deviation of the calculated vapour pressures is smaller than 0.01% in the whole temperature range considered. Furthermore sublimation pressures calculated with the own alpha-function are reproduced within 0.45% at temperatures down to 233.15 K (-40°C). Below this temperature, at 223.15 K for example, the absolute deviation of the sublimation pressures ($p_{s,calc}$-$p_{s,ref}$) is smaller than 0.09 Pa (while $p_{s,ref}$ = 3.9 Pa). Extrapolation of sublimation pressures beyond the temperature range considered (223.15 K ≤ T < 313.15 K) will lead to increased deviations, which is indicated by the function course.

With exception of water, for all other natural gas components the original alpha-function according to equation (A.24) and (A.25) was retained.

## 4.3 Data Base for the Parameter Optimisation

To complete the database for aqueous systems, in addition to the own measurements a broad literature survey has been carried out. Starting with the literature reviews by [51] [197] and [198], emphasis was put on vapour liquid equilibrium data. The major important binary systems were:

- Water - Methane
- Water - Ethane
- Water - Propane
- Water - Butane
- Water - Carbon Dioxide
- Water - Nitrogen

Figure 4.2 gives an overview about experimental water content data for the system water-methane, available in literature. Additionally, experimental data from this work are included. For a better comprehension, the desired application range of the new calculation model is indicated. Table F.1 (in annex F.2) contains a summary of the literature evaluation, with respect to the number of experimental points, the temperature and pressure range, as well as a list of the measured quantities. Water content data, which were measured under hydrate conditions (according to the authors statements) are not included in table F.1 (see table F.3).

Figure 4.2 and table F.1 give a strong indication, that no experimental data for the binary systems are available for a major part of the pressure and temperature range, considered for the model design. Among other reasons, for ethane and higher hydrocarbons this is caused by the limitation of the vapour pressure curve. Above the vapour pressure curve of pure hydrocarbons a second liquid phase may occur.

Measured quantities from literature were evaluated with respect to the uncertainty in a second step. The results are presented in table F.2 (in annex F.2). A final assessment of the experimental data based on this information, however, has only a limited value, since in many cases only estimations were used and no uniform procedure to determine the uncertainties could be applied.



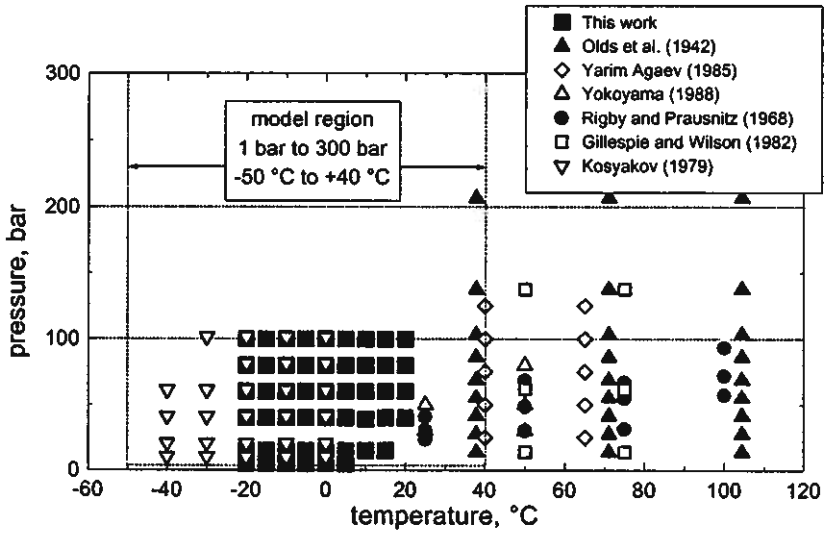


Figure 4.2: P,T-diagram with water content data of the water-methane system, available in literature and data from this work [248].

A preliminary consistency test of all available data (literature and this work) has been carried out using different kinds of graphic plots. Unfortunately it was not possible to check the experimental data with thermodynamic consistency tests (e.g. equation by Gibbs-Duhem), because required data were missing in some cases [199]. Experimental data, which showed an untypical behaviour within these tests, were excluded from the data pool (e.g. all methane-water data by Yarym-Agaev [207] ).

## 4.4 Binary Interaction Parameter ($k_{ij}$)

The reproducibility of phase equilibria of mixtures, calculated with equations of state is crucially affected by the cross-term $a_{ij}$ of the $a$-parameter, or the binary interaction parameter $k_{ij}$ , respectively. Interaction parameters usually are determined by fitting to experimental data. A generalised procedure to estimate these parameters from the specific properties of the components, however, did not succeed so far [221] [222] [223].

Because of the changed alpha-function, the binary interaction parameters for systems containing water had to be refitted. Binary systems measured within this work and those data from literature, which were classified as „accurate", have been selected for the data base (see discussion in chapter 4.3). Experimental data of multicomponent systems have not been used.

In this work dew point pressures have been used to optimise the binary interaction parameters, instead of bubble point pressures, which is more common in literature. The dew points have been used because of two reasons. First, only gas phase compositions have been measured and second,

the major objective of this work is the description of dew point curves. However, their course (over a large pressure range) is substantially more steep compared to the bubble point curve. Therefore, a small variation of the gas phase composition may lead to a large change in pressure. The effect for the calculated water content is, that water contents do not depend sensitively on dew point pressures. For the parameter optimisation a performance function $S$ has been minimised, which expresses the sum of the squares of the deviations between calculated and experimental dew point pressures.

$$S = \sum_i \left(p_{calc,i} - p_{exp,i}\right)^2 = Min. \tag{4.4}$$

During the parameter optimisation for the methane-, ethane- and carbon dioxide-water binary systems it became obvious, that temperature dependent interaction parameters are required for an optimum reproduction. The temperature dependence of the interaction parameters was approached as follows:

$$k_{ij}(T) = k_{ij,0} + k_{ij,1} \cdot \left(\frac{T}{273.15K} - 1\right) \tag{4.5}$$

At a temperature of 273.15 K (0°C) $k_{ij}$ becomes identical to $k_{ij,0}$. Data points of the methane-water and ethane-water binary systems, which were measured under hydrate conditions, were weighted slighter. Because of the metastable conditions, the kind of the condensed phase was not exactly determinable. This fitting procedure results in a temperature dependent $k_{ij}$-function, which is essentially determined by experimental data outside the hydrate region. The $k_{ij}$-function for the important binary system methane-water, is particularly supported by data of Olds et al. [202] up to high temperatures and pressures (right border of the model region).

For the examples of the binary systems methane-water and nitrogen-water, the good reproduction of experimental data with the PR-EOS is demonstrated. Figures 3.5 and 3.6 in chapter 3.2.1 show the results of the calculation program (GERGWATER) developed in this work, using the adjusted $k_{ij}$-functions. Apart from a few points (at high pressures of the -20°C-isotherm of methane-water, 40 and 60 bar data of the 0°C-isotherm of the nitrogen-water system) the calculated water contents are located within the uncertainty of the experimental data. Additionally one has to bear in mind, that the experimental data presented, are not correlated and some of the data exhibit a slight deviation from the trend. As an example the methane-water binary system (at 80 bar/ -20°C) is mentioned (see figure 3.1), where the experimental water content date is located slightly above the trend.

Only experimental data within the temperature range -40°C to +50°C have been taken for the $k_{ij}$-adjustment of the binary water containing systems. A usage of the $k_{ij}$-functions outside this range is not advisable. $K_{ij}$-values of the other binary systems (without water) have been taken from literature. A sensitivity study proved, that water content and dew point calculation of the mixtures considered show an insignificant dependence on the binary interaction parameters only. Annex F.3 contains a complete table of the compound properties used (pure and binary data), as well as the corresponding literature sources.



## 4.5 Extent of the Analysis

Natural gas is a multicomponent mixture with an undefined number of components. Depending on the analytical techniques applied, one yields a different extent of the natural gas analysis. Against this background, an extensive sensitivity study has been carried out, to fix the extent of the gas analysis required. The objective of this study was to find out the minimum necessary analysis, to calculate dew point temperatures (at a given pressure and water content) within an uncertainty of ±2 K. Two gas chromatographically (GC) determined standard analyses with a different extent were available as a potential input data base:

- a gaschromatographic natural gas standard analysis according to ISO 6974-4 [147]
- (extent: 11 components - $N_2$, $CO_2$ and hydrocarbons $C_1$ to $C_5$ and $C_{6+}$)
- an extended gaschromatographic natural gas standard analysis according to ISO 6974-3 [146] (extent: 24 components - $H_2$, helium, inert gases and hydrocarbons up to $C_8$)

In the natural gas standard analysis according to ISO 6974-4 [147] , n-hexane and the sum of all hydrocarbons equal to and higher than $C_6$ are lumped together into a pseudo component $C_{6+}$. Analyses with this extent can be carried out with a portable GC-device. So, a field analysis is possible, for example. This analysis does not contain the components helium and argon, which is valid for natural gases with a negligible content of these gases [147]. For the more complex natural gas analysis according to ISO 6974-3 [146] , more accurate and high sophisticated GC-devices are required. So, this procedure usually is carried out in stationary laboratories.

An evaluation of several natural gas analyses showed, that the concentration of higher hydrocarbons (> $C_8$) is extremely small (some ppm). Because of the objective of this work, to calculate water dew points and no hydrocarbon dew points, the ISO 6974-4 analysis has been identified as sufficient. This was proven by the sensitivity study.

The study has been carried out for the dew point calculation, as well as for the water content calculation. A detailed description of the procedure and the graphic plots of the results (concerning to the influence of single components to dew point and water content ) are included in annex F.4. The results may be summarised as follows (see table 4.2):

- If the extended natural gas analysis according to ISO 6974-3 is applied (column B in table 4.2), at low temperatures possibly, hydrocarbon dew points instead of water dew points are calculated. But these hydrocarbon dew points, could not be observed in any case in experimental dew point mirror measurements.
- Only the main components (≤ comp. No. 8, n-butane) have a distinct influence on the location of the water dew point (or water content respectively).
- The results using both analyses are nearly identical. This means, that the higher information content of the extended gas analysis has no advantages over the "small" standard analysis, with respect to water dew point or water content calculations.

Based on these results, the extent of the natural gas standard analysis according to ISO 6974-4 has been defined as sufficient for the objectives of this work. In addition, the pseudo component $C_{6+}$ is treated like n-hexane in the calculations.

## 4.6 The Calculation Program (GERGWATER)

Table 4.2: Input data base for the calculation
Col. A: Components from natural gas analysis according to ISO 6974-4 [147]
Col. B: Components from extended natural gas analysis acc. to ISO 6974-3 [146]

| No. | Component | A | B | No. | Component | A | B |
|---|---|---|---|---|---|---|---|
| 1 | Water | | | 14 | 2,3-Dimethyl butane ($C_6H_{14}$) | $C_{6+}$ | x |
| 2 | Methane | x | x | 15 | 3-Metylpentane+2-Methylpentane | $C_{6+}$ | x |
| 3 | Ethane | x | x | 16 | n-Hexane | $C_{6+}$ | x |
| 4 | Nitrogen | x | x | 17 | Cyclohexane ($C_6H_{12}$) | $C_{6+}$ | x |
| 5 | Carbon dioxide | x | x | 18 | Benzene | $C_{6+}$ | x |
| 6 | Propane | x | x | 19 | n-Heptane | $C_{6+}$ | x |
| 7 | 2-Methyl propane | x | x | 20 | Methyl cyclohexane ($C_7H_{14}$) | $C_{6+}$ | x |
| 8 | n-Butane | x | x | 21 | Toluene | $C_{6+}$ | x |
| 9 | 2,2-Dimethyl propane | x | x | 22 | n-Octane | $C_{6+}$ | x |
| 10 | 2-Methyl butane | x | x | 23 | Helium | | x |
| 11 | n-Pentane | x | x | 24 | Hydrogen | | x |
| 12 | Cyclopentane ($C_5H_{10}$) | | x | 25 | Oxygen | | x |
| 13 | 2,2-Dimethyl butane | $C_{6+}$ | x | | | | |

Within the model development, some of the core routines from the process simulation package *K-BP*[2] ("Karlsruhe-Berliner-Prozeß-Berechnungs-Paket" [228]) were used. With a suitable integration of these routines and the inclusion of own subroutines, the program was adapted to the specific requirements, which became obvious during the implementation and the following verification of the performance of many types of EOS, or their modifications, respectively.

Based of these subroutines, a new calculation program GERGWATER was developed in FORTRAN. A WINDOWS compatible program containing the GERGWATER-method is available from RUHRGAS AG, D-54138 Essen (Germany). Flow sheets of the water content and dew point calculations are included in annex F.5.



# 5 Model Validation

This chapter is dedicated to the validation of the calculation procedure GERGWATER developed in chapter 4. The binary methane - water system as well as the multicomponent systems (natural gases) NG1 to NG7 were taken as test systems. The calculated values for water content and for the dew point were compared to the experimental data. As the large number of measuring data for the natural gases were not used when developing the calculation procedure the comparison of the calculated results with the experimental data gives an indication of the predictability of the model. Table 5.1 gives a summary of the composition range covered by the natural gases under investigation.

Table 5.1: Mixture composition covered by the natural gases NG1 to NG7

| Component | Min. mole-% | Max. mole-% | Component | Min. mole-% | Max. mole-% |
|---|---|---|---|---|---|
| Helium | - | 0.152 | Propane | 0.189 | 1.763 |
| Hydrogen | - | 0.001 | 2-Methylpropane | 0.029 | 0.293 |
| Oxygen | - | 0.01 | n-Butane | 0.038 | 0.584 |
| Nitrogen | 0.840 | 10.351 | 2.2-Dimethylpropane | 0.001 | 0.006 |
| Carbon dioxide | - | 25.124 | 2-Methylbutane | 0.007 | 0.08 |
| Methane | 70.144 | 98.197 | n-Pentane | 0.004 | 0.082 |
| Ethane | 0.564 | 8.360 | $C_{6+}$ | - | 0.118 |

### 5.1 Dew Point

Figure 5.1 shows the absolute deviations between the calculated dew point and the outlet temperature of the second condenser TIR4 (actual value for the dew point) for the binary system methane-water, for the ternary methane-ethane-water (T1-97/3) and for the seven natural gases NG1 to NG7. The tables G.3-G.6 and G.9 give the listing of the respective data. The calculated value of the dew point is smaller (greater) than the actual value for the dew point when a negative (positive) difference is shown. For calculation of the dew points the respective input data were pressure, the dry mixture composition according to ISO 6974-4 [147] and the experimental water content (see chapter 3 as well as the data in annex G.2.1).

Figure 5.1 indicates that the deviations are nearly equally distributed around the zero axis[23]. The deviations between the calculated and the actual value of the dew point decreases with increasing temperature. Except of one value for natural gas NG5 at 100 bar, -10°C deviations larger than +2 K only occur at the low temperatures -10° and -20°C at the high pressures 80 and 100 bar for

[23] The mean deviation of all data points is -0.09 K.

five of the eight gases shown. Only 10 of the 327 data points are located outside the prediction range accuracy of ±2 K for the dew point. One has to take into account that all the data points deviating by more than ±2 K are within the range of extremely low water content. Here the relative uncertainty of the water contents measured with the coulometric Karl-Fischer titration is high (up to 20%, see annex D.2). The estimation of annex D.3.1 shows that only the uncertainty of the water content estimation can lead to deviations of more than 1 K at low water contents. As also the dew point calculation reacts very sensitive to the necessary input value of water content at the conditions of low water contents inevitably the high uncertainty of the experimentally determined water content also leads to high deviations in the calculated dew point. Nevertheless figure 5.1 justifies the statement that the uncertainty of the calculated dew point is significantly less than 2 K [248].

When using the calculation procedure in an area of extrapolation, that is in a region not covered by experiments, the trend shown in table G.9 should be taken into consideration. The deviations in the dew point calculation increase slightly when simultaneously lowering the temperature and increasing the pressure. From the slope of the data in this property range one can conclude that the dew point will be predicted at too high a temperature. Therefore water condensation in reality only occurs at a lower temperature. For operational point of view in pipelines the calculated value is on the „safe" side. The adjustment of a dew point in gas drying which lies far below the calculated value for the dew point (= calculated dew point minus an uncertainty of 2 K), however, in view of avoidance of a condensed phase causes unnecessary additional cost.

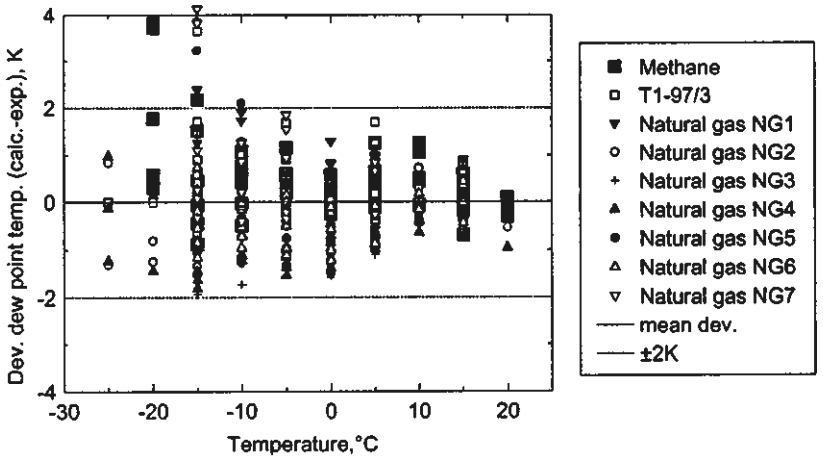


Figure 5.1: Deviation between calculated dew point (GERGWATER) and experimentally determined dew point temperature for 327 data.



## 5.2 Water Content

Figure 5.2 shows the deviations between the calculated and the measured water content. The respective data are listed in tables G.2 and G.8 in annex G.2.1. The number of components of a gas analysis according to ISO 6974-4 [147] were taken into consideration for a dry gas composition as input for the calculation of the water content (see table 4.2).

Figure 5.2 indicates that positive and negative deviations are equally distributed for water contents below 500 mg/Nm³. The comparatively low number of data at high water contents indicate that in this area one has to expect positive deviations, which means that the calculated water contents are higher than the measured ones.

The greatest deviations occur at high temperatures and low pressures (the range of high water contents, WC >500 mg/Nm³). However, the relative deviation for water contents greater than 500 mg/Nm³ for those data points which show a large deviation from the measured water content always is below 7%[24]. The relative deviation between the calculated and the measured water content increases in the direction of lower water contents to a maximum value of 34% (data point natural gas E5, 100 bar,-15 °C, ΔWC= -6.8 mg/Nm³, $Wc_{exp.}$= 20.3 mg/Nm³). When evaluating these figures again one has to take into consideration the relative high uncertainty of the experimentally determined water contents in this range. The enlarged uncertainty of the water content estimation $U_{95,tot}$ (see annex D.3.1) also shown in figure 5.2 allows a comparison of the

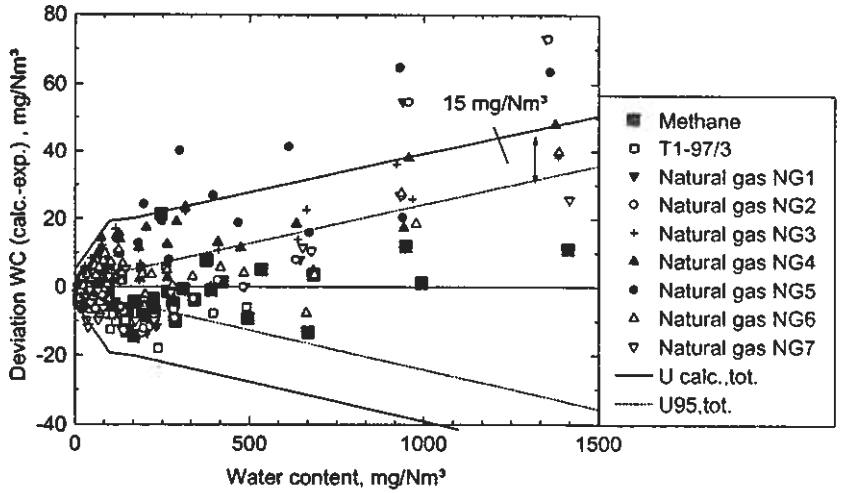


Figure 5.2: Deviation between calculated water content (GERGWATER) and experimentally determined water content ($U_{95,tot}$ = extended uncertainty of the water content determination according to annex D.2)

[24] Relative deviation = $(WC_{calc}/Wc_{exp}-1)\cdot 100$

differences between the calculated and the measured water contents with the measuring uncertainty of the experimental data. The courses of the curves show that the course of the uncertainty of the calculation procedure $U_{calc,tot}$ can be estimated from the course of enlarged uncertainty $U_{95,tot}$ plus a constant value of 15 mg/Nm³ taken from the diagram. At water contents below 100 mg/Nm³ the uncertainty of the calculation procedure decreases linearly to the uncertainty which is fixed by the measuring exactitude of the KF-coulometer applied at its lower analysing limit (=10 µg water). As for the experimentally determined water contents the relative uncertainty of the estimated water content is very high at low water contents (ppm-range, WC < 200 mg/Nm³) for the calculated water contents.

In a simplified manner the following functional expression can be given for the (predictive) uncertainty of the water content ($WC_{calc}$) calculated with the GERGWATER-method:

5 mg/Nm³ ≤ $WC_{calc}$ < 100 mg/Nm³:

$$U_{WC,calc}(WC_{calc}) = \left\{ 3.3\ mg/Nm^3 + 0.167 \cdot WC_{calc} \right\} \tag{5.1}$$

$WC_{calc.}$ ≥ 100 mg/Nm³:

$$U_{WC,calc.}(WC_{calc.}) = \left\{ 17.9\ mg/Nm^3 + 0.021 \cdot WC_{calc} \right\}$$

From this it follows:

$$WC_{calc.,tot} = WC_{calc} \pm U_{WC,calc} \tag{5.2}$$

For a calculation result below 5 mg/Nm³ the lower limit of $WC_{calc.,tot}$ is the value of the water free probe ($WC_{calc.,tot}$ = 0 mg/Nm³); the upper limit of $WC_{calc.,tot}$ in these cases can be estimated from the uncertainty from equation (5.1).

The tendency of the calculation procedure to calculate too high dew points at high pressures and low temperatures (< -10°C; range of low water contents: WC <50 mg/Nm³) as indicated in sub chapter 5.1 in return has the consequence that at the these boundary conditions too low water contents are found for this property range when calculating the water contents. When applying the calculation procedure when designing or adjusting a gas drying plant this predictive behaviour should be taken into consideration. In these cases, at high pressures and low temperatures, it is recommended to take the upper limit of the water content resulting from adding the (positive value) uncertainty to the calculated water content.

The slightly „worse" reproduction of the measured water contents by the calculation procedure ensures that the result of the dew point calculation in all cases is on the safe side (see the preceding chapter 5.1).



# 6 Comparison with Methods from Literature

In this chapter selected experimental data of this work (see chapter 3) are compared with several estimation methods for water content or dew points (calculation, diagram) from literature, as well as the own method (GERGWATER). Emphasis is put on methods, which are widely used in natural gas industries for calculation of water content and dew points.

Besides the own calculation method (GERGWATER), in particular the ASTM 1142-95 [59] correlations are considered (eq. (E.1), eq.(E.4) respectively). To distinguish between the two correlations given by ASTM 1142-95, results of equation (E.4) are called as „ASTM" and the results of equation (E.1) are marked with the authors name (Bukacek et al. [155]).

As particularyly practical methods for water content - dew point conversion, the diagram by McKetta et al. [150] in the revised version of Wichert [157] and a diagram by GASUNIE were selected. The GASUNIE-diagram [149] is a converted water content diagram (into SI-units and standard conditions) by Campbell [148], which is almost identical to that one developed by McCarthy [151]. The calculation programs CSMHYD by Sloan et al. (the 1998 version [28], in the following called CSMHYD98 and the 1990 version, called CSMHYD90 [29]) have been included into the investigations, though a dew point calculation for a given water content is not provided. But the use of this programs makes it possible, to calculate water contents in the gaseous phase above a solid hydrate phase. The physical standard condition has been choosen as reference state for all methods and the dry gas mixture as reference gas volume (values in "mg/Nm³"; see discussion in chapter 1.1.2). If necessary the results of the several methods have been converted into this reference state.

A preliminary comparison between the calculation methods CSMHYD, GERGWATER and experimental results of the methane-water binary system is already presented in figure 3.5 (chapter 3.2.1). It is shown, that calculation results by CSMHYD98 and CSMHYD90 (the preceeding version) deviates in some cases (e.g. the 0°C-isotherm)[25]. This indicates a modification of the calculation method, referring to this important binary system. The CSMHYD98-values are comparable to the experimental data by Kosyakov, in contrast to the CSMHYD90-values. The results of the CSMHYD90 method, however, are (apart from pressures higher than 80 bar) in very good agreement to the own experimental data and the GERGWATER method, respectively. For the example of the natural gas NG4 (in figure 6.2), the slightly better reproduction of the own experimental data by CSMHYD90 compared to CSMHYD98 becomes obvious. In figure 6.1 and 6.2 it is proved at the 100 bar example, that both methods exhibt only negligible differences at high pressures and low temperatures (see also figure 3.5). For the comparison only that part of the 100 bar-isobar could be used, which is located in the hydrate region. This is caused by the application range of the CSMHYD methods, wich are limited to

[25] No deviations have been found for the binary system nitrogen-water, however.

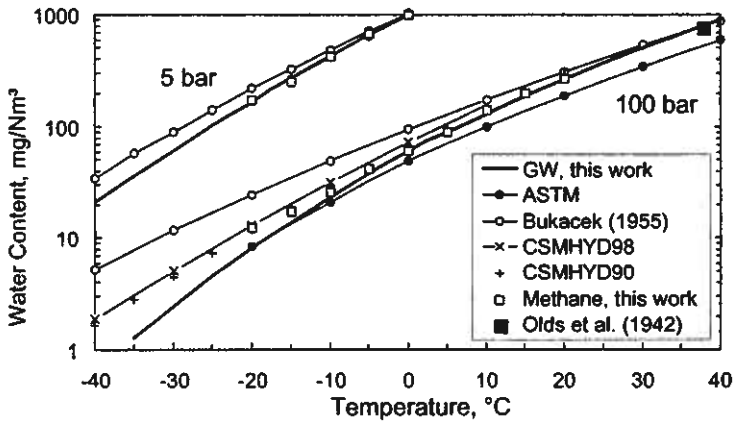


Figure 6.1: Comparison of the calculation results for water contentsof several methods (Bukacek [59],[155]; ASTM [59]; CSMHYD98 [28]; GERGWATER see chapter 4) with experimental data from this work and one experimental point by Olds (103 bar, 38°C) [202] for the methane-water binary system.

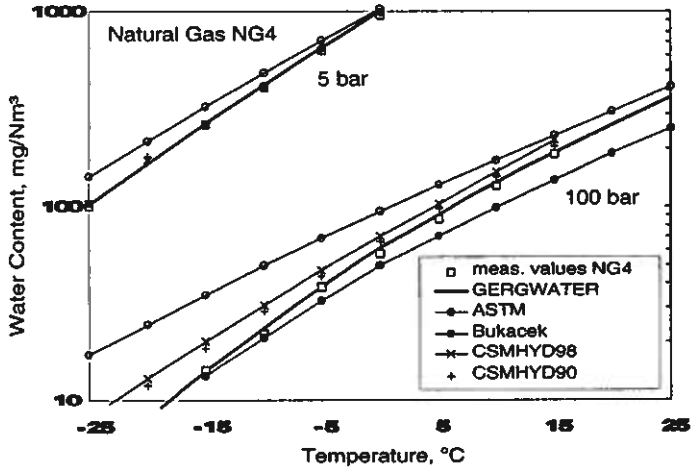


Figure 6.2: Comparison of the calculation results for water contents of several methods (Bukacek [59],[155]; ASTM [59]; CSMHYD90 [28]; GERGWATER see chapter 4) with experimental data from this work (natural gas NG4).



water contents at hydrate conditions[26]. For the 5 bar isobar of natural gas NG4, calculation results of the CSMHYD-methods were available at low temperatures only, since the hydrate region is limited to temperatures below -17°C. The methane-water binary system, however, does not exhibit hydrates at 5 bar. The good agreement to the 5 bar data and the fact, that experimental data of the 100 bar isobar are located slightly below water contents calculated with the CSMHYD-methods, give a strong indication, that measurements have been carried out under hydrate conditions, where the condensed phase was solid hydrate. The deviations between water contents, calculated with the CSMHYD-methods and experimental data for the multicomponent mixture NG4 are larger. At low temperatures (-15°C) a deviation of already 4 K is observed.

Water content calculations with the ASTM-method were only possible with an approach contrary to the standard, which prescribes a calculation procedure according to equation (E.2) and a pressure reduction to ambient pressure before the dew point measurement. This rule is derived from equation (E.2), which stems from the ideal gas law. In this work, however, dew points have been measured under high pressure conditions. So, the equilibrium pressure (PIR4) is used in equation (E.1) instead of the ambient pressure. In the same way, the equilibrium temperature (TIR4) was used for the dew point temperature, unlike the rules given in the standard.

The ASTM-method in this form, equals the simple Raoult's law, on the whole. But the specific saturated vapour volume of pure water is taken into account, instead of vapour pressures. A conversion can be done using the ideal gas law directly. As it is proved by figure 6.1 and 6.2, the reproduction of experimental data is excellent at low pressures (5 bar). The 5 bar points coincide the symbols of experimental data. That's why they are hardly recognisable in the figures. At 100 bar, the low temperature course approaches the course of the experimental data. A preliminary estimation of the water content is often done by the Raoult's law in practise (eq. (E.3)), because of its simpleness and speed. The Raoult's law exhibits a comparatively good reproduction of water contents of methane rich mixtures up to high pressures, which is proved for the temperature range from -20° up to -5°C by experimental data (see figures 3.5, 6.1 and 6.2). But a comparison to nitrogen-water data (figure 3.6) makes it clear, that high errors may occur with increasing pressure. Figures 3.5 and 3.6 prove in combination with figures 6.1 and 6.2, that the Raoult's law generally does not give reliable results in this region.

Furthermore the figures show, that particularly at high temperatures and pressures, the real gas behaviour is insufficiently described by the simple ASTM-approach, or Raoult's law, respectively. In the low pressure range ($p < 15$ bar), however, both approaches represent an acceptable method for the water content estimation.

[26] In the CSMHYD90 version input values are not checked against the application range of the model. So this method could be used to extrapolate water contents into the hydrate free region. With increasing distance to the hydrate region large errors were observed, as expected. For the methane-water system e.g. at 60 bar and +20°C the error was already >15%.

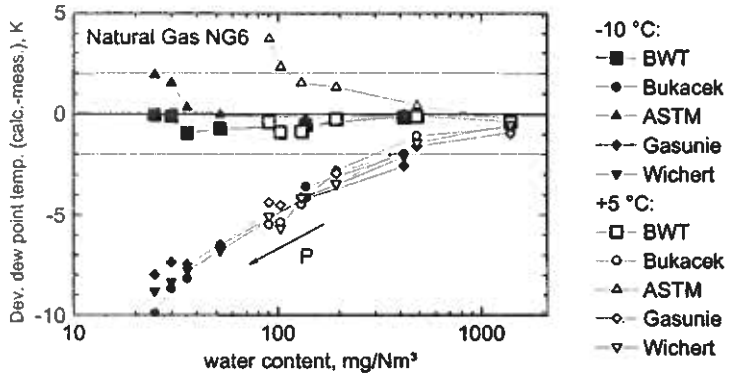


Figure 6.3: Comparison of experimental dew point values with predicted ones for severals calculation methods. Input values were water content data of natural gas NG6 at given temperatures (-10°C, +5°C) and pressures (100, 80, 60, 40, 15, 5 bar) [248]

The correlation by Bukacek gives a good reproduction of the experimental data of the methane-water system up to high pressures and temperatures. Because Bukacek used Old's data [202] for the development of his method, this was to be expected. The good connection of the own calculation method (GERGWATER) to Old's data is shown in figure 6.1 (data point 103 bar, +37.8°C). Together with figure G.2 it may be concluded, that Bukacek's values are located above the own experimental data for low temperatures ($\vartheta$ <+10°C at 100 bar, $\vartheta$ <0°C at 5 bar), independent of the hydrate region. The reproduction of water contents for natural gas NG4 is not satisfactory for high temperatures, too. These statements can be transferred to results obtained with the water content diagrams by Wichert and GASUNIE, because the diagram values are similar to those of Bukacek's method (see chapter 6.3)[27].

In figure 6.3 deviations between calculated dew points (or readings from the diagram) and measured equilibrium temperatures (outlet temperature TIR4 of condenser K2) are plotted for two isotherms (-10°C and +5°C) of natural gas NG6. The objective of this figure is to examine the prediction capabilities of the different methods. The results of all calculations methods, mentioned in the beginning of this chapter, are presented, except the method of Sloan[28]. Figure 6.3 shows clearly, that overestimated water contents (Bukacek, Wichert[29], GASUNIE) correspond to underestimated dew points. At small water contents the deviations exceed 7 K. It is proved by the almost equal deviations, that the methods by Bukacek, Wichert and GASUNIE are based on an identical data base. It is assumed, that the experimental data used in these correlations

[27] The results of Wichert and GASUNIE were not included into figure 6.1 and 6.2, because of clearness. As it is shown in figure 6.3, the results of the methods by Bukacek, Wichert and Gasunie deviate approximately 1-2 K. These differences are in between the uncertainties of the methods (see discussion in annex E).

[28] As already mentioned, a dew point calculation for a given water content is not provided by the CSMHYD-programs.

[29] Correction values: $C_S$=1; $C_G$=1



correspond to water content data in a metastable equilibrium phase[30], which is supported by the course of the deviations (see annex E).

These results confirm the statements by Jamieson and Sikkenga [57], which investigated methane-water and methane-ethane-water mixtures and found out, that all diagrams read too low dew points in comparison to the measurements. But the autors neither report the experimental data nor the diagrams investigated.

In figures 6.1 and 6.2 it becomes obvious, that the (modified) ASTM-method reproduces the experimental dew points at low temperatures and low pressures with a sufficient accuracy. But at high pressures and low temperatures the deviations become significantly higher than 2 K. The calculated dew points are always too high [248]. From figure 6.3 one may conclude, that the courses of all methods converge for high water contents[31]. In that range, all methods predict dew points within an accuracy of ±2 K.

For a given water content, too low dew points are predicted with the methods by Bukacek, Wichert and GASUNIE. From this follows, that these methods predict water contents (at a given dew point), which are higher than the experimental ones (see figure 6.4). If water contents, calculated by these methods, are used to control the drying process, a water condensation may occur already before the prescibed dew point is reached. To avoid a premature water condensation, a lower water content has to be adjusted in the drying process.

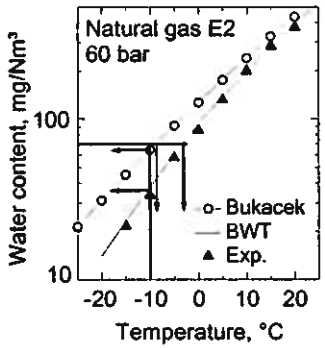


Figure 6.4: Difference between predicted water content (dew point, resp.) at given dew point (or water content, respectively).

Only the method developed in this work (GERGWATER) and the CSMHYD-methods by Sloan (which are restricted to a limited application range, however) allow the input of accurate gas compositions. Wichert's (McKetta's) method makes use of a correction value, which is coupled to the molecular weight. For the natural gases NG1 to NG7, all values were determined to unity, because of the small differences in the molecular weight. Figure 3.9 shows, that relative deviations between the water content courses of natural gases with different compositions may become large in the region of low water contents. This proves, that the gas composition has to be considered as accurate as possible, particular in this region, though only a limited number of components exhibit a significant influence (see chapter 4.5).

[30] The water content diagram by Wichert (or McKetta, respectively) contains an explicit hint, that the courses of the water content lines in the hydrate region are a matter of metastable phase equilibria, while the corresponding stable equilibrium values are lower.

[31] In this work, high water contents occur at low pressures only, because of the limited temperature range considered.

The own method (GERGWATER) has been developed, aiming at the accurate prediction of water contents and dew points of natural gases. Only data of binary systems have been employed for the development. Data of multicomponent mixtures (e.g. natural gases), however, have not been regarded. The standard gas analysis according to ISO 6974-4 [147] has been applied to create the input data base for the dry natural gas compositions (see table 4.2).

The figures show, that the GERGWATER-method is in good agreement with experimental data, for all natural gases. At high pressures (100 bar) and low temperatures ($\vartheta < -10°C$), the predicted water contents are slightly higher than experimental data for the methane-water binary system. As it is proved in chapter 5, the dew point calculation (at a given water content) for natural gases distributed in the European pipeline network, is possible within an accuracy of ±2 K, for the whole pressure range of 1 up to 100 bar and temperatures from -25° up to +20°C [248]. Additionally, figure 6.3 shows, that the GERGWATER-method is superior to all other calculation and conversion methods available, which are applied in practice.

The GERGWATER already has been successfully employed in multiple European gas companies.



# 7 Summary

Numerous operational problems in gas processing plants as well as in transportation lines can be attributed to the trace compound water. In combination with acid forming natural gas constituents water can lead to corrosion or water can mechanically damage measuring and control equipment by droplet erosion or by pressure shock. Gas hydrates which are thermodynamically stable also at temperatures well above 0°C can form in water containing hydrocarbon mixtures. Especially the formation of undesired ice or hydrate deposits in production and transportation lines can lead to major financial losses. A reduction of gas flow with the possibility of blockage of the complete pipe line cross section may be the consequence of the deposits formed. The most effective means to avoid the damages of interruptions of operation and consequent cost due to water, is the removal of water to a great extent from the natural gas. In order to safely exclude the formation of a condensed water phase during pipeline transportation operation the natural gas has to be dried sufficiently. For an optimal design and an economical operation of the gas drying plants one has to know the water content and the dew point as a function of pressure, of temperature and of gas composition as exactly as possible.

An experimental set up following the dynamic method has been constructed for investigating the dew point and the water content of gases. First in a saturator the gas flow is being saturated with water at a temperature above the respective dew point temperature. Then the gas is cooled successively in two condensers in series to the desired dew point temperature and the excessive water is being condensed. A video endoscope system allows to visually inspect the inner condenser chamber. Water contents and dew points, respectively, can be adapted in the pressure range of 1 to 100 bar and for temperatures between -25 and +20 °C. The dew point is measured with a dew point mirror. Coulometric Karl-Fischer titration is applied for measuring the water content (near ambient pressure). The experimental set up for determining the water content corresponds to the guidelines of the currently applicable international standard ISO 10101-3:1993(E).

The adjustment of a equilibrium condition for pre set conditions was proven in first experiments and via a sensitivity analysis. In addition the sensitivity analysis showed that for a set up for measuring the water content according to ISO 10101-3 the sealing liquid of the wet gas meter has to be replaced in regular intervals in order to stay within pre set error limits. This result was taken into account during the water content measurements.

A detailed analysis of uncertainties according to DIN recommendations was carried out to establish the uncertainty of the water content measurement. The major source of uncertainty in the range of low water contents (high pressures, low temperatures) turned out to be the measuring accuracy of the Karl-Fischer titrators, whereas in the range of high water contents (low pressures, high temperatures) the uncertainty of the pressure measurement dominates. At low water contents (to 100 mg/Nm³) the uncertainty in the water content amounts up to 20% of the value measured. The relative uncertainties become especially high when approaching the analysing limits of the Karl-Fischer titrators.

For water contents above100 mg/Nm³ the uncertainty is ≤ 2.5% of the value measured within the range of properties under consideration.

In this work binary mixtures of water with the main components of natural gas methane, ethane and nitrogen and with argon were measured at temperatures between -25° and +20°C and for pressures from 5 to 100 bar. In addition a ternary methane-ethane-water system (dry gas composition: 97 mole-% methane, 3 mole-% ethane) and seven multicomponent-water mixtures (natural gas-water) were investigated in the same range of properties. The natural gases in their respective composition correspond to the major natural gases distributed in the European pipeline network. The range of properties investigated covers the major parts of the pressure and temperature range relevant for the supraregional pipeline transportation. The own measurements represent a substantial enlargement of the data available in open literature. The magnitude of the new data base becomes clear when considering the number of more than 13000 water content measurements carried out here. For part of the measurements (about 25%) a fully automatic variant of the experimental set up according to ISO 10101-3 was applied. A computer controlled major parts of the manual operational duties. No difference between the data obtained in manual and in automatic operation could be noted. During evaluation the results were also checked according to the criteria given in DIN ISO 5725-6:1994-12(E).

The experimental results were compared to the few data available in open literature. Except of a few exceptions the deviations were within the uncertainty of the estimation of the water content. A comparison of the water contents measured in this work for the seven natural gases resulted in the finding that the course of the water content is mainly influenced by the major component methane. At low pressures the differences in the courses of the water content for the different natural gases are small. At high pressures and low temperatures (region of low water contents), however, a recognizable influence of the gas composition was found. There were significant differences in the courses of the water contents.

During the dew point measurements only cooling velocities of minimum 3-5 K/min at the dew point mirror could be verified. In spite of this restriction the dew point temperature in the majority of measurements could be estimated with an accuracy better than ±2 K. With three natural gases a region of retrograde condensation occurred during the dew point measurements. When evaluating the experimental data it was found that, contrary to the dew point measurements, the water content measurements were nearly not influenced by this condensation of small amounts of hydrocarbons in the high pressure part.

For the hydrocarbon mixtures under investigation a large number of the measuring points were located in a region in which a solid hydrate phase forms the thermodynamically stable condensed phase (hydrate region). Due to kinetic hindrance inside the hydrate region a metastable ice or liquid water phase can prevail instead of the stable hydrate phase. As the condensed phase is decisive for the measured water content in the gas phase more detailed investigations with respect to the condensed phase were carried out for the ternary methane-ethane-water mixture following special experimental procedures. It could be concluded from these results as well as from the pictures taken with the video endoscope system that to a high probability hydrate has been the



condensed phase determining the equilibrium inside the hydrate region. There were only very few cases in which indications of a metastable subcooled liquid water phase could be noted.

The theoretical part of this work showed clearly that a very accurate representation of the vapour and the sublimation pressure of pure water is decisive for a accurate calculation of the water content and the dew point of the mixture, respectively. The equation of Peng and Robinson was chosen as the basis for developing an optimised calculation method.

For improving the reproduction of the vapour and sublimation pressure of pure water the generalised temperature function of parameter a had to be replaced by a individual temperature function. The coefficients of this modified function were directly fitted to the vapour and sublimation pressures of pure water, respectively. For all other components except water the generalised temperature function of a as given by Peng and Robinson was kept. The simple one parameter mixing rules of van der Waals were used.

The binary interaction parameters were determined from literature data as well as from the own data for the binary systems. Emphasis was laid on a good representation of the dew point when adjusting the binary interaction parameters. From numerous test calculations it turned out that the standard analysis according to ISO 6974-4:1984 was a sufficient input base for the dry gas composition.

As only data for binary systems were used for establishing the calculation procedure the data for the multicomponent systems, especially for the seven natural gases investigated, could be used to validate the calculation procedure as these data were not used for adapting the procedure. It could be shown that the dew point temperature can be predicted by the calculation procedure developed with an accuracy of better than ±2 K in the pressure range 5 to 100 bar and temperature range -25° to +20°C. In addition by comparing the experimental data and the calculated results for the natural gases the uncertainty of the calculated water content could be estimated.

Calculation methods and conversion procedures in common use in natural gas industry were taken from literature. The comparison of the own calculation procedure with these calculation methods and conversion procedures and the own experimental data revealed that the errors in the prediction of the water content or the dew point, respectively, is substantially reduced by applying the own simple calculation procedure.

Summarising it can be stated that the new experimental data represent a substantial and important enlargement of the existing literature data base. Compared to standard methods used today in natural gas industry for prediction of the water content and the dew point the own newly developed calculation procedure results in a considerable improvement of accuracy.

The newly established calculation procedure was transformed into a computer program which is easy to handle and allows the calculation of the water content and/or the dew point temperature taking into account the composition of the natural gas. The program already proved to be useful for application in European gas companies. A WINDOWS compatible program containing the GERGWATER-method is available from Ruhrgas AG, D-54138 Essen (Germany).

# Annex A

# Thermodynamic Principles

## A.1 Phase Equilibrium Thermodynamics

The phase equilibrium calculation of multicomponent mixtures is based on the concept of chemical potentials, which was introduced by J.W. Gibbs. A thermodynamic system, which does not exchange heat or work with the ambient is completely specified by the state function $U(S,V,n_i)$, where $S$ is the entropy, $V$ the volume of the system and $n_i$ the number of moles of each component in equilibrium. The total energy $U$ becomes minimal in equilibrium. If the partial derivatives of the state function $U$ are substituted by the thermodynamic state variables temperature $T$, pressure $p$ and the chemical potential of a component $\mu_i$, one yields the fundamental property relation (A.2).

$$T \equiv \left(\frac{\partial U}{\partial S}\right)_{V,n_i}; p \equiv -\left(\frac{\partial U}{\partial V}\right)_{S,n_i}; \mu_i \equiv \left(\frac{\partial U}{\partial n_i}\right)_{S,V} \tag{A.1}$$

$$dU = TdS - pdV + \sum_i \mu_i dn_i \tag{A.2}$$

In 1923 G.N. Lewis introduced the fugacity $f$, which is equivalent to the chemical potential and has a unit of pressure.

$$d\mu_i = RT\, d(\ln f_i). \tag{A.3}$$

In real gases the fugacity may be considered as a corrected partial pressure, which is shown by the fugacity coefficient $\varphi_i$

$$\varphi_i = \frac{f_i}{\zeta_i p} \tag{A.4}$$

with $\zeta_i$, the mole fraction of a component $i$ in the phase considered. The fugacity coefficient indicates the deviation to the ideal gas law. So, for ideal gases the fugacity coefficient becomes unity.

It is followed by application of the extremal principle to a heterogeneous self-contained system with $N$ components and $P$ phases, that temperature, pressure and fugacities of all components $i$ in all phases $P$ must be identical.



$$\begin{aligned} T^\alpha &= T^\beta = \ldots = T^P \\ p^\alpha &= p^\beta = \ldots = p^P \\ f_i^\alpha &= f_i^\beta = \ldots = f_i^P \ (i = 1,..,N) \end{aligned} \tag{A.5}$$

In a two component vapour-liquid equilibrium system (index V=vapour, L=liquid) the set of equations is reduced to:

$$\begin{aligned} T^L &= T^V \\ p^L &= p^V \\ f_i^L &= f_i^V \ (i = 1, 2) \end{aligned} \tag{A.6}$$

An equilibrium condition (A.7) can be derived for each component $i$ from the equilibrium of matter (A.6) using the definition of the fugacity coefficient (A.4), where $x_i$ is the mole fraction of component $i$ in the liquid phase and $y_i$ is the mole fraction in the gaseous phase.

$$\varphi_i^L x_i = \varphi_i^V y_i \ \ (i = 1..N) \tag{A.7}$$

The relation between the fugacity coefficient of a component $i$ in any phase and the state variables of this phase usually are linked to thermal equations of state. For an equation of state, explicit in pressure, the fugacity coefficient reads:

$$\ln \varphi_i = \frac{1}{RT}\int_V^\infty \left[\left(\frac{\partial p}{\partial n_i}\right)_{T,V,n_{j\neq i}} - \frac{RT}{V}\right] dV - \ln Z \tag{A.8}$$

with compressibility factor Z: $Z = \dfrac{pV}{nRT}$. (A.9)

The compressibility factor is a measure of the deviation from the ideal gas law, for which Z equals unity.

## A.2 Equations of State

Thermal equations of state give a relation between the pressure $p$, the volume $V$ and the temperature $T$ for a pure compound.

$$f(p,V,T) = 0 \tag{A.10}$$

The most simple equation of state is the ideal gas law:

$$pV = nRT \tag{A.11}$$

The ideal gas model is based on the assumptions, that molecules do not interact with each other and their inherent volume is negligible. So, the ideal gas law is valid for low densities only, where these assumptions (nearly) are justified. Because of the neglected attractive forces between the molecules, condensed phases cannot be described with this model. To overcome these

restrictions, many equations of state have been developed, which include the ideal gas law as boundary condition. The equations may be divided into groups as follows [9] [10]:

- semi-empirical (cubic) equations,
- modified virial equations,
- pVT-calculations based on the principle of corresponding states,
- equations based on statistical thermodynamics.

In this chapter, only a selected part of these groups will be discussed, since emphasis is put on semi-empirical (cubic) equations in chapter 4, where the own calculation method (BWT) is presented. For a more detailed description of the other groups, the treatises by Dohrn [9], Walas [11] and Anderko [12] may be recommended.

The first cubic equation of state has been developed by J.D. Van der Waals in 1873 [14].

$$\left(p+\frac{a}{v^2}\right)(v-b)=RT \quad \text{or} \quad p=\frac{RT}{v-b}-\frac{a}{v^2}=p_{Repulsion}+p_{Attraction} \tag{A.12}$$

Attractive forces between the molecules are taken into account by the correction term for pressure $-a/v^2$. The quantity $b$ is called co-volume. It is a measure for the inherent volume of the molecules and characterises the repulsive forces. The Van der Waals (VDW) equation was the first one, which succeeded in a quantitative reproduction of the behaviour of fluids in the gas and liquid phase simultaneously (with one equation, only). But it turned out, that this equation shows an insufficient accuracy for many applications. So numerous cubic equations have been developed in the last century, which often retain the division into attraction and repulsion term. Though all those modifications differ in many details, they may be reduced to a general five parameter structure ([9] [12] [13]).

$$p=\frac{RT}{v-b}-\frac{\Theta\,(v-\eta)}{(v-b)\,(v^2+\delta v+\varepsilon)} \tag{A.13}$$

The variables $\Theta$, $\delta$, $\varepsilon$ and $\eta$ for some important cubic equations of state are given in table A.1 .

Table A.1: Variables for equation (A.13)

| Equation of state | Abbr. | $\Theta$ | $\delta$ | $\varepsilon$ | $\eta$ |
|---|---|---|---|---|---|
| Van der Waals (1873) [14] | VDW | $a$ | 0 | 0 | $b$ |
| Soave-Redlich-Kwong (1972) [15] | SRK | $a(T)$ | $b$ | 0 | $b$ |
| Peng-Robinson (1976) [16] | PR | $a(T)$ | $2b$ | $-b^2$ | $b$ |
| Patel-Teja (1982) [17] [18] | PT | $a(T)$ | $b+c$ | $-c\,b$ | $b$ |



For the 2-parameter equations, both parameter ($a$ and $b$) can be determined from the critical point condition. The critical isotherm of a pure fluid exhibits a saddle point in the p,V-diagram, at the critical point.

$$\left(\frac{\partial p}{\partial v}\right)_{T=Tcrit}=0 \quad ; \quad \left(\frac{\partial^2 p}{\partial v^2}\right)_{T=Tcrit}=0 \tag{A.14}$$

For equations with more than two parameter, additional boundary conditions have to be defined.

Among all the improvements of the Van der Waals (VDW) equation, the Peng-Robinson (PR) equation [16] stands out. Originally developed for gas condensate systems, it proceeded as a standard tool in many applications. Compared to VDW, the PR-equation has a modified attraction term only. The PR-equation reads:

$$p(T,v)=\frac{RT}{v-b}-\frac{a(T)}{v^2+2bv-b^2} \tag{A.15}$$

From the critical point conditions (eq. (A.14)) follows:

$$a(T_{crit})=0.45724\,\frac{R^2T_{crit}^2}{p_{crit}} \tag{A.16}$$

$$b(T_{crit})=0.0778\,\frac{RT_{crit}}{p_{crit}} \tag{A.17}$$

For temperatures different from $T_{crit}$, a temperature dependent function $\alpha(T_R)$ is introduced, to obtain a better reproduction of the vapour pressure curve.

$$a(T)=a(T_{crit})\,\alpha(T_R) \tag{A.18}$$

$$b(T)=b(T_{crit}) \tag{A.19}$$

$$T_R=\frac{T}{T_{crit}} \tag{A.20}$$

Term $\alpha(T_R)$ is a non-dimensional function of the reduced temperature $T_R$. At the critical temperature it becomes unity. The $b$-parameter of the PR-equation is temperature independent.

Peng and Robinson found the functional form of the $\alpha$-term using vapour pressures from literature. They formed a linear relation between $\alpha^{1/2}$ and $T_R^{1/2}$:

$$\alpha(T_R)^{1/2}=1+\kappa(1-T_R^{1/2}) \tag{A.21}$$

The coefficient $\kappa$ is a substance specific constant, which is generalised using the acentric factor $\omega$.

$$\kappa=0.374640+1.54226\omega-0.26992\omega^2 \tag{A.22}$$

**Mixtures**

To apply equations of state for the calculations of mixture properties, the equation parameters ($a$, $b$,...) of the pure compounds have to be substituted by mixing parameters ($a_M$, $b_M$,...). The relation between mixing parameters and pure compound parameters is established by mixing rules. This procedure is based on the "one-fluid"-theory [9]. It is assumed, that a (hypothetical) pure fluid exists, which behaves (under the given conditions p,T) similar to the mixture. The most simple mixing rules available are the symmetric rules developed by Van der Waals. For a 2-parameter equation of state it reads:

$$a_M(T) = \sum_{i=1}^{n}\sum_{j=1}^{n} x_i x_j a_{ij}(T) \tag{A.23}$$

$$b_M = \sum_{i=1}^{n} x_i b_i \tag{A.24}$$

$$a_{ij}(T) = \sqrt{a_{ii}a_{jj}}(1-k_{ij}) \tag{A.25}$$

$$k_{ij} = k_{ji} \tag{A.26}$$

$$k_{ii} = k_{jj} = 0 \tag{A.27}$$

The mole fraction $x_i$ of the several components in the mixture is used as a weight factor for the parameters. Additionally, the cross coefficients $a_{ij}$ of the a-term are corrected with a binary interaction parameter $k_{ij}$. These $k_{ij}$-values frequently are determined by fitting to vapour liquid equilibrium data of binary mixtures. Though interaction parameters obtain only small values in most cases, they have a strong influence on the reproducibility of phase equilibria, particular at high pressures. In literature many mixing rules and modifications do exist [19], which provide several problem specific advantages (e.g. [20] [21] [181]).

## A.3 Phase Behaviour

From the equilibrium conditions (A.5) and (A.6) follows, that some of the intensive state variables and compositions in the several phases can not be chosen independently for a system, which is in (a checkless) equilibrium state. For a heterogeneous system, the number of free eligible variables is determined by Gibbs's phase rule [24] [25]:

$$F = 2 - P + N \tag{A.28}$$

with: $F$ = degree of freedom N = number of compounds P = number of phases



From this phase rule (A.28) can be derived, that the most crucial quantities for the water content in the gaseous phase are pressure, temperature and gas composition. All those main quantities have an influence on the intermolecular forces and the phase equlibria. The influence of the gas composition depends strongly on the kind of the species regarded. Above all, this is valid for gas mixtures with strongly different molecular properties. An essential quantity is the molecular charge distribution [175]. The charge distribution affects the phase equilibria particular at high densities, i.e. at high pressures, or in liquids. The hydrocarbons, occurring in natural gases, are non or weak polar substances. Water however, belongs to the strong polar substances, due to its high dipole momentum. The hydrogen bondings between water molecules in the dense liquid phase enables the formation of gas hydrates (clathrates).

In the next paragraphs, examples for phase behaviour in equlibrium systems are discussed by means of p,T-phase-diagrams at constant composition. Using schematic temperature-concentration-phase-diagrams at constant pressure, the effects of temperature, pressure and the phase location on the water content is discussed.

### A.3.1 Phase Behaviour of Pure Water

Figure A.1 shows a schematic phase diagram of pure water. At the triple point *TP*, the system has no degree of freedom, since already three phases exist (solid, liquid and gaseous water). The vapour pressure curve runs from *TP* to the critical point *CP*. At the vapour pressure curve gas and liquid water coexist. The sublimation pressure curve divides the ice region from the vapour region. Water exhibits eight different ice modifications [27]. In the pressure and temperature range, considered in this work, ice exists in modification *ice I*.

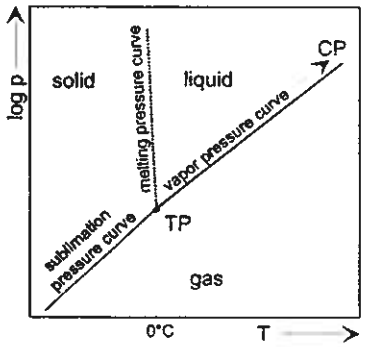


Figure A.1: Schematic phase diagram of pure water in the p,T-range of this work.

### A.3.2 Hydrates and Phase Behaviour of Hydrate Forming Mixtures

Most of the measuring points of this work are located in the hydrate region of the wet hydrocarbon mixtures investigated. To convey a basic comprehension, a short survey on gas hydrates is given first, before phase behaviour of hydrate forming mixtures is discussed in detail.

**Hydrates (Clathrates)**

Mixtures of hydrocarbons with water may form gas hydrates as a solid phase. Gas hydrates are gas inclusion compounds, similar to ice, which may exist in a solid phase at high temperatures essentially above 273.15 K, the melting point of ice. The main difference to salt, or ion hydrates

is, that gas hydrates do not perform chemical bonds. Favourably, gas hydrates are formed at low temperatures and high pressures, if molecules with low molecular weight are in equilibrium with water.

At hydrate formation, water molecules are ordered in molecule cages of different size caused by hydrogen bondings. The cavities are stabilised by the hydrocarbon molecules included (guest molecules). Each cavity is occupied by one hydrocarbon molecule at most. But cavities may remain empty. Gas hydrates belong to the class of non-stoichiometric compounds. Three different kinds of hydrate structures have been identified, so far. They are called structure I, structure II and structure H. The structures are specified by an unit cell. The unit cell of structure I and structure II is composed of cages with two different cavity sizes, respectively. Structure I consists of 2 small and 6 large cavities. Structure II however, consists of 16 small and 8 large cavities (see figure G.1). Structure H hydrates are formed by gas mixtures only. The unit cell is composed by three cages of different size. At least two guest molecules must fit, to create structure H hydrates. The question, which structure is formed and which cavities are occupied depends on the size of the guest molecules and the gas composition.

Among the natural gas compounds, structure I is formed by "small" molecules like methane, ethane, carbon dioxide and hydogen sulphide. Nitrogen, propane and isobutane, however, stabilize structure II hydrates. Hydrates containing larger molecules (e.g. n-butane, 2-methyl butane) are only formed when small hydrate forming molecules are present, too. Natural gases mainly form structure II hydrates, because sufficient amounts of hydrate formers are contained, as a rule [28]. The phase behaviour of structure I and II hydrates is nearly identical. So, it is not distinguished between both structures, in the following paragraphs[32].

Nucleation plays an important part in the formation of hydrates. Therefore a number of theoretical approaches has been developed. But an experimental confirmation is still extremely difficult, since the structure fragments (cluster) are in the order of ten to some hundred molecules only. The clusters are caused by hydrogen bondings and are invisible with the naked eye. In the beginning of the nucleation, near order structures between several water molecules and the guest molecule are formed, which are subject to a continuous growth and decay process. An accelerated hydrate forming and a macroscopic hydrate growth starts first, if a critical nucleation size is passed, due to the unification of metastable hydrate cluster [22]. Dependent on the system considered and the boundary conditions, the time until critical nucleation size is reached (called induction time), may vary between minutes and days.

A necessary condition for a continuous hydrate growth, is a sufficient availability of water, as well as hydrate forming guest molecules. That's the reason, why hydrate forming favourably happens at phase boundaries [30] (liquid water-gas, or ice-gas, etc.). An intensive contact between the

[32] One condition for the formation of structure H hydrates is the existence of a liquid or solid hydrate former phase. But only one mixture (at a few measuring points) exhibited a liquid hydrocarbon phase (see chapter 3.1), in the investigations of this work. Furthermore the p,T-phase behaviour of structure H hydrates is similar to that of structures I and II, according to the state of the art ([28], p.173). That's why structure H is not mentioned separately, in the following.



phases, caused by stirring or by turbulent flow, reduces the induction time, i.e. favours the hydrate forming. An extensive treatise of the hydrate subject can be taken from Sloan [28] [29], Makogon [30], Nixdorf [31] and Englezos [32].

## Phase Behaviour of Hydrate Forming Mixtures

As already mentioned in the preceding section, nearly all of the major compounds in natural gases are hydrate formers. The discussion of the phase behaviour of hydrate forming mixtures is carried out with emphasis on volatile hydrocarbons, since this hydrocarbon group amounts to the largest concentrations in natural gas.

The phase behaviour of hydrate forming mixtures differs essentially from the phase behaviour of pure water, or the phase behaviour of dry hydrocarbon mixtures, respectively. Already simple binary water-hydrocarbon mixtures exhibit a complex phase behaviour [29] [33]. Water-hydrocarbon systems generally are characterised by the partial solubility into each other. Compared to the good solubility of the natural gas compounds nitrogen and carbon dioxide in the aqueous phase, the solubility of hydrocarbons is negligible. The solubility of n-alkanes, for example, is in the order of some hundred ppm. At low temperatures, a solid ice or hydrate phase may be formed. At very low temperatures, which are beyond the temperature range considered in this work, a solid hydrocarbon phase may be formed additionally.

In figure A.2, some typical pressure-temperature phase diagrams for hydrate forming mixtures are presented. The vapour pressure curve of pure water courses at the lower border of each diagram (triple point pressure = 6.11 mbar) and therefore is not included into the diagrams. The following abbreviations have been used for the several phases: $V$ for the vapour phase, $L_W$ for the water rich liquid phase, $L_{HC}$ for the hydrocarbon rich liquid phase, $I$ for the solid ice phase and $H$ for the solid hydrate phase. The lines correspond to the equilibrium lines between the several coexisting phases. At the quadruple points $Q_i$, four phases are in equilibrium. At $Q_1$, for example, hydrate,

Table A.2: Hydrate structure and location of the quadruple points $Q_i$ for selected molecules (sorted by increasing size of the guest molecules) [30]

| Guest molecule | Molecule Ø (nm) | $T_{crit.}$ (K) | T (K), P(bar) at $Q_1$ | T (K), P(bar) at $Q_2$ | Hydrate structure | Occupied cavity |
|---|---|---|---|---|---|---|
| Argon | 0.38 | 150.69 | 272.4, 87.00 | no $Q_2$ | II | small + large |
| Nitrogen | 0.41 | 126.26 | 271.9,143.38 | no $Q_2$ | II | small + large |
| Methane | 0.436 | 190.55 | 272.9, 25.63 | no $Q_2$ | I | small + large |
| Carbon dioxide | 0.512 | 304.21 | 273.1, 12.56 | 283.0, 44.99 | I | small + large |
| Ethane | 0.55 | 305.33 | 273.1, 5.30 | 287.8, 33.9 | I | small + large |
| Propane | 0.628 | 369.85 | 273.1, 1.72 | 278.8, 5.56 | II | large |
| i-Butane | 0.65 | 407.85 | 273.1, 1.13 | 275.0, 1.67 | II | large |

ice, gas and liquid water ($H$-$I$-$V$-$L_W$) coexist. The phase behaviour will be discussed at the example of the change of state from point (1) to point (3) in figure A.2 .

At state point (1) the gaseous and the aqueous liquid phase coexist. Point (2) is located on the equilibrium line ($L_W$-$H$-$V$). The three phases liquid water, hydrate and gas are in equilibrium, for all points on this line. Crossing this line by a further temperature reduction towards point (3), the liquid phase vanishes, so that only gas and hydrate phases are present.

The binary systems methane-water, nitrogen-water and argon-water (figure A.2a) do not exhibit an upper quadruple point $Q_2$, because of the supercritical states of the gases. The critical temperature of methane, nitrogen and argon is far below $Q_1$ (see table A.2). This is the major difference to the hydrocarbon-water systems (figure A.2b).

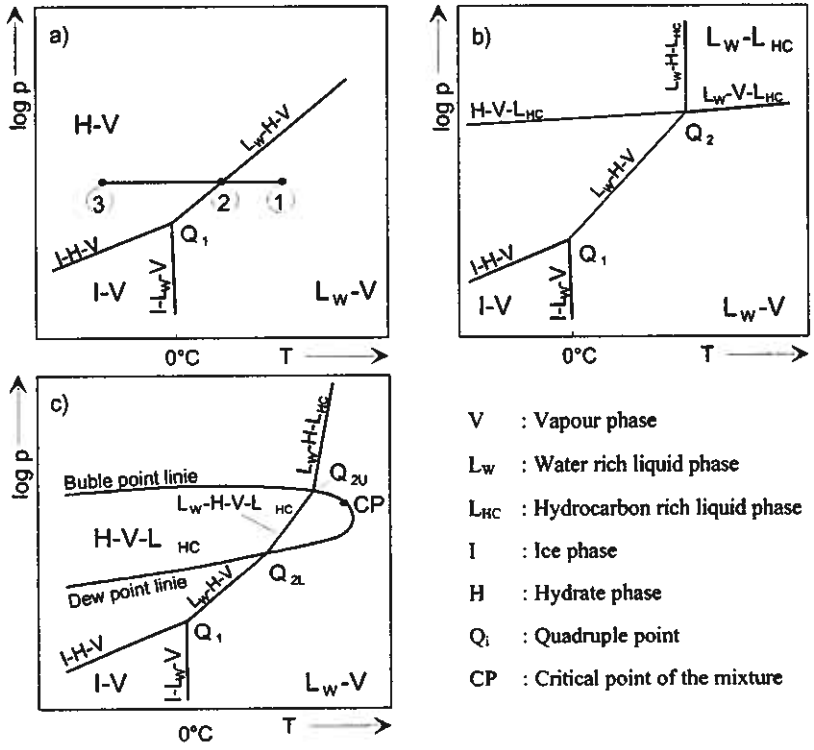


V : Vapour phase

$L_W$ : Water rich liquid phase

$L_{HC}$ : Hydrocarbon rich liquid phase

I : Ice phase

H : Hydrate phase

$Q_i$ : Quadruple point

CP : Critical point of the mixture

Figure A.2: Schematic p,T-phase diagrams including the hydrate region (according to Sloan [28])

a) Methane-water, nitrogen-water and argon-water systems

b) Hydrocarbon-water system (e.g. ethane-water)

c) Multicomponent natural gas-water system with retrograde condensation.



If the hydrocarbon rich liquid phase $L_{HC}$ is formed by a mixture of hydrocarbons, then the upper quadruple point $Q_2$ is transformed into a quadruple line $Q_{2L}$-$Q_{2U}$ (figure A.2c). A hydrocarbon rich liquid phase is present in between the area, which is spread by the dew point curve and the bubble point curve. Dependent on the location of the critical point of the mixture, a retrograde phase behaviour may be observed. Natural gases, which do not obtain a hydrocarbon rich liquid phase in this state, exhibit a phase behaviour according to figure A.2a. A phase behaviour according to figure A.2b occurs, if a hydrocarbon rich liquid phase is formed, which is observed

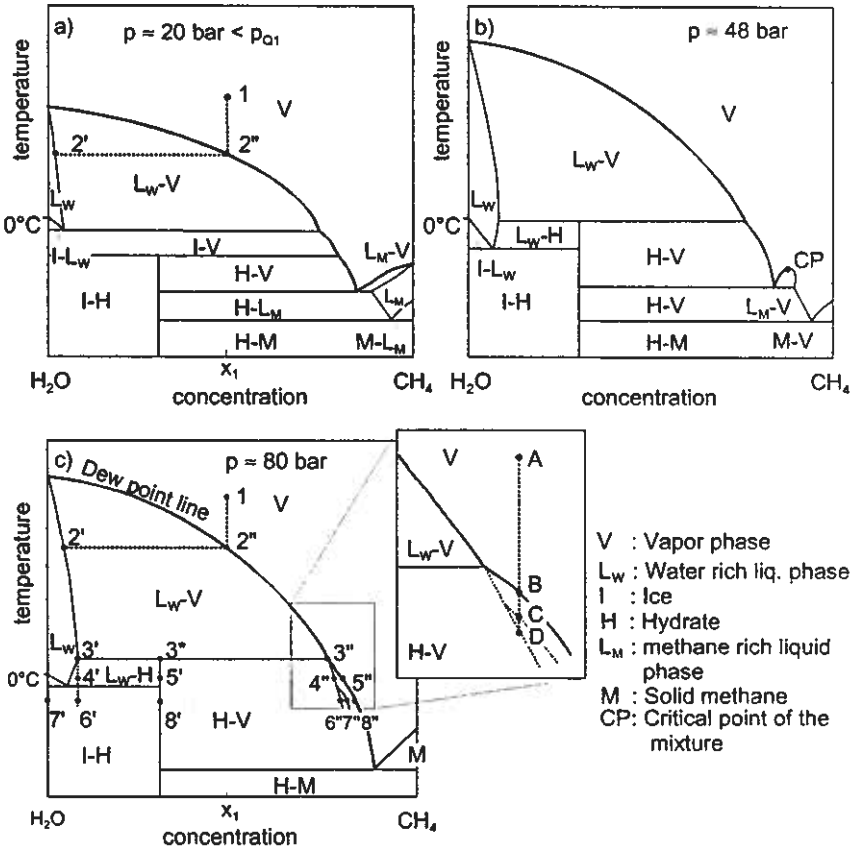


V : Vapor phase

$L_W$ : Water rich liq. phase

I : Ice

H : Hydrate

$L_M$ : methane rich liquid phase

M : Solid methane

CP: Critical point of the mixture

Figure A.3: Schematic temperature-concentration-diagrams for the methane-water binary system [35] [36]:

a) Pressure p ≈ 20 bar (below the quadruple point $Q_1$)

b) Pressure p ≈ 48 bar (just above the critical point of pure methane)

c) Pressure p ≈ 80 bar

for binary systems with volatile hydrocarbons (e.g. water-ethane, or water-propane).

Table A.2 gives an overview about the location of the quadruple points and the kind of the hydrate structures formed, for selected pure substances. It is conspicuous, that the relatively small molecules argon and nitrogen form structure II hydrates, which is contrary to the expectation from the analysis of the molecule size. The reason is, that these molecules do not stabilise the large cavities sufficiently, due to their small size. In structure II, the ratio between small to large cavities is higher, than in structure I. So a unit cell of structure II is more stabilised on an average. Methane however, forms hydrates of structure I, because of a better stabilisation of the large cavities [22].

Due to the induction time (to form the critical nucleation size) a crossing of the equilibrium line into the hydrate region is possible, without forming of a hydrate phase. This phenomenon is called metastable behaviour (see [28]-[31])[33].

Since natural gases are multicomponent mixtures, a clear presentation of the complex phenomena is not possible in a pressure-, or temperature-concentration-diagram. But figure A.3 shows for example three schematic temperature-concentration-diagrams for methane-water binary systems at different pressures, since methane is the major component of natural gas. In the matter of this work, particular the range of low water concentrations is of interest. To improve the resolution of these regions, temperature and concentration axis in the diagrams are represented not to scale. Especially the region of low water concentration is scaled up.

A methane rich liquid phase is formed at temperatures below the critical temperature (CP)[34], far beyond the range considered in this work. A solid methane phase exists below 91 K only. For a preliminary information, the triple temperature of pure water (0.01°C) is included into the diagram. Triple point lines appear horizontal in the T,x-projection. Furthermore the solubility of methane in liquid water is drawn exaggerated. Actually it is less than 0,1 mol% [28].

Figure A.3a gives an overview about the phase locations of the methane-water binary mixture at a pressure below the quadruple point $Q_1$. Four phases ($I$-$L_W$-$H$-$V$) coexist at the quadruple point. If pressure is increased in direction to the quadruple pressure ($p_{Q1}$=25.6 bar), then the $I$-$V$ area is diminished until $Q_1$ vanishes. The triple point lines $I$-$L_W$-$V$ and $I$-$H$-$V$ become identical at the quadruple point (see figure A.3b).

Figure A.3b shows the course of the equilibrium lines at a pressure just above the critical pressure of pure methane ($p_{crit.,CH4}$ = 46 bar). Finally, the phase behaviour of the methane-water system at 80 bar is presented in figure A.3c. In this figure selected states are marked, as reference for the following discussion. The superscript " stands for a gaseous state, while the superscript ' or * describes the corresponding equilibrium phase(s).

If temperature is decreased isobarically in a under-saturated methane-water mixture with a

[33] Gibbs's phase rule is applicable for stable systems only. If metastable phases occur, it is not valid any more.

[34] The critical temperature of a binary methane-water mixture with a low water concentration is almost similar to the critical temperature of pure methane [35].



composition $x_1$ (state point 1 in figure A.3a and A.3c), then a liquid phase occurs at temperature (2). The composition of the aqueous liquid phase reads state point (2'), in this example. At this temperature the vapour phase is completely saturated with water. Temperature (2) therefore corresponds to the dew point. The equilibrium line, where point (2") is located, will be called dew point line. At a further temperature decrease, the state points (2') and (2") courses along the equilibrium lines (see figure A.3c). If the triple point temperature (3) is reached, the three phases $L_W$-$H$-$V$ coexist. Phase $L_W$ has the composition (3'), the hydrate phase (3*) and the vapour phase (3"). Below the triple point line $L_W$-$H$-$V$ the hydrate phase $H$ coexists with the vapour phase $V$ (state points 5 and 8), in the case of a stable equilibrium. But under certain conditions (e.g. moderate cooling rate, missing nucleation cores, etc.) a metastable phase equilibrium may occur [29]. At a further temperature reduction, the states follow the extrapolated dew point and solubility lines first. From this follows for example, that state point 4' (and 6') corresponds to a subcooled liquid water phase, where state point 4" (and 6") represents the coexisting vapour phase. But if the metastable equilibrium is disturbed, a transformation into the stable equilibrium suddenly sets in. In this example, the metastable liquid phase (4' and 6') transforms to the stable hydrate phase (5' and 8'). At low water concentrations also a metastable ice phase (state point 7') may occur. The water content in the vapour phase depends on the kind of the coexisting phases. At a given temperature, the water content in the vapour phase is highest for a subcooled liquid (6'") and lowest above a hydrate phase (8"). Water contents above a metastable ice phase are measured in between these values. Makogon carried out investigations[35] on water contents above the three condensate phases ($L_W$, $I$, $H$) at constant conditions [30] (see table 3.5). The deviations in water content, for 100 bar and -10°C for example, were 3.9 mg/Nm³ ($L_W$-$I$) and 10.1 mg/Nm³ ($I$-$H$). The detail in figure A.3c shows the effect of the phase location on the result of a dew point measurement. Dependent on the kind of the condensed phase, which formed during the temperature reduction, several dew points are measured. If a gas is cooled down (isobarically and at a constant water content) starting at point $A$, the following dew point temperatures may be measured: point $B$ at a stable hydrate-gas phase equilibrium, point $C$ at a metastable ice-gas phase equilibrium and point $D$ above a subcooled liquid water phase.

A comparison of the diagrams in figure A.3 highlights, that the phases which are formed depend on the composition of the starting point ($x_1$) and on pressure. In the pressure and temperature range considered in this work, a aqueous liquid phase, an ice phase, or a hydrate phase may be formed as a stable condensed phase. Liquid water, a subcooled aqueous liquid phase, or an ice phase may exist in the metastable region. An intensive treatise to the subject of the complex phase behaviour of hydrate forming mixtures may be taken from [29] [33] and [34].

[35] Makogon himself does not give any citation of the data. It is not evident, if the water contents are measured values or calculated ones.

# Annex B

# Measurement of Traces of Humidity in Gases: State of the Art

This annex first gives a classification of the different ranges of gas humidity. A short listing of requirements for an optimal measurement technique is followed by a classification of methods available. The measurement techniques - dew point mirror and coulometric Karl-Fischer titration - used in this work are described in detail. Some remarks on gas sampling will conclude this annex.

## B.1 Measurement of Traces of Gas Humidity

The synonym humidity is used when water is contained in solids, liquids or gases. Depending on the application and the measuring technique in practice different quantities are applied for indicating the humidity [38], some of them are only of interest for meteorological considerations [39]. In natural gas industry the humidity content of a gas is given as dew point or water content, respectively. In drying and air conditioning it is customary to give the relative humidity, the ratio of the amount of water vapour measured to the maximum possible (at saturation). This figure is not generally used in natural gas industry.

When measuring humidity it is common to distinguish between different ranges [55]: range of traces of humidity, range of relative humidity and range of high humidity. Figure B.1 indicates this classification as a function of dew point and the corresponding water contents at ambient pressure. The range of high humidity covers a large part of drying technique. Most of the applications in air conditioning are found in the range of relative humidity. In the following we will concentrate on the range of traces of humidity.

There are many areas in technique in which the determination of traces of humidity have become important in recent years. Even though the water content in the gas phase in most applications is extremely small, gas humidity has a profound influence on optimal process configuration, on product properties and product quality. In addition to natural gas industry controlling of remainders of humidity plays a role in protective gases for welding [40] [41], in gases for semiconductor fabrication [42] [50] as well as in educt flow for metallo-organic catalysed reaction in polymer chemistry [43]. The numerous areas of application of measurement of gas humidity gives rise to the fact that the results cover a large range of values. Even when limiting the dew point interval to the range of traces of humidity the water vapour partial pressure can change over six orders of magnitude or else, covers a concentration range from some µg/Nm³ to a few 100 g/Nm³ [44].



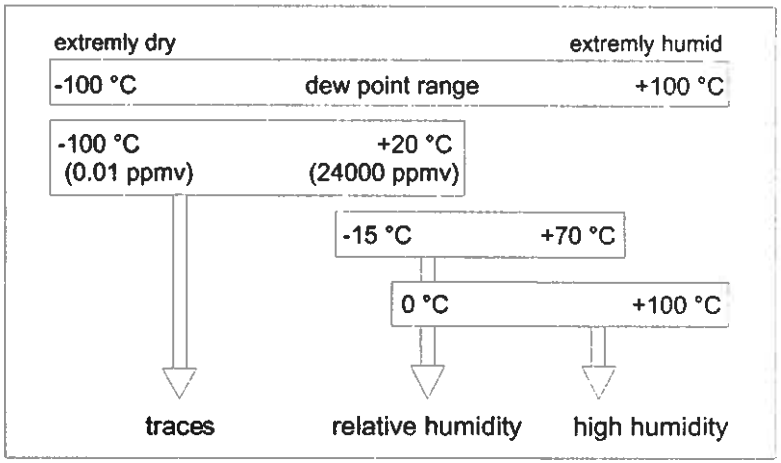


Figure B.1: Ranges of humidity at 1 bar (by Weber [55])

## B.2 Classification of Measuring Techniques

Techniques for measuring the humidity already have been applied since several centuries [46]. Over a long period the development of measuring devices for the water content closely had been connected to the progress in the area of air humidity measurements.

Several overview articles dealing with measuring techniques for traces of humidity can be found in literature [6] [39] [42] [44] [47] [57] [68] [71]. Even though their description mainly deals with the application of the measuring techniques in meteorology or measuring the air humidity the findings are basic statements also for other applications. Due to the background of this work the following exposition will concentrate on the techniques used in natural gas industry.

Several requirements have to be met by an optimum measuring technique [51] [52] [54] [72]:

- small static and dynamic measuring errors, high measuring precision, no cross sensitivity, no sensitivity on pressure and temperature variation, resistance against aggressive media, contamination and extreme changes of operation conditions (for instance liquid hammer).
- fast and sensitive reaction, possibility of continuous measuring
- long term stability, long maintenance intervals or free of maintenance, possibility of remote maintenance
- fulfilling explosion proof rules, the rules for electromagnetic compatibility
- long operation time,
- low cost (investment, operation, maintenance).

Even though a large number of measuring techniques already have been developed one has not succeeded to fulfil all the requirements with a single technique. This is not surprising as fulfilling one requirement in some cases can lead to violation of another. Therefore it is left to the user to choose the measuring technique most suitable to him.

The respective systems (measuring devices) obtain advantages and disadvantages typical to the system, which in part can be traced back to the underlying physical measuring principles. Among the physical processes used are phase transitions (dew point mirror), sorption of water vapour (with salts, $Al_2O_3$, $P_2O_5$) or the interaction with electromagnetic waves (spectroscopy) [58]. In general one can say that either the water is separated from the gas (quantitative measuring of the water content) or the special properties of water (dipole, absorption, etc.) or the consequences of the water content on a substance can be considered [46]. Table B.1 gives an overview over the principles of measurement of some selected methods.

Table B.1: Survey of selected measuring principles (following [57])

| **Measuring technique** | **Measuring principle** |
|---|---|
| Gravimetric hygrometer | Increasing mass by adsorption of water. |
| Karl-Fischer titration | Titration of absorbed water vapour by iodine. |
| Dew point mirror | Measurement of the temperature, where water droplets condense on the surface of a cooled mirror. |
| Electrolysis hygrometer | Electrolysis-current through $P_2O_5$ is proportional to the amount of absorbed water. |
| Oscillating crystal hygrometer | Frequency shift of a hygroscopic covered quartz crystal. |
| Capacitive hygrometer | Shift of the dielectric properties by sorption of water. |
| Conduction hygrometer | Shift of the electric conductivity of a glycol/ salt-solution. |

One can divide the methods of gas humidity measurement following different points of view [46] [52]. Whereas Lück [46] sorts the methods according to the different principles of effects, Heinze [52] classifies the methods according to the exchange of energy between the measuring agent and the measuring system. In addition to system characteristics Berliner [53] chooses the type of output signal, distinguishing between electric and non electric signal as a criterion. Jamieson et al [57] carried out a broad study to document the commercially available measuring devices for gas humidity. For sorting the basic principles they divide between direct and indirect measuring techniques as is done in general.

The direct methods directly measure the dew point as temperature (or the water content as mass of water). In the ideal case no calibration is necessary. Therefore these techniques also are called absolute techniques. The following measuring methods belong to the direct methods:



- the dew point mirror,
- Karl-Fischer-Titration and
- the Gravimetric Hygrometer.

With the **indirect** methods a physical property depending on the humidity is measured from which the dew point or the water content has to be calculated. The indirect methods, being relative methods, always require calibration. When calibrating the relation between the property measured (conductivity, capacity, frequency etc.) and the water content or the dew point is fixed empirically by comparing with a reference method. The indirect methods can be divided into three sub groups:

- spectroscopic,
- chromatographic and
- hygroscopic methods.

The following two sub chapters contain a detailed discussion of the measuring methods applied here - the dew point mirror and the coulometric Karl-Fischer titration.

## B.3 The Dew Point Mirror

This measuring method is standardised in DIN 51871 [5], ISO 6327 [64] and ASTM D1142-95 [59].

### B.3.1 Description of the Measuring Method

For determination of the dew point with a dew point mirror the gas flows over a metal mirror - a small high polished plate of gold, rhodium, platinum or nickel - in a pressure tight chamber. During cool down of the mirror condensate forms on the mirror at the dew point temperature. Condensate is detected by suitable means. The mirror temperature is measured with a resistance thermometer directly attached to the back side of the mirror. Small scratches on the mirror surface serve as condensation nuclei.

In general optical methods which use the change in reflection characteristics at condensate formation are applied for determining the dew point. The simplest method is to illuminate the mirror surface and to directly observe the mirror through an ocular. Cool down velocity is controlled manually. The dew point mirror temperature in general is controlled opto-electronically in automated systems [62] [63] [70] [72].

Cascaded Peltier elements are used for cooling down the mirror in automated systems. In manual systems a refrigerant which is throttled in pressure by a manually operated valve near the mirror flows on the back side of the mirror. Re-heating is accomplished by heat ingress from ambient or by electric heating. The mirror temperature is measured by means of a resistance thermometer placed directly on the back side of the mirror. The accuracy of the temperature measurement is strongly influenced by the measuring device, the accuracy class, the response time and the calibration of the temperature sensor. Figure B.2 shows a schematic of the measuring chamber of a dew point mirror.

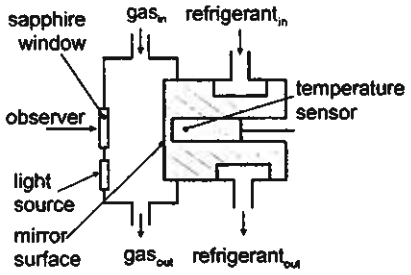


Figure B.2: Schematic design of the measuring chamber of a dew point mirror

For temperatures above 0°C the accuracy of the dew point mirror is about ±0.2 K, for temperatures below 0°C ±0.03 K, respectively. The reproducibility is better than ±0.03 K [55]. The measuring method with the dew point mirror is a recognised laboratory transfer standard [60].

## B.3.2 Possible Problems Occurring During Dew Point Measurement

Possible sources of errors or problems occurring during the measurement of the dew point are:

- the accurate temperature measurement at the mirror, the adjustment of low cooling down velocities of the mirror,
- the hindrance/disturbance of water condensation by simultaneously condensing gas compounds (especially higher hydrocarbons) or accompanying substances from gas conditioning (for instance glycols, mono-ethanol amine from drying or methanol from hydrate inhibition),
- lacking condensation sites,
- the influence of the dew point by solved gases of foreign matter (dust, rust) on the mirror surface,
- the identification of the type of condensed phase (subcooled liquid, ice or in hydrocarbon containing gases the possibility of hydrate formation),
- The exact determination of the dew point at very low water concentrations (extremely low amounts of condensate),
- temperature gradients occurring in the material of the mirror and in the gas phase can lead to the fact that the temperature measured is not exactly that of the dew point.

The condensation point can also be determined with a cooled mirror [69] [70]. Due to the different reflection characteristics the condensation point can clearly be distinguished from the dew point. In case higher hydrocarbons condense prior to water no exact dew point measurement is possible. The surface tension of hydrocarbon condensate is about 24 mN/m², the one of water ≈72 mN/m² [65]. Hydrocarbon condensate forms big, flat film like droplets because of the smaller surface tension and the smaller wetting angle. Hydrocarbon condensation therefore also is called film condensation [70]. Water condenses as light grey layer becoming "foggy" white at



temperatures below 0°C. When enough water has condensed small droplets or -depending on temperature small ice crystals - are forming. A closed ice surface is white.

In case the condensate does not only consist of pure water the measured dew point is shifted from that of pure water. Already impurities at extreme low concentrations can have a significant influence on the dew point and therefore cannot be neglected a priori. The shifting of the dew point temperature due to solved gases is called "Raoult effect" [66].

In case highly accurate measurements of the dew point are intended one also has to take into consideration the reduction of dew point temperature due to droplet formation on the mirror surface [68]. Because of the surface tension of the droplets the vapour pressure is shifted to higher values. The influence of droplet formation is called "Kelvin effect" [66].

Raoult and Kelvin effects in many cases show different signs so that they compensate each other to a certain extent [66]. Depending on additional components in the condensate the Raoult effect can cause errors in measurements of a few Kelvin and predominates the Kelvin effect. Cremonesi [112] investigated the influence of additional compounds resulting from gas conditioning on the dew point of natural gas under pipeline conditions and found out that already a few ppm of methanol in total water content rises the dew point by a few degrees. Glycol had no significant influence on the dew point, mono ethanol amine lowered the temperature. ISO 6327 [64] offers the possibility to recalculate the "true" dew point for gases which were treated with methanol for hydrate inhibition from tables showing the dependence of methanol content on the shifting of the dew point temperature.

The dew point mirror has to be cleaned in regular intervals to remove any impurities which may have accumulated. For "cleaning" the mirror surface electronic dew point mirror systems often have the option of a special temperature program in which the mirror first is sub-cooled to very low temperatures with a subsequent re-heating. The larger amounts of condensate formed during the cooling cycle shrink during evaporation to small droplets and thus concentrate the impurities to a few spots on the mirror surface [42] [55]. By this procedure the time between maintenance intervals for the mirror is increased. It does, however, not replace the manual cleaning of the mirror. Pragnell [61] describes proven techniques for cleaning of the mirror. He recommends always to use distilled ore de-ionised water in the last cleaning step. In order to safely remove traces of condensed hydrocarbons the mirror should be heated in regular intervals to temperatures well above the dew point.

At low cooling down velocities the condensate will be a subcooled liquid at temperatures below 0 °C. Only at temperatures between -5 °C and -20 °C a phase change to solid (ice) occurs. In some special cases the water can prevail as subcooled liquid to even lower temperatures. In gases containing hydrocarbons the possibility of formation of gas hydrates exists. As at a given water content sub-cooled water, ice and hydrate condense at different temperatures (see annex A.3) also the type of equilibrium phase must be known when estimating the dew point. Determining which of the possible phases has formed is very difficult and requires a lot of experience from the operating personal observing the mirror surface. Pragnell [60] in detail discusses the different images of the mirror depending on the different phases and on the time elapsed after their

occurrence. He also stresses the influence of solid and soluble impurities on the appearance of the dew and frost point. He does not, however, take into account the formation of a hydrate phase from hydrate forming gas compounds in his discussions.

Lück [46] indicates that on the surface of the mirror about 50 µg/cm² water have to be formed in order to recognise the dew point. According to Berliner [53] condensate can be detected with the help of optical methods already from about 3 µg/cm². Different lead times for accumulating a certain amount of condensate have to be taken into account as a constant amount of water is being carried with the gas stream to the mirror. During this time, however, the mirror is being cooled down continuously. The error resulting from surpassing the dew point temperature, therefore, is minimised when keeping the right balance between a short adjustment time (high cooling velocity) and a low cooling velocity (long adjustment time).

Throttling the gas to near ambient pressure prior to the dew point measurement - according to the recommendation of ASTM D1142-95 - has the advantage that the measurement in general is being carried out outside the hydrate formation region. In case crystals form on the mirror surface these will be ice crystals (frost point). Compared to the measurement under pressure a smaller amount of water per unit volume is passed over the mirror, thus making the dew point estimation more difficult due to this "dilution" effect caused by throttling.

## B.4 The Karl-Fischer Titration

The determination of water content in natural gases with the help of Karl-Fischer (KF) titration is laid down in ISO 10101. Part 3 of ISO 10101 [89] as well as DIN 51869 [90] especially deal with the coulometric KF titration. Based on the Bunsen reaction

$$2\,H_2O + I_2 + SO_2 \rightarrow H_2SO_4 + 2\,HI \qquad (B.29)$$

the petrochemist Karl Fischer in 1935 developed an analytical method for determining water by shifting the reaction equilibrium to the right in giving excess sulphur dioxide and by neutralising the resulting acid by an organic base. Out of the substances investigated pyridine ($C_5H_5N$) proved to be an optimal base to have the existing water react stochiometrically with sulphur dioxide and iodine. Therefore the first KF reactant consisted of a solution of iodine and sulphur dioxide in a water free solvent mixture of pyridine and methanol [73] [74]. The indication of the equivalence point of the reaction was visualised by change of colour when titrating the water containing probe with the dark brown KF reactant.

Until today research goes on [75] on clarifying the steps involved in the KF reaction and on determining the equivalence point. The KF-reactants as well as the apparatuses used are continuously being developed and adjusted to specific analytical problems [77]. The improved methods for following the reaction allow deeper and deeper insight into the interdependence of the reactions of the components which turn out to be complex on closer inspection [78] [79].

Different stochiometries have been formulated in the course of years for the KF-reaction which take into account the new reactions or intermediate products, respectively. The work of Scholz



[73], Wieland [74] and Fischer [80] document the progress made in this area. One of the major recognition is the fact that methanol first believed only to be a solvent also takes part in the reaction. Among others methanol reacts with sulphur dioxide to form mono-methyl-sulphite-ion which in turn act as reactive compound.

$$2\,CH_3OH + SO_2 \leftrightarrow CH_3OH_2^+ + SO_3CH_3^- \qquad (B.30)$$

Taking this into account Scholz [73] has established the following system of reaction equations (B.3) and (B.4):

$$CH_3OH + SO_2 + RN \leftrightarrow [RNH]SO_3CH_3 \qquad (B.31)$$

$$H_2O + I_2 + [RNH]SO_3CH_3 + 2\,RN \rightarrow [RNH]SO_4CH_3 + 2\,[RNH]I \qquad (B.32)$$

with RN = Base

Also other alcohols can be used instead of methanol. Sulphur dioxide reacts with the alcohol to form an ester which is being neutralised by the base. When using methanol the anion of the alkyl-sulphuric acid forms the reactive component. It is oxidised by iodine to alkyl-sulphate consuming water [83].

Pyridine, having been used over a long time develops a unpleasant odour and being questionable from industrial medical point of view has finally been replaced by other bases by Scholz [73] [81]-[85] in the early 80-ies. Imidazol has proven to be a very good replacement for pyridine, as it leads to faster and more exact titrations. By using a pyridine free buffer solution with imidazol as the base the equilibrium also is shifted completely to the right in equation (B.4). In recent investigations Cedergren [79] confirms the superiority of the base imidazol over pyridine as well as the fact that the KF-reaction is of first order with respect to water, iodine and sulphur dioxide.

The KF-titration can be divided into two basic analytic groups with respect to dosing or production of iodine, respectively:

- the volumetric titration and
- the coulometric titration.

During volumetric KF-titration the water containing probe is solved in a suitable alcoholic solvent and is titrated with a KF-solution. The volumetric titration is applied for estimation of larger amounts of water in the range of 1 to 100 mg [83].

Compared to that the coulometric KF-titration is a micro method. Here, iodine is not dosed in form of a solution but is directly produced in a iodine containing solution via anodic oxidation. Due to its high analytic accuracy it is suited for estimation of extremely low amounts of water (10 µg to 50 mg). Therefore, for measuring the water content of gases the coulometric KF-titration is the preferred choice. Two types of cells are being distinguished for the coulometric KF-titration:

- titration cells with diaphragm (two component cell, Figure B.3a) and
- titration cells without diaphragm (one component cell, Figure B.3b).

In both cases the measuring cell consists of a closed titration vessel made of glass. The connections for gas entering and leaving are done via grinding with the one piece glass cell. The gas enters directly into the KF solution via a glass frit or a capillary. By doing so a lot of small gas bubbles are generated having a large surface for mass transfer so that all the water contained in the gas is completely absorbed by the hygroscopic KF-solution. A magnetic stirrer guarantees an optimal admixing of the reacting substances in the cell. In the two component cell the large anode chamber is divided from the small cathode chamber by a diaphragm (in general a ceramic membrane). Both chambers are filled with a special KF-solution, respectively. Both, the cathode and the anode are circular latticed electrodes located directly above and below the diaphragm, respectively.

In the one component cell the contents of the anode chamber and the smaller cathode chamber are in direct contact, not separated by a diaphragm. Only one KF-solution is used in both chambers interconnected by a hole in the bottom of the cathode chamber. In order to prevent a reduction of the iodine at the cathode, both, anode and cathode are separated over a longer distance, the cathode only consisting of a fine wire. Large openings on the circumference in the lower part of the cathode chamber in addition to the open bottom area enhance the exchange of chemicals between the electrodes as well as the anode and cathode chambers. When choosing the solution composition care was taken that no substances will form at the cathode which are oxidised by iodine which could falsify the measuring result [83]. By avoiding the diaphragm the one component cell is easier to clean and can be dried faster.

In both types of cells the iodine necessary for the analysis is generated directly in the solution at the anode by oxidising iodide to iodine. The anode reaction is:

$$2\,I^- \leftrightarrow I_2 + 2\,e^- \qquad \text{(B.33)}$$

In parallel a reduction reaction of a solved ammonium salt takes place at the cathode with formation of hydrogen [86]. The corresponding anion travels into the anode chamber - in case of

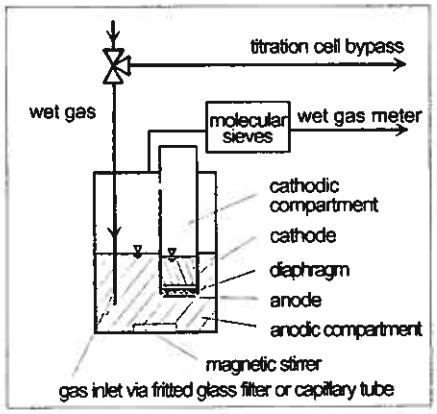


Figure B.3a: KF-cell with diaphragm

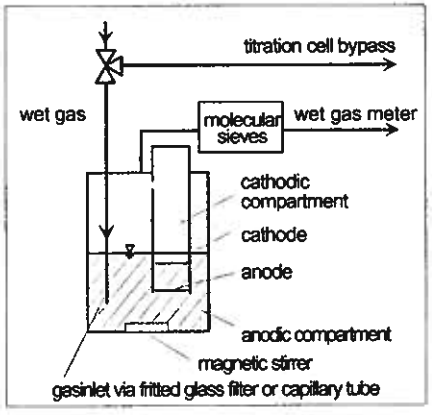


Figure B.3b: KF-cell without diaphragm



a two chamber cell through the diaphragm - and so closes the current loop.

$$2\,[RN]H^+ + 2\,e^- \leftrightarrow 2\,RN + H_2 \qquad \text{(B.34)}$$

In the reaction according to equation (B.4) a water molecule reacts with a iodine molecule. For generating a iodine molecule or for reaction of a water molecule two electrons have to be taken up by the anode according to equation (B.6). According to Faraday's law it follows:

$$\frac{m_{H2O}}{M_{H2O}} = \frac{m_{Iod}}{M_{Iod}} = \frac{1}{2}\frac{m_{Iodid}}{M_{Iodid}} = \frac{1}{2}\frac{Q}{F} \qquad \text{(B.35)}$$

$$\frac{Q}{m_{H2O}} = 10.71\frac{C}{mg\,H_2O} \qquad \text{(B.36)}$$

with $m_i$ : mass of component i; F : Faraday's-constant (96485 C/mole)

$M_i$ : molecular weight of i; Q : charge (in Coulomb)

during conversion of 1 mg $H_2O$ a charge of 10.71 Coulomb is flowing, which means that one directly can conclude from the charge required for the electrolysis on the amount of water contained in the measuring gas. The titration is ended when the equivalence point - also called end point - is reached. At the equivalence point free iodine is found in the anode solution. The determination of the equivalence point in general is done by means of a indicating electrode, either bipotentiometric (voltametric) or biamperometric [73] [75].

According to ISO 10101.3 [89] a water content between 5 mg/Nm³ to 5000 mg/Nm³ is a meaningful range of application for the coulometric method. Here, the lower limit is coupled to the analytical limit of the commercially available KF-apparatuses, which currently is at an absolute analysable amount of 10 µg water. There are, however, types of new cells under development which have a lower analytical limit of 0.1 µg [91]. When lowering the analytical limit a further reduction of the diffusive ingress of the air humidity becomes one of the deciding factors.

There are extensive representations about the wide areas of application of the KF-titration [83]. Scholz [73], and Wieland [74]. In addition to an overview over the methods these presentations include numerous different experimental set ups optimised for special applications as well as a number of recommendations and techniques (up to prescriptions for laboratories) for the practical user.

## B.5 Sampling Systems

In practice the humidity content of a gas at a defined location is of interest. In order to be able to exactly determine the water content or the dew point, respectively, the choice of a probe sampling system is of fundamental importance. In the ideal case the analysis should be performed directly in the gas system (here pipeline) under operating conditions. Due to the sorption effects of the water, as already mentioned, sampling a probe and consequent transportation of the gas probe in a closed pressure vessel to the analytical device is not suited for highly exact measurements.

Sampling systems which are connected directly - as close as possible - to the gas containing system via a bypass line are a proven method. Ample purging, the avoidance of dead volumes and possibly trace heating of the probe lines ensure a representative sampling. It is optimal to purge the bypass line continuously with measuring gas. Filters integrated into the bypass line as well as separation vessels for conditioning of the gas can prolong the time for reaching a stable equilibrium considerably. The systems have to be maintained regularly in order not to influence the measuring results. Mayeaux [111] and Cremonesi [112] both describe iso-kinetic systems for sampling from natural gas pipelines. ISO 10715 "Natural Gas: Sampling guidelines" [113] contains additional recommendations and hints for this application.



# Annex C

# Supplements to the Experimental Setup

## C.1 Data Acquisition

To allow the automatic acquisition of all relevant data, a respective program has been written which calls the data from a 6 ½ digit multimeter (DMM 6001, Prema, Mainz) via a IEEE-488.2 controller (National Instruments, Texas) in fully automatic mode. The 10 channel multimeter measures the voltage signal of the pressure transmitters and the resistance of the temperature sensors.

### C.1.1 Pressure Measurement and Control

The pressure is measured at PIR2 and PIR4 by absolute pressure transmitters (WIKA, Klingenberg, 1-100 bar, class 0.05% of end value), which include a stainless steel thin film sensor. The pressure sensors are connected via three line technique and posess a maximum outlet signal of 10 V. Even though the manufacturer guarantees an internal temperature compensation in the range of -10°C to +40°C the pressure sensors PIR2 and PIR4 are held at constant temperature above ambient by means of a PID controlled heating tape (Isopad, Heidelberg) inside an insulated cabin. Therefore any influence of room temperature is excluded from the measurement. To avoid condensation and eventual hydrate formation the lines near the pressure sensors PIR2 and PIR4 are trace heated by the same heating tape. PIR7, a relative pressure transducer (Burster, Gernsbach, 0-200 bar, class 0.1% of end value) allows to check the pressure at the dew point mirror.

All pressure transducers are installed in vertical position with the connection at the bottom and short connecting lines. The energy is delivered from highly accurate constant voltage units.

Calibration of the pressure sensors was verified in built in condition with an oil pressure balance (Desgranges&Huot, Rodgau) with the exception of the pressure sensor used for measuring the ambient pressure (WIKA, Klingenberg, 0-2.5 bar, class 0.05% of end value) which was calibrated against a mercury barometer. The calibration was checked several times a year. Observed deviations were within the measuring accuracy.

The plant pressure is adjusted and held constant by an electronic pressure control unit. The pressure control unit (Type 250C, MKS, München) consists of a PID-controller and the respective electronic control valve (Type 248A - valve V2 in figure 2.2, max. operation pressure 103 bar). In normal operation the pre pressure for the pressure control unit is adjusted in the pressure reducing unit PIC1 according to the desired pressure. Final control is done by the electronic control unit, the requested pressure is pre set in the control unit by a potentiometer.

The control unit is reset by a PC via a digital-to-analogue converter (DA 1326 ERMA-Electronic, Immendingen) for a new operating point. The 12-bit card allows a minimum pressure change of 25 mbar steps. For controlling the plant pressure via the DA card a software program was written which allows a ramp wise pressure change by pre setting the end pressure and the pressure change per time interval. By doing so the pressure can be adjusted more smoothly and slower than by hand.

The outlet signal of the pressure transmitter PIR2 is taken parallel to the multimeter as input signal for the control unit. There are two reasons not to take the signal from PIR4. First the equilibrium state is defined by TIR4 and PIR4. An eventual false measuring value of PIR4 due to the parallel off take which may weaken the shielding is not tolerable. In addition dependent on operation conditions one can suspect hydrate or ice formation between PIR2 and PIR4 as both condensers are located between them. By reducing the cross section for the flow a considerable pressure reduction can result in a pressure reduction and pretend a fall in plant pressure. When using PIR4 as control input signal, the controller would register a too low plant pressure and so open the valve. In extreme cases the full pressure after the pressure reducer could so be verified. This miss operation is excluded by choosing the adapted procedure. As a potential ice or hydrate formation near PIR2 is prevented due to the pre heating PIR2 always is upstream of a possible throttling position. Even when the pressure would be reduced after the throttling the position of the control valve would not change, the plant pressure would stay constant up to the throttling position. During trouble free operation the pressure drop between PIR2 and PIR4 was max. 0.07 bar.

### C.1.2 Temperature Measurement

Platinum resistance thermometer (Pt100, class A, supplied by Senycon, Hanau) were used for temperature measurement. The transducers were placed inside a stainless steel pipe with a 1/8" pipe connector. The electrical connection was established via a 4-line technique with shielded cabling and LEMO-gold contacts (Lemosa, München). The 20 mm long sensor is located near the connection free end of the jacket pipe. According to the measuring positions, pipes with a length of 100 to 200 mm were assembled.

Inside the saturator (TIR2) and the condensers (TIR3 and TIR4) the sensors are located replaceable inside protection tubes (se also figures C.2a and C.3).

The protection tubes are stainless steel capillary tubes (3.0x0.3 mm) closed at one end and welded to the respective vessel. The choice of this installation has the advantage that the sensors can be taken out any time for re-calibration [118]. So possible problems with tightness or damage of the sensor pipes resulting from opening and closing of high pressure threads are excluded. To achieve a good heat transfer the opening of the capillary protection tubes are located below the surface of the thermostat fluid thus ensuring that the small distance between sensor and protection pipe is filled with fluid. Inside the plant the protection pipes are located such that the measured fluid always flows around them. As the temperature inside the vessels is held constant over several



hours during the phase equilibrium measurements the somewhat retarded sensor reaction due to the encapsulation did not influence the accuracy.

In order to improve the measuring accuracy at the dew point mirror the original temperature sensor was replaced by a platinum thin film thermometer class A (Model S 105 PD 4A, Telemeter Electronic, Donauwörth). The sensor was fixed on a piece of Teflon and fixed in a protection tube, the cylindrical part of which was made of stainless steel, the top of copper, against which the sensor was pressed. The outside of the copper head was directly contacted with the back of the mirror. To improve heat transfer thermal conduction paste was applied on the areas. So the sensor is only separated from the mirror by the thin copper plate. To take up possible tension and prevent possible ingress of humidity the connecting cables were glued to the protection tube.

Calibration of the temperature sensors was verified against a Pt25-standard calibrated according to ITS-90 inside the thermostat which was used to control the temperature for condenser K2 [119]. Always the whole measuring line from sensor to data acquisition computer was calibrated as also done for the pressure transmitters. The overall error of the temperature measurement was ±20 mK. The calibration of the temperature sensors was checked at least once a year. The observed deviations were within the error limit.

### C.1.3 Volume and Volumetric Flow Measurement

The flow is controlled by a rotameter (Rota Yokogawa, Wehr). The gas flowing through the Karl-Fischer apparatus is measured in a wet gas meter (Elster, Mainz). De-ionised water was used as fluid in the wet gas meter. After filling the water was purged with the test gas for several hours in order to remove all traces of inert gases. To secure the exactitude of the measurements the filling level of the water was controlled before every measurement and the liquid renewed in regular intervals.

The rotameter had to be re-calibrated when the gas was changed. This was done against the wet type gas meter. In operation the wet type gas meter was used to measure the gas flow through the Karl-Fischer unit. The wet type gas meter had been delivered with a 9 point calibration from the manufacturer. The protocol indicates a deviation of +0.23% for a flow of 30 $dm^3/h$ at ambient conditions (about 27 $Ndm^3/h$).

## C.2 Safety Devices

As the experimental set up is operated at high pressures (up to 100 bar) with flammable and - by appropriate mixing with air even explosible - gases different safety devices were installed into and also around the set up, to prevent operational disruptions or to reduce possible effects.

A metal sinter filter (pore size 5-9 µm) was installed between the gas supply bottle and the pressure reduction unit in order to prevent ingress of solid particles. As the gas bottles used in this work were filled with natural gas directly from the pipeline it could not be precluded that dust and rust particles might have entered into the bottles. Solid particles in the plant aside from polluting the plant could also lead to possible damage of the control units; for instance a particle deposited

on the membrane of the pressure reducer can influence the correct throttling of the gas flow. As an additional safety device an over pressure valve was installed between pressure reducer and control valve. In case of malfunction of the pressure reducer the over pressure valve SV1 opens at a pressure of 125 bar and the gas is led to ambient via a separate purge line.

When being mixed with air the hydrocarbons examined in this work show a lower and upper explosion limit [120] [121]. As all parts of the plant are always operated at pressures above ambient an explosible mixture can only be formed after leakage of the gas into the surrounding. To avoid formation of an ignitable mixture (primary explosion safety) several measures were taken. To prevent igniting of a explosible mixture (secondary explosion safety) parts of the set up were carried out in explosion proof manner [123] [124] [125].

Besides a regular control of the tightness with leakage detectors the whole laboratory is de aerated by a ventilator during operation of the plant. Due to the high air flow rate of about 3500 Nm³/h the whole air of the room is changed within 2.5 min. In addition the main parts of the plant are enclosed by a cover (see flow scheme figure 2.2) which possesses a separate ventilator of about 1000 Nm³/h. The design of the housing was executed in accordance with DIN 12924 [126]. Ventilator and plant were grounded in order to prevent static electricity. For a secure operation of the de aeration unit the correct design of the ventilator system is decisive. The two extreme cases of a sudden release of the gas from the main components and of a continuous release of gas with sonic velocity at maximum plant pressure were taken into account.

In order to prevent release of the whole content of the gas bottle in case of a leakage a gas warn unit with two independent alarm levels (Auer EX-Alarm ED-90, Auer, Berlin) was installed for surveillance of the set up. The gas sensor (Type 7600) which is located in the upper part of the protective housing in the air flow continuously controls the passing air. When the pre set concentration is reached a optical pre-alarm is issued. When the concentration set for the main alarm is reached an acoustic alarm is started, magnetic valve MV2 is closed so that the plant is disconnected from gas supply. The explosion proof ventilator still sucks in the air- hydrocarbon mixture delivering it to outside ambient. The plant pressure in addition is reduced via the off gas line. Even when lower concentrations are reached the main alarm is self hold, SV2 remains closed. SV2 also closes in case of power failure (locked closed position). In both cases the valve can only be opened after the operation personnel has accepted the alarm. The gas warn unit was checked in regular intervals with a test gas mixture.

## C.3 Optical Installations (Video Endoscope System)

Already during the first measurements it became evident that in the area of the condensers interruptions of the experimental operation occurred. They could be detected through a pressure drop between PIR2 and PIR4. Due to these problems one wanted to have more information about the status of the condensers. An optical system had been integrated into the condenser flanges. One can observe a large portion of the inside of both condensers via the installed Video Endoscope System. The visible portion can be seen in figure C.3. Selected photographs are included in chapter G.1.3.



A sapphire window in each condenser allows to observe their content. The sapphire glass was designed for a maximum pressure of 400 bar. In order to avoid any reflections the glasses were annealed optically. As the condensers are located inside the cryostats completely surrounded by thermostated liquid a guiding tube was installed on the pressure less side of the windows ending above the liquid surface. Through the guiding tube a wide angle endoscope (Opticon, Karlsruhe) is led to the window. The 90 ° wide angle as well as the 30 ° angle of the head end ensure that the gas entrance opening as well as the wall opposite to it can be observed (grey shaded area in figure C.3). To avoid possible condensation of air humidity inside the guiding tubes the intermediate area is purged with nitrogen via an additional connection. Light is being provided from a 150 W cold light source (FLQ 150, Hund, Wetzlar) via glass light fibres which are integrated into the endoscope. No influence on the thermal equilibrium from the video system could be detected. The pictures from the endoscope are taken by a CCD video camera and are shown on a monitor after processing by a PC equipped with a video card. A dedicated video documentation system offers the possibility to digitalise the pictures, to archivate them with corresponding information and to process them further at a later stage. Both condensers were equipped with a corresponding endoscope and a video camera. A scheme of the complete optical installation can be seen on figure C.1.

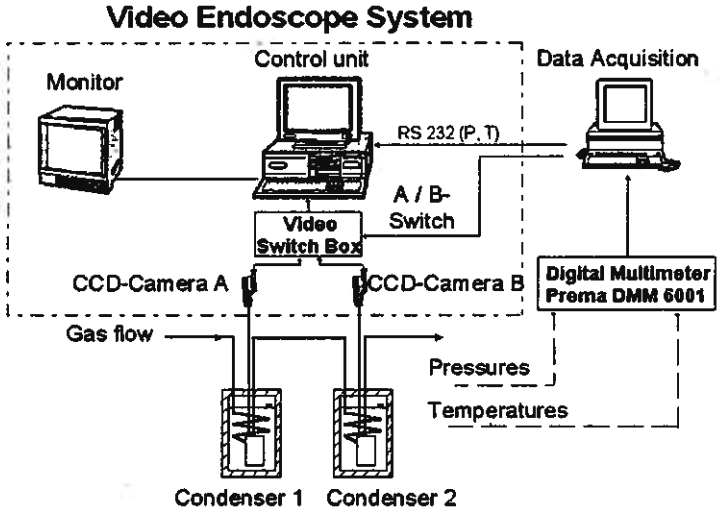


Figure C.1: Schematic set up of the optical system

In order to be able to have a computerised automatic picture storage during non supervised operation of the set up a communication routine has been implemented into the data processing as well as into the picture processing system which allows remote control of both. This software is located on a separate PC (see figure C.1). According to the programming the data acquisition program can start picture taking and processing with the video card. The necessary accompanying data for the respective picture, like date, time, measuring data recognition, operation parameter

etc. are transferred via RS-232-interface as well. The computer can switch over from condenser 1 to condenser 2 camera via a Video Switch Box.

## C.4 Particular Requirements of the Humidity Trace Analysis

When carrying out measurements with traces of humidity, additional factors (which get more important the lower the humidity values are) have to be taken into account compared to measurements of high humidity [47] [44]. In addition to the water adsorbed on the inner surface the large difference of humidity of the measuring gas inside the set up and the ambient air demands highest requirements to extreme tightness of the plant. Following nitrogen and oxygen water vapour represents the third largest amount in the composition of the atmosphere. At room temperature up to 2.5 Vol-% of the air can be made up by water [39]. The high concentration difference between measuring gas and ambient air provides a large driving force for back diffusion of water into the plant [48]. As even in "tight" high pressure plants a certain leakage rate can not be avoided this back diffusion can lead to a permanent base humidity value [50]. The number of gasket joints therefore were kept to a minimum in the relevant parts of the plant. [48] [50] [71] give approximate values of back diffusion through small openings which allow to estimate a humidity ingress into the high pressure part of the set up to be less than 0.1 ppm/h. The influence of humidity carry over into the low pressure part has been discussed together with the water content estimation with Karl-Fischer coulometry. To achieve an optimal drying of the plant via the dry gas flow, dead spaces as well dead end lines were avoided as far as possible.



## C.5 Drawings

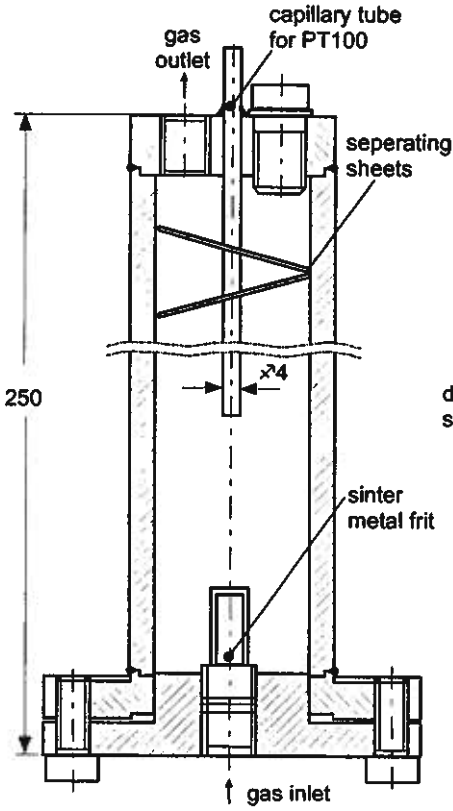


Figure C.2a: Sectional drawing of the saturation unit

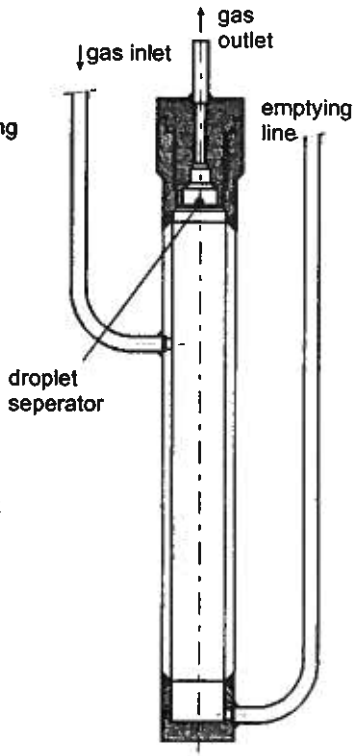


Figure C.2b: Sectional drawing of the compensation vessel

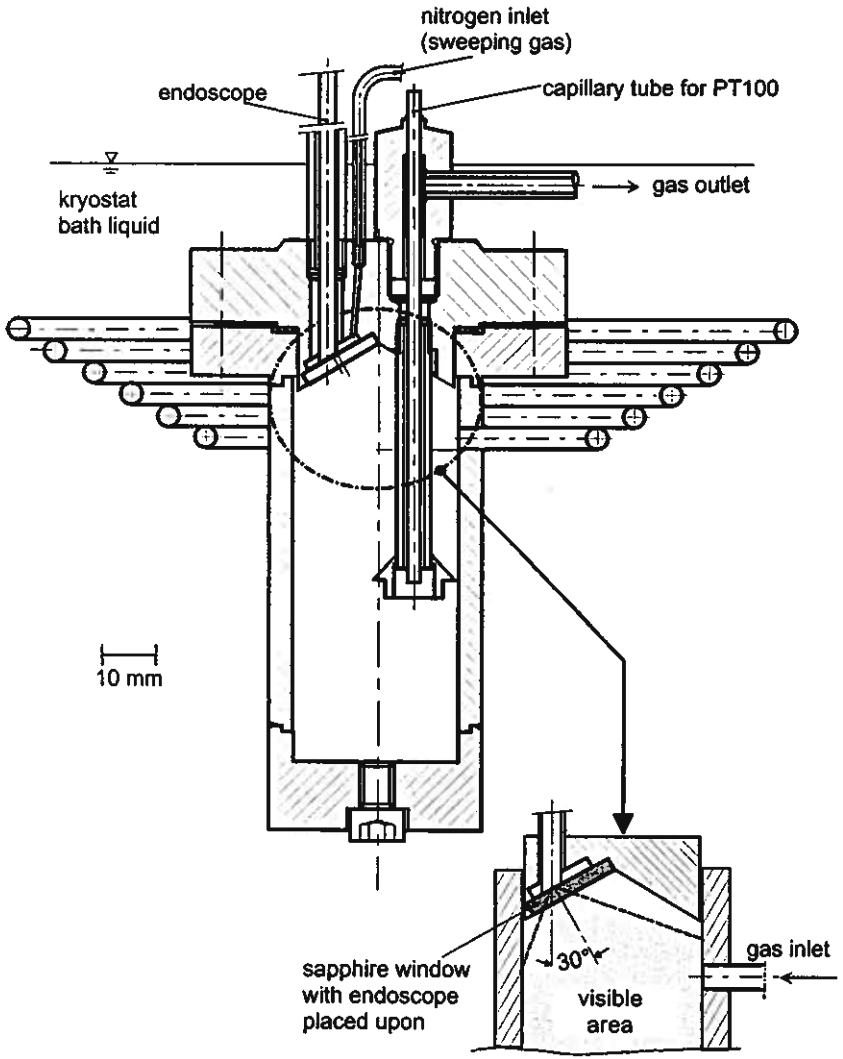


Figure C.3: Sectional drawing of the condenser and a sketch of the autoclave window for the video endoscope system.



## C.6 Variants of the Gas Flow Routing

**Variant 1: Direct measurement of dew points**

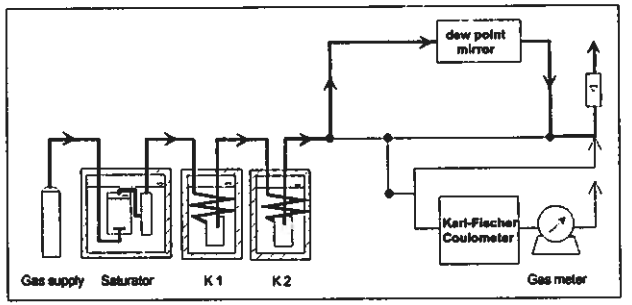


Figure C.4: Direct measurement of the dew point

In this flow routing the dew point is measured directly. Gas is conducted over the dew point mirror fist, and flows into the vent after passing the wet type gas meter.

**Variant 1: Direct measurement of water contents**

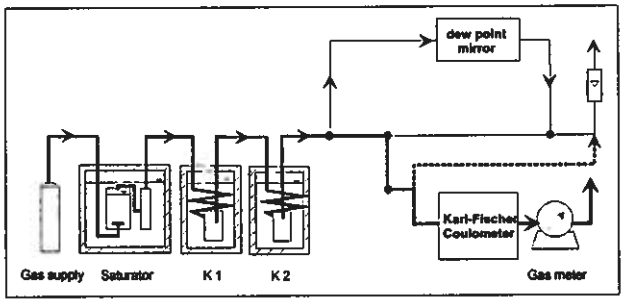


Figure C.5: Direct measurement of the water content

In this flow routing the water content is measured by the Karl-Fischer-coulometer. Between two water content measurements the gas is routed through the bypass line (dashed line). The gas flow is controlled by the Rotameter.

**Variant 3: Series connection of dew point mirror and Karl-Fischer cell**

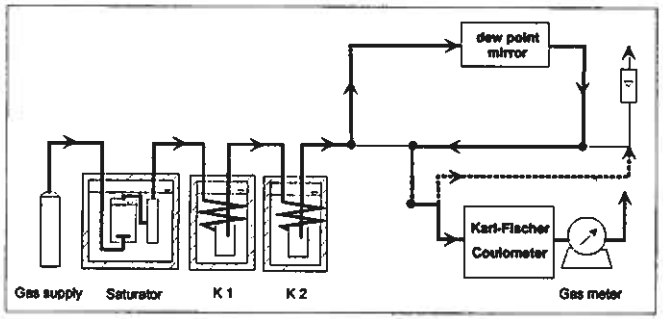


Figure C.6: Series connection of dew point mirror and KF-cell

In this variant dew point mirror and KF-cell are connected in series. Gas is routed over the dew point mirror first, followed by the KF-coulometer.



# Annex D

# Supplement to the Evaluation of Experiments

## D.1 Execution and Evaluation of Experiments

### D.1.1 Operating Points

In order to guarantee equilibrium conditions as well as reproducible and comparable experimental results also with different gases, all experiments were conducted according to a fixed time and experimental scheme and were all evaluated according to a fixed data digression scheme. The main points of these schemes to be obeyed are presented hereafter. In addition the measures taken in order to avoid and to react on interruptions of measuring operation due to ice and/or hydrate deposits are described. The text refers to figure 2.2.

#### D.1.1.1 Measuring Program

The measured values are within a pressure range of 5 to 100 bar with the temperature being varied between -25 and +20°C. A detailed list of the respective measuring points already was given in Chapter 3.

The determination of the water content at individual operating points were carried out two times independently. The second measurement was only taken after all measurements of the first run had been performed. The first run was taken at constant pressure with random temperature selection, the second run with increasing temperature. In both cases the pressures were varied from high to low pressure. Due to this procedure the water content of each operating point was measured at least twice from different pre installations.

#### D.1.1.2 Variants of Flow Routing

By selecting a certain position of 3-way valves H15 and H23 the dew point mirror and the Karl-Fischer cell can be operated in series. The different possible variants of flow are presented in appendix C.6.

#### D.1.1.3 Start up of the Set up of a New Operating Point

Prior to measuring with the gas the set up is purged thoroughly with nitrogen (quality 4.6). Then the measuring gas bottle is connected to the pressure reduction station and the whole plant is purged for several hours with measuring gas at a pressure slightly above ambient. During this purging time drying of the plant can be achieved via a by-pass along the saturator if requested. This can be controlled by the video system. Water droplets on the sapphire window of the condensers are a sign of high humidity in the plant.

During all operating conditions of the plant a flow of 30 dm³/h at ambient conditions (abt. 27 Ndm³/h) is selected. The volumetric flow is adjusted by needle valves V14 and V23 and controlled regularly with the rotameter and the wet gas meter.

Prior to setting a new operating point, the temperature set point of the saturator is fixed first. The thermostat is set to a minimum of +18°C. When choosing the operating temperature one has to keep in mind that the saturator temperature always is located below the ambient temperature in order to avoid the condensation of water in the lines prior to the condensers. In addition, the temperature in the saturator at the specified pressure always has to be chosen definitely above a possible hydrate formation temperature. The location of the hydrate equilibrium curve of the gas under consideration can be estimated with the program CSMHYD of Sloan [28] [29].

The temperatures of the thermostats for the condensers are pre set in the thermostat heads. The temperature of the first condenser is dictated by the one of the second. In case the temperature of the second condenser is at or above 0°C the temperature of the first condenser is set 5 K above that value. In case the temperature of the second condenser is below 0°C the temperature of the first is set to +2°C. By doing this a possible formation of ice in condenser K1 is avoided.

In order to avoid a possible water ingress into condenser K2 and into the downstream analytical section when going to high pressure a low temperature was pre selected (generally K1: +2°C, K2: -10°C) and the desired temperatures of the thermostats were only set after reaching the pressure set point.

When going to higher plant pressure first a suitable pressure for the control valve is adjusted in the pressure reducer. Following that the plant pressure is increased step wise by the control station. Experience has shown that a too fast pressure increase can complicate reaching a stationary condition in the plant. A pressure increase of 0.2 to 0.5 bar per minute has proven to be adequate. In case the new operation pressure is below the prior installed the new value is taken for the pressure control. Due to the constant volume flow at the exit of the plant the plant pressure is also reduced slowly when following this procedure.

### D.1.1.4 Running-in Period

As soon as the temperatures in the thermostats and the plant pressure have reached the prescribed values prior to measurement the running-in period of three hours starts. During this time the dew point mirror is purged continuously with measuring gas as it is the dew point that will be determined first. After completing the dew point measurements the gas flow is re-routed through the Karl-Fischer branch. The gas is routed directly up to the cell and by respective adjustment of 3-way valve H27 bypassed to the KF-cell into the wet gas meter. Purging time for the short (about 1 m) line from needle valve V23 to the KF-cell is at least one hour prior to the start of the water content measurements. In case no dew point measurement have been carried out prior to KF-measurements the KF-branch is purged during the whole three hour running-in period. It has been proved by sensitivity analysis that the chosen running-in times warrant reaching equilibrium conditions (see annex D.4.1). Pressure PIR4 and temperature TIR4 at the outlet of condenser K2 are regarded as the equilibrium pressure and temperature, respectively.



### D.1.1.5 Handling of Disturbances Caused by Hydrate Precipitation

When changing from a operating point with high equilibrium water content to one with considerable lower water content in some cases deviations from normal operation were observed due to the high humidity ingress. Also operation of the plant over several days at high pressures and low temperatures turned out to be problematic. The disturbances were detected by a pressure drop between PIR2 and PIR4, that is the pressure difference between condensers K1 and K2 increased. The cause for this were ice and/or hydrate deposits which reduced the free flow cross section. In extreme cases the pressure drop increased up to 0.3 bar per minute.

During operation of the phase equilibrium plant care was taken that all parts - except of the condensers - stayed outside the temperature range of possible solid phase formation. So due to the comparatively low temperatures only in a few cases in the surrounding of the condensers ice and/or hydrate formation conditions prevailed. The relatively small cross section together with the sudden re-routing of the flow in the head of condenser K1 (figure C.3) made this section a prominent place for formation of flow induced deposition. Obviously here are optimum conditions for hydrate formation. Ice formation in condenser K1 is excluded as temperature TIR3 is always kept above or equal to +2°C. In most cases the obstruction could be removed by partly taking the condenser out of the thermostat bath and heating with a blower in the area of gas outlet line. During this approximately 2-3 min. operation condenser K2 remained inside its bath. The described procedure ensured a minimum disturbance of the equilibrium point and condenser K1 fast reached the set temperature again.

Compared to the first condenser substantially less blockages of flow were registered in condenser K2. Thermodynamically this is to be expected as the amount of water possible for deposition and the water concentration in the gas is much lower, so the water available for solid formation is much less. Disturbances in K2 influence the phase equilibrium much more, however. Deposits were observed as well in the entry line as well as in the gas outlet line. No certain point at which the problems occurred (as in K1) could be observed in K2. In general, measuring had to be broken off as the pressure de-routed from the set pressure again soon after heating as the hydrate-/ice deposition was not removed completely and intervention from outside became necessary in lesser intervals. To safely remove all traces of hydrates the whole condenser unit had to be heated to a temperature well above hydrate formation temperature. According to literature [29] [30] ordering structures can survive in case the hydrate formation temperature is only surpassed slightly. This leads to an acceleration of renewed hydrate formation.

Due to the direct feedback of the measuring system on a change of operation conditions the reaction to the above described operations were not detectable after a short period, which means that the system fast comes into equilibrium conditions again (see also the response of the system on drastic changes in operating conditions in annex D.3.1). In case small deviations from the setpoint were observed prior to start of measurements and immediate countermeasures taken the running-in time was prolonged respectively. In case of disturbance and immediate successful removal during the dew point and Karl-Fischer measurements all respective measuring values were marked and the series of measurements were increased. The marked values underwent a

special critical evaluation. If during estimation of water content measurements disturbances occurred several times and the series of measurements showed an increased number of outliers all measuring data were discarded and the respective operating point was re-measured at a later stage. In case greater deviations from the set values were detected the measuring points were discarded and the series was measured again at a later stage.

#### D.1.1.6 Documentation of Measurements

All measuring values taken by the digital multimeter were displayed on the screen of the data acquisition computer and were continuously updated. During the running-in time and during measuring operation all data were logged in files. To complete documentation a lab book was kept.

### D.1.2 Dew Point Mirror Measurements

A manually regulated dew point mirror (Type 1300, Marquis, Witten) was used for determining the dew point. Observation of the surface of the mirror is achieved via an enlarging ocular. The cooling down is controlled by adjusting a refrigerant flow via a hand valve. The refrigerant flows on the back side of the mirror. The re-heating of the mirror is effected solely by heat ingress from the ambient. A schematic of the dew point mirror is shown in figure B.2 in annex B.3.1.

For operation the dew point mirror has been modified slightly compared to the original design. The original mounted temperature sensor was replaced by a platinum thin film sensor (see annex C.1.2) which was connected to the data acquisition system. By doing so it is possible to document the temperature changes during the dew point measurements. In addition the computer calculates the cooling velocity from the temperature values and displays it on the monitor.

For cooling of the mirror the manufacturer recommends $CO_2$ from a pressure bottle. Here cooling was verified by a fluorocarbon vapour compression cycle. This reconstruction allowed to keep the requirement of refrigerant to a minimum in spite of the numerous measurements carried out. First R12 ($CCl_2F_2$) was used as refrigerant, at the start of 1995 the cycle was retrofitted with R134a ($C_2H_2F_4$).

A special optic was constructed to accommodate one of the CCD video cameras which was used on one of the condensers. So the surface of the mirror could be observed via the video camera on the monitor of the video system. By doing so the observations on the mirror surface could be documented and also several persons could observe the dew point estimation on the monitor at a time.

The dew point measurements were carried out according to the recommendations of DIN 51871 [5]. At the start of the dew point measurements the dew point mirror (under operating pressure) is subcooled to about 5 K below the expected dew point temperature in order to activate as many condensation nuclei as possible.

The measurement of a dew point consists of a cooling and an re-heating phase. By adjusting different refrigerant flows via a throttle valve directly connected to the mirror the mirror temperature as well as the cooling down and re-heating velocity can be controlled. Starting at a



temperature about 5 K above the expected dew point temperature the mirror is cooled continuously until dew is observed on the mirror surface. The corresponding temperature is marked. Then the refrigerant flow is reduced followed by a slow warming up of the mirror due to heat ingress from ambient. The temperature at which the dew vanishes is also marked. Marking is done via the keyboard of the data acquisition computer.

For documentation purposes the marked temperatures as well as the respective cooling and re-heating velocities are stored by the computer. The dew point is found from the arithmetic mean value of both marked temperatures. In total ten measuring cycles are carried out in order to arrive at a sound statistical mean value for the dew point temperature.

It became evident during the dew point measurements that the cooling down velocities of 1 K/min and a step wise cooling or re-heating of 0.1 K/min near the dew point temperature according to DIN 51871 except of a few cases could not be realised. The measurements therefore were carried out with a cooling velocity of 3 to 5 K/min.

### D.1.3 Water Content Measurements

The water content measurements were carried out taking into consideration ISO 10101-3 [89] and DIN 51869 [90].

#### D.1.3.1 The Karl-Fischer Apparatus

Three different Karl-Fischer (KF-) apparatuses were available for the estimation of the water content, all of which worked according to the coulometric principle:

- Mitsubishi Moisture Meter CA-02 with a two component cell
- Mitsubishi Moisture Meter CA-06 with a two component cell and
- Metrohm 684 KF-Coulometer with a one component cell[36].

Mitsubishi Coulometer CA-06 is a follow up model of CA-02. Compared to CA-02, CA-06 includes a more developed electronic control and operation unit, the execution of the KF-cell remained unchanged, that is, both coulometers work with identical cells. Table D.1 gives a listing of the suggested measuring range and the accuracy given by the manufacturer.

[36] In the Metrohm Coulometer KF-684 the gas is led into the cell via a capillary. This capillary was replaced by a glass pipe with a frit as literature indicated that gas inlet via a capillary is only recommended for gas flow rate up to 15 dm³/h [83]; here a volume flow of 30 dm³/h was fixed.

Table D.1: Measuring range and accuracy of the Karl-Fischer Coulometer used

| Type | Measuring range | Measuring accuracy |
|---|---|---|
| Mitsubishi CA-02 | 10 µg - 30 mg $H_2O$ | ±5 µg for m($H_2O$) ≤ 1 mg<br>≤0.5 % of meas. Value for m($H_2O$) >1 mg |
| Mitsubishi CA-06 | 10 µg -100 mg $H_2O$ | ±3 µg for m($H_2O$) ≤ 1 mg<br>≤0.3 % of meas. value for m($H_2O$) >1 mg |
| Metrohm KF-684 | 10 µg - 10 mg $H_2O$ | ±5 µg for m($H_2O$) ≤ 1 mg<br>≤0.5 % of Meas. value for m($H_2O$) >1 mg |

A detailed description of the construction of the two and the one component cell is given in annex B.4 together with a description of the analytic principle of the KF-titration. The KF-cell was incorporated into the plant according to figure 3.4. This flow diagram corresponds fully with the prescriptions of ISO 10101-3 [89].

The connection from the stainless steel line to and from the glass connections of the cell were realised with short Viton hoses. To facilitate the operation of the water content measurements with KF-titration part of the measurements were taken via a automatic data acquisition scheme. No difference in the results obtained manually and in automatic mode could be noted.

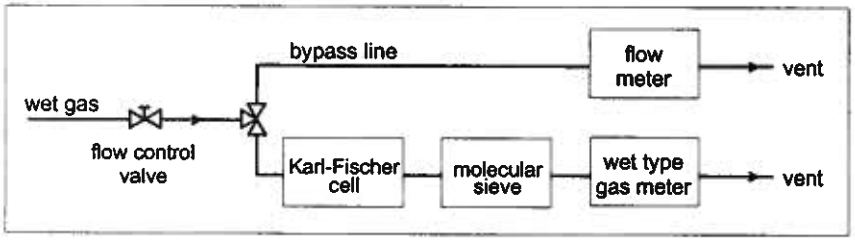


Figure D.1: Schematic design of the Karl-Fischer-titration set up for the humidity measurement of wet gases.

### D.1.3.2 Chemicals

Exclusively products of HYDRANAL® from Riedel-de Haen, Seelze were used. For all the three titrators HYDRANAL-Coulomat AG was used as anode solution. For the two component cells HYDRANAL-Coulomat CG was used as cathode solution. For checking the conditioning of the KF-cell reference solution HYDRANAL-Water Standard 0.1 and 1.0 was used (called standard liquid hereafter).

### D.1.3.3 Operational Check of the Apparatus

Prior to the estimation of the water content the KF-cell is checked with the standard liquid, the water content of which is known exactly. A small quantity of standard liquid is injected into the KF-cell through a septum via a 2 ml one way syringe made of plastic. It is advisable that the syringe including the injection needle is purged two or three times with the standard liquid prior to



injecting to remove all possible traces of humidity from the inner walls. The injected quantity of water is measured by weighing the syringe immediately before and after injection with a high precision balance (Mettler AT, resolution 0.01 mg). This value is compared with the reading of the coulometer. The difference between both values should not exceed 1-2 µg, else the KF-cell will have to be reconditioned. During conditioning of the cell the chemicals are changed, the glass connection checked and the molecular sieves are changed. Due to the high sensitivity of the measuring principle the cell has to be extremely tight against humidity from ambient by greasing the ground-in connectors. Used chemicals as well as non-tight cells are recognised by a high drift of the KF-apparatus. More detailed information for preparation and servicing of the KF-cell can be found in [73] [74] [83] (see also annex B.4).

Experience has shown that with a start drift of more than 4 µg/min water content measurements can show a reduced reproducibility. In general a start drift of more than 6 µg/min led to measurements with slopes no more tolerable. The data taken after each other showed a strong oscillation about a mean value with changing in- and decreasing slope with non uniform trend.

### D.1.3.4 Performing the Water Content Measurements

Only when the KF-cell is conditioned sufficiently measurements of the water content can commence. The KF- apparatus is started and the humid gas is led through the KF-cell to determine the water content. The volume of the gas led through is controlled by the indication of the wet gas meter. The volume taken is approximately 2 l. Depending on the amount of water led through the coulometer needs additional time until ending the titration. In the measuring protocol the exact probe volume, the temperature of the gas, the over pressure to ambient of the gas led through the wet gas meter as well as the pressure PIR4 and temperature TIR4 in condenser K2 are noted. In addition the analysed absolute water content, the duration of the titration and the (background) drift prior to and after the titration are taken.

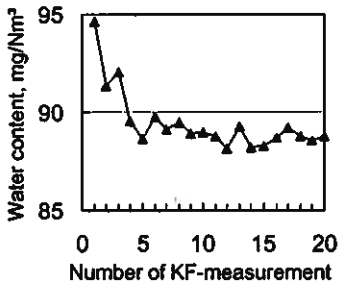


Figure D.2: Typical course of a KF-measuring series [248]

A minimum of 20 KF-measurements are taken directly one after the other per operating point. Figure D.2 gives a typical slope of such a KF-measuring series. At the start a clear running-in effect occurs which ceases after about 4 to 7 measurements. This effect is mainly to be attributed to the adsorption equilibrium, occurring during the first measurements due to the non purged parts of the lines to the KF-cell, the connecting line to three way valve H27 to and including the glass frit as well as the saturation of the KF-solution with the measuring gas. In order to eliminate this running-in effect the first ten measurements were not taken into account for the evaluation.

### D.1.3.5 Calculation of Water Content

The calculation of the water content WG in milligram per normal cubic meter of dry gas is done according to eq. (D.1):

$$WC = \frac{m_{W,KF} \cdot (273.15 + \vartheta_{NGZ}) \cdot 1013.25}{V_{NGZ} \cdot p_{Gas,dry} \cdot 273.15} \left[\frac{mg}{Nm^3}\right] \tag{D.1}$$

with the values for one individual measurement:

WC : Water content at standard conditions in [mg/Nm³]
$m_{W,KF}$ : Analysed mass of water by KF-coulometer in probe volume in [µg]
$\vartheta_{NGZ}$ : Temperature of the gas in the wet gas meter in [°C]
$V_{NGZ}$ : Gas volume passed through the KF-cell in [dm³]
after correction with the calibration factor of the wet gas meter
$p_{Gas,dry}$ : Absolute pressure of the dry gas in the wet gas meter in [hPa], see eq. (D.2)

The pressure $p_{Gas,dry}$ is made up of the parts shown in equation (D.2):

$$p_{dryGas,I} = p_{GasNGZ} - p_{SFK}(\vartheta_{NGZ}) = p_{amb} + p_{\ddot{u},NGZ} - p_{oW}(\vartheta_{NGZ}) \tag{D.2}$$

with:

$p_{GasNGZ}$: pressure of the humid gas in wet gas meter in [hPa]
$p_{SFK}$ : vapour pressure of the sealing liquid (SFK) at wet gas meter temperature $\vartheta_{NGZ}$ in [hPa]
$p_{amb}$ : ambient pressure in [hPa]
$p_{\ddot{u},NGZ}$ : over pressure of wet gas meter volume compared to ambient in [hPa]
$p_{oW}$ : vapour pressure of pure water according to eq. (D.14) in annex D.5

## D.2 Statistical Evaluation of Water Content Measurements

### D.2.1 Check of the Results with Respect to Outliers

As already mentioned 20 KF-measurements were carried out in series per operating point. As a standard the first ten measurements were left out, the remaining ten measurements were checked in a statistical test (test according to Nalimov [136] [138])for outliers immediately after taking them. In case that the test indicates an outliers the respective measuring value is redone and replaced by an immediate re-measurement. In annex D.6 the applied outlier test, the detailed procedure of the data checking as well as the evaluation criteria are indicated.



### D.2.2 Estimating the Mean Value of the KF-Measurement

The water content is calculated as the (outlier free) mean value of the last ten experimental values together with the standard deviation $s_{SM}$ :

$$WC_{SM} = \frac{\sum_{i=1}^{10} WC_i}{10} \tag{D.3}$$

$$s_{SM} = \frac{\sum_{i=1}^{10} (WC_i - WC_{SM})^2}{10 \cdot (10-1)} \tag{D.4}$$

with:

$WC_i$ : result of the $i^{th}$ individual measurement
$WC_{SM}$ : water content of the KF-measurements in a series
(= mean value of the last 10 individual measurements excluding outliers)
$s_{SM}$ : standard deviation of $WC_{SM}$

### D.2.3 Checking the Results by Means of Repeatability and Reproducibility Limits

The experimental design chosen, results in at least two independent KF-measurements were available for each operating point, in addition all measurements could be checked for consistency according to the criteria of repeatability "r" and reproducibility "R" with reference to DIN ISO 5725-6 [135]. During this checking the differential value of the arrived mean values is compared to a critical differential value which is calculated with the help of repeatability limit in case of repeatability conditions or with the reproducibility limit in case of comparative conditions, respectively.

Prior to fixing the values of the repeatability and reproducibility limits for the evaluation a round robin test was carried out between different labs, which arrived at the respective values evaluated according to ISO 5725 [132] [133]. Figure D.3 gives an overview of the slope of both evaluation criteria including the respective indications of ISO 10101-3 [89] and DIN 51869[90]. It is obvious that the functional correlation for the repeatability and reproducibility limit used here obviously is more stringent than the respective values from ISO 10101-3[37]. The values of "r" and "R" for the water contents in this work are below those of DIN 51869 for values less than 60 mg/Nm³; for values above 60 mg/Nm³ slightly higher values result compared to DIN. The horizontal slope of the "r" and "R" curve of this work, among others, takes into consideration the incertitude of the analysis at extremely low water content when applying the KF-coulometer.

[37] When comparing the graphs for the repetitive and comparative limits in DIN 51869 and in ISO 10101-3 it is obvious that for a fixed value of the repetitive and comparative limit the respective water mass concentration in ISO 10101-3 is greater by the factor of 10 compared to DIN 51869. It is most probable that a transmission error has occurred when transferring the data from DIN to ISO standard.

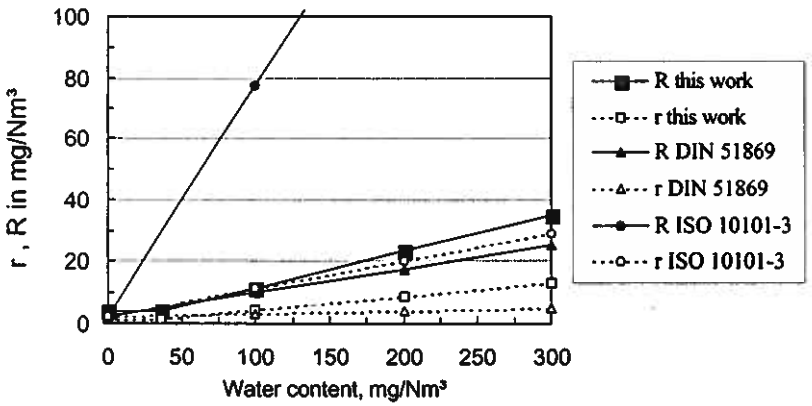


Figure D.3: Repeatability "r" and reproducibility "R" for coulometrically determined water contents using the Karl-Fischer-method. Values of this work as well as according to DIN 51869 and to ISO 10101-3.

Only those mean values of a operation point fulfilling the critical differential value criterion were taken into consideration for calculation of the total mean value for the respective operating point. Mean values not fulfilling the criterion were discarded. During the evaluation approximately 5% of the mean values were discarded due to this limit. A thorough description of the checking of the repeatability and reproducibility limits, respectively, is given in annex D.15. Here also the prerequisites for applying the repeatability limit (repetition conditions) and the reproducibility limit (comparison conditions) are given.

### D.2.4 Overall Mean Value for an Operating Point

All mean values of the KF-measurements that satisfied the statistical checking with the repeatability and reproducibility limit were used in calculating the overall mean value. By performing additional measurements it always was secured that a minimum of two KF-measuring campaigns was available for finding the overall mean value. The calculated overall mean values are listed in appendix G.2 for all gases investigated.

$$WC_{OP}(T,P) = \frac{\sum_{j=1}^{k} WC_{SM,j}}{k} \qquad (D.5)$$

with:

k : number of mean values with positive statistical evaluation

$WC_{OP}$ : Overall mean value of the operating point

$WC_{SM,j}$ : Water content of $j^{th}$ Karl-Fischer measurement of a series (= mean value of 10 single measurements satisfying the criterion)



## D.3 Uncertainty of the Water Content Determination

This sub-chapter deals with the definitions and rules according to the "Guidelines for the specification of the uncertainty of measuring" [139] (hereafter called DIN ISO-guidelines) for determining the uncertainty of measurements.

By carrying out a measurement the measuring result gives a value for the property measured. The (measuring) uncertainty is a measure for the scatter of the values that are dedicated to the property measured. It reflects the inadequate knowledge of the exact value of the measured property. Whereas the exact value of the deviation of the measured result from the "true" value is unknown - cannot be known - the uncertainty connected with systematic and random influences leading to the measurement deviation can be obtained [139].

Two different methods are distinguished for calculating the uncertainty. Method A is based on several observations of property $x_i$. The connected standard uncertainty - it is also called standard uncertainty of type A - of property $x_i$ is calculated with the help of the standard deviation s and the number n of the observations (measurements) [139]:

$$u_A(x_i) = \frac{s}{\sqrt{n}} \qquad (D.6)$$

The standard deviation s characterises the "fluctuation width" of the measuring results. According to equation (D.6) the standard uncertainty of type A can be reduced by increasing the number of measurements *n*.

For method B information of the manufacturers, reference data, calibration papers etc. are used. The standard uncertainty type B in general refers to reference data from handbooks and known limits for the property $x_i$ (for instance the upper and lower error limit). As a rule a rectangle distribution of all possible measuring result is assumed for the boundaries in which $x_i$ is located. Assuming the boundaries 2a, the standard uncertainty of type B is calculated as follows [139]:

$$u_B(x_i) = \frac{a}{\sqrt{3}} \qquad (D.7)$$

In case the property y cannot be measured directly but has to be calculated from N additional properties $x_1, x_2, .., x_N$ via a function $f$

$$y = f(x_1, x_2, .., x_N), \qquad (D.8)$$

the combined standard uncertainty $u_c$ is calculated as

$$u_c^2(y) = \sum_{i=1}^{N} \left(\frac{\partial f}{\partial x_i}\right)^2 \left[u_A^2(x_i) + u_B^2(x_i)\right] = \sum_{i=1}^{N} u_i^2(x_i) \qquad (D.9)$$

Equation (3.9) also is called uncertainty propagation law[38]. By multiplying the combined uncertainty $u_c$ with an extension factor $k_p$ one gets the extended uncertainty $U_p$:

$$U_p(y) = k_p\, u_c(y) = t_p\, u_c(y). \tag{D.10}$$

The extended uncertainty $U_p$ indicates an area $Y = y \pm U_p$, from which it can be expected that it contains a portion p of the distribution of values that, with confidence, can be assigned to the measuring property Y. As a first approximation for calculating the extended uncertainty for $k_p$ a value from the normal distribution can be used. For improvement generally a value from the t-distribution is taken.

When looking at the uncertainty of the determination of the water content prevailing at an operating point with temperature TIR4 and pressure PIR4 three main sources can be distinguished:

- Uncertainties which stem from adjustment of the equilibrium water content,
- Uncertainties that appear during KF-coulometry
- Uncertainties which occur during recalculating the analysis results to normal conditions.

The discussions of the uncertainties are done for the gas methane for two operating points located at the edge of the temperature and pressure range, respectively. The result of these considerations can be transferred to all other gases investigated, however. The very low water content of 17.6 mg/Nm³ of operation point 1 corresponds to an equilibrium water content at a temperature of -15°C and a pressure of 100 bar, the high water content of 1390 mg/Nm³ of operation point 2 corresponds to an equilibrium water content at a temperature of +5 °C and a pressure of 5 bar.

By rearranging equation (D.1) incorporating eq. (D.2) one obtains:

$$WC = \frac{m_{W,KF}}{V_{NGZ}\left(1 - \frac{p_{SFK}(\vartheta_{NGZ})}{P_{amb} + P_{e,NGZ}}\right)} \cdot \frac{(273.15 + \vartheta_{NGZ}) \cdot 1013.25}{(P_{amb} + P_{e,NGZ}) \cdot 273.15} \tag{D.11}$$

In the first term the mass of water analysed by the KF-apparatus $m_{W,KF}$ is referred to the dry probe volume, in the second term the recalculation to normal conditions is performed. As a result one yields:

$$WC = f(m_{W,KF}, \vartheta_{NGZ}, P_{amb}, p_{e,NGZ}, V_{NGZ}) \tag{D.12}$$

The mass of water in the probe volume transferred to the KF-apparatus is only dependent on the prevailing operating conditions (pressure PIR4 and temperature TIR4) assuming stationary conditions.

[38] Proceeding according to the DIN-ISO guidelines compared to [140] shows the advantage, that the estimated standard uncertainties of type A and type B can be treated the same way in further calculations. The results of the calculations therefore can be also applied when calculating the combined standard uncertainties for other applications.



$$\frac{m_W}{V_N} = WC = f'(TIR4, PIR4) \tag{D.13}$$

To estimate the influence of the uncertainties of TIR4 and PIR4 on the measured result, simplified correlations for the water content were applied which were found on the basis of the measurements carried out in this work (see eq. (D.29) to (D.31)). This procedure is considered to be of adequate accuracy as the correlations fitted isothermally or isobarically, respectively, represent the course of the water contents well.

Table D.2: Typical input values for the standard uncertainty calculation (type A)

| measured quantity | reference values example 1: 17.6mg/Nm³,-15°C,100bar | typical standard deviations | reference values example 1 1350mg/Nm³,+5°C, 5bar | typical standard deviations |
|---|---|---|---|---|
| $m_{W,KF}$[39] | 30.8 µg | 0.4 µg | 2320 µg | 10 µg |
| $\vartheta_{NGZ}$ | 26°C | 0.06 K | 26°C | 0.06 K |
| $P_{amb}$ | 1000 mbar | 0.3 mbar | 1000 mbar | 0.3 mbar |
| $P_{0,NGZ}$ | 0.1 mbar | - | 0.1 mbar | - |
| $V_{NGZ}$ | 2.0 dm³ | 5 cm³ | 2.0 dm³ | 5 cm³ |
| TIR4 | 258.15 K | 0.01 K | 278.15 K | 0.01 K |
| PIR4 | 100 bar | 0.01 bar | 5 bar | 0.01 bar |

In table D.2 typical values for the standard deviations of the measured properties are given for the two operating points chosen. The reference values as well as the standard deviations in each case are based on ten individual measurements. The listed figures serve as input for estimation of standard uncertainty A according to equation (D.6). The comparatively high standard deviation for the volume measurement takes into consideration the change of composition of the sealing liquid on the volume measurement (see also results of the sensitivity analysis in chapter D.4.2) in addition to the uncertainty of the reading.

Table D.3 contains the corresponding listing of input figures for calculating the standard uncertainties type B as well as the main causes for these uncertainties. The listed values are taken from manuals and data sheets of the measuring devices. In case of the KF-coulometers it was assumed that the uncertainties of the digital reading (the titrated water mass is given in µg to one digit after the decimal point) as well as a possible hysteresis in the measuring system already are included in the error limits given by the manufacturer. Due to its smaller error limits KF-apparatus CA-06 is treated separately from CA-02 and KF-684 in the uncertainty consideration of the water content estimation. The deviations of the characteristic curves of the pressure transmitters were

[39] As the operation manuals of the KF-apparatuses did not contain hints as to whether the error limits for the water mass estimation given by the manufacturers already contain type A uncertainties the indicated error limits for $m_w$ exclusively were considered to be of type B and an additional uncertainty part for type A was taken into consideration. In case the manufacturers already would have included a type A uncertainty in the indicated error limits one would have taken the type A part twice into consideration. The error caused by this, however, would be relatively small as the part of type A in $m_w$ is comparatively small in relation to that of type B standard uncertainty in the combined uncertainty $u_c$ (see table D.4).

Table D.3: Input values for the calculation of standard uncertainties of type B

| measured quantity | Maximum input value for the standard uncertainty (Type B) | Main source of uncertainty |
|---|---|---|
| $m_{W,CA-02}$ $m_{W,KF-684}$ | 5 µg for ≤ 1 mg 0.5% for > 1 mg | Error limit CA-02, KF-684, resp. |
| $m_{W,CA-06}$ | 3 µg for ≤ 1 mg 0.3% for > 1 mg | Error limit CA-06 |
| $\vartheta_{NGZ}$ | max. 20 mK | Stability + ageing of A/D-converter |
| $P_{amb}$ | ≤ 2.5 mbar p.a. | Stability + ageing of pressure tranducer |
| $P_{0,NGZ}$ | 0.02 mbar | Reading error (estimated) |
| $V_{NGZ}$ | - | - |
| TIR4 | max. 20 mK | Stability + ageing of A/D-converter |
| PIR4 | ≤ 0.1 bar p.a. | Stability + ageing of pressure tranducer |

got from the calibration against the oil pressure balance (see chapter C.1.1) and corrected via a calibration curve. The resulting deviations of the characteristic curves with max. 0.025% always remained well below that given by the manufacturer of 0.05%. The positive systematic deviation of 0.23% for the wet gas meter at a volume flow of 30 dm³/h already is included in a correction factor (see eq. D.1) and therefore does not have to be taken into account in the calculation of the uncertainty[40]. The standard uncertainties of type B can be calculated with equation (D.7) from the values listed in table D.9. To calculate the combined uncertainty the partial derivatives of $f$ (eq. (D.25)) and $f'$ (eq. (D.26)) with respect to the measured property are needed, respectively. A summary of the partial derivatives is given in table D.9 in annex D.8.

The calculated standard uncertainties of type A and B as well as the single contributions of the components to the combined uncertainty estimated according to equation (D.9) are listed in table D.4. It can be seen from table D.4 that the uncertainty of the water measurement with the KF-apparatus dominates the total uncertainty at low water contents, that is, at high pressures and at low temperatures. At high water contents, that is at low pressures and at high temperatures, the uncertainty of the water content estimation is of the same order of magnitude as those for the pressure and temperature measurements. In example 2 the largest contribution to the uncertainty is due to the pressure PIR4. The high uncertainty of pressure PIR4 is mainly due to type B uncertainty part, which means the uncertainty due to lack of stability or due to ageing of the

[40] In case the hydrogen produced at the cathode is not led to ambient via the drying tower but is routed through a small opening into the anode chamber as is done in the newer version of the Mitsubishi KF-cells the hydrogen is added to the gas measured by the wet gas meter. For small water contents the amount of hydrogen produced can be neglected. At the high water content, for example 1350 mg/Nm³ (example 2, table D.3) 1.68 Nml $H_2$/Ndm³ hydrogen is produced at the cathode. In case the volume correction due to the added hydrogen is not carried out, the calculated water content is too small by 2.27 mg/Nm³. This corresponds to an error of 0.17%. So the error is smaller than the uncertainty part from recalculating to normal conditions (see also table D.6). As errors of this magnitude only occur at these high water contents the hydrogen generation was not taken into account in the evaluation. During the calculation of the uncertainty it was assumed that it already is included in the error limits of the KF-coulometer.



Table D.4: Calculated standard uncertainties of type A and B as well as the contributions of the respective measuring quantities to the combined uncertainty (according to eq.(D.9)) for examples 1 and 2.

| Measured quantity $x_i$ | Example 1 (-15°C, 100bar) | | | Example 2 (+5°C, 5bar) | | |
|---|---|---|---|---|---|---|
| | $u_A(x_i)$ | $u_B(x_i)$ | $u_i(x_i)$ | $u_A(x_i)$ | $u_B(x_i)$ | $u_i(x_i)$ |
| $m_{W,CA-02}$ $m_{W,KF-684}$ | 0.0126 | 2.8868 | 1.6496 | 3.1623 | 6.6973 | 4.3097 |
| $m_{W,CA-06}$ | 0.0126 | 1.7321 | 0.9898 | 3.1623 | 4.0184 | 2.9755 |
| $\vartheta_{NGZ}$ | 0.0190 | 0.0115 | 0.0021 | 0.0190 | 0.0115 | 0.1588 |
| $P_{amb}$ | 0.0949 | 1.4434 | 0.0263 | 0.0949 | 1.4434 | 2.0207 |
| $P_{0,NGZ}$ | 0 | 0.0115 | 0.0002 | 0 | 0.0115 | 0.0161 |
| $V_{NGZ}$ | 0.0016 | 0 | 0.0139 | 0.0016 | 0 | 1.0673 |
| TIR4 | 0.0032 | 0.0115 | 0.0199 | 0.0032 | 0.0115 | 1.0735 |
| PIR4 | 0.0032 | 0.0577 | 0.0064 | 0.0032 | 0.0577 | 15.4101 |

pressure transmitter. The listed values indicate clearly that for an uncertainty calculation ageing and stability of the pressure transducers used cannot be neglected. Unfortunately in many publications the uncertainty of pressure measurement only is given as the deviation of the characteristic curves of the pressure transmitters. Especially with high precision pressure transmitters - as is also the case in this work - this deviation as a rule is smaller than the deviations due to ageing or the long term stability of the pressure transmitters. The results highlight that calibration in regular intervals is necessary in order to exclude eventual ageing influences. Example 2 indicates that a reduction of the uncertainty at low pressures can be achieved by applying pressure transmitters with smaller ageing or/and a higher stability (see indications in table D.3). The extended uncertainty can be obtained by applying equation (3.9) from the combined standard uncertainty from equation (3.9). Here a single value for $t_p$, $t_{95} = 2$ is used to calculate the extended uncertainty $U_{95}$ for a confidence interval of 95 % taking into consideration the recommendation of the DIN-ISO guideline [139][41].

Table D.5 shows a listing of the extended uncertainties; in table D.6 the uncertainties are shown in relative figures. The contributions from recalculating to normal conditions ($U_{95,NB}$), from Karl-Fischer analysis and recalculation to normal conditions ($U_{95,KF+NB}$) as well as setting equilibrium ($U_{95,T4P4}$) for the total extended uncertainty ($U_{95,tot}$) are listed separately in both tables. At low

[41] When going from the combined uncertainty to the extended uncertainty an additional problem occurs in that for fixing the extension factor $k_p$ exact knowledge of the distribution functions of all influencing variables is assumed. The central limit theorem requests that the variance of non normally distributed variables for calculating the measuring property is significantly smaller than the variance of the measuring property. As the rectangle distribution $u_B$ ($m_{H2O}$) at very low water contents as well as $u_B$(PIR4) at very low pressures give a high contribution to the combined standard uncertainty $u_C$(WC) the requested conditions for the central limit theorem may not be fulfilled. Using a $k_p$ value from a normal or t-distribution for calculating the extended uncertainty then leads to higher $k_p$ values. For a confidence interval of 95% (p=0.95) the value of the rectangle distribution is $k_p = k_{95} = 1.65$. For the sytem under consideration an effective degree of freedom of $\nu_{eff} > 30$ is calculated from the Welch-Satterthwaite formula [139]. Taking this into account for $t_p$ a value of $t_{95} = 2$ results from the t-distribution assuming a confidence interval of 95%.

water contents the uncertainties from the titration are decisive. At high water contents the uncertainties from setting equilibrium dominate. Due to different error limits of the KF-coulometers the measurements carried out with Mitsubishi coulometer CA-06 possess a smaller uncertainty. The relative part of the uncertainty due to recalculation ($U_{95,NB}/WC_j$) is independent from the measured water content.

Table D.5: Calculation of the extended uncertainties (eq. (D.10))

| Values in mg/Nm³ | Example 1 (-15°C, 100bar) | | Example 2 (+5°C, 5bar) | |
|---|---|---|---|---|
| | CA-06 | CA-02, KF-684 | CA-06 | CA-02, KF-684 |
| $U_{95,NB}$ | 0.06 | 0.06 | 4.54 | 4.54 |
| $U_{95,KF+NB}$ | 1.98 | 3.3 | 7.51 | 9.76 |
| $U_{95,T4P4}$ | 0.04 | 0.04 | 30.9 | 30.9 |
| $U_{95,tot}$ | 1.98 | 3.30 | 31.79 | 32.40 |

Table D.6: Calculation of the relative extended uncertainties

| | Example 1 (-15 °C, 100 bar, $WC_1$= 17,6 mg/Nm³) | | Example 2 (+5 °C, 5 bar, $WC_2$= 1350 mg/Nm³) | |
|---|---|---|---|---|
| | CA-06 | CA-02, KF-684 | CA-06 | CA-02, KF-684 |
| $U_{95,NB}/WC_j$ | 0.0034 | 0.0034 | 0.0034 | 0.0034 |
| $U_{95,KF+NB}/WC_j$ | 0.1125 | 0.1875 | 0.0056 | 0.0072 |
| $U_{95,T4P4}/WC_j$ | 0.0024 | 0.0024 | 0.0229 | 0.0229 |
| $U_{95,tot}/WC_j$ | 0.1126 | 0.1875 | 0.0236 | 0.024 |

Figure D.4 allows an overview over the course of the uncertainties as a function of the set equilibrium pressure in the saturation apparatus and of the water content. To draw-up this diagram the uncertainties at different points were calculated. To do so measuring points from the reference system methane - water were used. The respective calculated uncertainties were connected with lines for the respective isobars in figure D.4. As the uncertainty contribution of temperatures $\vartheta_{NGZ}$ as well as TIR4 are relatively small, in the overall uncertainty temperature has not to be taken into account as an additional parameter in this diagram. Due to different error limits one has to distinguish between the different KF apparatuses, however. For the region investigated here and the water contents measured the courses of the uncertainties for pressures above 15 bar coincide with that at 15 bar. The reasoning is given in the preceding paragraph. At the high pressures low water contents are measured. The uncertainty part from setting equilibrium is small. The extended uncertainty therefore mainly is fixed by the uncertainty of the water content measurement.

Summarising one can conclude that in the area of small water contents (up to 100 mg/Nm³) the uncertainty is up to 20% of the value measured. The uncertainties become especially high when



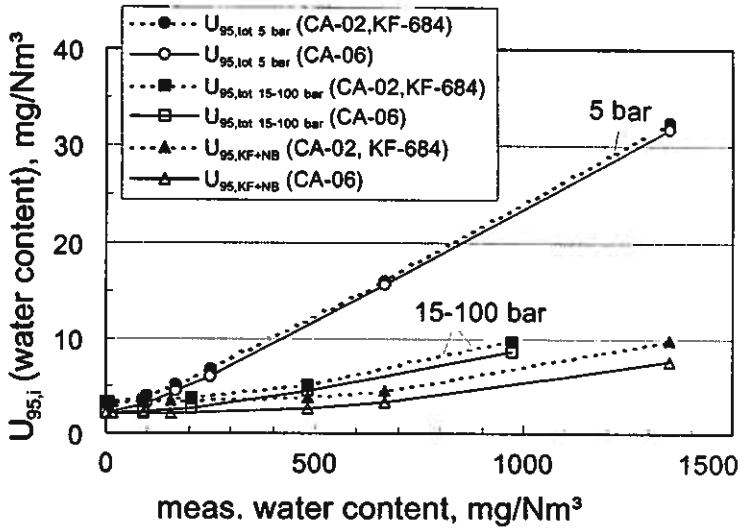


Figure D.4: Uncertainties of experimentally determined water contents in dependence of equilibrium pressure and water content (measured values).
($U_{95,KF+NB}$: Uncertainty of the Karl-Fischer analysis and the conversion to standard conditions; $U_{95,tot.}$: extended uncertainty)

approaching the analytic limit of the Karl-Fischer titration. For water contents higher than 100 mg/Nm³ the uncertainty in the investigated range lies ≤2.5% of the measuring value for KF-coulometer CA-06 (and ≤3.8% for CA-02 and KF 684, respectively).

## D.4 Sensitivity Analysis

### D.4.1 Investigation Concerning the Running-in Period

In order to reach equilibrium conditions the dew point mirror and the lines were purged for three hours at constant operating conditions. During first start up of the plant numerous measurements have shown that in every case equilibrium conditions are reached for a volume flow of 30 dm³/h.

Automation of the Karl-Fischer (KF) titration opened up the possibility to carry out a very large number of KF-measurements in series. As a result, the influence of a change in temperature of the second condenser TIR4 on the measured water content could be investigated as well as the influence on reaching adsorption equilibrium with the walls of the pipeline and the measuring gas.

Figure D.5 shows a typical result of such an experiment over a long period of time. For the data shown the dew point mirror and the KF-cell were switched in series (variant 3, see annex C.6). The pressure set point was set 40 bar. Nitrogen was used as measuring gas. Over a period of 12 hours in total 80 KF-measurements were carried out. Temperature TIR4 for the first eleven measurements was set to +20°C. After showing the typical running-in behaviour (measurements 1

to 5) the measured water content stabilises at 375 mg/Nm³. After the tenths KF-measurement the temperature of the cryostat bath was changed from +20°C to -20°C. Due to the cooling of the bath temperature TIR4 drops immediately. The water content follows correspondingly; it follows with a time gap of a quarter of an hour (or 15 minutes). This can be seen when crossing 0°C, which also can be traced back for the water content. The cryostat needs about 3.5 hours for reaching the new set temperature of -20°C. From the point of reaching the set temperature (320th minute) the measured water contents are shown in an enlarged scale. (The slight fluctuation of TIR4 at 300 minutes shortly prior to reaching the set temperature is due to the PID-control of the cryostat temperature).

When reaching the set-point temperature as a rule the three hours of running-in time start to guarantee stationary conditions at the start of measurements. In the detailed section the mean value (MV) of all measurements after the end of the running-in period (500th minute) is shown as a dotted line. In addition the uncertainty calculated in annex D.3.1 is shown. Already one hour after reaching the new set temperature TIR4 = -20 °C all analysed water contents fall within the uncertainty area of the final value of the measuring set. The measurements first still show a slight downward trend before they oscillate around the mean value from the 380th minute. The variations, however, are within the uncertainty limits and mainly are due to the conditions of the chemicals caused by the large number of measurements. The slight drop in the measured values after the 620th minute was caused by an increase of the drift from 0.00 µg/sec to 0.01 µg/sec and therefore is no indication of a change in adsorption equilibrium in the lines leading to the KF-cell.

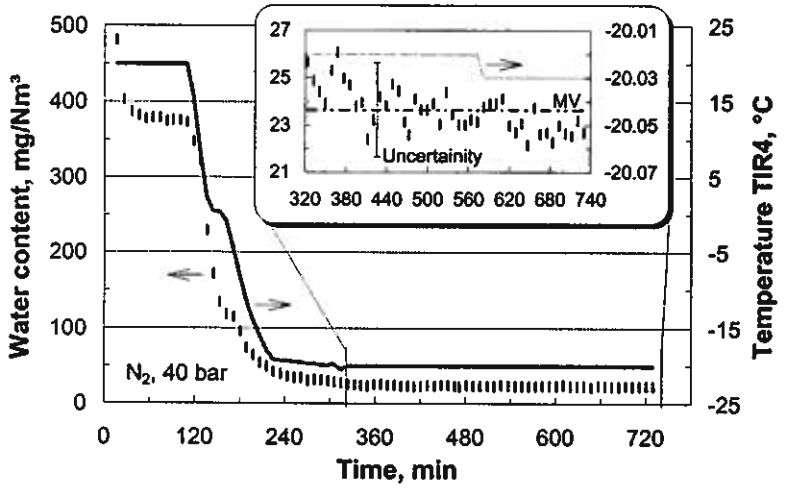


Figure D.5: Long term measurement over a period of 13 hours. The operating temperature of condenser K2 (TIR4) was lowered from +20°C to -20°C. Constant operating pressure: 40 bar. Operating gas: nitrogen



The course of the measurements clearly indicates the large influence of a changing drift during the measurement of small water contents. Experience tells that an increase in the drift leads to output of smaller analysed water contents.

By means of the long term measurements it became evident that a new stationary equilibrium was reached after a short period. If one takes into consideration, that the routing of the gas during these measurements (series of dew point mirror and KF-cell) was about four times as long as with a normal KF-measurement, the running-in time of three hours guarantees in all cases a new equilibrium of the plant prior to the start of the actual measurement.

## D.4.2 Gas Volume Measurement

The exact knowledge of the dry gas volume is a prerequisite for an exact calculation of the water content in the gas phase from the mass of water analysed with the KF-coulometer (see eq. D.1). In dedicated measurements the influence of the sealing liquid on the volume measurements was investigated more closely.

When calculating the water content according to ISO 10101-3 it is assumed that the gas flow at the exit of the wet type gas meter is completely saturated with water. First this assumption was checked via water content measurements at the exit of the wet gas meter. The result was that with the given boundary conditions the gas flow was not saturated 100 % but in average only 92.5%. At a gas meter temperature of +23 °C this leads to an error of +0.22% in dry volume or -0.22% in water content compared to complete saturation. Details are given in appendix D.9.1 "volume measurement with the wet type gas meter".

The phenomenon of a decrease of liquid in the anode chamber of the KF-cell when larger amounts of gas were led through the KF-cell was a second major point of investigation. As methanol forms the major part of the anode liquid as a first guess it was assumed that the decrease of the liquid in the KF-cell was only caused by the loss of methanol. A mass balance for the methanol loss in the KF-cell showed that the gas stream leaving the KF-cell nearly was saturated with methanol.

Due to its strong hygroscopic properties methanol is being removed from the gas stream in the following wet gas meter (at the start being pure water). The consequence is that with each KF-measurement the methanol content of the water increases. In case the gas stream entering the wet gas meter is free of methanol - as is the case when bypassing the KF-cell - the gas is being loaded with methanol when passing through the liquid of the wet gas meter. During this period the methanol content of the liquid decreases slightly. During a complete measuring sequence consisting of the bypass and measuring period the overall methanol content of the liquid slightly increases. The methanol water mixture formed possesses a vapour pressure which is higher than that of pure water. The difference between both vapour pressures increases with increasing methanol content and increasing temperature in the wet gas meter.

In order to assess the quality of those water content measurements taken prior to the knowledge of these facts the error resulting from it was estimated. The higher vapour pressure of the methanol-water mixture compared to pure water leads to an error in the calculation of the dry gas volume according to equation (D.1) which counteracts the error of incomplete saturation. By

using a computation model the admissible methanol content was estimated for different boundary conditions. If the relative maximum error of the estimation of the dry volume (insufficient saturation and influence of methanol) is fixed at ±0.25% the model results in a allowable maximum of 6.7 mass-% methanol in the wet gas meter liquid at a temperature of +23°C. For the boundary conditions of this work (volume flow 30 dm³/h, running-in time 3 h, volume of the wet gas meter liquid 2.5 dm³) the consequence is that the wet gas meter sealing liquid will have to be changed latest after 460 KF-measurements (or 23 KF-series of measurements of 20 measurements each) at a temperature of +23°C. A detailed description of the calculations performed can be found in chapters D.9.2 and D.9.3 in Annex D. All measurements carried out prior to these investigations were checked using the laboratory book and all series of measurement lying outside the required interval of sealing liquid change were discarded.

In general the consequence from these investigations indicate that the enrichment of parts of the KF-chemicals (especially methanol) in the wet gas meter sealing liquid has to be taken into consideration for water content measurements carried out according to ISO 10101-3. In order to avoid high methanol content and errors in the estimation of the dry gas volume resulting from this fact the wet gas meter liquid has to be changed within the intervals estimated. Several modification of the set up were tested in order to get rid of the methanol and saturation problems, two of which are described here.

An easy to handle and cheap solution was to lead the gas stream through a washing bottle filled with de-mineralised water prior to the wet gas meter to get rid of the methanol and simultaneously saturating the gas stream with water. Prior to each series of measurements the relatively small amount of water in the washing bottle can be changed fast and easy. The experiments with the washing bottle failed, however, as the pressure in the KF-cell increased such that problems with the tightness of the cell were observed. Ground joints were lifted resulting in a loss of gas from the cell and an increase in the drift. A solution to these problems is only possible by modifying the KF-cells. For the coulometers used in this work (Mitsubishi CA-02 and CA-06) a change of the KF cell in the area of ground joints would be necessary (for instance use of ground-in stopper clamps) to allow a higher pressure in the KF-cell and to guarantee an optimum tightness. Another solution not applied here would be to extract the methanol by means of adsorption on active carbon filter. The gas free from methanol and water then is led through a wet gas meter using oil as sealing liquid. By using an oil with low vapour pressure one would not have to correct for vapour pressure when estimating the dry gas volume. It can be anticipated that for this variation, too, the KF-cell would have to tolerate a higher pressure due to the additional activated carbon bed. In addition the break through time of the activated carbon for the operating conditions (volume flow, temperature of KF-cell, etc.) would have to be estimated in additional experiments. This would have to be observed during normal operation.

Within this work solely the set up according to ISO 10101-3 [89] was used (see figure D.1) without washing bottle or activated carbon and with water as sealing liquid in the wet gas meter. A change of sealing liquid in regular intervals was the consequence of the sensitivity analysis carried out. The relative maximum overall error fixed at ±0.25% was taken into consideration



when estimating the standard uncertainty of type A (see annex D.3.1). As the investigation of the uncertainty resulted in a small contribution to the overall uncertainty no modifications of the set up according to ISO 10101-3 or in the procedure of evaluation of the water content described in annex D.1.3.5 were made.

# D.5 Vapour- and Sublimation Pressure Curves

## D.5.1 Water

**Vapour Pressure Curve**

Vapour pressures of pure water $p_{oW}$ may be calculated using Magnus's equation [127]. The specific coefficients $A_W$, $B_W$, $C_W$ were particularly fitted for the temperature range 0° to +40°C [128].

$$p_{oW} = \frac{\exp\left\{\frac{A_W \cdot \vartheta}{B_W + \vartheta} + C_W\right\}}{100}\ hPa \qquad \text{for } 0°C < \vartheta \le 40°C \tag{D.14}$$

With the set of coefficients[42]: $A_W = 17.438$; $B_W = 239.78°C$; $C_W = 6.4147$

The calculation of pseudo-experimental vapour pressures for the purpose of the parameter optimisation of the alpha-function (see chapter 4.2), however, has been carried out using the equation by Pruss and Wagner [130].

**Sublimation Pressure Curve**

For the calculation of sublimation pressures $p_{ol}$, equation (D.15) has been used (Wagner et al. [129]):

$$\ln\left[\frac{P_{ol}}{P_{tr}}\right] = A_l\left(1-\left(\frac{T}{T_{tr}}\right)^{-1.5}\right) + B_l\left(1-\left(\frac{T}{T_{tr}}\right)^{-1.25}\right) \tag{D.15}$$

with $A_l = -13.9281690$ Triple point temperature: $T_{tr} = 273.16$ K

$B_l = 34.7078238$ Triple point pressure: $P_{tr} = 611.657$ Pa

The coefficients of equation (D.15) are related to the ITS-90 temperature scale. For the temperature range $T \ge 250$ K an accuracy of $\le \pm 0.1\%$ is stated by Wagner et al., while the accuracy for the reproduction of sublimation pressures is $\le \pm 0.5\%$ for temperatures $T < 250$ K.

[42] The coefficients given in eq. (D.14) are related to the IPTS-68 temperature scale. Due to project-related reasons, temperatures were not converted into the ITS-90 scale. However, the maximum difference between IPTS-68 and ITS-90 is about -10 mK in the temperature range considered [141]. Therefore, the error in calculated water content is negligible. Equation (D.14), however, only was applied to calculate vapour pressures in the wet gas meter, as well in the uncertainty estimation (see annex D.8).

### D.5.2 Methanol

The vapour pressure curve of methanol (MeOH) in the temperature range between +15°C and $T_{crit}$ reads [131]:

$$\ln\left[\frac{P_{oMeOH}}{P_{krit}}\right]=\frac{T_{crit}}{T}\left[A_M\left(1-\frac{T}{T_{crit}}\right)+B_M\left(1-\frac{T}{T_{crit}}\right)^{1.5}+C_M\left(1-\frac{T}{T_{crit}}\right)^{3}+D_M\left(1-\frac{T}{T_{crit}}\right)^{6}\right] \quad \text{(D.16)}$$

Using the coefficients: $A_M$ = -8.54796; critical pressure MeOH: $P_{crit}$ = 80.9 bar;
$B_M$ = 0.76982; critical temperature MeOH: $T_{crit}$ = 512.6 K;
$C_M$ = -3.1085;
$D_M$ = 1.54481.

## D.6 Supplement to the Statistical Evaluation of the Karl-Fischer Measurements

The water content has been determined in $k$ series of measurements ($k_{min}$=2) for every operation point and every type of gas. The extent of the series amounts at least to 20 points. Due to running-in effects, the first 10 points have been discarded. Therefore, only the last 10 measuring points contribute to the mean value of a Karl-Fischer measuring series. The correctness of each value has been checked using a statistical test by Nalimov (see next section). The verification on outliers has been carried out directly after the 20th KF-measurement. This procedure made it possible, to identify outliers at once, and they were substituted by a following (21st measurement, etc.). Until the end of one measuring series, 24 measurements have been carried out at most, as a result of this procedure. If the series still failed in a final check, the operating point has been measured at a later date.

The statistical tests and the supervision of the measuring process has been controlled by a program running on the process control computer. Since at least two series have been measured for each operating point, the data were evaluated using the reproducibility and repeatability limits (according to ISO 5725-6 [135]) in a second step. According to DIN ISO 5725-1 [134] the quantities repeatability limit „r" and reproducibility limit „R" are defined as follows:

- **Repeatability limit, r:** That range, in which the absolute difference between two individual measured values, determined under conditions of repeatability, may be expected within a probability of 95%.
- **Reproducibility limit, R:** That range, in which the absolute difference between two individual measured values, determined under conditions of reproducibility, may be expected within a probability of 95%.

Conditions of repeatability exist, if measurements are carried out by the same operator, the same experimental method, in the same laboratory, in small time intervals for identical objects of measurement. For conditions of reproducibility, these requirements are reduced to the identical



object of measurement and the application of the same experimental method. In this work, therefore conditions of repeatability have been assumed, if the same coulometer was applied. In the case, if results obtained by different types of coulometers (e.g. Metrohm KF-684 and Mitsubishi CA-06) and results by external laboratories were compared, conditions of reproducibility have been assumed.

From the repeatability or reproducibility limit, respectively, a critical differential value can be derived which shall not be exceeded by the absolute difference of two mean values estimated at the respective prevailing conditions. In case the absolute difference of two mean values exceeds the critical differential value the mean values have to be questioned and additional investigations have to be carried out in order to clarify the causes of exceeding the limit.

In this work for each operating point the mean values of the first and second run were taken to form the differential value which was compared to the critical differential value which in turn had been calculated according to the prevailing conditions (repeatability and reproducibility conditions, respectively. See also the following chapter „Critical Difference Test by Means of the Reproducibility and Repeatability Limit"). For calculating the values of the repeatability and reproducibility limit always the group mean value of the water contents under consideration were inserted. In case of exceeding the critical difference as a rule at least one additional run was carried out.

In case more than two mean values were available the mean values were arranged in descending manner ($WC_{SM,A} \geq WC_{SM,B} \geq WC_{SM,C} \geq$..) and it was checked whether the differential value of two neighbouring mean values were greater than the critical differential value. Mean values not satisfying the difference criterion with any neighbouring mean value were taken out of the group.

The overall mean value for the operating point is the group mean value of the remaining consistent mean values.

### D.6.1 Outlier-Test by Nalimov (r-Test) [136] [138]

The mean value $WC_{SM}$ and the standard deviation $s_{SM}$ of the KF-measurement run were calculated.

$$WC_{SM}=\frac{\sum_{i=1}^{n} WC_i}{n} \quad \text{(D.17)}$$

$$s_{SM}=\frac{\sum_{i=1}^{n}\left(WC_i-WC_{SM}\right)^2}{n\,(n-1)} \quad \text{(D.18)}$$

For the value $WC_i^*$ most suspect to runaway or outlier, that is, the measuring value $i$ which shows the greatest difference to the mean value the following test value ($PG^*$) was calculated:

$$PG^*=\frac{\left|WC_i^*-WC_{SM}\right|}{s_{SM}}\sqrt{\frac{n}{n-1}} \quad \text{(D.19)}$$

With the help of this test value the measuring value is classified by comparing with a triple of judgement scales (BG). The values of the r-distribution for the statistical probability of 95%, 99% and 99.9% were taken as judgement scales. It follows:

$PG^* < BG(95)$ : no outlier detectable

$BG(95) < PG^* < BG(99)$ : $x^*$ is probably an outlier

$BG(99) < PG^* < BG(99.9)$ : $x^*$ is a significant outlier

$BG(99.9) < PG^*$ : $x^*$ is a highly significant outlier

A test result of outlier-free data has to be interpreted in a way that no outlier can be detected statistically within the data set checked. No absolute judgement about existence or non existence of an outlier in the data set under consideration is possible with any outlier test [137], however.

The outlier test according to Dixon as given in DIN ISO 5725 is less stringent than the Namilov-test [136] used in this work as the respective comparison values for the same statistical security are greater for the Dixon test.

As a standard in this work ten individual measuring values ($Wc_i$) were used for arriving at the mean value ($n = 10$). When taking this value, equation (D.17) to (D.10) can be modified according to:

$$WC_{SM} = \frac{\sum_{i=1}^{10} WC_i}{10} \tag{D.20}$$

$$s_{SM} = \frac{\sum_{i=1}^{10} \left(WC_i - WC_{SM}\right)^2}{90} \tag{D.21}$$

$$PG^* = \frac{\left|WC_i^* - WC_{SM}\right|}{s_{SM}} \sqrt{\frac{10}{9}} = \frac{\left|WC_i^* - WC_{SM}\right|}{s_{SM}} \cdot 1.0541 \tag{D.22}$$

In this case with eight degrees of freedom $f_{r\text{-Test}}=n-2=8$) from the r-distribution the judgement scales resulted as BG(95) = 1.895, BG(99) = 2.294 and BG(99.9) = 2.616 [137].

## D.6.2 Critical Difference Test by Means of the Reproducibility and Repeatability Limit

According to ISO 5725-6 [135] the difference between the mean value $WC_{SM,A}$ of the measuring values $n_{SM,A}$ and the mean value $WC_{SM,B}$ of the measuring values $n_{SM,B}$ for two measuring runs $A$ and $B$ under repeatability conditions has to be smaller than the critical difference $CrD_{95}$ which can be calculated with the help of the repeatability limit $r$.

$$CrD_{95}\left(\left|WC_{SM,A} - WC_{SM,B}\right|\right) = r\sqrt{\frac{1}{2\,n_{SM,A}} + \frac{1}{2\,n_{SM,B}}} \tag{D.23}$$



In case only reproducibility conditions prevail for the measuring runs $A$ and $B$ the critical difference of the mean values is calculated from these runs by applying the reproducibility limit $R$ and the repeatability limit $r$ according to:

$$CrD_{95}\left(\left|WC_{SM,A} - WC_{SM,B}\right|\right) = \sqrt{R^2 - r^2\left(1 - \frac{1}{2\,n_{SM,A}} - \frac{1}{2\,n_{SM,B}}\right)} \tag{D.24}$$

the index „95" of the critical differential values $CrD_{95}$ indicates that they are given for a probability level of 95%.

For repeatability conditions equation (D.23) simplifies to

$$CrD_{95}\left(\left|WC_A - WC_B\right|\right) = r\sqrt{0.1} = 0.3162 \cdot r \tag{D.25}$$

as in this work as a standard ten measuring data are taken for generating the mean value ($n_{SM,A}=n_{SM,B}=10$). When reproducibility conditions prevail equation (D.24) simplifies to

$$CrD_{95}\left(\left|WC_A - WC_B\right|\right) = \sqrt{R^2 - r^2\,0.9} \tag{D.26}$$

In case the differential value for measuring runs A and B is smaller than the relevant critical difference, both mean values are valid and according to the standard. They can be summarised into a total mean value.

The values for the repeatability limit r and for the reproducibility limit R have been established in a round robin test prior to the start of this work [133]. The following functional relation depending on the water content has been used for the respective limits:

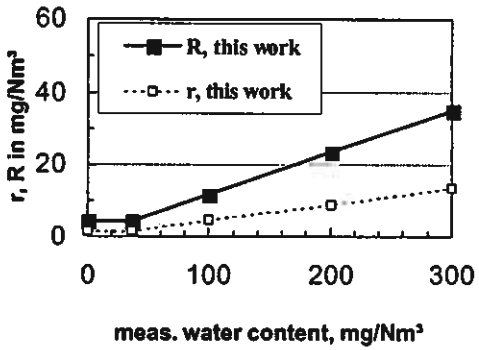


Figure D.6: Repeatability limit r and reproducibility limit R, applied in this work, for determination of critical differences $CrD_{95}$ between two mean values.

Repeatability limit, r:

0 mg/Nm³ < WC < 36 mg/Nm³

r = 1.6 mg/Nm³ (constant)

36 mg/Nm³ ≤ WC

r = (1.6/36) · WC

Reproducibility limit, R:

0 mg/Nm³ < WC < 36 mg/Nm³

R = 4.2 mg/Nm³ (constant)

36 mg/Nm³ ≤ WC

R = (4.2/36) · WC

WC: water content as measured (in mg/Nm³)

As shown in figure D.6 straight lines with constant slope result for water contents greater than or equal to 36 mg/Nm³.

## D.7 Correlation of the Water Content Data

In order to be able to carry out the uncertainty calculation in chapter 3.4.1 a simple dependence of the water content on pressure and on temperatures is needed. Therefore - standing in for all gases under investigation - the measured water content of the main natural gas component methane was correlated isobaric and isothermal.

### Correlation of the isobaric Data Sets

The isobaric water content was fitted to a simple cubic polynomial:

$$\log(WC_{F,ib}) = a_0 + a_1 t + a_2 t^2 + a_3 t^3 \qquad (D.27)$$

with

$$t = \frac{T}{T_N} \qquad (D.28)$$

T : temperature of operation point in Kelvin ($T_N$ = 273.15 K)

$a_{0\text{-}3}$ : fit parameter

Table D.7: Coefficients for the isobaric correlation of the water contents according to equation (D.27)

| Methane | 100 bar | 80 bar | 60 bar | 40 bar | 15 bar | 5 bar |
|---|---|---|---|---|---|---|
| a0 | -21.5484 | -26.3171 | -26.0143 | -23.7037 | -21.8300 | -20.9229 |
| a1 | 36.8888 | 46.8598 | 46.6196 | 42.2120 | 39.3917 | 32.0217 |
| a2 | -13.4565 | -18.6412 | -18.6024 | -16.3796 | -15.0195 | -1.0203 |
| a3 | -0.0927 | -0.0098 | -0.0102 | -0.0023 | -0.0151 | -7.0928 |

The temperature range of -25°C to + 20°C corresponds to reduced temperatures of 0.9085 to 1.0732. By reducing, the coefficients $a_o$ to $a_3$ show nearly the same order of magnitude. When choosing an optimal fit function it turned out that splitting the isobaric data set into two sub-domains to take care of the corresponding solid and liquid phase, respectively, due to the relatively small temperature range under consideration gave no superior results compared to the polynomial approach. In addition, the exact transition temperature between the solid and the liquid phase cannot be determined unambiguously from the data available. The continuous description of the temperature interval with one cubic polynomial in addition has the advantage of not showing a discontinuity. As a draw back of this approach a limited extrapolaribility is to be expected.

### Correlation of the isothermal Data Sets

$$WC_{F,it} = \frac{y_W}{1-y_W} \cdot \frac{M_W P_N}{R T_N} = \frac{y_W}{1-y_W} \cdot 803745 \frac{mg}{Nm^3} \qquad (D.29)$$



with

$$y_W = b_1 \cdot \frac{P^*}{P} \exp\left\{\frac{P - P^*}{b_0}\right\} \qquad (D.30)$$

$P^*$ : saturation vapour pressure $P_{oW}$ (t >0°C) and sublimation vapour pressure $P_{oI}$ for pure water according to equation.(D.14) and. (D.15), respectively

$b_0$, $b_1$ : fit parameter

Table D.8: Coefficients for the isothermal correlation of the water contents acc. to eq. (D.29)

| Methane | -20°C | -15°C | -10°C | -5°C | 0°C | 5°C | 10°C | 15°C | 20°C |
|---|---|---|---|---|---|---|---|---|---|
| b1 | 265.60 | 256.89 | 674.83 | 470.42 | 482.68 | 340.15 | 254.30 | 276.75 | 275.95 |
| b2 | 1.0003 | 0.9185 | 0.9973 | 1.0119 | 1.0062 | 1.0194 | 0.9844 | 0.9923 | 0.9794 |

The approach for calculating the mole fraction of the water $y_W$ in the isothermal correlation has been derived from the phase equilibrium equation. As a maximum of six experimental data per isotherm were available for fitting (according to the pressures normally measured 5, 15, 40, 60, 80, 100 bar), an additional pseudo experimental value was added for the correlation at 1 bar (see figure D.7). This pseudo experimental value was calculated according to simple Raoult's law (see equation (E.2)) from the vapour pressure of water and the pressure of 1 bar. By enlarging the data basis in this thermodynamically consistent way the influence of the greater number of points at the higher pressures is levelled out and the extrapolaribility of the correlation to lower pressures is improved.

The minimisation of the sum of squares of the errors between measured and calculated water contents was chosen as objective function. In addition the differences in water contents were weighted with the standard deviation of the experimental values.

$$Min = \sum_{i=1}^{N} \left( \frac{WC_{exp,i} - WC_{calc,i}}{s_{exp,i}} \right)^2 \qquad (D.31)$$

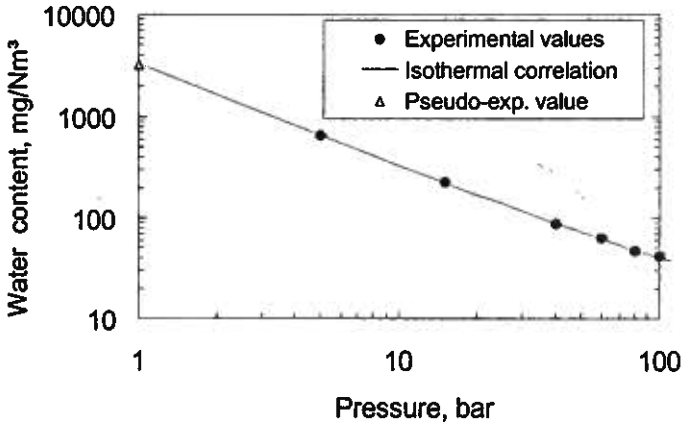


Figure D.7: Example for an isothermal correlation.

An artificial standard deviation had to be assumed for the pseudo experimental values calculated according Raoult's law from the vapour pressure of pure water. The highest standard deviation of the real measuring data in the data set under consideration additionally was weighted with the factor five and was assigned to the pseudo experimental value. By doing so it was ensured that the pseudo experimental value obtained a reduced influence compared to the measuring data while fitting the values. The accuracy of both correlations stays within the uncertainty when neglecting the indicated unsecured measuring values of the preceding evaluation (see annex D.3.1).

The correlations were only used for the uncertainty considerations in annex D.3.1. The fitting of the model parameters in chapter 4 as well as model validation in chapter 5 was based only on experimental values. No values from the correlations according to equations (D.27) and (D.29) were used in these cases, respectively.

## D.8 Supplement to the Uncertainty Evaluation

With the help of equation (D.27) the influence of the extended uncertainty on the dew point in determining the water content can be estimated for a given operating point.

$$U_{95}(T_{TP}) = \left(\frac{\partial t}{\partial WC}\right)_{T,P} \cdot U_{95}(WC) \qquad \text{(D.32)}$$

The results for methane can be taken from figure D.8. From the uncertainty in water content estimation a maximum deviation in the dew point of 0.5 K or more can only result in water contents below 80 mg/Nm³. Figure D.9 shows the maximum deviation in dew point when only the uncertainties from the Karl-Fischer titration and from the conversion to standard conditions are taken into consideration. The comparison of both figures clarifies the fact that the higher deviations in the dew point at lower water contents is mainly a direct consequence of the uncertainties of the

Karl-Fischer titration due to the small influence of the conversion to standard conditions. For practical purposes one can also conclude that, even with exact knowledge of the functional influence between dew point and water content, the calculated dew point always is connected with a uncertainty of up to 2 K at low water contents (< 30-40 mg/Nm³) due to the uncertainty of the water content estimation.

As can be expected the smaller the uncertainty (error limit) of the Karl-Fischer coulometer the more exact the dew point can be calculated. A remarkable reduction in uncertainty over the whole range under consideration results from the smaller error limit by 2 µg or 0.2% of CA06 compared to the other two coulometers used (CA02, KF684).



Table D.9: Listing of the partial derivatives of WC with respect to the measuring properties

| Measuring property $x_i$ | partial derivative: $c_i = \frac{\partial f}{\partial x_i} = \frac{\partial WC}{\partial x_i}$ |
|---|---|
| $m_{W,KF}$ | $\frac{WC}{m_{W,KF}}$ |
| $\vartheta_{NGZ}$ | $\frac{WC}{\vartheta_{NGZ}+273.15K}\cdot\left\{1+\frac{(\vartheta_{NGZ}+273.15K)\cdot\frac{\partial P_{SFK}}{\partial \vartheta_{NGZ}}}{P_{amb}+P_0-P_{SFK}}\right\}$<br>In case the sealing liquid (SFK) is pure water it follows from eq. (D.14):<br>$\frac{\partial P_{SFK}}{\partial \vartheta_{NGZ}} = \frac{\partial P_{oW}}{\partial \vartheta_{NGZ}} = \frac{A\,B}{(B+\vartheta_{NGZ})^2} P_{oW}$ |
| $P_{amb}$ | $-\frac{WC}{p_{Gas,dry}} = -\frac{WC}{P_{amb}+P_0-P_{SFK}}$ |
| $P_0$ | $-\frac{WC}{p_{Gas,dry}} = -\frac{WC}{P_{amb}+P_0-P_{SFK}}$ |
| $V_{NGZ}$ | $-\frac{WC}{V_{NGZ}}$ |
| TIR4 | $\frac{1}{T_N}\frac{WC}{\log(e)}\left\{a_1+2a_2\left(\frac{TIR4}{T_N}\right)+3a_3\left(\frac{TIR4}{T_N}\right)^2\right\}$ |
| PIR4 | $\frac{WC}{(1-y)}\left(\frac{1}{b_o}-\frac{1}{PIR4}\right)$ |

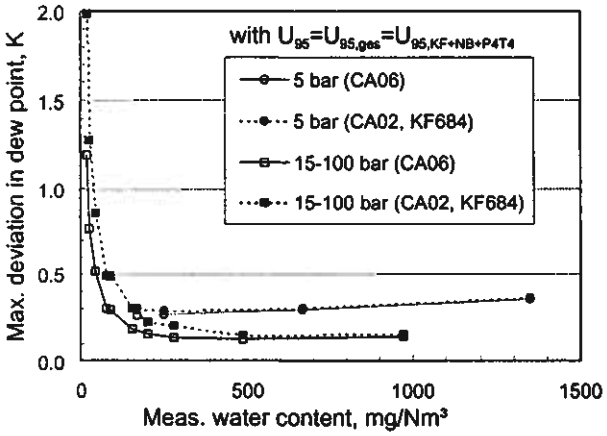


Measured Values:

| T | P | WC |
|---|---|---|
| °C | bar | mg/Nm³ |
| -20 | 5 | 170 |
| -15 | 5 | 249 |
| -5 | 5 | 668 |
| 5 | 5 | 1350 |
| -15 | 100 | 18 |
| -15 | 60 | 27 |
| -5 | 100 | 45 |
| -5 | 60 | 79 |
| 5 | 100 | 90 |
| 5 | 60 | 155 |
| -5 | 15 | 203 |
| 15 | 60 | 281 |
| 5 | 15 | 485 |
| 15 | 15 | 970 |

Figure D.8: Maximum deviation in dew point temperature according to the extended uncertainty $U_{95,gas}$

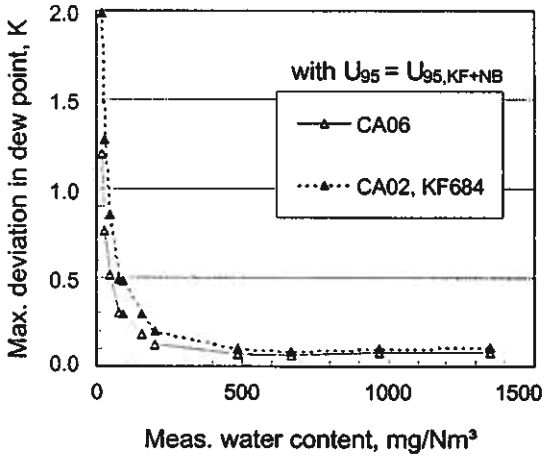


Measured Values:

| T | P | WC |
|---|---|---|
| °C | bar | mg/Nm³ |
| -15 | 100 | 18 |
| -15 | 60 | 27 |
| -5 | 100 | 45 |
| -5 | 60 | 79 |
| 5 | 100 | 90 |
| 5 | 60 | 155 |
| -5 | 15 | 203 |
| 5 | 15 | 485 |
| -5 | 5 | 668 |
| 15 | 15 | 970 |
| 5 | 5 | 1350 |

Figure D.9: Maximum deviation in dew point temperature according to the extended uncertainty $U_{95,KF+NB}$ in the measured water contents.



# D.9 Supplement to the Sensitivity Analysis

## D.9.1 Volume Measurement with the Wet Type Gas Meter

### D.9.1.1 Measurement of the Gas Meter Exhaust Humidity

The surface of the sealing liquid (SFK) as well as the continuously wetted rotating measuring chambers represent a large area for mass transfer for the gas flowing through the wet gas meter (NGZ). Therefore when determining the dry gas volume the volume part resulting from the vapour pressure of the sealing liquid $p_{SFK}$ has to be deducted from the measured volume. If ideal gas phase is considered the following results:

$$V_{dry} = V_{NGZ} \cdot \frac{p_{NGZ} - p_{SFK}(\vartheta_{NGZ})}{p_{NGZ}} \tag{D.33}$$

$p_{NGZ}$ = pressure of the humid gas in the wet gas meter

In case the sealing liquid (SFK) of the wet gas meter is not pure water, the dry gas volume $V_{dry}$ cannot be determined solely with the saturation vapour pressure $p_{oW}$ of pure water at the temperature of the wet gas meter $\vartheta_{NGZ}$ (see equation 3.2). If, however, the sealing liquid still is regarded as being pure water, the following error results when estimating the dry gas volume:

$$\frac{\Delta V}{V_{dry}} = \frac{V_{dry} - V_{dry(SFK=water)}}{V_{dry}} = 1 - \frac{p_{NGZ} - p_{oW}(\vartheta_{NGZ})}{p_{NGZ} - p_{SFK}(\vartheta_{NGZ})} \tag{7.34}$$

In order to check the assumption of a one hundred per cent saturation of the gas phase at the exit of the wet gas meter measurements were carried out with pure water as the sealing liquid in the wet gas meter.

**Measurement of the degree of humidity $\varphi_{water}$:**

Figure D.10 shows the experimental set up for determination of the degree of humidity after flowing through the wet gas meter NGZ. Prior to the start of the measurements NGZ was freshly filled with de-mineralised water.

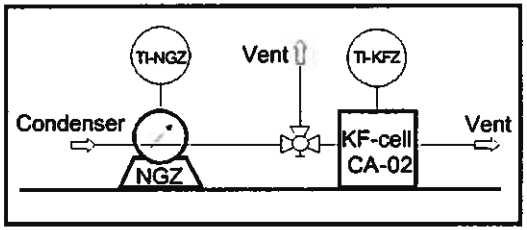


Figure D.10: Measurement of the degree of humidity (experimental set up).

Argon 5.0 has been used as gas. With a slight over-pressure to ambient the gas flows from the plant into NGZ in which it is in mass exchange with the SFK. By positioning the three way ball valve (DWH) first purging of the line connecting to the Karl-Fischer measuring device for about three hours is accomplished in order to guarantee thermal and mass equilibrium between measuring gas and the wall of the connecting hose. A Mitsubishi moisture meter (model CA-02) was used as analysing device. In order to prevent

premature condensation the temperature of the connecting line and of the KF-cell were kept above that of the NGZ.

**Evaluation:**

The volume indicated by the wet gas meter is corrected with the correction factor of the NGZ ($V_{corr}$= $f_{corr.}$*$V_{reading,NGZ}$) and is used as reference value for calculation of the water content from the mass of water measured in the CA-02.

The degree of humidity is estimated by comparing the measured water content to the theoretical value at a one hundred per cent saturation (degree of humidity $\varphi_{water}$= 1). The water content at complete saturation is calculated from the saturation vapour pressure of pure water according to equation (D.14) with the water temperature of the NGZ $\vartheta_{NGZ}$ by assuming an ideal gas mixture:

$$WC_{theo.} = \frac{m_{wat.,theor.}}{V} = \frac{p_{oW}(\vartheta_{NGZ}) \cdot M_{water}}{R \cdot T_{NGZ}} \quad \text{with} \quad R = 8.3145 \frac{J}{mol \cdot K}, \quad M_{water} = 18.02 \frac{g}{mole} \tag{D.35}$$

The degree of humidity is defined by: $\varphi_{water} = \frac{m_{water,meas.} / V_{corr.}}{WC_{theor.}}$ (D.36)

By taking into account the measuring uncertainty this water content measurement showed that the gas at the exit of the wet gas meter was only saturated to about 92.5% ($\varphi_{water}$= 0.925). With

$$p_{SFK}(\vartheta_{NGZ}) = \varphi_{humid} \cdot P_{oW}(\vartheta_{NGZ}) \tag{D.37}$$

the following relative errors in the measurement of the volume result for two chosen conditions:

$p_{NGZ}$ = 1 bar and $\vartheta_{NGZ}$ = 23°C: $\frac{\Delta V}{V_{dry}} = 1 - \frac{10^5 - 2610}{10^5 - 0.925 \cdot 2610} = 0.22\%$ (D.38)

$p_{NGZ}$ = 1 bar and $\vartheta_{NGZ}$ = 30 °C: $\frac{\Delta V}{V_{dry}} = 1 - \frac{10^5 - 4246}{10^5 - 0.925 \cdot 4246} = 0.33\%$ (D.39)

### D.9.1.2 Methanol Losses During the KF-Measurement

When carrying out several KF-measurements directly one after the other decrease of the liquid level in the anode chamber of the KF-cell can be detected. As the anode liquid mainly consists of the solvent methanol, in first order one can assume that the decrease in the liquid level in the KF-cell can be attributed solely to a loss of methanol[43].

[43] This assumption is backed by the recommendation of the manufacturer of the KF-chemicals used in this work to use pure water free methanol (water content max 0.005%) for refilling [83].



**Measurements of the degree of humidity $\varphi_{Methanol}$:**

In order to estimate the mass losses of methanol during the KF-measurement the whole KF-cell unit (analytic cell + magnet stirrer unit) was mounted on an analytic scale. The connection to and from the cell were routed as tension free as possible. The remaining influences from ambient (vibration etc.) were taken into consideration by assuming a weighing error of ±2 g.

Due to the construction of the KF-cell a direct measurement of the temperature of the anode liquid inside the glass cell was not possible. Therefore the KF-cell was inserted into a thermostated box thus insulating it from ambient. The temperature inside the box was measured. The error compared to a direct measurement of the anode liquid temperature was estimated to be ±1 K.

**Evaluation:**

As had been done for checking the degree of saturation at the exit of the wet gas meter the mass loss of methanol measured was referred to a theoretical value. The theoretical value corresponds to a complete saturation of the gas with methanol when flowing through the KF-cell. The vapour pressure of methanol was calculated from equation (D.16) for the respective temperature of the KF-cell. The theoretical contents of methanol is being calculated assuming ideal gas mixture according to:

$$\frac{m_{MeOH,theor.}}{V} = \frac{p_{oMeOH}(\vartheta_{KFZ}) \cdot M_{MeOH}}{R \cdot T_{KFZ}} \quad \text{with} \quad R = 8.3145 \frac{J}{mole \cdot K}, \quad M_{MeOH} = 32.04 \frac{g}{mole} \tag{D.40}$$

The ratio of the value measured to the theoretical one at complete saturation gives the degree of saturation with which the gas leaves the KF-cell.

$$\varphi_{MeOH} = \frac{m_{MeOH,meas.}}{m_{MeOH,theor.}} \tag{D.41}$$

The results of the measurements showed that in average the gas was saturated to 94.3% ($\varphi_{MeOH}$= 0.943)with methanol at the exit of the KF-cell.

### D.9.1.3 Mass Transfer in the Wet Type Gas Meter

The highly hygroscopic methanol carried along with the gas from the anode liquid of the KF-cell is being absorbed by the sealing liquid (mainly water) and causes an increase in methanol content in the SFK. Due to the higher vapour pressure of the methanol-water mixture compared to that of pure water an error results when calculating the dry volume according to equation (D.1) which counteracts the error due to incomplete saturation. In order to estimate the maximum allowable methanol content of the SFK a simple calculation model is established for the methanol enrichment of the sealing liquid. With the help of this calculation model and assuming a maximum allowable relative error of ±0.25% (lack of complete saturation of the gas flow with sealing liquid in the NGZ and influence of methanol) when estimating the dry gas volume it is estimated after

how many KF-measurements the sealing liquid has to be replaced at the latest. This has been done for different boundary conditions.

**Estimation of the enrichment of methanol in the wet gas meter (NGZ):**

In order to estimate the momentary methanol content a mass balance around the NGZ is being performed with the following simplifications:

- Assuming an ideal gas mixture and ideal liquid phase one has:

the ideal gas law: $$p \cdot V = n \cdot R \cdot T \quad \text{(D.42)}$$

Raoult's law: $$p_{tot} \cdot y_i = x_i \cdot p_{oi}(T) \quad \text{(D.43)}$$

Dalton's law: $$p_{tot} = \sum_i p_i \quad \text{(D.44)}$$

- The system NGZ as well as the incoming and the outgoing streams are isothermal and isobaric.
- At the outlet of the KF-cell the gas stream is completely saturated with methanol.
- At the outlet of the NGZ the gas stream is completely saturated with the sealing liquid SFK.
- The change in moles of the sealing liquid is neglected.
- The gas solubility of the components of the dry gas stream in the SFK is neglected.

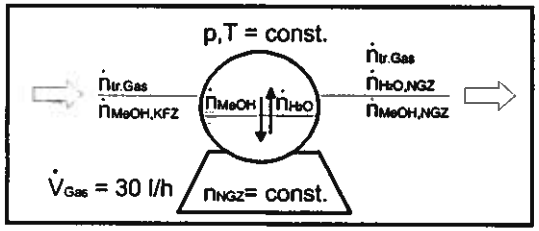


Figure D.11: Entering and leaving mole streams for a balance around the NGZ gas phase (saturation case)

One has to distinguish between the enrichment of methanol in the sealing liquid during the KF-measurement (saturation case, see figure D.11) and the de-saturation during the three hours of purging with methanol free (humid) gas prior to the start of a water content measurement.



**Balance of methanol during saturation:**

$$\frac{dn_{MeOH}}{dt} = \dot{n}_{Gas} \cdot (y_{MeOH,in} - y_{MeOH,out}) \quad \text{(D.45)}$$

$$n_{NGZ} \cdot \frac{dx_{MeOH}}{dt} = \frac{p_{oMeOH}(T) \cdot \dot{V}_{Gas}}{R \cdot T}\left(1 - x_{MeOH}\right) \quad \text{(D.46)}$$

$$\int_{x_{MeOH,t0}}^{x_{MeOH,t1}} \frac{1}{1 - x_{MeOH}} dx_{MeOH} = \frac{p_{oMeOH}(T) \cdot \dot{V}_{Gas}}{n_{NGZ} \cdot R \cdot T} \cdot \int_{t0}^{t1} dt \quad \text{(D.47)}$$

$$\boxed{x_{MeOH,t1} = 1 - (1 - x_{MeOH,t0}) \cdot \exp\left\{-\frac{p_{oMeOH}(T) \cdot \dot{V}_{Gas}}{n_{NGZ} \cdot R \cdot T}(t_1 - t_0)\right\}} \quad \text{(D.48)}$$

**Balance of methanol during de-saturation:**

$$\frac{dn_{MeOH}}{dt} = \dot{n}_{Gas} \cdot (y_{MeOH,in} - y_{MeOH,out}) = -\dot{n}_{Gas} \cdot y_{MeOH,out} \quad \text{(D.49)}$$

$$n_{NGZ} \frac{dx_{MeOH}}{dt} = -\frac{p_{oMeOH}(T) \cdot \dot{V}_{Gas}}{R \cdot T} \cdot x_{MeOH} \quad \text{(D.50)}$$

$$\int_{x_{MeOH,t0}}^{x_{MeOH,t1}} d\ln x_{MeOH} = -\frac{p_{oMeOH}(T) \cdot \dot{V}_{Gas}}{n_{NGZ} \cdot R \cdot T} \cdot \int_{t0}^{t1} dt \quad \text{(D.51)}$$

$$\boxed{x_{MeOH,t1} = x_{MeOH,t0} \cdot \exp\left\{-\frac{p_{oMeOH}(T) \cdot \dot{V}_{Gas}}{n_{NGZ} \cdot R \cdot T}(t_1 - t_0)\right\}} \quad \text{(D.52)}$$

**Validation of the model for estimating the methanol accumulation:**

In order to check the model samples of the sealing liquid were taken over a longer period and the methanol content was estimated by means of gas chromatography (GC)[44]. Figure D.12 gives a comparison of the results from the GC-measurements and the calculated results.

$V_{NGZ} = 2.5\ dm^3$ (= filling volume SFK in NGZ)

Model constants used: $\rho_{H_2O} = 1\ kg/dm^3$

$$n_{NGZ} = \frac{\rho_{H_2O} \cdot V_{NGZ}}{M_{H_2O}} = 138.7\ mole$$

Figure D.12 indicates that the values obtained from the model at higher methanol contents always are slightly above the measured ones. Among others this is a consequence of the model

assumption that the gas always leaves the KF-cell and also the NGZ completely saturated. The course of the methanol concentration in the sealing liquid is correctly represented by the model.

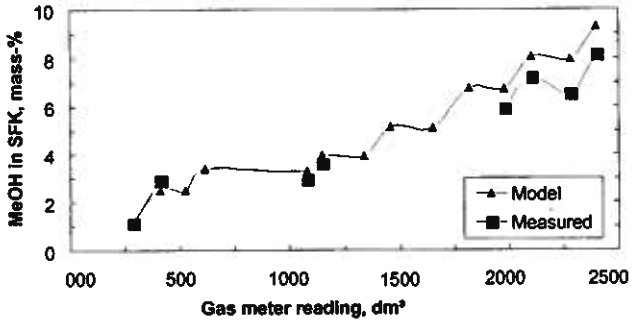


Figure D.12: Comparison of the values of methanol content in the sealing liquid from model and from GC-measurements

**Consequences on the realisation of the KF-measurements:**

The allowable methanol content can be calculated with the help of the developed model for different boundary conditions in order not to exceed the relative over all error of ±0.25% (from incomplete saturation in the NGZ and influence of methanol) when estimating the dry volume.

The calculations were carried out for two representative temperatures of +23 °C and + 30 °C. As the temperature of the wet gas meter and the KF-cell is determined mainly at room temperature these two temperatures are representative for winter and summer operation of the measuring device, respectively. Figures (D.13) and (D.14) give the results of the model calculations for measuring runs of 20 and 30 individual KF-measurements. The running in time of three hours with 30 l/h for reaching stationary operation (mass transfer and temperature equilibrium between gas and pipe wall) corresponds to the 90 litres assumed for purging. The start and the end of a measuring run is marked, respectively. In order to stay within the error limit of 0.25% for the determination of the dry gas volume the methanol content in the sealing liquid shall not exceed the value of 6.7 mass-% (4.7 mass-%) at +23°C (+30°C). Due to this reason the sealing liquid must be completely replaced after 460 single KF-measurements (or 23 KF-measurement runs of 20 single measurements each) at + 23°C. As the vapour pressure of the methanol containing sealing liquid rises more sharply with temperature than the vapour pressure of pure water at +30°C, here a change of sealing liquid already is required after 7 and 11 KF-measurement runs, respectively.

[44] We would like to thank Miss Zimmermann of the Institut für Thermische Verfahrenstechnik der Fakultät für Chemieingenieurwesen und Verfahrenstechnik der Universität Karlsruhe (TH) for carrying out the GC-measurements.



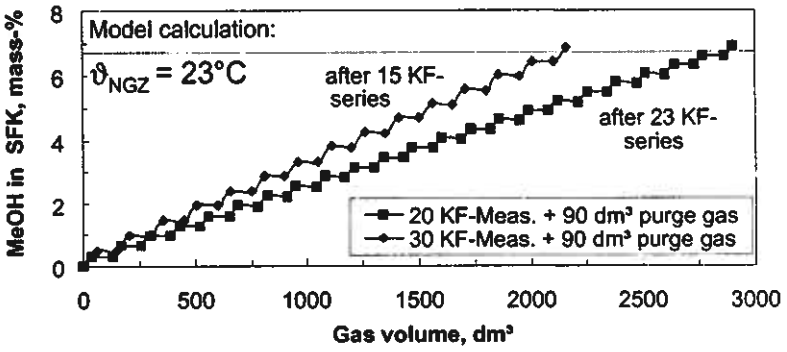


Figure D.13: Results of model calculation for a methanol content at a wet gas meter temperature of +23 °C

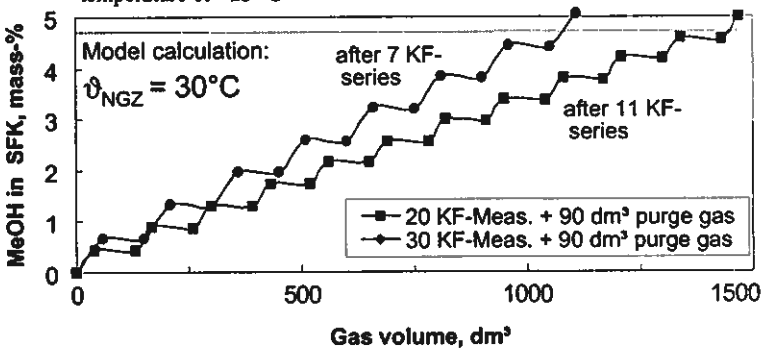


Figure D.14: Results of model calculation for a methanol content at a wet gas meter temperature of +30 °C

As the model predicts slightly higher methanol contents compared to the GC-measurements (see figure D.12) there is a certain safety margin with respect to the intervals for changing the sealing liquid. For the real operation, therefore, one can tolerate one or two additional KF-measuring runs between changing intervals.

## D.9.2 Water Content Measurements with a "Well Defined History"

For the ternary mixture methane (97 mole-%)-ethane (3 mole-%)-water (see chapter 3.2.2), water content measurements have been carried out at temperatures of -15°, -5°, +5° and +15°C and pressures of 100, 80, 60 and 40 bar, as well as for 15 bar at -15°, -5° and +5°C. Each operating point has been approached by a fixed route, to carry out measurements with a "well defined history". The objective of this investigations was to find out, if a distinct statement about the kind of the condensed phase (in condenser K2) is possible, in connection with the knowledge of the "history" of the measuring point. From the "history" the kind of the phase(s) may be derived. Besides the thermodynamically stable phase (see states in figure D.15), metastable phases may

occur as a result of kinetic inhibition (ice or liquid water, dependent on the location of the operating point, see annex A.3.2). For the route through the ice-region it is to be expected, that first a metastable ice phase is present, after reaching the hydrate-region. In the case of a route through the liquid-water-region, a metastable liquid water phase is expected due to the kinetic inhibition. This section treats the experimental procedure and results in detail.

**Experimental Procedure**

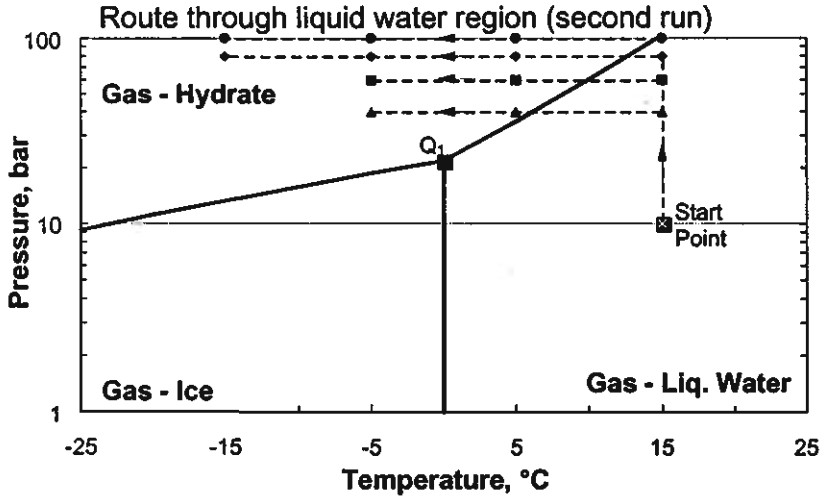


Figure D.15: Route through the liquid-water-region (2nd run)

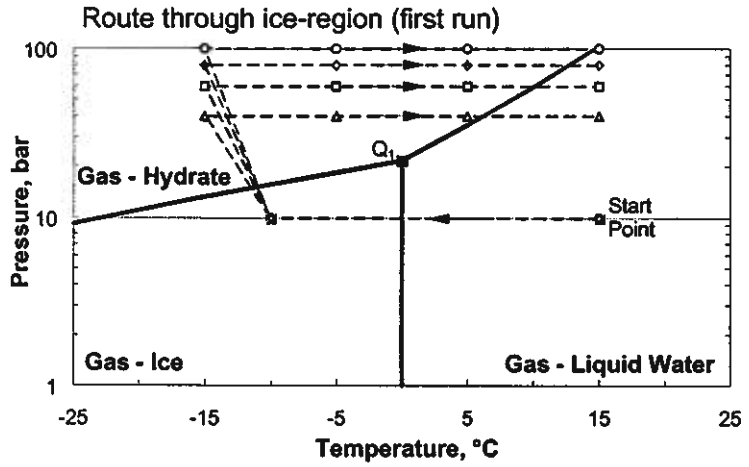


Figure D.16: Route through the ice-region (1st run)



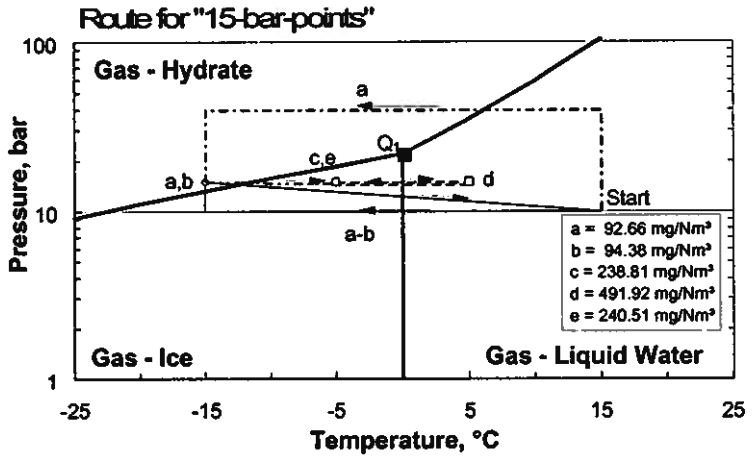


Figure D.17: Modified routes at 15 bar pressure

The pressures have been measured (in the order 100, 80, 60, 40 bar) in a first run through the ice-region (see figure D.16) and in a second run through the liquid-water-region (see figure D.15), starting at 10 bar and +15°C each.

After changing pressures or temperatures, a time interval of at least three hours was passed to ensure equilibrium states. For the operating points -15°C/ 60bar and -15°C/ 40bar however, only a first run has been carried out. At the beginning of each run, the sealing liquid of the wet gas meter was changed and the KF-cell was conditioned (change of chemicals and molecular sieve). Since the hydrate boundary is below the melting temperature of ice for the 15 bar-isobar, the approaching route had to be modified according to figure D.17. Therefore, the sealing liquid and KF-chemicals have been changed after measuring point "c".

Additional information about the kind of the condensed phase could be obtained by visual investigations of the condenser K2, using the video-endoscope-system. Three different kinds of visual states were noticed.

- **FREE:** No precipitation on the sapphire window are visible. The condenser walls are free of precipitation, too.
- **GREY:** The sapphire window is clear, but the walls appear with a "white-grey" cover.
- **HUMID:** At temperatures above the melting point, the sapphire window is covered, but the walls are free of precipitation.

The respective water contents of each pressure- and temperature stage are listed in Table D.10, together with the visual states from the endoscope system. At the measuring point "e" (15 bar),

the sapphire window was covered by light scattering small particles, which were assumed to be ice-crystals, but not liquid water droplets.

Table D.10: Water content and visual state inside condenser K2 (from video endoscope system). First run routes through the ice-region and second run through the liquid water region.

| | WC in mg/Nm³ | -15 °C | -5 °C | +5 °C | +15 °C |
|---|---|---|---|---|---|
| 100 bar | $WC_{first\ run}$ | 20.2 (FREE) | 44.2 (FREE) | 95.6 (FREE) | 197.9 (HUMID) |
| | $WC_{second\ run}$ | 19.9 (GREY) | 44.1 (GREY) | 108.4 (HUMID) | 200.3 (HUMID) |
| 80 bar | $WC_{first\ run}$ | 19.9 (FREE) | 48.0 (FREE) | 111.7 (FREE) | 228.2 (HUMID) |
| | $WC_{second\ run}$ | 21.0 (GREY) | 49.2 (GREY) | 122.3 (HUMID) | 231.4 (HUMID) |
| 60 bar | $WC_{first\ run}$ | 25.1 (FREE) | 61.5 (FREE) | 138.9 (FREE) | 281.1 (HUMID) |
| | $WC_{second\ run}$ | - | 63.6 (GREY) | 152.3 (HUMID) | 284.9 (HUMID) |
| 40 bar | $WC_{first\ run}$ | 36.5 (FREE) | 88.5 (FREE) | 202.4 (FREE) | 398.0 (HUMID) |
| | $WC_{second\ run}$ | - | 87.7 (GREY) | 208.0 (HUMID) | 395.8 (HUMID) |

| | a (-15 °C) | b (-15°C) | c (-5 °C) | d (+5 °C) | e (-5°C) |
|---|---|---|---|---|---|
| 15 bar | 94.4 (GREY) | 92.7 (GREY) | 238.8 (GREY) | 491.5 (HUMID) | 240.5 (HUMID) |

The absolute differences between the respective measured water content values ($WC_{first\ run}$ - $WC_{second\ run}$) are plotted in figure D.18. The differences in water content are within the experimental uncertainty, for measuring points in the hydrate region below the melting temperature and for measuring points, where liquid water or ice exists as a stable phase. For temperatures above +5°C and pressures above the hydrate boundary ($p_{Hyd.}$(+5°C) = 35.4 bar, calculated with CSMHYD [28]), deviations between the different routes have been observed, which were larger than the experimental uncertainty (see annex D.3.1).

The large deviations between the +5°C-measuring points may be attributed to the occurrence of different kinds of condensed phases. This assumption is supported by the different kind of visual states in condenser K2. In the first run, neither a solid nor a liquid phase has been observed on the images. But after crossing the hydrate boundary, a droplet like precipitation covered the sapphire window immediately. In the second run, droplets have been observed on the sapphire window, which did not vanish during the temperature reduction from +15°C to +5°C (into the hydrate region). The water content, measured at +5°C was significantly higher in the second round than in the first run measurements.



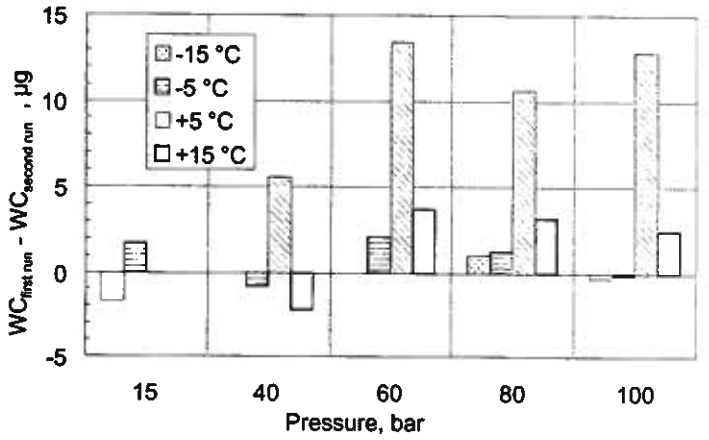


Figure D.18: Absolute differences in measured water content values, with respect to different approaching routes. (First run routes through the ice-region and second run through the liquid water region.)

A further cooling down to -5°C showed two effects. First, the droplet like precipitation vanished and a white-grey cover was formed on the condenser walls. Second, a short-time temperature peak of about +0.3 K was observed in the condenser K2. This effect may be attributed to the heat of phase transition during the hydrate- or ice forming[45].

To determine the kind of the precipitation, the temperature of condenser K2 was increased isobaric up to +15°C, after the second run of the 60 bar-isobar was finished. The white-grey cover vanished at about +10°C under formation of small droplets on the sapphire window. The corresponding hydrate boundary was calculated using the CSMHYD-program [28] to be +10.1°C, which confirms the assumption, that the observed precipitation have been hydrates.

The following hypotheses may be suggested referring to the kind of condensed phase, based on measured values and visual observations via the video endoscope system:

Measuring points located in the hydrate region, which were routed through the ice region, exhibited a metastable ice phase, directly after crossing the hydrate boundary. A complete transformation into a stable hydrate phase can be excluded with a high certainty, because of the relatively short residence time of maximum 20 hours (see chapter 3.3). Though the high induction time observed ([22] [28], see annex A.3), a partial transformation might have happened with increasing residence time in the hydrate region. From this follows, that a metastable ice- and a stable hydrate phase might have coexisted. Moreover, one may assume, that after crossing the melting temperature of ice, the remaining ice inside the cooling coil began to melt. Hwang et al.

[45] On the other hand, this effect possibly may be attributed to the PID-control of the cryostat bath, since this behaviour has been observed in some cases outside a hydrate region (long-term measurements with nitrogen-water, see annex D.4.1).

[145] report, that hydrate formation proceeds much faster in the presence of melting ice compared to "dry" ice. The heat of phase transition, emitted by the exothermal hydrate forming process will be absorbed by the endothermal melting process. Additionally, the re-orientation of water molecules is quite possible in the liquid phase. These reasons support the high probability that water molecules, dismissed from the ice crystals during the melting process, are directly incorporated into the hydrate structures. This is proved by the fact, that the condenser was dry at the first run at +5°C, while a typical white-grey cover has been observed at -15°C/ 15 bar and at point "b". Furthermore it may be concluded, that in the first run at +5°C/ (40-100 bar), hydrate was solely present, by all means. This statement is supported by the heavy water release after leaving the hydrate region. The importance of the conditions inside the condenser (besides the cooling coil) can be derived from the second-run results. In the case, if a humid atmosphere is present inside the condenser (recognisable by multiple droplets on the sapphire window), so the (essentially higher) water content above the metastable liquid phase will be measured. Due to the high differences in water contents for +5°C measurements, the presence of a possibly coexisting hydrate phase is of subordinate importance to the water content. From this follows, that the liquid phase plays a decisive role on the equilibrium phase composition, if the formation of droplets is observed on the sapphire window.

The comparison of water contents of the first and second run shows that measuring points at -5°C and -15°C differ only slightly. The measured values in the second run were higher, as well as lower than the values in the first run, respectively. An influence of pressure was not observed. Because of the negligible deviations between the two runs in the hydrate region (on an average $< 2$ µg), the existence of a metastable liquid water phase can be excluded. In the case of a metastable liquid water phase, the differences between first and second run might have been substantially higher, corresponding to Makogon (see. table 3.5).

A comparison of measuring points "c" and "e" inside the ice region shows, that "e" has a slightly higher water content (1.7 mg/Nm³). A distinct statement, if this observation can be attributed to the existence of a subcooled liquid aqueous phase is not possible, since the deviations are within the uncertainties.



# Annex E

# Methods for Water Content - Dew Point Conversion

For the user the knowledge of the dew point or the water content, respectively, is of interest depending on the application. The dew point directly gives the information at which temperature water starts to condense at isobaric temperature decrease; the water content is needed for balancing of water amounts. As in practice, however, either the dew point or the water content is estimated depending on the procedure applied it is necessary to convert the properties into one another. Due to the strong non-ideal behaviour of most mixtures there is no simple thermodynamic interrelation between both properties. In the literature several procedures for recalculations can be found. Up to now no exclusive method exists. Sometimes large differences in water content / dew point are estimated with different methods [148].

In this chapter selected methods are presented in more detail. Here methods which are used in practice are considered. The existing methods can be classified into procedures

- which are based on mainly empirical correlation (sometimes some input parameters have to be read from diagrams or tables),
- which merely are based on diagrams (nomograms) and
- which apply equations of state.

A strict separation of the methods is not possible. Often correlations also are available in diagram form or correlations were developed on the basis of diagrams.

## E.1 Empirical Correlations

The correlation of Bukacek [155] which is an equation developed according to Raoult's law is one of the most used correlations in the natural gas industry. It is listed as the standard method for calculating the water content WC from the dew point in ASTM D1142-95 [95]:

$$WC_{humid}\left(p, T_{dew}\right) = \frac{A(T_{dew})}{p} + B(T_{dew}) \left[\frac{g_{H2O}}{m^3_{Gas,humid}}\right] \qquad (E.1)$$

In addition to the pressure a constant A proportional to the vapour pressure of pure water and a temperature dependent constant B which is fitted to experiments is used[31]. Gas composition has been taken into consideration indirectly when setting up the correlation as the data base for

[31] Constants A and B are listed in tables in [59] and [155] for a temperature range of -40 to +460 °F (-40°C to +238°C) (reference state: 14.7 psia, 60 °F).

determining B was the water content measured for methane [202], methane - ethane [203] and for six natural gases.

At lower temperatures (hydrate region) Bukacek only had water content data available for one multicomponent mixture. These were the data of Skinner [204] who had measured the water content for a nearly nitrogen free natural gas. The exactitude of these data is questioned by Sloan et al. [219]. These authors assume, that the condensed phase during measurements could have been a metastable ice or liquid water phase but not a stable hydrate phase. Also McKetta and Wehe [151] and McCarthy [150] used the data of Skinner as a major basis for their water content diagrams in the area of low temperatures. Bukacek indicates that the water contents in natural gases can be reproduced within the experimental uncertainties. When considering the uncertainties of the data used for setting up the correlation Bukacek guesses the error of his correlation with roughly ± 4 % of the water content under consideration. This estimated error in water content leads for instance at 60 bar, -5°C (≈91 mg/Nm³) to an uncertainty of only ±0.5 K for the dew point.

As most of the correlations have been developed for calculation of the water content a simple determination of the dew point from a given water content often is not possible. As a rule the dew point can only be calculated from the water content by iteration.

## E.2 Diagrams

In practice preference is given to diagrams showing the water content in semi-logarithmic scale over dew point temperature as they allow a fast and simple allocation of a measured water content to a dew point temperature and vice versa. Out of the numerous published diagrams the one of McCarthy et al. (1950 [151]) and the one established in 1958 by McKetta and Wehe [150] have found the widest distribution. These diagrams mainly were based on the relatively few measurements from the 1940ies (among others Olds et al. [202], Skinner [204]). Due to the data used when developing the diagrams they are only valid for sweet natural gases with a low content of nitrogen and higher hydrocarbons. (sweet natural gases are nearly free of sulphur hydrogen and of carbon dioxide [152]). The exact gas composition is not taken into consideration. Contrary to McCarthy, McKetta and Wehe try to take into consideration the influence of the gas composition with a correction factor depending on the relative density of the gas (density of the natural gas at standard conditions divided by the density of air at standard conditions). McKetta and Wehe already took into consideration the hydrate formation region when setting up the diagram. Except of a re-scaling of the axes due to a recalculation to SI-units the diagram of McKetta and Wehe still is in use today nearly unchanged compared to the original version [152] [153][32]. In 1993 Wichert et al. [157] extended it for use at high pressures (from 689 to 1000 bar) and high temperatures (from 149 to 200°C) by means of computer simulations. Campbell [148] has based his diagram on the work of McKetta, McCarthy and Bukacek. Compared to the version of

[32] Kazim [156] only recently has published a correlation between the water content and the dew point based on the diagram of McKetta and Wehe.



McCarthy the diagram of Campbell shows nearly identical values. At low pressures the water contents are slightly higher. In the mean time the diagrams set up for sweet natural gases also can be used for sour natural gases. With the help of additional diagrams the values for the sweet natural gases are corrected according to the contents of carbon dioxide and sulphur hydrogen [149] [154] [157] [158].

It is plausible that an exact determination of the water content or of the dew point with the help of diagrams only is quite limited. In addition to the insufficient consideration of the gas composition during establishing and evaluation, interpolation and reading errors pose an additional source of errors. Campbell [148] indicates an error of 6-10 % for the water contents read from his diagram. At 60 bar, -5°C (≈88 mg/Nm³) the error of 10 % would correspond to an error of about ± (1.5 K to 2 K) in the dew point taking into consideration the additional sources of errors when evaluating the diagrams.

## E.3 Equations of State

The simplest and thermodynamically founded equation for calculating the water content is Raoult's law derived from equation (A.10) assuming ideal behaviour and neglecting the Poynting term:

$$p\, y_W^V = p_{oW}\, x_W^L \tag{E.2}$$

In case the liquid phase is considered as pure water due to the small gas solubility ($x^L_W$=1) it follows:

$$y_W^V = \frac{p_{oW}(T_{dew})}{p} \tag{E.3}$$

The calculation of the mole fraction of the water $y^V_W$ in the gas phase only with the saturation of pure water $p_{oW}$ and the system pressure p, however, only leads to an acceptable prediction as ideal gas behaviour is being assumed. Cambpell [148] therefore only suggests the application of equation (E.3) up to a pressure of 4 bar. Transferring the mole fraction into water content is achieved by applying equation (1.3).

In addition to the correlation of Bukacek ASTM D1142-95 [59] gives an additional equation for estimating the water content from measured dew points which can be deducted directly from equation (E.3) with the assumption of ideal gas.

$$WC_{humid}\left(p, T_{dew}\right) = \frac{1}{v^V_{oW}(T_{dew})} * \frac{p_b}{p} * \frac{T_{dew}}{T_b} \left[\frac{g_{H2O}}{m^3_{Gas,humid}}\right] \tag{E.4}$$

According to equation (E.4) the water content is proportional to the reciprocal value of the specific volume of pure water $v^V_{oW}$ at the dew point temperature $T_{dew}$. The remaining terms merely serve to recalculate the water content from pressure p and dew point temperature $T_{dew}$ of the measurement to the reference condition b. The ASTM-standard prescribes that the gas is let down to near ambient pressure prior to dew point measurement if the water content shall be

estimated with the help of equation (E.4). Numerical values for $v^{V}_{ow}$ that are taken from water vapour tables ([159] [160]) are listed for a temperature range of 0 to 100°F (-18 to +38°C).

In addition to these „simple" methods which are based on the assumption of ideal gas behaviour and do not take into account the gas composition the literature contains numerous, sometimes very complicated, equations of state which were especially fitted or developed by the authors to the application of hydrocarbon - water systems and which, in principle, allow to calculate the water content or the dew point. An evaluation of these methods revealed that no calculation procedure can be recommended without restrictions for the aims of this work - the calculation of water contents and dew points into each other for multicomponent systems, for a pressure range of 1 to 300 bar and at temperatures of -50 to +40°C. The results of this evaluation are summarised hereafter.

The evaluation of the literature revealed that the equations of state in most cases were developed or fitted to describe the phase equilibria at comparatively high temperatures. The consequence is that the equations either do not cover the temperature range of this work (-50 to +40°C) (Eubank [161]) or cover only the high temperature side (for instance, Victorov [165], Peng, Robinson [166], Soreide [168], Lovland [170], Kabadi [181]). With a few exceptions the recommended application range of the equations of state starts only at temperatures above +25°C. By doing so the authors exclude the region of a possible solid phase (ice or hydrate) [165]. Some authors explicitly do not recommend an extrapolation of the equations of state beyond the application range indicated [181]. When extrapolating the equations of state beyond the range of properties used for establishing the method in general one has to expect an increase in errors. Test calculations with selected equations of state revealed that the water contents were predicted increasingly worse in a temperature range below +25 °C. One of the main reasons is the inexact representation of the water vapour pressure of pure water in this temperature region.

As the water content in the vapour phase of hydrocarbon mixtures can be represented sufficiently well by modified equations of state above ambient temperature and from low to high pressures, during the last years further developments of equations of state for hydrocarbon-water mixtures aimed at a good reproduction of the concentrations of all phases with one calculation procedure. Especially the description of the liquid liquid equilibria (water and hydrocarbon rich phases) and the representation of the gas solubility in the liquid water phase pose high demands on the quality of an equation of state (or the mixing rules, respectively).

In addition one tries to take into account effects of association occurring at extreme high pressures and in the presence of salts in water hydrocarbon mixtures when developing the equations of state [172] [173]. This also includes trying to take into account the influence of hydrogen bounds on the interactions of the molecules in more detail [175]. By developing procedures based to a great extent on theoretical foundation the complexity of the equations rise more and more up to now, representing the phase behaviour only partly with sufficient accuracy [171] [174]. When representing the water solubility in the hydrocarbon rich vapour in general these equations show a nearly identical behaviour leading to the fact that the more complex equations are not superior to the simple ones, in most cases cubic equations [171] [176].



The calculation procedures which include the temperature range below the water triple point mainly were developed to predict the hydrate formation conditions as accurately as possible (for instance Sloan [28] [29], Anderson [162], Du [167], Wu [171]). In these cases the gas phase is described with help of a cubic equation of state. For description of the solid phase models describing the occupancy of the hydrate cages with gas molecules analogous to an adsorption are used (model of van der Waals and Platteeuw). The intermolecular interactions between the water molecules forming the cages are described using intermolecular potentials (for instance the Kihara potential [31] [163]). With the help of these comparatively complex methods the equilibrium water content above a solid hydrate phase can be calculated. However, the known calculation procedures were not developed for an exact representation of the water content in the vapour phase. The calculation procedure of Sloan et al. is available under the name „CSMHYD.EXE"[33] as a computer program for DOS and is included in the books of Sloan [28] and [29] on a disk, respectively. For the new edition the program has been revised, too. According to the year of publication the different versions of the program hereafter will be called CSMHYD90 [28] and CSMHYD98 [29]. However, as the computer code of the programs is not available, a detailed description of the calculation procedure is not possible.

[33] CSMHYD =Colorado School of Mines HYDrate Prediction Program

# Annex F

# Supplements to the Model Design

## F.1 Alpha-Function by Stryjek and Vera

The alpha-function for the Peng-Robinson equation of state [16] as modified by Stryjek and Vera (PRSV) [191] reads:

$$\alpha_{PRSV}(T_R)^{1/2} = 1 + \kappa\ (1 - T_R^{1/2}) \tag{F.1}$$

$$\kappa = \kappa_0 + \kappa_1 \left(1 + T_R^{1/2}\right)\left(0{,}7 - T_R\right) \tag{F.2}$$

$$\kappa_0 = 0.378893 + 1.4987153\,\omega - 0.1731848\omega^2 + 0.0196554\omega^3 \tag{F.3}$$

$\omega$ : acentric factor ($\omega_{H2O}$= 0.3438 [191])

$\kappa_1$ : substance specific parameter ($\kappa_{1,H2O}$= -0.06635 [191])

## F.2 Survey of Literature Data

Table F.1: Survey of phase equilibrium data for selected binary mixtures containing water, available in literature (condensed phase according to the authors: **ice or liquid water**).

| **Methane - Water** Author | Year | Number of points | No. exp. points ≤40°C u. 300bar | Measured variables | Temperatures in °C | Pressure range in bar |
|---|---|---|---|---|---|---|
| Olds et al. [202] | 1942 | 27 | 9 | $Y_W$ | 38, 71, 104 | 14 ÷ 207 |
| Yarym-Agaev [207] | 1985 | 15 | 5 | $Y_W$ , $X_G$ | 25, 40, 65 | 25 ÷ 125 |
| Yokoyama [208] | 1988 | 6 | 2 | $Y_W$ , $X_G$ | 25, 50 | 30, 50, 80 |
| Rigby, Prausnitz [205] | 1968 | 12 | 3 | $Y_W$ | 25,50,75,100 | 20 ÷ 101 |
| Gillespie, Wilson [206] | 1982 | 16 | 0 | $Y_W$ , $X_G$ | 50 ÷ 316 | 14 ÷ 169 |
| Kosyakov [200] | 1979 | 27 | 27 | $Y_W$ | -40 ÷ 0 | 10 ÷ 101 |



| **Ethane -Water** Author | Year | Number of points | No. exp. points ≤40°C u. 300bar | Measured variables | Temperatures in °C | Pressure range in bar |
|---|---|---|---|---|---|---|
| Song, Kobayashi [220] | 1994 | 4 | 4 | $Y_W$ | 15 ÷ 31 | 3,4 ÷ 4,7 |
| Reamer et al. [209] | 1943 | 41 | 3 | $Y_W$ | 37 ÷ 230 | 22 ÷ 680 |
| Anthony,McKetta [210] | 1967 | 4 | 1 | $Y_W$ , $X_G$ | 35,70,100,135 | 26 ÷ 108 |
| Anthony,McKetta [211] | 1967 | 21 | 8 | $Y_W$ , $X_G$ | 38, 71, 104 | 35 ÷ 347 |
| Coan, King [212] | 1971 | 18 | 4 | $Y_W$ | 25,50,75,100 | 24 ÷ 36 |

| **Propane-Water** Author | Year | Number of points | No. exp. points ≤40°C u. 300bar | Measured variables | Temperatures in °C | Pressure range in bar |
|---|---|---|---|---|---|---|
| Song, Kobayashi [220] | 1994 | 4 | 4 | $Y_W$ | 9 ÷ 27 | 6 ÷ 9 |
| Kobayashi, Katz [213] | 1953 | 74 | 8 | $Y_W$ , $X_G$ | 35 ÷ 145 | 7 ÷ 193 |

| **Butane-Water** Author | Year | Number of points | No. exp. points ≤40°C u. 300bar | Measured variables | Temperatures in °C | Pressure range in bar |
|---|---|---|---|---|---|---|
| Reamer, Olds [214] | 1944 | 26 | 1 | $Y_W$ | 38 ÷ 150 | 3,6 ÷ 44 |
| Wehe [215] | 1961 | 5 | 1 | $Y_W$ , $X_G$ | 38 ÷ 105 | 3,6 ÷ 18 |
| Anthony [210] | 1967 | 8 | 0 | $Y_W$ | 71 | 8,6 ÷ 8,7 |
| Reamer [217] | 1952 | 13 | 2 | $Y_W$ | 38 ÷ 105 | 1,4 ÷ 13,8 |

| **Nitrogen-Water** Author | Year | Number of points | No. exp. points ≤40°C u. 300bar | Measured variables | Temperatures in °C | Pressure range in bar |
|---|---|---|---|---|---|---|
| Rigby, Prausnitz [205] | 1968 | 13 | 3 | $Y_W$ | 25,50,75,100 | 21 ÷ 102 |
| Kosyakov [201] | 1978 | 22 | 22 | $Y_W$ | -40 ÷ 0 | 10 ÷ 101 |

| **Carbon dioxide-Water** Author | Year | Number of points | No. exp. points ≤40°C u. 300bar | Measured variables | Temperatures in °C | Pressure range in bar |
|---|---|---|---|---|---|---|
| Gillespie, Wilson [206] | 1982 | 21 | 6 | $Y_W$ | 16 ÷ 121 | 7 ÷ 203 |
| Coan, King [212] | 1971 | 22 | 5 | $Y_W$ | 25,50,75,100 | 23 ÷ 51 |
| Song,Kobayashi [216] | 1986 | 8 | 8 | $Y_W$ | -18 ÷ 25 | 34,5 ÷ 138 |

| Argon-Water<br>Author | Year | Number of points | No. exp. points ≤40°C u. 300bar | Measured variables | Temperatures in °C | Pressure range in bar |
|---|---|---|---|---|---|---|
| Rigby, Prausnitz [205] | 1968 | 12 | 12 | $Y_W$ | 25,50,75,100 | 20 ÷ 93 |
| Kosyakov [201] | 1978 | 22 | 22 | $Y_W$ | -40 ÷ 0 | 10 ÷ 101 |

Table F.2: Overview about uncertainties of measured quantities from literature (see Table F.1) (hatched fields = quantity not measured;* : estimated)

| Methane-Water | Uncertainty | | | |
|---|---|---|---|---|
| Author | T | P | $Y_W$ | $X_G$ |
| Olds et al. | 0.06 K | 0.2 bar | 2% | |
| Rigby, Prausnitz | 0.03 K | 0.3% | ≈1% | |
| Gillespie, Wilson | void | void | void | void |
| Yarym-Agaev* | 0.1 K | 0.5 bar | 0.04%* | $10^{-11}$* |
| Yokoyama | 0.03 K | 10 mbar | 5% | 5% |
| Kosyakov | 0.1 K | 0.4% | 0.2 ppm | |

| Ethane-Water | Uncertainty | | | |
|---|---|---|---|---|
| Author | T | P | $Y_W$ | $X_G$ |
| Song, Kobayashi | 0.06 K | 0.2 bar | 6% | |
| Reamer et al | 0.06 K | 0.2 bar | ≈3% | |
| Antony, McKetta | 0.12 K | 35mbar/0.2% | 4.6% | 5% |
| Antony, McKetta | 0.12 K | 35mbar/0.2% | 4.6% | 5% |
| Coan, King | 0.05 K | void | void | |

| Propane-Water | Uncertainty | | | |
|---|---|---|---|---|
| Author | T | P | $Y_W$ | $X_W$ |
| Song, Kobayashi | 0.06 K | 0.2 bar | 6% | |
| Kobayashi, Katz | 0.4 K | 1% | void | void |



| Butane-Water | Uncertainty | | | |
|---|---|---|---|---|
| Author | T | P | $Y_W$ | $X_G$ |
| Reamer, Olds | 0.06 K | 0.1% | 0.001 | |
| Wehe | 0.12 K | 35mbar/0.2% | 4.5% | void |
| Antony | 0.12 K | 35mbar/0.2% | 4.6% | |
| Reamer | 0.06 K | 0.1% | 0.001 | |

| Nitrogen-Water | Uncertainty | | | |
|---|---|---|---|---|
| Author | T | P | $Y_W$ | in $X_G$ |
| Rigby, Prausnitz | 0.03 K | 0.3% | ≈1% | |
| Kosyakov | 0.1 K | 0.4% | 0.2 ppm | |

| Carbon dioxide-Water | Uncertainty | | | |
|---|---|---|---|---|
| Author | T | P | $Y_W$ | $X_G$ |
| Gillespie, Wilson | void | void | void | void |
| Coan, King | 0.05 K | void | void | |
| Song, Kobayashi (RR #99) | 0.06 K | 0.2 bar | 4% | |

| Argon-Water | Uncertainty | | | |
|---|---|---|---|---|
| Author | T | P | $Y_W$ | in $X_G$ |
| Rigby, Prausnitz | 0.03 K | 0.3% | ≈1% | |
| Kosyakov | 0.1 K | 0.4% | 0.2 ppm | |

Table F.3: Survey of phase equilibrium data for selected binary mixtures containing water, available in literature (condensed phase according to the authors: **hydrate**).

| Author | Year | No.exp. points | System | Measured quantities | Temperature in °C | Pressure range in bar |
|---|---|---|---|---|---|---|
| Aoyagi et al. [218] | 1979 | 12 | Methane - Water | Yw | -33,-23,-13,-3 | 34.5, 69, 103 |
| Sloan et al. [219] | 1976 | 12 | „ | Yw | -24 ÷ +7 | ca.70, ca.103 |
| Song,Kobayashi [220] | 1994 | 3 | Ethane - Water | Yw | 3 ÷ 10.5 | 24.8 |

## F.3 Compound Properties and Binary Interaction Parameters

Table F.4: Compound properties used in the calculation program (GERGWATER) [228].

The listed compounds correspond to the standard analysis according to ISO 6979-4, besides argon and water (see table 3.4 and table 4.2).

| Compound | No. | Acentric factor - | Molecular weight g/mol | $P_{crit}$ bar | $T_{crit}$ K |
|---|---|---|---|---|---|
| *Water* | 1 | 0.34437 | 18.0152 | 220.64 | 647.14 |
| Nitrogen | 4 | 0.03593 | 28.014 | 33.99 | 126.26 |
| Carbon dioxide | 5 | 0.22394 | 44.009 | 73.86 | 304.21 |
| Methane | 2 | 0.0114 | 16.043 | 45.99 | 190.55 |
| Ethane | 3 | 0.09909 | 30.069 | 48.72 | 305.33 |
| Propane | 6 | 0.15611 | 44.097 | 42.46 | 369.85 |
| 2-Methyl propane | 7 | 0.18465 | 58.124 | 36.4 | 407.85 |
| n-Butane | 8 | 0.19777 | 58.124 | 37.84 | 425.14 |
| 2,2-Dimethyl propane | 9 | 0.19528 | 72.151 | 31.96 | 433.75 |
| 2-Methyl butane | 10 | 0.22606 | 72.151 | 33.7 | 460.39 |
| n-Pentane | 11 | 0.24983 | 72.151 | 33.64 | 469.69 |
| Hexane / $C_{6+}$ | 12 | 0.296 | 86.178 | 30.2 | 507.85 |
| *Argon* | | -0.00234 | 39.948 | 48.65 | 150.69 |



Table F.5:Binary interaction parameters used in the calculation program (GERGWATER)[228].

| No. (i) | No. (j) | $k_{ij,0}$ | $k_{ij,1}$ | Citation |
|---|---|---|---|---|
| 1 | 2 | 0.651 | -1.385 | This work |
| 1 | 3 | 0.635 | -0.93 | This work |
| 1 | 4 | 0.48 | 0 | This work |
| 1 | 5 | 0.184 | 0.236 | This work |
| 1 | 6 | 0.53 | 0 | This work |
| 1 | 7 | 0.69 | 0 | This work |
| 1 | 8 | 0.69 | 0 | This work |
| 1 | 9 | 0.5 | 0 | This work |
| 1 | 10 | 0.5 | 0 | This work |
| 1 | 11 | 0.5 | 0 | This work |
| 1 | 12 | 0.5 | 0 | This work |
| 2 | 3 | -0.0026 | 0 | Knapp (1982) |
| 2 | 4 | 0.0311 | 0 | Knapp (1982) |
| 2 | 5 | 0.0919 | 0 | Knapp (1982) |
| 2 | 6 | 0.0140 | 0 | Knapp (1982) |
| 2 | 7 | 0.0256 | 0 | Knapp (1982) |
| 2 | 8 | 0.0133 | 0 | Knapp (1982) |
| 2 | 9 | 0.0180 | 0 | Kordas (1995) |
| 2 | 10 | -0.0056 | 0 | Knapp (1982) |
| 2 | 11 | 0.0230 | 0 | Knapp (1982) |
| 2 | 12 | 0.0422 | 0 | Knapp (1982) |
| 3 | 4 | 0.0515 | 0 | Knapp (1982) |
| 3 | 5 | 0.1322 | 0 | Knapp (1982) |
| 3 | 6 | 0.0011 | 0 | Knapp (1982) |
| 3 | 7 | -0.0067 | 0 | Knapp (1982) |
| 3 | 8 | 0.0096 | 0 | Knapp (1982) |
| 3 | 9 | 0.0230 | 0 | Nishiumi (1988) |
| 3 | 10 | 0.0160 | 0 | Nishiumi (1988) |
| 3 | 11 | 0.0078 | 0 | Knapp (1982) |
| 3 | 12 | -0.010 | 0 | Knapp (1982) |
| 4 | 5 | -0.017 | 0 | Knapp (1982) |
| 4 | 6 | 0.0852 | 0 | Knapp (1982) |
| 4 | 7 | 0.1033 | 0 | Knapp (1982) |
| 4 | 8 | 0.08 | 0 | Knapp (1982) |
| 4 | 9 | 0.093 | 0 | Avlonitis (1994) |
| 4 | 10 | 0.0922 | 0 | Knapp (1982) |
| 4 | 11 | 0.1 | 0 | Knapp (1982) |
| 4 | 12 | 0.1496 | 0 | Knapp (1982) |
| 5 | 6 | 0.1241 | 0 | Knapp (1982) |
| 5 | 7 | 0.12 | 0 | Knapp (1982) |
| 5 | 8 | 0.1333 | 0 | Knapp (1982) |
| 5 | 9 | 0.126 | 0 | Kordas (1994) |
| 5 | 10 | 0.1219 | 0 | Knapp (1982) |
| 5 | 11 | 0.1222 | 0 | Knapp (1982) |
| 5 | 12 | 0.11 | 0 | Knapp (1982) |
| 6 | 7 | -0.0078 | 0 | Knapp (1982) |
| 6 | 8 | 0.0033 | 0 | Knapp (1982) |
| 6 | 10 | 0.0111 | 0 | Knapp (1982) |
| 6 | 11 | 0.0267 | 0 | Knapp (1982) |
| 6 | 12 | 0.0007 | 0 | This work |
| 7 | 8 | -0.0004 | 0 | This work |
| 7 | 9 | 0 | 0 | - |
| 7 | 10 | 0 | 0 | - |
| 7 | 11 | 0 | 0 | - |
| 7 | 12 | 0 | 0 | - |
| 8 | 9 | 0 | 0 | - |
| 8 | 10 | 0 | 0 | - |
| 8 | 11 | 0.0174 | 0 | Knapp (1982) |
| 8 | 12 | -0.0056 | 0 | K-BP[2] |
| 9 | 10 | 0 | 0 | - |
| 9 | 11 | 0 | 0 | - |
| 9 | 12 | 0 | 0 | - |
| 10 | 11 | 0.06 | 0 | Knapp (1982) |
| 10 | 12 | 0 | 0 | - |
| 11 | 12 | 0 | 0 | - |

Allocation to the compound numbers see table F.4 and structure of the $k_{ij}(T)$-function see equation (4.4).

**Citations:**

Avlonitis et al. (1994) [224]
Knapp et al. (1982) [225]
Kordas et al. (1994) [226]
Kordas et al. (1995) [227]
K-BP[2] (1994) [228]
Nishiumi et al. (1988) [222]

## F.4 Influence of Mixture Compounds on Dew Points and Water Contents

The objective of the preliminary investigations, described in this section, was to find out the minimum extent of the gas analysis required. The prescribed accuracy of the dew point prediction (at given pressure, temperature and water content) was to be at least ±2 K (see chapter 4.5).

To determine the influence of each gas compound on the dew point, or the water content respectively, the extent of the input data base was reduced gradually, starting at the detailed gas analysis according to ISO 6974-3.

Typical compositions of natural gases were selected for the investigations. The calculations have been carried out using the calculation program developed within this work (GERGWATER (GW), see chapter 4). Binary interaction parameters according to chapter 4.4 have been applied.

### Calculation Procedure

In a first run, the complete extent of the natural gas analysis according to ISO 6974-3 (Water + 24 natural gas compounds) was used as input data base. Table 4.2 contains a list of the complete initial composition. The gas composition was normalised prior to the first run. After each calculation run, the component with the highest number was removed from the input data base. The remaining mole fraction of this component was added to the methane composition. Due to this procedure, the input composition of the second run was free of oxygen (component number 25) and of the third run free of oxygen and hydrogen. In the last calculation run (N=2) only two mixture components remained (methane-water). In the following presentation of the results, only the compound numbers are used, because of clearness.

### Typical Calculation Results

Figure F.1 presents some typical results of the calculation runs with respect to the dew point at four temperatures for the 100 bar isobar of natural gas NG6. Additionally, the dew point calculated with the initial composition (ISO 6974-4, see table 4.2, column A), has been plotted on the ordinate axis. Figure F.2 represents the corresponding results with respect to the water content. In figure F.2, the water content calculated with the initial composition has been plotted on the ordinate axis analogous to figure F.1.

One may conclude from the figures, that only the main compounds of natural gas (No. 1 to 8) significantly influence the dew point and water content. In these examples the dew point can be reproduced within the prescribed uncertainty of ±2 K, if natural gas is treated as pure methane. But the figures clearly indicate, that at least the first five components (besides water: methane, ethane, nitrogen and carbon dioxide) are required to represent the mixture composition sufficiently. The fact, that differences between the calculated and measured dew points are independent from temperature indicates, that the water content (as input parameter for the dew point calculation) has a strong influence on the calculation results, too. Since the water content usually is an experimental value, it implies an experimental uncertainty, which should be



considered (see remarks in annex D). A comparison of the calculation results obtained with a ISO 6974-4 composition (points at the ordinate axis) and with the ISO 6973-3 composition (=No. 25) shows, that the reduction of the input data base from 24 to 11 compounds and the lumping of higher hydrocarbons to the $C_{6+}$ pseudo component leads to nearly the same values. The larger information content of the extended gas analysis does not lead to more accurate results compared to the "small" analysis, if dew points and water contents are regarded.

Based on these findings, the extent of the standard natural gas analysis according to ISO 6974-4 has been considered as being sufficient to predict dew points within an accuracy of ±2 K.

Based on the diagrams, furthermore, the behaviour of dew point and water content may be predicted, if compounds are added to a given mixture. It should be taken in mind, however, that the presented results do not correspond exactly to a gradually adding of further compounds, as in the calculation procedure the remaining amount of the removed components was added to methane. However, the calculations showed, that the water content decreases slightly (and the dew point increases) if ethane is added to methane. But own experiments did not prove this behaviour clearly. Also a comparison of experimental water content data for the binary methane-water mixture and the ternary methane-ethane-water mixture gives no final evidence. Higher water contents (or lower dew points respectively) are calculated, if nitrogen and carbon dioxide are added to methane. By adding higher hydrocarbons in the range of 100 to some 1000 ppm (according to the content in natural gases), only a negligible influence is observed. In some cases, however, already small amounts of high molecular hydrocarbons may lead to a hydrocarbon dew point, which occurs prior to the water dew point. An accurate dew point measurement or calculation is impossible in this case.

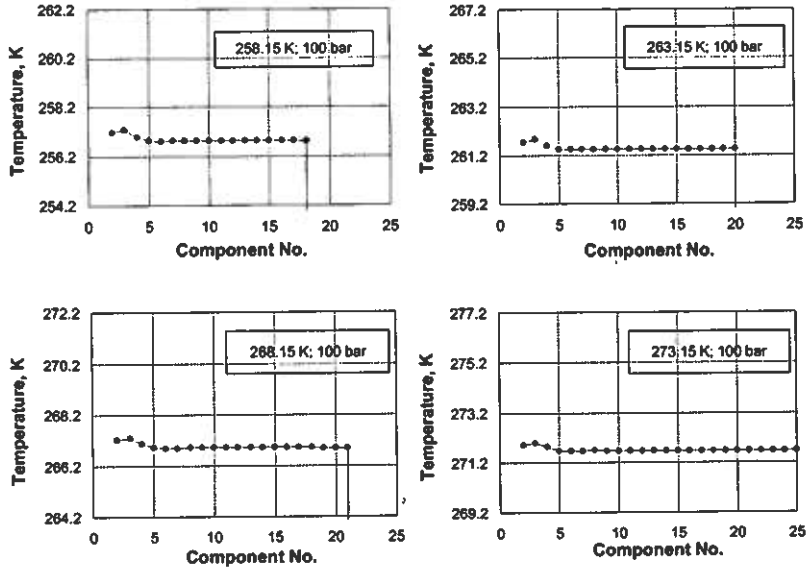


Figure F.1: Influence of several compounds on the water dew point (natural gas NG6)

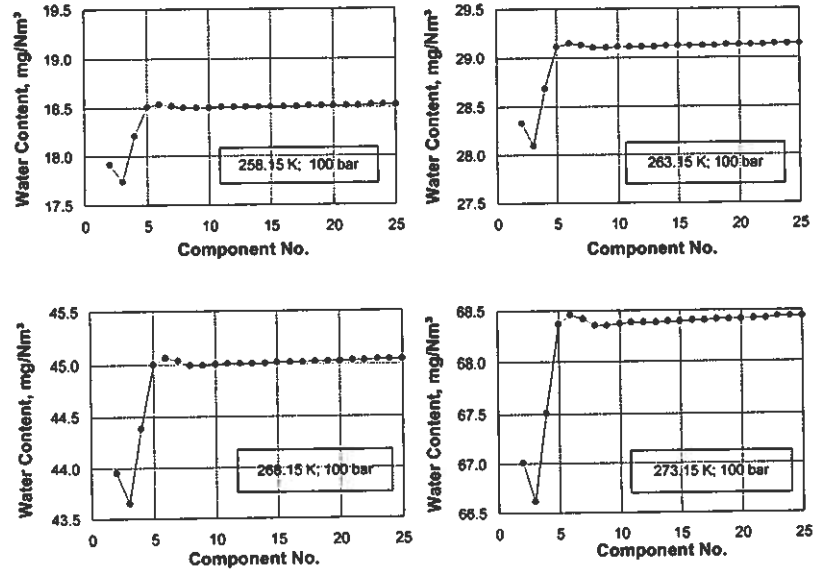


Figure F.2: Influence of several compounds on the water content (natural gas NG6)



## F.5 Flow Sheets

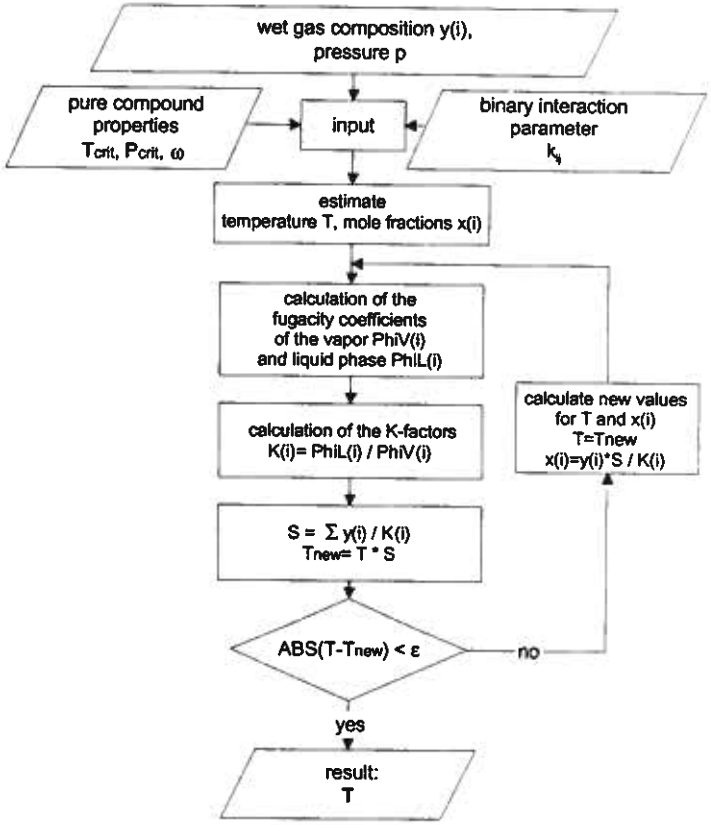


Figure F.3: Flow sheet for the calculation of dew points [228]

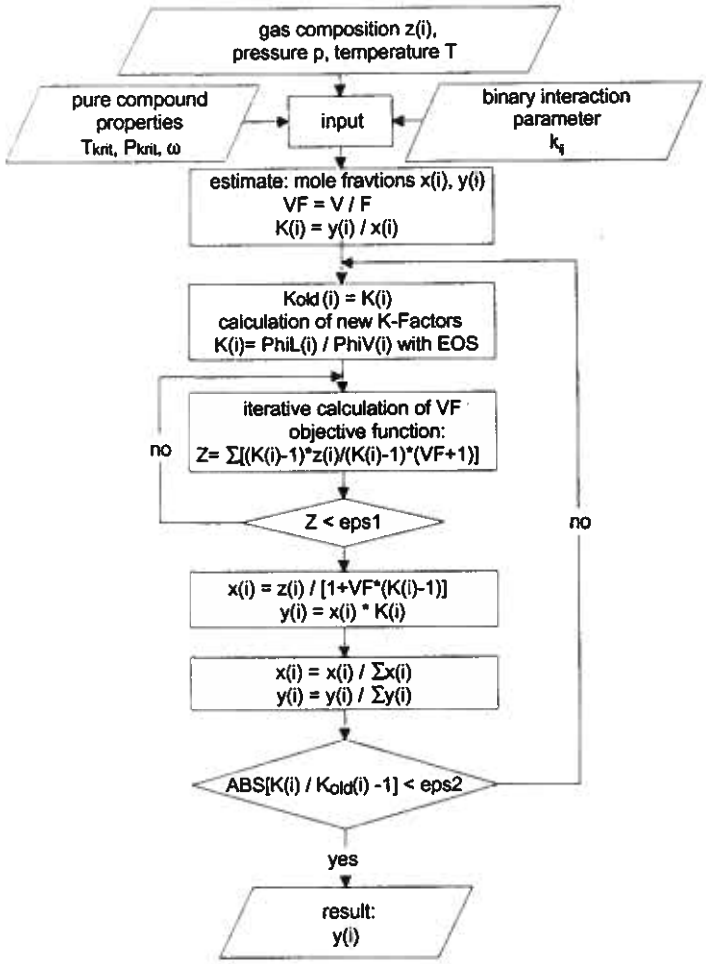


Figure F.4: Flow sheet for the calculation of water contents [228]



# Annex G - Figures and Tables

## G.1 Figures

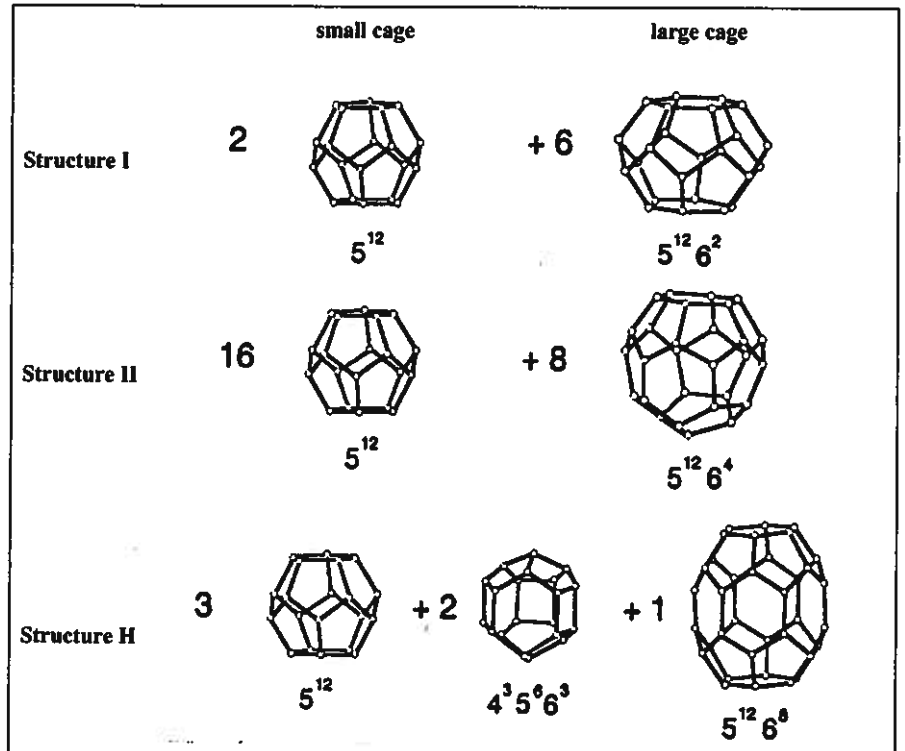


**Structure I:** 2 small cages with 12 pentagonal surfaces (notation: $5^{12}$, Dodecahedron)
+ 6 large cages with 12 pentagonal and 2 hexagonal surfaces
(notation: $5^{12}6^2$, Tetrakaidecahedron)

**Struktur II:** 16 small cages with 12 pentagonal surfaces (notation: $5^{12}$, Dodecahedron)
+ 8 large cages with 12 pentagonal and 4 hexagonal surfaces
(notation: $5^{12}6^4$, Hexakaidecahedron)

**Struktur H:** 3 cages ($5^{12}$, Dodecahedron)
+ 2 cages ($4^3 5^6 6^3$)
+ 1 cage ($5^{12}6^8$)

Figure G.1: Composition of the hydrate structures [31]

## G.1.1 Hydrate Equilibrium Lines

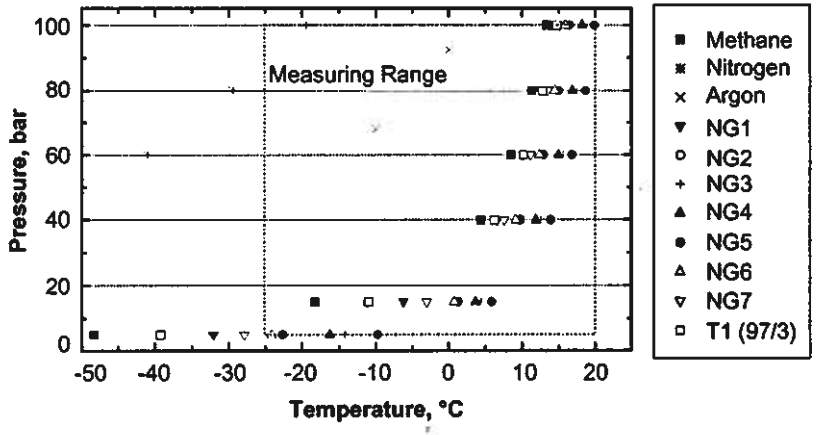


Figure G.2: Location of the hydrate equilibrium lines at six pressures (calculated with the CSMHYD-program by Sloan [29] ). Argon is not considered in the CSMHYD-program. So, argon-water data were taken from [245].

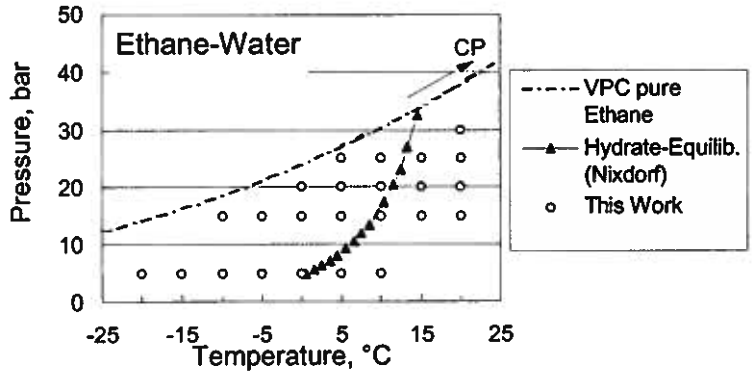


Figure G.3: Overview over the location of the measuring points of this work for the ethane-water binary system, with respect to the hydrate equilibrium line (Nixdorf [31]) and the vapour pressure curve of pure ethane [131].



## G.1.2 Experimental Results of the Water Content Measurements

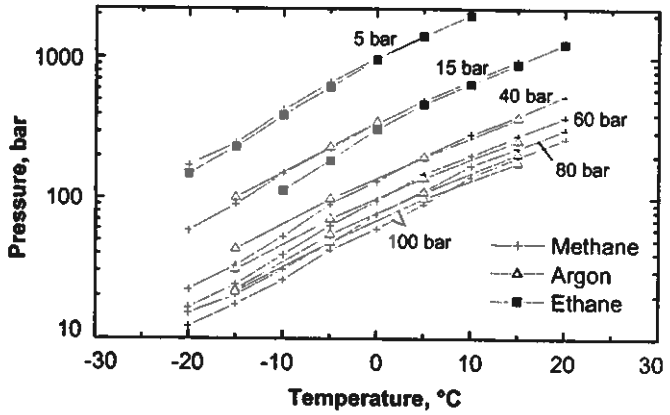


Figure G.4: Comparison of the water contents for methane-, ethane- and argon-water binary systems

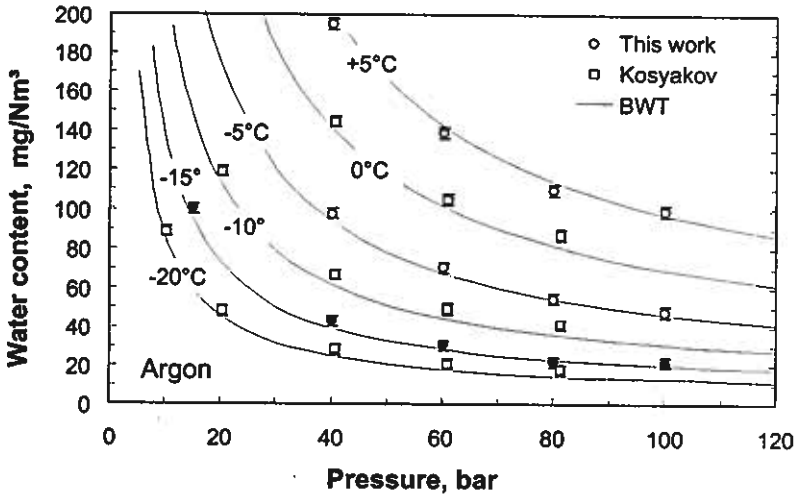


Figure G.5: Experimental water content data for argon. Comparison of data of this work, with data by Kosyakov [200] and calculated water contents (GERGWATER-method, see ch. 4).

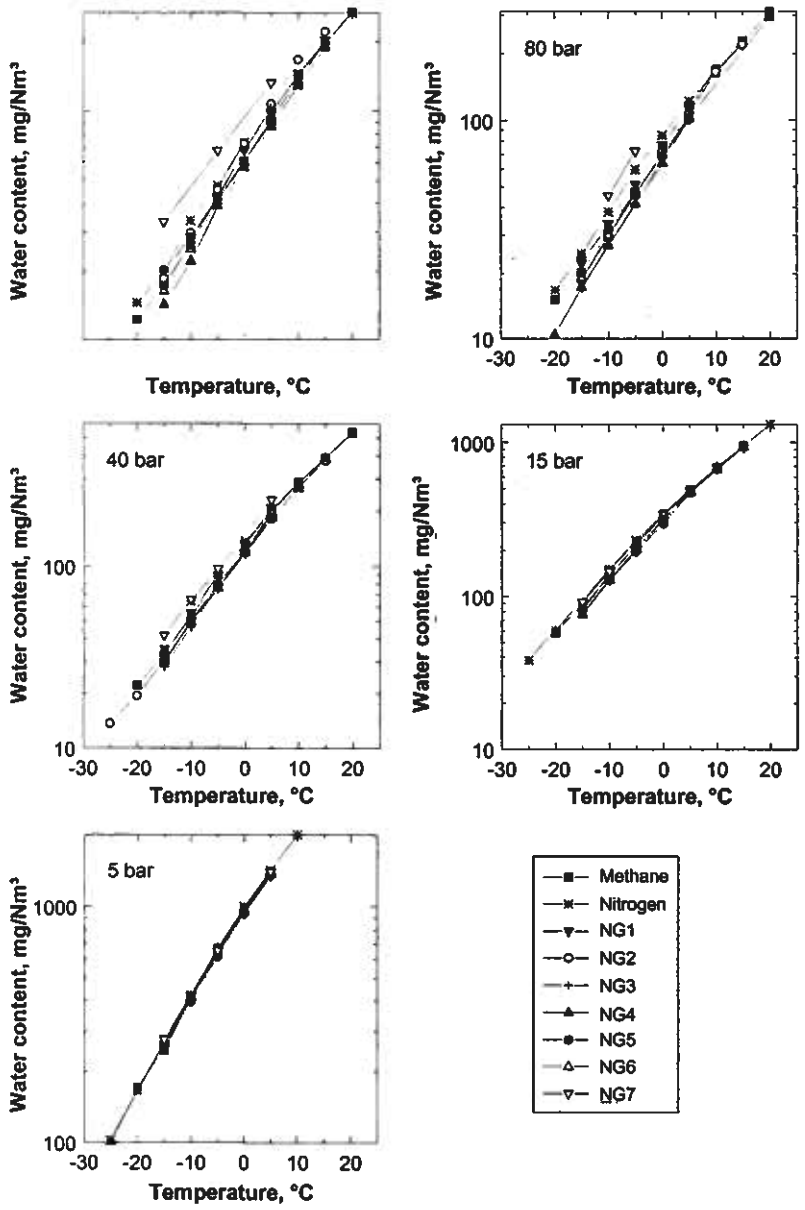


Figure G.6: Comparison of the courses of experimental water content data for the natural gases NG1 until NG7, and the binary systems methane-water and nitrogen water. (60 bar see figure 3.9)



## G.2 Experimental Data and Results of the Model Validation

The following tables contain results of the water content measurements and results of the model validation (see chapter 5). The data were sorted by the states investigated. The headings of the columns and rows contain the equilibrium conditions during the measurement (pressure PIR4 and temperature TIR4 at the outlet of condenser K2).

All values are given in "mg/Nm³ " and refer to the dry gas mixture.

### G.2.1 Binary Mixtures

Table G.1: Experimental water contents determined in this work, for the binary systems methane-, ethane-, nitrogen- and argon-water.

| *methane N5.5, mg/Nm³* | | | | | | | | | | |
|---|---|---|---|---|---|---|---|---|---|---|
| **bar/°C** | **-25** | **-20** | | **-10** | | **0.** | | **10** | | **20** |
| | | 171.3 | 246.6 | 421.0 | 667.2 | 993.6 | 1412.3 | | | |
| **15** | | 58.0 | 89.5 | 149.9 | 225.3 | 342.5 | 495.5 | 684.2 | 948.0 | |
| **40** | | 22.2 | 32.8 | 52.6 | 90.0 | 131.0 | 200.6 | 287.0 | 390.3 | 535.0 |
| **60** | | 16.6 | 24.1 | 39.0 | 63.0 | 94.9 | 140.8 | 201.4 | 281.5 | 377.9 |
| **80** | | 15.1 | 20.2 | 30.8 | 47.1 | 75.9 | 112.3 | 169.6 | 228.2 | 310.5 |
| **100** | | 12.2 | 17.4 | 25.9 | 42.2 | 60.1 | 89.9 | 141.6 | 196.2 | 266.8 |

| *ethane N3.5, mg/Nm³* | | | | | | | | | | |
|---|---|---|---|---|---|---|---|---|---|---|
| **bar/°C** | **-25** | **-20** | **-15** | **-10** | **-5** | **0.** | **5** | **10** | **15** | **20** |
| **5** | | 148.5 | 232.3 | 390.0 | 616.1 | 971.6 | 1411.8 | 1967.9 | | |
| **15** | | | | 112.9 | 183.8 | 311.3 | 467.7 | 651.4 | 903.7 | 1245.6 |
| **20** | | | | | | 237.0 | 328.9 | 480.8 | 669.7 | 959.8 |
| **25** | | | | | | | 271.6 | 387.0 | 533.8 | 737.9 |
| **30** | | | | | | | | | | 603.0 |

| *nitrogen N5.0, mg/Nm³* | | | | | | | | | | |
|---|---|---|---|---|---|---|---|---|---|---|
| **bar/°C** | **-25** | **-20** | **-15** | **-10** | **-5** | **0.** | **5** | **10** | **15** | **20** |
| **5** | 101.6 | 166.8 | | 427.1 | | 1002.0 | 1433.2 | 2017.5 | | |
| **15** | 38.4 | 60.6 | | 151.7 | 233.6 | 343.0 | 483.1 | 674.1 | | 1313.6 |
| **40** | | | | 64.2 | | 137.3 | | 284.8 | | 525.6 |
| **60** | 11.5 | 17.9 | 27.9 | 45.0 | 68.4 | 101.9 | 142.7 | 199.5 | | 375.7 |
| **80** | | 16.7 | 24.8 | 38.3 | 59.7 | 85.4 | 121.5 | 164.4 | | 301.7 |
| **100** | | 14.5 | 19.8 | 33.4 | 47.5 | 72.9 | 98.1 | 141.2 | | 262.5 |

| argon N5.0, mg/Nm³ | | | | | | | | | | |
|---|---|---|---|---|---|---|---|---|---|---|
| bar/°C | -25 | -20 | -15 | -10 | -5 | 0. | 5 | 10 | 15 | 20 |
| 15 | | | 100.3 | | 231.5 | 352.8 | | | | |
| 40 | | | 43.1 | | 97.7 | | 195.2 | | 375.0 | |
| 60 | | | 30.6 | | 70.2 | | 138.5 | | 258.4 | |
| 80 | | | 22.0 | | 54.4 | | 109.4 | | 206.9 | |
| 100 | | | 21.4 | | 47.6 | | 98.7 | | 178.3 | |

Table G.2: Deviations in the water content ($WC_{calc.}$-$WC_{exp.}$) calculated with the GERGWATER-method.

| Methane, ΔWC [mg/Nm³] | | | | | | | | | | |
|---|---|---|---|---|---|---|---|---|---|---|
| bar / °C | -25 | -20 | -15 | -10 | -5 | 0. | 5 | 10 | 15 | 20 |
| 5 | | -4.58 | 21.27 | 1.32 | -13.41 | 1.17 | 11.10 | | | |
| 15 | | -2.29 | 0.60 | -7.29 | -3.57 | -3.90 | -9.33 | 3.68 | 11.87 | |
| 40 | | -1.25 | 1.49 | 2.48 | -3.28 | 2.85 | -6.51 | -10.04 | -0.96 | 5.00 |
| 60 | | -2.77 | -1.06 | -1.51 | -3.37 | -1.97 | -13.10 | -6.05 | -4.95 | 7.71 |
| 80 | | -4.92 | -2.86 | -2.18 | -1.00 | -3.37 | -5.37 | -14.58 | -7.37 | -0.74 |
| 100 | | -4.16 | -3.51 | -2.59 | -4.30 | 0.26 | -0.14 | -10.53 | -8.15 | -1.58 |

| Ethane, ΔWC [mg/Nm³] | | | | | | | | | | |
|---|---|---|---|---|---|---|---|---|---|---|
| bar / °C | -25 | -20 | -15 | -10 | -5 | 0. | 5 | 10 | 15 | 20 |
| 5 | | 14.21 | 29.67 | 23.78 | 25.36 | 5.84 | -11.21 | 10.61 | | |
| 15 | | | | 18.25 | 21.88 | 5.26 | -10.13 | -0.18 | 9.93 | 18.87 |
| 20 | | | | | | -6.15 | 7.49 | 1.03 | 9.84 | -15.13 |
| 25 | | | | | | | -11.56 | -10.53 | 1.52 | 11.21 |
| 30 | | | | | | | | | | 10.41 |

| Nitrogen, ΔWC [mg/Nm³] | | | | | | | | | | |
|---|---|---|---|---|---|---|---|---|---|---|
| bar / °C | -25 | -20 | -15 | -10 | -5 | 0. | 5 | 10 | 15 | 20 |
| 5 | 3.10 | 4.13 | | 2.65 | | 3.91 | 2.31 | 2.84 | | |
| 15 | -1.44 | -0.47 | | -1.37 | -2.19 | 7.24 | 15.46 | 26.04 | | 14.41 |
| 40 | | | | -0.71 | | 9.02 | | 4.81 | | 19.04 |
| 60 | 0.37 | 1.15 | 2.08 | 1.51 | 2.33 | 4.10 | 6.91 | 8.85 | | 13.56 |
| 80 | | -0.96 | -0.06 | -0.25 | -1.95 | 0.75 | -0.26 | 3.81 | | 10.45 |
| 100 | | -0.66 | 1.88 | -0.24 | 2.61 | 1.57 | 6.29 | 3.15 | | 3.83 |

| Argon, ΔWC [mg/Nm³] | | | | | | | | | | |
|---|---|---|---|---|---|---|---|---|---|---|
| bar / °C | -25 | -20 | -15 | -10 | -5 | 0. | 5 | 10 | 15 | 20 |
| 15 | | | -5.60 | | -2.92 | -6.67 | | | | |
| 40 | | | -3.68 | | -3.45 | | 6.26 | | 14.60 | |
| 60 | | | -2.03 | | -2.56 | | 5.19 | | 17.83 | |
| 80 | | | 1.17 | | 0.22 | | 5.76 | | 13.26 | |
| 100 | | | -1.32 | | -0.68 | | -0.41 | | 8.54 | |



Table G.3: Deviations in the dew points ($T_{dew,calc.}$-$T_{dew,TIR4}$) calculated with the GERGWATER-method (see chapter 4). TIR4 = outlet temperature of condenser K2. The indented values indicate that deviations are above 2 K.

| methane N5.5, ΔDP [K] | | | | | | | | | | |
|---|---|---|---|---|---|---|---|---|---|---|
| bar / °C | -25 | -20 | -15 | -10 | -5 | 0. | 5 | 10 | 15 | 20 |
| 5 | | 0.28 | -0.89 | -0.04 | 0.24 | -0.01 | -0.11 | | | |
| 15 | | 0.41 | -0.07 | 0.55 | 0.19 | 0.16 | 0.27 | -0.08 | -0.19 | |
| 40 | | 0.58 | -0.46 | -0.50 | 0.42 | -0.25 | 0.45 | 0.51 | 0.04 | -0.15 |
| 60 | | 1.76 | 0.45 | 0.42 | 0.61 | 0.27 | 1.25 | 0.43 | 0.26 | -0.31 |
| 80 | | 3.70 | 1.50 | 0.76 | 0.23 | 0.57 | 0.65 | 1.25 | 0.48 | 0.04 |
| 100 | | 3.80 | 2.15 | 1.06 | 1.14 | -0.05 | 0.02 | 1.05 | 0.60 | 0.09 |

| ethane, ΔDP [K] | | | | | | | | | | |
|---|---|---|---|---|---|---|---|---|---|---|
| bar / °C | -25 | -20 | -15 | -10 | -5 | 0. | 5 | 10 | 15 | 20 |
| 5 | | -0.94 | -1.28 | -0.66 | -0.47 | -0.07 | 0.11 | -0.08 | | -0.24 |
| 15 | | | | -1.62 | -1.27 | -0.20 | 0.30 | 0.00 | -0.16 | 0.25 |
| 20 | | | | | | 0.34 | -0.31 | -0.03 | -0.22 | -0.23 |
| 25 | | | | | | | 0.57 | 0.38 | -0.04 | -0.25 |
| 30 | | | | | | | | | | |

| nitrogen, ΔDP [K] | | | | | | | | | | |
|---|---|---|---|---|---|---|---|---|---|---|
| bar / °C | -25 | -20 | -15 | -10 | -5 | 0. | 5 | 10 | 15 | 20 |
| 5 | -0.30 | -0.25 | | -0.07 | | -0.05 | -0.02 | -0.02 | | |
| 15 | 0.38 | 0.08 | | 0.10 | 0.11 | -0.26 | -0.45 | -0.57 | | -0.18 |
| 40 | | | | 0.13 | | -0.79 | | -0.25 | | -0.58 |
| 60 | -0.33 | -0.67 | -0.80 | -0.39 | -0.41 | -0.50 | -0.70 | -0.67 | | -0.59 |
| 80 | | 0.64 | 0.03 | 0.08 | 0.41 | -0.11 | 0.03 | -0.36 | | -0.57 |
| 100 | | 0.51 | -1.03 | 0.09 | -0.66 | -0.27 | -0.94 | -0.35 | | -0.25 |

| argon, ΔDP [K] | | | | | | | | | | |
|---|---|---|---|---|---|---|---|---|---|---|
| bar / °C | -25 | -20 | -15 | -10 | -5 | 0. | 5 | 10 | 15 | 20 |
| 15 | | | 0.63 | | 0.16 | 0.27 | | | | |
| 40 | | | 1.01 | | 0.45 | | -0.44 | | -0.58 | |
| 60 | | | 0.79 | | 0.47 | | -0.51 | | -1.03 | |
| 80 | | | -0.54 | | -0.01 | | -0.72 | | -0.95 | |
| 100 | | | 0.77 | | 0.22 | | 0.11 | | -0.70 | |

## G.2.2 Ternary Mixture (Methane-Ethane-Water)

Table G.4: Experimental water contents determined in this work, for the methane-ethane-water ternary system (dry gas composition: 96,94 mol% methane; 3,06 mol% ethane).

| *methane-ethane (97/3), mg/Nm³* | | | | | | | | | | |
|---|---|---|---|---|---|---|---|---|---|---|
| bar/°C | -25 | -20 | -15 | -10 | -5 | 0. | 5 | 10 | 15 | 20 |
| 15 | | | 93.5 | | 238.8 | | 491.9 | | | |
| 40 | | | 36.5 | | 88.2 | | 205.2 | | 396.9 | |
| 60 | | | 25.1 | | 62.6 | | 145.6 | | 283.0 | |
| 80 | | | 20.5 | | 48.6 | | 117.0 | | 229.8 | |
| 100 | | | 20.1 | | 44.1 | | 102.0 | | 199.1 | |

Table G.5: Deviations in the water content ($WG_{calc.}$-$WG_{exp.}$) for the methane-ethane-water ternary system. Calculated with the GERGWATER-method (see chapter 4).

| *Methane-Ethane (97/3), ΔWC [mg/Nm³]* | | | | | | | | | | |
|---|---|---|---|---|---|---|---|---|---|---|
| bar / °C | -25 | -20 | -15 | -10 | -5 | 0. | 5 | 10 | 15 | 20 |
| 15 | | | -3.54 | | -18.05 | | -5.99 | | | |
| 40 | | | -2.27 | | -1.62 | | -11.46 | | -7.81 | |
| 60 | | | -2.17 | | -3.15 | | -9.99 | | -6.81 | |
| 80 | | | -3.29 | | -2.80 | | -10.36 | | -9.28 | |
| 100 | | | -6.36 | | -6.49 | | -12.55 | | -11.37 | |

Table G.6: Deviations in the dew points ($T_{dew,calc.}$-$T_{dew,TIR4}$). Calculated with the GERGWATER-method (see chapter 4). TIR4 = outlet temperature of condenser K2. The indented values indicate that deviations are above 2 K.

| *methane-ethane (97/3), ΔDP [K]* | | | | | | | | | | |
|---|---|---|---|---|---|---|---|---|---|---|
| bar / °C | -25 | | | | | | | | | |
| | | | 0.41 | | 0.91 | | | | | |
| 40 | | | 0.66 | | | | 0.79 | | 0.30 | |
| | | | 0.91 | | 0.57 | | | | 0.36 | |
| 80 | | | | | 0.64 | | 1.23 | | | |
| 100 | | | 3.65 | | | | 1.70 | | 0.84 | |



## G.2.3 Multicomponent Mixtures (Natural Gases)

Table G.7: Experimental water contents determined in this work, for the natural gases NG1-NG7

| *natural gas NG1, mg/Nm³* | | | | | | | | | | |
|---|---|---|---|---|---|---|---|---|---|---|
| bar/°C | -25 | -20 | -15 | -10 | -5 | 0. | 5 | 10 | 15 | 20 |
| 5 | | | 262.6 | 420.5 | 646.0 | 940.3 | 1350.5 | | | |
| 15 | | | 91.1 | 150.2 | 233.8 | 342.4 | 486.4 | 677.6 | 933.3 | |
| 40 | | | 35.1 | 55.2 | 89.4 | 130.9 | 207.8 | | | |
| 60 | | | 26.1 | 39.7 | 63.1 | 99.2 | 142.2 | 201.9 | 286.0 | |
| 80 | | | 22.2 | 33.9 | 51.5 | 77.4 | 115.5 | | | |
| 100 | | | 17.6 | 28.2 | 42.2 | 67.1 | 98.2 | 144.2 | 200.6 | |

| *natural gas NG2, mg/Nm³* | | | | | | | | | | |
|---|---|---|---|---|---|---|---|---|---|---|
| bar/°C | -25 | -20 | -15 | -10 | -5 | 0. | 5 | 10 | 15 | 20 |
| 5 | | | 260.4 | 409.3 | | 957.5 | 1355.8 | | | |
| | | | 81.9 | 139.0 | | 340.1 | 481.9 | | 937.2 | |
| 40 | | 19.4 | 30.3 | | 78.9 | 121.1 | | 269.4 | 376.0 | |
| | | | 21.7 | 33.7 | | 85.2 | 131.4 | | 286.3 | 374.1 |
| | | | 18.6 | 29.5 | | 72.2 | 106.8 | | 218.9 | |
| 100 | | | | 26.1 | 38.9 | | 88.8 | 139.8 | | 262.0 |

| *natural gas NG3, mg/Nm³* | | | | | | | | | | |
|---|---|---|---|---|---|---|---|---|---|---|
| bar/°C | -25 | -20 | -15 | -10 | -5 | 0. | 5 | 10 | 15 | 20 |
| 5 | | | 260.9 | 411.4 | 639.6 | 968.5 | 1384.6 | | | |
| 15 | | | 77.8 | 126.9 | 204.4 | 316.1 | 473.7 | 664.1 | 922.4 | |
| 40 | | | 28.1 | 46.4 | 75.0 | 116.1 | 182.3 | | | |
| 60 | | | 21.6 | 35.2 | 52.3 | 80.7 | 124.0 | 187.4 | 262.4 | |
| 80 | | | 17.1 | 27.0 | 41.7 | 67.4 | 103.0 | | | |
| 100 | | | 15.4 | 23.2 | 36.8 | 56.7 | 84.9 | 127.8 | 184.8 | |

| *natural gas NG4, mg/Nm³* | | | | | | | | | | |
|---|---|---|---|---|---|---|---|---|---|---|
| bar/°C | -25 | -20 | -15 | -10 | -5 | 0. | 5 | 10 | 15 | 20 |
| 5 | 100.6 | | 265.5 | 409.7 | 635.6 | 957.3 | 1376.0 | | | |
| 15 | | | 76.1 | 129.1 | 204.7 | 315.8 | 475.3 | 683.5 | 942.8 | |
| 40 | | | 30.0 | 49.4 | 75.9 | 119.4 | 183.2 | 265.1 | 389.9 | |
| 60 | 7.1 | 11.9 | 19.7 | 34.0 | 52.9 | 83.2 | 126.7 | 190.8 | 280.0 | 377.9 |
| 80 | 6.5 | 10.4 | 17.3 | 26.9 | 41.6 | 63.6 | 101.9 | | | 291.2 |
| 100 | | | 14.2 | 22.1 | 38.5 | 56.9 | 85.7 | 127.7 | 186.5 | |

| natural gas NG5, mg/Nm³ | | | | | | | | | | |
|---|---|---|---|---|---|---|---|---|---|---|
| bar/°C | -25 | -20 | | -10 | -5 | | 5 | 10 | | 20 |
| 5 | | | 249.0 | 395.9 | 613.0 | 930.6 | 1360.5 | | | |
| 15 | | | 81.7 | 127.8 | 198.0 | 299.1 | 467.9 | 672.5 | 940.1 | |
| 40 | | | 29.6 | 49.5 | 78.4 | 120.2 | 181.7 | | | |
| 60 | | | 23.0 | 38.4 | 58.8 | 83.4 | 126.5 | 190.2 | 269.5 | |
| 80 | | | 23.6 | 32.0 | 47.3 | 68.5 | 100.4 | | | |
| 100 | | | 20.3 | 28.2 | 41.2 | 58.5 | 88.3 | 130.2 | 196.3 | |

| natural gas NG6, mg/Nm³ | | | | | | | | | | |
|---|---|---|---|---|---|---|---|---|---|---|
| bar/°C | | -20 | -15 | -10 | -5 | 0. | 5 | 10 | 15 | 20 |
| 5 | | | 264.0 | 418.0 | 663.2 | 978.3 | 1386.2 | | | |
| 15 | | | 83.9 | 137.2 | 220.0 | 337.9 | 484.8 | 687.4 | 935.8 | |
| 40 | | | 33.5 | 52.9 | 81.2 | 125.5 | 193.3 | | | |
| 60 | | | 21.5 | 35.6 | 55.8 | 86.0 | 135.1 | 201.5 | 280.3 | |
| 80 | | | 19.0 | 30.0 | 46.1 | 69.7 | 103.4 | | | |
| 100 | | | 16.3 | 24.9 | 40.3 | 60.2 | 92.9 | 133.9 | 198.7 | |

| natural gas NG7, mg/Nm³ | | | | | | | | | | |
|---|---|---|---|---|---|---|---|---|---|---|
| bar/°C | -25 | -20 | -15 | -10 | -5 | 0. | 5 | 10 | 15 | 20 |
| 5 | | | 275.0 | | 653.0 | | 1417.0 | | | |
| 15 | | | 92.8 | 145.5 | | | | | | |
| 40 | | | 41.8 | 65.7 | 97.0 | | 227.8 | | | |
| 60 | | | 33.6 | 51.9 | 80.9 | | 173.2 | | | |
| 80 | | | | 45.4 | 72.0 | | | | | |
| 100 | | | 32.9 | | 67.0 | | 131.3 | | | |

Table G.8: Deviations in the water content ($WC_{calc.}$-$WC_{exp.}$) calculated with the GERGWATER-method.

| natural gas NG1, Δ WC [mg/Nm³] | | | | | | | | | | |
|---|---|---|---|---|---|---|---|---|---|---|
| bar / °C | -25 | -20 | -15 | -10 | -5 | 0. | 5 | 10 | 15 | 20 |
| 5 | | | 5.39 | 1.97 | 7.93 | 54.62 | 73.05 | | | |
| 15 | | | -1.01 | -7.43 | -11.91 | -3.58 | -0.05 | 10.47 | 26.81 | |
| 40 | | | -0.70 | -0.04 | -2.55 | 3.09 | -13.59 | | | |
| 60 | | | -3.05 | -2.09 | -3.37 | -6.09 | -6.16 | -6.32 | -9.20 | |
| 80 | | | -4.77 | -5.18 | -5.37 | -4.75 | -8.34 | | | |
| 100 | | | -3.63 | -4.85 | -4.11 | -6.61 | -8.18 | -12.86 | -12.22 | |



| natural gas NG2, Δ WC [mg/Nm³] | | | | | | | | | | |
|---|---|---|---|---|---|---|---|---|---|---|
| | -25 | -20 | -15 | -10 | -5 | 0. | 5 | 10 | 15 | 20 |
| 5 | | | 7.84 | 13.40 | 21.15 | 37.89 | 68.40 | | | |
| 15 | | | 8.48 | 4.05 | 9.63 | -0.82 | 5.03 | 10.46 | 23.86 | |
| 40 | -1.15 | 1.68 | 4.25 | 6.23 | 8.36 | 13.43 | 3.01 | 8.64 | 14.75 | |
| 60 | | | 1.52 | 4.11 | 2.56 | 8.41 | 5.41 | -3.88 | -8.32 | |
| 80 | | | -1.08 | -0.55 | 0.94 | 1.09 | 1.15 | -8.51 | 3.65 | |
| 100 | | | -2.33 | -2.50 | -0.45 | 1.22 | 2.07 | -7.21 | -6.83 | |

| natural gas NG3, Δ WC [mg/Nm³] | | | | | | | | | | |
|---|---|---|---|---|---|---|---|---|---|---|
| bar / °C | -25 | -20 | -15 | -10 | -5 | 0. | 5 | 10 | 15 | 20 |
| 5 | | | 6.90 | 10.75 | 13.88 | 25.77 | 38.14 | | | |
| 15 | | | 12.05 | 15.45 | 16.98 | 21.99 | 11.61 | 22.63 | 35.99 | |
| 40 | | | 5.87 | 8.23 | 11.16 | 16.96 | 10.76 | | | |
| 60 | | | 0.90 | 1.63 | 6.50 | 11.17 | 10.66 | 6.50 | 12.41 | |
| 80 | | | -0.47 | 0.74 | 3.37 | 3.91 | 2.58 | | | |
| 100 | | | -2.20 | -0.82 | 0.06 | 2.35 | 3.52 | 1.79 | 1.68 | |

| natural gas NG4, Δ WC [mg/Nm³] | | | | | | | | | | |
|---|---|---|---|---|---|---|---|---|---|---|
| bar / °C | -25 | -20 | -15 | -10 | -5 | 0. | 5 | 10 | 15 | 20 |
| 5 | 1.26 | | 2.66 | 13.01 | 18.58 | 37.94 | 47.91 | | | |
| 15 | | | 14.26 | 13.91 | 17.41 | 23.30 | 11.35 | 4.77 | 17.36 | |
| 40 | | | 4.55 | 5.96 | 11.19 | 14.94 | 11.35 | 12.30 | -0.17 | |
| 60 | 1.05 | 1.97 | 3.52 | 3.74 | 7.02 | 10.14 | 9.71 | 5.11 | -3.01 | 7.92 |
| 80 | -0.70 | -0.16 | 0.10 | 1.87 | 4.73 | 9.28 | 5.60 | | | 19.03 |
| 100 | | | -0.27 | 1.31 | -0.33 | 3.81 | 4.67 | 4.15 | 2.40 | |

| natural gas NG5, Δ WC [mg/Nm³] | | | | | | | | | | |
|---|---|---|---|---|---|---|---|---|---|---|
| bar / °C | -25 | -20 | -15 | -10 | -5 | 0. | 5 | 10 | 15 | 20 |
| 5 | | | | 26.79 | | 64.67 | 63.55 | | | |
| | | | 8.58 | 15.13 | | 40.05 | 18.83 | | 20.33 | |
| 40 | | | | 5.70 | 8.47 | | 12.75 | | | |
| 60 | | | | -1.01 | 0.79 | | 9.66 | 5.72 | | |
| 80 | | | -6.69 | | -1.49 | 3.89 | | | | |
| 100 | | | -6.84 | | -3.64 | 1.74 | | 1.78 | -6.55 | |

| natural gas NG6, Δ WC [mg/Nm³] | | | | | | | | | | |
|---|---|---|---|---|---|---|---|---|---|---|
| bar / °C | -25 | -20 | -15 | -10 | -5 | 0. | 5 | 10 | 15 | 20 |
| 5 | | | 4.81 | 5.63 | -7.75 | 18.53 | | | | |
| 15 | | | 7.10 | | 3.53 | 2.98 | | 3.46 | 27.49 | |
| | | | 1.85 | 3.67 | | 10.79 | 3.67 | | | |
| | | | 2.61 | 3.37 | | 9.60 | 4.00 | | 0.33 | |
| 80 | | | | 0.26 | 2.15 | | 7.01 | | | |
| 100 | | | | 0.08 | -0.05 | | 0.65 | 1.52 | | |

| natural gas NG7, ΔWC [mg/Nm³] | | | | | | | | | | |
|---|---|---|---|---|---|---|---|---|---|---|
| bar / °C | -25 | -20 | -15 | -10 | -5 | 0. | 5 | 10 | 15 | 20 |
| 5 | | | -1.73 | | 11.57 | | | | | |
| 15 | | | 2.88 | | | | | | | |
| 40 | | | -0.97 | | 2.93 | | -9.77 | | | |
| | | | -3.31 | -3.84 | | | -9.99 | | | |
| 80 | | | | -4.89 | -8.91 | | | | | |
| | | | -9.92 | | -9.85 | | | | | |

Table G.9: Deviations in the dew points ($T_{dew,calc.}$-$T_{dew,TIR4}$). Calculated with the GERGWATER-method (see chapter 4). TIR4 = outlet temperature of condenser K2. The indented values indicate that deviations are above 2 K.

| natural gas NG1, ΔDP [K] | | | | | | | | | | |
|---|---|---|---|---|---|---|---|---|---|---|
| bar / °C | -25 | -20 | -15 | -10 | -5 | 0. | 5 | 10 | 15 | 20 |
| 5 | | | -0.22 | -0.05 | -0.14 | -0.68 | -0.75 | | | |
| 15 | | | 0.12 | 0.57 | 0.61 | 0.14 | 0.00 | -0.23 | -0.43 | |
| 40 | | | 0.21 | 0.01 | 0.33 | -0.27 | 0.93 | | | |
| 60 | | | 1.25 | 0.57 | 0.61 | 0.82 | 0.60 | 0.45 | 0.48 | |
| 80 | | | 2.39 | 1.72 | 1.19 | 0.80 | 0.99 | | | |
| 100 | | | 2.21 | 1.90 | 1.09 | 1.28 | 1.13 | 1.27 | 0.90 | |

| natural gas NG2, ΔDP [K] | | | | | | | | | | |
|---|---|---|---|---|---|---|---|---|---|---|
| bar / °C | -25 | | -15 | -10 | | 0. | 5 | | 15 | 20 |
| | | | -0.32 | -0.36 | -0.38 | -0.47 | -0.70 | | | |
| 15 | | | -1.05 | -0.32 | -0.51 | 0.03 | -0.15 | -0.23 | -0.38 | |
| 40 | 0.83 | -0.82 | -1.35 | -1.28 | -1.13 | -1.23 | -0.21 | -0.45 | -0.58 | |
| 60 | -1.32 | | -0.68 | -1.20 | -0.48 | -1.08 | -0.54 | 0.28 | 0.44 | -0.54 |
| 80 | -1.32 | -1.25 | 0.58 | 0.19 | -0.22 | -0.17 | -0.14 | 0.74 | -0.24 | |
| 100 | | | 1.45 | 1.01 | 0.12 | -0.22 | -0.30 | 0.72 | 0.50 | -0.32 |

| natural gas NG3, ΔDP [K] | | | | | | | | | | |
|---|---|---|---|---|---|---|---|---|---|---|
| bar / °C | -25 | -20 | -15 | -10 | -5 | 0. | 5 | 10 | 15 | 20 |
| 5 | | | -0.28 | -0.29 | -0.25 | -0.32 | -0.39 | | | |
| 15 | | | -1.52 | -1.27 | -0.92 | -0.81 | -0.34 | -0.49 | -0.58 | |
| 40 | | | -1.94 | -1.74 | -1.55 | -1.59 | -0.79 | | | |
| 60 | | | -0.40 | -0.47 | -1.28 | -1.48 | -1.10 | -0.48 | -0.68 | |
| 80 | | | 0.27 | -0.27 | -0.82 | -0.63 | -0.32 | | | |
| 100 | | | 1.42 | 0.35 | -0.02 | -0.44 | -0.52 | -0.19 | -0.13 | |

| natural gas NG4, ΔDP [K] | | | | | | | | | | |
|---|---|---|---|---|---|---|---|---|---|---|
| bar / °C | -25 | -20 | -15 | -10 | -5 | 0. | 5 | 10 | 15 | 20 |
| 5 | -0.12 | | -0.11 | -0.35 | -0.34 | -0.47 | -0.49 | | | |
| 15 | | | -1.82 | -1.13 | -0.94 | -0.86 | -0.33 | -0.10 | -0.28 | |
| 40 | | | -1.45 | -1.22 | -1.54 | -1.38 | -0.83 | -0.65 | 0.01 | |
| 60 | -1.24 | -1.45 | -1.64 | -1.10 | -1.37 | -1.18 | -0.99 | -0.37 | 0.16 | -0.32 |
| 80 | 0.97 | 0.14 | -0.05 | -0.69 | -1.15 | -1.18 | -0.70 | | | -0.96 |
| 100 | | | 0.18 | -0.57 | 0.09 | -0.71 | -0.68 | -0.43 | -0.18 | |



| natural gas NG5, ΔDP [K] | | | | | | | | | | |
|---|---|---|---|---|---|---|---|---|---|---|
| bar / °C | -25 | -20 | -15 | -10 | -5 | 0. | 5 | 10 | 15 | 20 |
| 5 | | | -0.80 | -0.73 | -0.76 | -0.81 | -0.65 | | | |
| 15 | | | -1.06 | -1.24 | -1.33 | -1.51 | -0.56 | -0.34 | -0.33 | |
| 40 | | | -1.54 | -1.17 | -1.15 | -1.28 | -0.93 | | | |
| 60 | | | 0.07 | 0.28 | -0.15 | -1.24 | -0.98 | -0.42 | -0.42 | |
| 80 | | | 3.22 | 1.27 | 0.34 | -0.62 | -0.85 | | | |
| 100 | | | 3.85 | 2.10 | 0.96 | -0.32 | -0.26 | -0.18 | 0.48 | |

| natural gas NG6, ΔDP [K] | | | | | | | | | | |
|---|---|---|---|---|---|---|---|---|---|---|
| bar / °C | -25 | -20 | -15 | -10 | -5 | 0. | 5 | 10 | 15 | 20 |
| 5 | | | -0.19 | -0.15 | 0.14 | -0.23 | -0.40 | | | |
| 15 | | | -0.86 | -0.53 | -0.18 | -0.11 | -0.12 | -0.07 | -0.44 | |
| 40 | | | -0.56 | -0.73 | -0.99 | -0.97 | -0.26 | | | |
| 60 | | | -1.16 | -0.96 | -1.12 | -1.23 | -0.91 | 0.17 | -0.02 | |
| 80 | | | 0.26 | -0.09 | -0.50 | -1.01 | -0.88 | | | |
| 100 | | | 0.73 | -0.03 | 0.01 | -0.58 | -0.09 | -0.16 | 0.43 | |

| natural gas NG7, ΔDP [K] | | | | | | | | | | |
|---|---|---|---|---|---|---|---|---|---|---|
| bar / °C | -25 | -20 | -15 | -10 | -5 | 0. | 5 | 10 | 15 | 20 |
| 5 | | | 0.07 | | -0.21 | | -0.26 | | | |
| 15 | | | -0.33 | -0.40 | | | | | | |
| 40 | | | 0.25 | 0.21 | -0.35 | | 0.63 | | | |
| 60 | | | 1.10 | 0.86 | 0.94 | | 0.84 | | | |
| 80 | | | 4.13 | 1.26 | 1.54 | | | | | |
| 100 | | | 3.83 | | 1.85 | | 0.67 | | | |

Table G.10: Molecular weight, compressibility factor (calculated with the AGA8-DC92 equation of state [246]), specific gravity and the Wobbe number of the natural gases investigated in this work.

| Natural Gas | NG1 | NG2 | NG3 | NG4 | NG5 | NG6 | NG7 |
|---|---|---|---|---|---|---|---|
| Molecular Weight, g/mol | 16.3448 | 17.2809 | 18.1434 | 18.2972 | 19.272 | 18.4856 | 23.8347 |
| Compressibility Factor $Z_N$ | 0.99758 | 0.99737 | 0.9969 | 0.99715 | 0.99659 | 0.99755 | 0.99672 |
| Specific Gravity | 0.5654 | 0.598 | 0.628 | 0.6326 | 0.6672 | 0.6395 | 0.8107 |
| Wobbe Number, MJ/m³ | 52.94 | 52.19 | 55.17 | 51.91 | 54.45 | 46.23 | |

# H Literature


[1] Pusch, G.; Rischmüller, H.; Weggen, K.: Die Energierohstoffe Erdöl und Erdgas: Vorkommen, Erschliessung, Förderung. Berlin: Ernst & Sohn Verlag 1995

[2] Recknagel, H.; Fasold, H.G.: Möglichkeiten und Grenzen des Gastransportes. In: Global link : interkontinentaler Energieverbund; Tagung Essen, Oktober 1994, VDI-Bericht No. 1129, Düsseldorf : VDI-Verlag, 1994, 55-72

[3] Schmidt, T.; Götzen, P.: Unterirdische Speicherung von Erdgas in Salzkarvernen und Porenspeichern. In: Global link: interkontinentaler Energieverbund; Tagung Essen, Oktober 1994, VDI-Bericht No. 1129, Düsseldorf : VDI-Verlag, 1994, 101-120

[4] Stephan, K.: Thermodynamik: Grundlagen und technische Anwendungen. Bd. 1. Einstoffsysteme. 14. Aufl., Berlin : Springer, 1992

[5] DIN 51871: Bestimmung des Wasserdampf-Taupunktes - Verfahren mit gekühltem Spiegel. Hrsg.: DIN, Deutsches Institut für Normung e.V. Berlin : Beuth-Verlag, Ausg. Dez. 1985

[6] Personal communication to Dr. Steinle, NAM, Nederland, Dec. 1998 (chairman of ISO/TC 193/SC 2 "Natural Gas - Measurement of Properties") ISO CD 15972 "Natural Gas - Measurement of Properties - Single Components and Condensation Properties - Part 1: Water Content and Water Dew-Point Measurement".

[7] Saul, A.H.: Eine Fundamentalgleichung für den fluiden Zustandsbereich von Wasser bis zu Drücken von 25000 Mpa und Temperaturen von 1273 K. Fortschr.-Ber. VDI Reihe 3, No. 149, Düsseldorf : VDI-Verlag, 1988

[8] Cohen, E.R.; Tayler, B.N.: The 1986 Adjustment of the Fundamental Physical Constants. CODATA Bulletin 63, Oxford : Pergamon Press 1986

[9] Dohrn, R.: Berechnung von Phasengleichgewichten. Vieweg Verlag, 1994

[10] Gmehling, J.; Kolbe, B.: Thermodynamik. 2. Überarb. Aufl., Weinheim : VCH, 1992

[11] Walas, St. M.: Phase equilibria in chemical engineering. 2 pr.- Boston : Butterworth, 1985

[12] Anderko, A.: Review: EoS Methods for the Modelling of Phase Equilibria. In: Fluid Phase Equilibria 61 (1990) 145-225

[13] Abbott, M.M.: Cubic EoS: An interpretive Review. In: Advances in Chemistry Series 182 (1979) 47-70

[14] Van der Waals, J.D.: Over de continuiteit van den gas- en vloestoftoestand. Dissertation Universität Leiden 1873

[15] Soave, G.: Equilibrium constants from a modified Redlich-Kwong equation of state. In: Chem. Eng. Sci., 27(1972) 1197-1203

[16] Peng, D.Y.; Robinson, D.B.: A New Two-Constant Equation of State. In: Ind. Eng. Chem. Fundam., Vol. 15 (1976) No. 1, 59-64

[17] Patel, N.C.; A.S. Teja: A new cubic equation of state for fluids and fluid mixtures. In: Chem. Eng. Science, 37 (1982) 463-473

[18] Patel, N.C.: Improvements of the Patel-Teja Equation of State. In: Int. J. of Thermophysics, Vol. 17 (1996) No. 3,

[19] Copeman, T.W. ; Mathias P.M.: Recent Mixing Rules for Equations of State. In: Equation of State: Theories and applications, Ed. K.C. Chao, ACS symposium series 300 (1986), p. 352-370

[20] Mansoori, G.A.: Mixing Rules for Cubic Equations of State. In: Equation of State: Theories and applications, Ed. K.C. Chao, ACS symposium series 300 (1986), p. 314-330

[21] Michel, S.; Hooper, H.H.; Prausnitz, J.M.: Mutual Solubilities of Water and Hydrocarbons from an Equation of State need for an unconventional Mixing Rule. In: Fluid Phase Equilibria, 45 (1989) 173-189





[22] Christiansen, R.L.; Sloan, E.D. jr.: Mechanisms and Kinetics of Hydrate Formation. In: Annals New York Academy of Sciences, Vol. 715 (1994), 283-305

[23] Mathias, P.M.; Klotz, H.C.; Prausnitz, J.M.: Equation-of-state mixing rules for multi-component mixtures: the problem of invariance. In: Fluid Phase Equilibria,67 (1991) 31-44

[24] Ricci, J.E.: The Phase Rule. New York: D. van. Nostrand Co. 1951

[25] Roozeboom Bakhuis, H.W.: Die heterogenen Gleichgewichte vom Standpunkt der Phasenlehre. 1. Heft, Braunschweig: Vieweg & Sohn 1901

[26] Sharma, S.C.: Equilibrium Water Content of Gaseous Mixtures. Ph.D. thesis, The University of Oklahoma, 1969

[27] Hobbs, P.V.. Ice physics. Oxford : Clarendon Press 1974

[28] Sloan, E. D., Jr.: Clathrate hydrates of natural gases. 2nd ed., rev. and expanded, New York : Marcel Dekker 1998

[29] Sloan, E. D., Jr.: Clathrate hydrates of natural gases.1st ed., NY : Marcel Dekker 1990

[30] Makogon, Y.F.: Hydrates of hydrocarbons. Tulsa, Oklahoma : PennWell Publishing Company 1997

[31] Nixdorf, J.: Experimentelle und theoretische Untersuchung der Hydratbildung von Erdgasen unter Betriebsbedingungen. Dissertation, Universität Karlsruhe (TH) 1996

[32] Englezos, P.: Reviews - Clatherate Hydrates. In: Ind. Eng. Chem. Res., 32(1993)1251-1274

[33] Harmens, A.; Sloan, E.D.: The Phase Behaviour of the Propane-Water System: A Review. In: CJChE, 68 (1990), 151-158

[34] Metha, A.P.; Makogon, T.Y. et al.: A composite phase diagram of structure H hydrates using Schreinemakers' geometric approach. In: Fluid Phase Equilibria 121 (1996), 141-165

[35] Kobayashi, R.; Katz, D.L.: Methane Hydrate at High Pressure. In: Petroleum Transaction AIME 186 (1949), 66-70

[36] Kobayashi, R.; Katz, D.L.: Metastable Equilibrium in the Dew Point Determination of Natural Gases in the Hydrat Region. In: PetroleumTransactions, AIME, 204 (1955)262-263

[37] Moisture and Humidity 1985 : Measurement and Control in Science and Industry; Proceedings of the 1985 International Symposium on Moisture and Humidity, Washington, DC, April 15-18, 1985

[38] Quinn, F.C.: The most common problem of moisture / humidity measurement and control. In: [37], 1-5

[39] Murphy, B.: Determination of water vapour content and hydrocarbon dew point in natural gas. In: International School of Hydrocarbon Measurement, Proceedings, Norman, Oklahoma, 59 (1984), 519-522

[40] Jefferies, J.: Product quality improvement with correct moisture measurement in thermal processes using electrolytic hygrometers. In: Industrial heating 60 (1993) October, 47-49

[41] Psares:, G.G.: The effects of the moisture contents of shielding gases on the formation of pores when aluminium is welded. In: Automat. Weld. 32 (1979) 10, 6-8

[42] McAndrew, J.J.; Boucheron, D.; Moisture Analysis in Process Gas Streams. In: Solid state technology 35 (1992) February, 55-60

[43] Sistig, E.: Kontinuierliche Bestimmung von Wasserspuren in Gasen mit Hilfe einer neuen Meßzelle. In: Chem. Ing. Tech., 43 (1971) No.19, 1061-1064

[44] Scholz, G.: Markanalyse: Sensoren und Meßgeräte für Gasfeuchte. In: Technisches Messen 59 (1992) 3, 88-109

[45] G.J. van Rossum (ed.): Gas Quality. Proceedings of the congress „Specification and measurement of physical and chemical properties of natural gas", Groningen, The Netherlands, 22-25 April 1986. Amsterdam : Elsevier Science Publishers B.V. 1986

[46] Lück, W.: Feuchtigkeit - Grundlagen, Messen, Regeln. München : R.Oldenburg, 1964

[47] Breitsameter, B.; Moritz, M.: Spurenfeuchtemessung in Gasen.
In: Chem.Techn., 37. Jg. (1985) Heft 1, 1-7
[48] Bhadha, P.M.: Control of Moisture and Contaminants in Shieldings Gases.
In: Welding Journal 73 (1994) No. 5, 57-63
[49] Sonntag, D.: Advancements in the field of hygrometry.
In: Meteorol. Zeitschrift, N.F. 3 (1994) April, 51-66
[50] Schön, H.: Spurenfeuchtebestimmung in Gasen im Hoch- und Niederdruck - Teil 1: Literaturübersicht und Apparatur zur Messung im vpb-Bereich.
In: Linde- Berichte aus Technik und Wissenschaft 72 (1994), 22-32
[51] Hebestreit, A.: Beitrag zur indirekten Wasserdampftaupunktbestimmung in Hochdruckgasen. Dissertation, TH Leipzig, 1988
[52] Heinze, D.: Einheitliche mathematische Beschreibung von Gasfeuchtemeßverfahren.
Dissertation, TH Ilmenau, 1981
[53] Berliner, M.A.: Feuchtemessung. Berlin : VEB Verlag Technik, 1980
[54] Scelzo, M.J.: Moisture analysis in natural gas. In: [45], p. 337-344
[55] Weber, D.: Technische Feuchtemessung in Gasen und Festkörpern. Essen : Vulkan, 1995
[56] The Institute of Measurement and Control (Publ.): A Guide to the Measurement of Humidity. London, 1996
[57] Jamieson, A.W.; Sikkenga, H.J.: On-line water dewpoint measurement in natural gas.
In: [45], p. 289-299
[58] Ulte, J.M.: Standards in der Feuchtemeßtechnik. In: Laborpraxis (1993) Juli, 26-29
[59] Water Vapour Content of Gaseous Fuels by Measurements of Dew Point Temperature.
American National Standard, ASTM D 1142-95
[60] Pragnell, R.F.: Dew and frost formation on the condensation dewpoint hygrometer. In: Measurement + Control, Vol. 26 (1993) October, 242-244
[61] Pragnell, R.F.: The modern condensation dewpoint hygrometer.
In: Measurement + Control, Vol. 22 (1989) April, 74-77
[62] Dadachanji, F.: Humidity measurement at elevated temperatures.
In: Measurement + Control, Vol. 25 (1992) March, 48-50
[63] Tobin, St.: Chilled Mirror Dew Point Sensor Optics.
In: Sensor - the Journal of Applied Technology, Vol. 11 (1994) No.10, 18-27
[64] ISO 6327-1981(E) : Gas Analysis - Determination of the water dew point of natural gas - Cooled surface condensation hygrometers.
Hrsg.: ISO, Internationale Organisation für Normung, Genf, 1981
[65] Bannell, J.L.K.; Dixon, A.G.; Davies T.P.: The monitoring of hydrocarbon dewpoint.
In: [45], p. 263-271
[66] Dosoretz, V.J.: A portable optical chilled mirror hygrometer. In: [37], 729-733
[67] Rötter, J.: New methods of dew point Measurement for natural gas. In: [45], 311-325
[68] Sonntag D.: Hygrometrie - Ein Handbuch der Feuchtigkeitsmessung in Luft und anderen Gasen. Berlin : Akademie-Verlag, 1967
[69] Schmidt, T.; Rennemann, D.; Schulz, T.: Natural Gas Treatment: Simultaneous Water and Hydrocarbon-Dew Point-Control - Part 1: Process Design, Adsorbent Selection and Performence. In: Erdöl und Kohle - Erdgas Bd. 46 (1993) 10, 366-374
[70] Bernhart, M.: Messung und Berechnung von Kondensationspunkten kohlenwasserstoffhaltiger Gasgemische. Dissertation, Universität Karlsruhe (TH) 1994
[71] Carr-Brion, K.: Moisture sensors in process control.
London: Elsevier Applied Science Publishers, 1986
[72] Retgien, P.P.I.: Silicon dew-point sensor for accurate humidity measurement systems. Delft University Press 1981



[73] Scholz, E.: Karl-Fischer-Titration. Berlin : Springer-Verlag, 1984
[74] Wieland, G.: Wasserbestimmung durch Karl-Fischer-Titration.Darmstadt: GIT-Verlag 1985
[75] Wünsch, G.; Schöffski, K.: Die voltametrische Indikation der Karl-Fischer-Titration.
In: Fresenius journal of analytical chemistry, 340 (1991), 691-695
[76] Wünsch, G.; Seubert, A.: Stöchiometrie und Kinetik der Karl-Fischer-Reaktion in Methanol als Reaktionsmedium. In: Fresenius Z. Anal. Chem., 334 (1989), p. 16-21
[77] Hahn, M.; Hartung, P.: Neue Einsatzgebiete fuer die Karl-Fischer-Titration.
In: Chemie in Labor und Biotechnik (1996) No. 9, 388-392
[78] Schöffski, K.: Elektrochemische Untersuchungen der Karl-Fischer-Reaktion. Dissertation, Universität Hannover 1992
[79] Cedergren, A.: Coulometric Study of Reaction Rates of Water in Pyridine- and Imidazole-Buffered Methanolic Karl Fischer Reagents Containing Chloroform.
In: Analytical chemistry, Vol. 68 (1996) No. 20, 3682-3687
[80] Fischer, W.; Krenn, K.-D.: The Stoichiometry in the Determination of Water using Karl Fischer Reagent. In: J. für prakt. Chemie-Chemiker-Zeitung 338 (1996)6,569-577
[81] Scholz, E.: Karl-Fischer-Reagentien ohne Pyridin (3) - Die Genauigkeit der Wasserbestimmung. In: Fresenius Z. Anal. Chem. 309 (1981), 30-32
[82] Scholz, E.: Karl Fischer-Reagentien ohne Pyridin (7) - Zweikomponenten-Reagentien mit Imidazol. In: Fresenius Z. Anal. Chem. 312 (1982), 462-464
[83] HYDRANAL-Praktikum. Riedel-de Haen AG, Seelze 1996
[84] Scholz, E.: Karl-Fischer-Reagentien ohne Pyridin (4) - Einkomponenten-Reagentien.
In: Fresenius Z. Anal. Chem. 309 (1981), 30-32
[85] Scholz, E.: Karl-Fischer-Reagentien ohne Pyridin (8) - Coulometrische Wasserbestimmung.
In: Fresenius Z. Anal. Chem. 314 (1983), 567-571
[86] Scholz, E.: Karl Fischer coulometry - the cathode reaction.
In: Fresenius Z. Anal. Chem. 348 (1994), 269-271
[87] Dietrich, A.: Karl-Fischer titration, Part 2: Standardization, equipment validation, and control techniques. In: American Laboratory, Vol. 26 (1994) 5, 33-39
[88] Kaesler, H.: Direkte Bestimmung des Wassergehaltes in Gasen nach Karl Fischer.
In: gwf-Gas/Erdgas 125 (1984) Heft 3, 125-131
[89] ISO 10101-3: Natural gas - Determination of water by the Karl Fischer method - Part 3: Coulometric procedure.
Hrsg.: ISO, Internationale Organisation für Normung, Genf, Ausg. 1993
[90] DIN 51869: Bestimmung des Wassergehaltes nach Karl Fischer. Hrsg.: DIN, Deutsches Institut für Normung e.V., Berlin : Beuth-Verlag, Ausg. Mai 1986
[91] Cedergren, A.: Diaphragm-Free Cell for Trace Determination of Water Based on the Karl Fischer Reaction Using Continuous Coulometric Titration.
In: Analytical chemistry, Vol.69 (1997), No. 15, p. 3100-3108
[92] Poynter, W.G.; Barrios, R.J.: Coulometric Karl Fischer titration simplifies water content testing. In: Oil & gas journal, Apr. 11 (1994), 53-54
[93] DVGW-Arbeitsblatt G 260/I: Technische Regeln für die Gasbeschaffenheit.
5. Auflage, Frankfurt/M. : ZfGW-Verlag, Ausg. April 1983
[94] Persönliche Mitteilung Fr. Dr. K. Schöffski, Fa. Riedel-de-Haen Laborchemikalien GmbH & Co. KG, Seelze, April 1998
[95] Margolis, S.A.: Sources of Systematic Bias in the Measurement of Water by the Coulometric and Volumetric Karl Fischer Methods.
In: Analytical chemistry,Vol.69 (1997) No. 23, p. 4864-4871
[96] Schön, H.; Ehrich, A.: Über die Änderung der Wasserdampfkonzentration in Druckgasbehältern bei Entnahme. In: Chemische Technik, 40. Jg. (1988) Heft 2, 85-88

[97] Schön, H.; Hille, J.; Ehrich, A. et al.: Die Analyse und das Verhalten von vpm-Mischungen Wasserdampf/Inertgas und Tellurdiethyl/Wasserstoff in Druckgasbehältern. In: Linde-Berichte aus Technik und Wissenschaft, 65 (1990), 17-25
[98] Ehrich, A.: Indirekte Bestimmung der Oberflächeneigenschaften von Druckgasbehältern. In: Chem. Technik, 45. Jg. (1993) Heft 4, 236-238
[99] Schön, H.: Spurenfeuchtebestimmung in Gasen im Hoch- und Niederdruck - Teil II: Das Seifenblasenphänomen in der Druckgasflasche. In: Linde-Berichte aus Technik und Wissenschaft 73 (1995), 41-48
[100] Ovarlez, J.: A Two Temperature Calibration System. In: [37], 235-241
[101] Pichlmaier, J.: Befeuchtung von Prüfgas für die Kalibrierung von Gas- und Feuchtesensoren. In: Technisches Messen 58 (1991) 12, 471-477
[102] Mermoud, F.; Brandt, M.D.; McAndrew, J.J.: Low-Level Moisture Generation. In: Analytical chemistry 63 (1991) No. 3, 198-202
[103] Pichlmaier, J.: Kalibriertechnik für Gassensoren. In: Technisches Messen 57 (1990) 11, 419-423
[104] Scelzo, M.; Pierce, R.: A High Precision Saturation / Dilution Calibration System for Water Vapour in a Carrier Gas. In: [37], 569-576
[105] Stier, St.: Grundlegende Untersuchungen zum Verhalten von chemischen Sensoren auf der Basis akustischer Oberflächenwellen und Einsatz zur Detektion komplexer flüchtiger organischer Stoffgemische. Forschungszentrum Karlsruhe, Wiss. Berichte FZKA 5817, 1997
[106] Walker, J.A.J.; Campion, P.: The Use of Electrolytic Hygrometers for the Determination of Water and Hydrogen. In: Analyst, Vol. 90 (1965) April, 199-209
[107] Siefering, K.L.; Whitlock, W.H.: Measurement and modeling of moisture adsorption properties of 316 stainless steel tubing samples. In: J.Vac. Sci. Technol. A, Vol. 12 (1994) No.5, 2685-2691
[108] Ohmi, T.; Nakamura, M. et al.: Trace Moisture Analysis in Specialty Gases. In: J. Electrochem. Soc. , Vol. 139 (1992) No. 9, 2654-2658
[109] Siefering, K.; Whitlock, W.; Athalye, A.: Modelling moisture adsorbtion and transport in ultra-high-purity gas piping systems. In: Microcontamination 12(1994) March,41-45
[110] Thiel, P.; Madey, T.: The Interaction of Water with Solid Surfaces: Fundamental Aspects. In: Surface science reports 7 (1987), 211-385
[111] Mayeaux, D.P.: Moisture analysis of contaminated gases. In: [37], 215-223
[112] Cremonesi, P.L.: Practical expiriences with on-line water dew point determination in natural gas transmission pipelines. In: [45], p. 301-310
[113] ISO 10715-1997 (E): Natural Gas: Sampling Guidelines. Hrsg.: ISO, Internationale Organisation für Normung, Genf, 1997
[114] Mersmann, A.: Auslegung und Maßstabsvergrößerung von Blasen- und Tropfensäulen. In: Chem. Ing. Tech., 49 (1977) 9, 679-691
[115] Fasold, H.-G.; Wahle, H.-N.: Joule-Thomson-Koeffizienten für in der Bundesrepublik Deutschland vermarktete Erdgase. In: gwf-Gas/Erdgas 135 (1994) No. 4
[116] Fasold, H.-G.; Wahle, H.-N.: Berechnung und Auslegung von Erdgas-Vorwärmanlagen. In: In: gwf-Gas/Erdgas 135 (1994) No. 4, 220-224
[117] Day, Ch.: Experimentelle und theoretische Untersuchung der kalorischen Eigenschaften von gasförmigen Mischungen aus Wasser, Methan und Ethan. Fortsch.-Ber. VDI Reihe 3 No. 397, Düsseldorf : VDI-Verlag 1995
[118] Lieneweg, F.: Handbuch der technischen Temperaturmessung. Braunschweig: Vieweg 1976
[119] Nicholas, J.V.; White, D.R.: Traceable Temperatures - An Introduction to Temperature Measurement and Calibration. Chichester : JohnWiley & Sons 1994



[120] Thiel-Böhm, A.: Explosionsgrenzen methanhaltiger Brenngasgemische. Fortschr.-Ber. VDI Reihe 3 No. 258, Düsseldorf : VDI-Verlag 1991
[121] Stickling, J.; Thiel-Böhm, A.: Der Einfluß des Druckes auf die Explosionsgrenzen gasförmigen Gemische. Fortschr.-Ber. VDI Reihe 3 No. 305, Düsseldorf : VDI-Verlag 1993
[122] Bartknecht, W.: Explosionsschutz. Berlin : Springer-Verlag 1993
[123] Dose, W.-D.: Explosionsschutz durch Eigensicherheit. Braunschweig : VDE-Verlag bei Vieweg 1993
[124] Olenik, H.; Rentzsch, H.; Wettstein, W.: Handbuch für Explosionsschutz. Hrsg. von Brown, Boveri & Cie AG Mannheim, 2., überarb. Aufl., Essen : Girardet Verlag 1984
[125] Lienenklaus, E.: Elektrischer Explosionsschutz nach DIN VDE 0165. VDE-Schriftenreihe 65, VDE-Verlag 1992
[126] DIN 12924 (Teil 1): Abzüge. Hrsg.: DIN, Deutsches Institut für Normung e.V., Berlin : Beuth-Verlag, Ausg. August 1991
[127] Sonntag, D.: Formeln verschiedenen Genauigkeitsgrades zur Berechnung des Sättigungsdampfdruckes über Wasser und über Eis und ihre Anwendung auf praktische Feuchtemeßaufgaben. Abhandlung des Meteorologischen Dienstes der Deutschen Demokratischen Republik No. 129 (Band XVII), Berlin : Akademie-Verlag 1982
[128] Wexler, A.; Greenspan, L.: Vapour pressure for water in the range 0 to 100°C. In: J. of research of the National Bureau of Standards, Vol. 75, A No.3, May-June 1971
[129] Wagner, W.; Saul, A.; Pruß, A.: International Equations for the Pressure along the Melting and along the Sublimation Curve of Ordinary Water Substance. In: J. Phys. Chem. Ref. Data, Vol. 23 (1994) No.3, 515-527
[130] Pruß, A.; Wagner, W.: New International Formulation for the Thermodynamic Properties of Ordinary Water Substance for General and Scientific Use. To be submitted to the J. Phys. Chem. Ref. Data (1997)
[131] Reid; Prausnitz; Poling: The Properties of Gases and Liquids. New York: McGraw-Hill Book Company, 1987
[132] ISO 5725: 1986 (E): Precision of test methods - Determination of repeatibility and reproducibility for a standard test method by inter-laboratory tests. Hrsg.: ISO, Internationale Organisation für Normung, Genf, Ausg. 1986
[133] Le Noe, O.; Schieppati, L.; Viglietti, B.; Oellrich, L.R.; Althaus, K.; Pot, F.; van der Meulen, L.; Kaesler, H.; Monco, G.; Wismann, G.: Development of a Mathematical Correlation Between Water Content and Water Dewpoint. In: 1995 International Gas Research Conference, Cannes, France,Vol. I, Chap. II : transmission and storage. 1995, 544-553
[134] DIN ISO 5725-1:1997-11: Genauigkeit (Richtigkeit und Präzision) von Meßverfahren und Meßergebnisssen, Teil 1: Allgemeine Grundlagen und Begriffe. Hrsg.: DIN, Deutsches Institut für Normung e.V., Berlin : Beuth-Verlag, Ausg. Nov. 1997
[135] ISO 5725-6:1994-12(E): Accurancy (trueness and precision) of measurements methods and results - Part 6: Use in practice of accurancy values. Hrsg.: ISO, Internationale Organisation für Normung, Genf, Ausg. Dez. 1994
[136] Gottschalk, G.; Kaiser, R.E.: Einführung in die Varianzanalyse und Ringversuche. BI-Hochschultaschenbücher Band 775, Bibliographisches Institut Mannheim 1976
[137] Gottschalk, G.; Kaiser, R.E.: Elementare Tests zur Beurteilung von Meßdaten. BI-Hochschultaschenbücher Band 774, Bibliographisches Institut Mannheim 1972
[138] Nalimov, V.V.: The application of mathematical statistics to chemical analysis. Oxford : Pergamon Press 1963
[139] Leitfaden zur Angabe der Unsicherheit beim Messen. Hrsg.: DIN, Deutsches Institut für Normung e.V., Berlin : Beuth-Verlag 1995
[140] Abernethy, R.B. et al.: ASME Measurement Uncertainty. In: Journal of Fluids Engineering, Vol. 107 (1985) June, 161-164

[141] Blanke, W.: Eine neue Temperaturskala - Die Internationale Temperaturskala von 1990 (ITS-90). Fachbeiträge, PTB-Mitteilungen 99 (1989) 6, 411-418
[142] Gilgen, R.: Präzisionsmessungen der thermischen Zustandsgrößen von Argon, Kohlendioxid und Schwefelhexafluorid. Fortschr.-Ber. VDI Reihe 3 No. 317. Düsseldorf : VDI-Verlag 1993
[143] API Technical Data Book - Petroleum Refining, Chapt. 9, Revised Edition 1985
[144] Sloan, E.D.; Fleyfel, F.: A Molecular Mechanism for Gas Hydrate Nucleation from Ice. In: AIChE Journal, Vol.37 (1991), No.9; 1281-1292
[145] Hwang, J.J.; Wright, D.A.; Kapur, A.; Holder, G.D.: An Experimental Study of Crystallization and Crystal Growth of Methane Hydrates from Melting Ice. In: J. of Inclusion Phenomina and Molecular Recognition in Chemistry 8 (1990), 103-116
[146] ISO 6974-3: Natural gas - Determination of composition with defined uncertainty by gas chromatography - Part 3: Determination of hydrogen, helium, inert gases and hydrocarbons up to $C_8$. Hrsg.: ISO, Internationale Organisation für Normung, Genf, 1984
[147] ISO 6974-4: Natural gas - Determination of composition with defined uncertainty by gas chromatography - Part 4: Determination of nitrogen, carbon dioxide and hydrocarbons ($C_1$ up to $C_5$ and $C_{6+}$) for a laboratory and on-line measuring system. Hrsg.: ISO, Internationale Organisation für Normung, Genf, 1984
[148] Campell, J.M: Gas Conditioning and Processing - Volume 1: Basic Principles. 7th Ed., 2nd printing, Campbell Petroleum Series, Norman, Oklahoma 1994
[149] GASUNIE - physical properties of natural gases. Publ. By N.V. Nederlandse Gasunie, June 1988
[150] McKetta, J.J.; Wehe, A.H.: Use this chart for water content of natural gases. In: Petroleum Refiner 37 (1958) 8, 153-154
[151] McCarthy, E.L.; Boyd, W.L.; Reid, L.S.: Water Content of Essentially Nitrogen-free natural gas saturated at various conditions of temperature and pressure. In: Petroleum transactions, AIME, Vol. 189, 1950
[152] Katz, D.L.; Lee, R.L.: Natural gas engineering: production and storage. Singapore: McGraw-Hill chemical engineering series 1990
[153] Engineering Data Book, 10th Ed., Gas Processors Suppliers Association, 1987
[154] Maddox, R.N. et al.: Estimating Water Content of Sour Natural Gas Mixtures. In: Laurance Reid Gas Conditioning Conference, March 8, 1988, p. 75- 97
[155] Bukacek, R. F.: Equilibrium Moisture Content of Natural Gases. Research Bulletin 8, Institute of Gas Technology, 1955
[156] Kazim, F.M.A.: Quickly calculate the water content of natural gas. In: Hydrocarbon processing (1996) 3, 105-110
[157] Wichert, C.G.; Wichert, E.: Chart estimates water content of sour natural gas. In: Oil & Gas Journal, Vol. 91 (1993) 13, 61-64
[158] Robinson, J.N.; Wichert, E.; Moore, R.G.: Charts help estimate H2O content of sour gases. In: Oil and Gas Journal 76 (1978) Feb. 6, 76-78
[159] Harr, L.; Gallagher, J.S.; Kell, G.S.: NBS/NRC Steam Tables. National Standard Reference Data System, 1984, p. 9
[160] Goff, J.A.; Gratch, S.: Low-Pressure Properties of Water from -160 to 212°F. In: Heating, Piping and Air Conditioning, Vol. 18 (1946) Feb., No.2, 125-136
[161] Eubank, P.T.; Scheloske, J.J.; Joffrion, L.L.: Dew points of wet gas mixtures: new data and a new correlation using interaction third virial coefficients. In: Fluid Phase Equilibria 30 (1986), 255-264
[162] Anderson, F.E.; Prausnitz , J.M.: Inhibition of gas hydrates by methanol. In: AIChE Journal, Vol. 36 (1986) No. 8, 1321-1333



[163] Parrish, W.R.; Prausnitz, J.M.: Dissociation Pressures of Gas Hydrates. In: Ing. Eng. Chem. Proc. Des. Dev., 11 (1972) 1, 26-35
[164] Mathias,P.M.; Klotz, H.C.: Take a Closer Look at Thermodynamic Property Models. In: Chem. Eng. Prog., (1994) June, 67-75
[165] Victorov, A.I.; Fredenslund, Aa.; Smirnova, N.A.: Fluid phase equilibria in water: natural gas component mixtures and their description by the hole group-contribution eos. In: Fluid Phase Equilibria, 66(1991) p.187-210
[166] Peng, D.-Y.; Robinson, D.B.: Two- and three-Phase Equilibrium Calculations for Coal Gasification and Related Processes. In: S.A. Newman (Ed.), Thermodynamics of Aqueous Systems with Industrial Applications; ACS Symposium Series; 133,(1980), p. 393-414
[167] Du, Y.; Guo, T.-M.: Prediction of Hydrate Formation For Systems containing Methanol. In: Chem. Eng. Sc., Vol. 45 (1990) 4, p. 893-900
[168] Soreide, I; Whitson, C.H.: Peng-Robinson predictions for hydrocarbons $CO_2$, $N_2$, and $H_2S$ with pure water and NaCl brine. In: Fluid Phase Equilibria, 77 (1992), 217-240
[169] Daridon, J.; Lagourette, B.: A cubic equation of state model for phase equilibrium calculation of alkane + carbon dioxide + water using a group contribution $k_{ij}$. In: Fluid Phase Equilibria, 91 (1993) 31-54
[170] Lovland. J. et al.: Water Content of Natural Gas in Equilibrium with Pure Water or with Saturated Salt Solutions. Paper präsentiert auf „8th International Conference on Properties and Phase Equilibria for Product and Process Design". 26.4.-1.5.1998 Noordwijkerhout, The Netherlands
[171] Wu, J.; Prausnitz, J. M.: Phase Equilibria for Systems Containing Hydrocarbons, Water, and Salt: An Extended Peng-Robinson Equation of State. In: Industrial and Engineering Chemistry Research, Vol. 37 (1998) 5, p. 1634-1643
[172] Economou , I.G.; Peters, C.J.; de Swaan Arons, J.: Water-Salt Phase Equilibria at Elevated Temperatures and Pressures: Model Development and Mixture Predictions. In: J. Phys. Chem., 99 (1995) 6182-6193
[173] Shinta, A.A.; Firoozabadi, A.: Equation of State Representation of Aqueous Mixtures Using an Association Model. In: Can. J. Chem. Engng. 73 (1995) June, p. 367-379
[174] Economou, I.G.; Donohue, M.D.: Equation of State with Multiple Association Sites for Water and Water-Hydrocarbon Mixtures. In: Ind. Eng. Chem. Res., 31 (1992), 2388-2394
[175] Economou, I.G.; Donohue, M.D.: Equations of State for Hydrogen Bonding Systems. In: Fluid Phase Equilibria 116 (1996) 518-529
[176] Economou, I.G.; Tsonopoulos, C.: Associating models and mixing rules in equations of state for water / hydrocarbon mixtures. In: Chem. Eng. Sc., Vol.52 (1997) 4, 511-525
[177] Han, S.J.; Lin, H.M.; Chao, K.C.: Vapour-Liquid Equilibrium of Molecular Fluid Mixtures by Equation of State. In: Chem. Eng. Sc., Vol.43 (1988) 9, 2327-2367
[178] Gibbons, R.M.; Laughton, A.P.: An Equation of State for Polar and Non-polar Substances and Mixtures. In: J. Chem. Soc. Faraday Trans., 2 (1984) 80, 1019-1038
[179] Larsen, E.R.; Prausnitz, J.M.: High-Pressure Phase Equilibria for the Water / Methane System. In: AIChE Journal, Vol. 30 (1984) 5, 732-738
[180] Tsonopoulos, C.; Heidman, J.L.: High-Pressure Vapour-Liquid Equilibria with cubic Equations of State. In: Fluid Phase Equilibria, 29 (1986) 391-414
[181] Kabadi, V. N.; Danner, R.P.: A Modified Soave-Redlich-Kwong Equation of State for Water-Hydrocarbon Phase Equilibria. In: Ind.Eng.Chem. Proc. Des. Dev. 24(1985)537-541
[182] Robinson, D.B. et al.: The development of the Peng-Robinson equation and its application to phase equilibrium in a system containing methanol. Fluid Phase Equilibria, 24 (1985) 25-41
[183] Heidemann, R.A.; Rizvi, S.S.H.: Correlation of ammonia-water equilibrium data with various modified Peng-Robinson eos. In: Fluid Phase Equilibria 29(1986), p. 439-446

[184] Voros, N.G.; D.P. Tassios: VLE in nonpolar/weakly polar systems with different types of mixing rules. In: Fluid Phase Equilibria 91(1993), p. 1-29
[185] Xu, Z.; S.I. Sandler: Temperature-dependent parameters and the Peng-Robinson eos. In: Ind. Eng. Chem. Res. 26 (1987) 26, p. 601-606
[186] Luedecke, D.; J.M. Prausnitz: Phase equilibria for strongly nonideal mixtures from an EOS with density dependent mixing rules. In: Fluid Phase Equilibria, 22 (1985), 1-19
[187] Panagiotopoulos A.Z., Reid R.C.: New Mixing Rule for Cubic EoS for Highly Polar, Asymetric Systems. In: ACS Symposium Series, 300 (1986), p.571-582
[188] Adachi, Y.; Sugie, H.: A new mixing rule - modified conventional mixing rule. In: Fluid Phase Equilibria 28(1986), p. 103-118
[189] Wong, D.S.H.; Sandler, S.I.: A theoretically correct mixing rule for cubic eos. In: AIChE 38 (1992) 5, p. 671-680
[190] Melhem, G.A.: A Modified Peng-Robinson Equation of State. In: Fluid Phase Equilibria, 47 (1989), 189-237
[191] Stryjek, R.; J.H. Vera: PRSV: An improved Peng-Robinson eos for pure compounds and mixtures. In: Can. J. Chem. Engng., 64 (1986) 4, p. 323-333
[192] Stryjek, R.; J.H. Vera: PRSV2: A cubic eos. Accurate VLE calculations. In: Can. J. Chem. Engng., 64 (1986) 10, p. 820-826
[193] Proust, P.; J.H. Vera: PRSV: The Stryjek-Vera modification of the Peng-Robinson eos. Parameters of other pure compounds of industrial interest. In: Can. J. Chem. Engng., 67 (1989) 2, p. 170-173
[194] Proust, P.; Meyer, E.; Vera, J.H.: Calculation of pure compound saturated enthalpies and saturated volumes with the PRSV eos. Revised k1-parameters for alkanes. In: Can. J. Chem. Engng. 71 (1993) 4, p. 292-298
[195] Twu, C.H.; Coon, J.E.; Cunningham, J.R.: A new generalized alpha function for a cubic equation of state Part 1. Peng-Robinson equation. In: Fluid Phase Equilibria 105 (1995), p. 49-59
[196] Mathias, P.M.; T.W. Copeman: Extention of the Peng-Robinson EOS to complex mixtures: Evaluation of the various forms of the local composition concept. In: Fluid Phase Equilibria, 13 (1983), p. 91-108
[197] Ed. Bradley, H.B.; Petroleum Engineering Handbook. 1st Ed., Richardson, Texas: Society of Petroleum Engineers 1987
[198] Heimlid, J.-R.: Water Content in Natural Gas. Diploma Work, University of Trondheim, 1995
[199] Jackson, P.L.; Wilsak, R.A.: Themodynamic consistency test based on the Gibbs-Duhem equation applied to isothermal, binary vapour-liquid equilibrium data: data evaluation and model testing. In: Fluid Phase Equilibria 103 (1995) 155-197
[200] Kosyakov, N.E.; Ivenka, B.I.; Krishtopa, P.P.: Solubility of moisture in compressed argon, methane, and helium at low temperatures. In: Russian journal of applied chemistry (1979), 881-882; Übersetzung von Zhurnai Prikladnoi Khimii, 52 (1979) 4, 922-923
[201] Kosyakov, N.E.; Ivenka, B.I.; Krishtopa, P.P.: Moisture contents of compressed nitrogen and hydrogen at low temperatures. In: Russian journal of applied chemistry (1978), 2436-2438; Übersetzung von Zhurnai Prikladnoi Khimii, 50 (1978) 11, 2568-2570
[202] Olds, R.H.; Sage, B.H.; Lacey, W.N.: Phase Equilibria in Hydrocarbon Systems. In: Industrial and Eng. Chemistry, Vol. 34 (1942) 10, 1223-1227
[203] Villarreal, J.F. et al.: Dew-Point Water Contents of Methane-Ethane-Mixtures at a Series of Pressures and Temperatures. In: Producers monthly, 18 (1954) May, 15-17
[204] Skinner, W.: The Water Content of Natural Gas at Low Temperatures. M.S. Thesis in Chem. Eng., U. of Oklahoma, 1948



[205] Rigby, M.; Prausnitz, J.M.: Solubility of Water in Compressed Nitrogen, Argon and Methane. In: The Journal of Physical Chemistry, Vol. 72 (1968) 1, 330-334
[206] Gillespie, P.C.; Wilson, G.M.: Vapour-Liquid- and Liquid-liquid-equilibria: Water-Methane, Water-Carbondioxide, Water-Hydrogensulfide, Water-n-Pentane. Research Report #48, Project 758-B-77, Gas Processors Association 1982
[207] Yarym-Agaev, N.L. et al.: Phase Equilibria in the Water-Methane and Methanol-Methane Binary Systems under High Pressures. Plenum Publishing Corporation (1985), 154-157
[208] Yokoyama, C. et al.: Vapour-Liquid Equilibria in the Methane-Diethylene Glycol-Water System at 298,15 and 323,15 K. In: J. Chem. Eng. Data, Vol. 33 (1988), 274-276
[209] Reamer, H.H. et. al.: Composition of Dew-Point Gas in Ethane-Water System. In: Ind. Eng. Chem., Vol. 35 (1943) 7, 790-793
[210] Anthony, R.G.; McKetta, J.J.: Phase Equilibrium in the Ethylene-Water System. In: J. Chem. Eng. Data, Vol. 12 (1967) 1, 17-20
[211] Anthony, R.G.; McKetta, J.J.: Phase Equilibrium in the Ethylene-Ethane-Water System. In: J. Chem. Eng. Data, Vol. 12 (1967) 1, 21-28
[212] Coan, C.R.; King Jr., A.D.: Solubility of Water in Compressed Carbon Dioxide, Nitrous Oxide, and Ethane. Evidence for Hydration of Carbon Dioxide and Nitrous Oxide in the Gas Phase". In: Journal of the American Chemical Society, Vol. 93 (1971), 1857-1862
[213] Kobayashi, R.; Katz, D.L.: Vapour-Liquid Equilibria for Binary Hydrocarbon-Water Systems. In: Ind. Eng. Chem., Vol. 45 (1953), 440-451
[214] Reamer, H.H. et al.: Compositions of the Coexisting Phases of n-Butane- Water System in the Three-Phase-Region. In: Ind. Eng. Chem., Vol. 36 (1944) 4, 381-383
[215] Wehe, H.H.; McKetta, J.J.: n-Butane-1-Butene-Water system in the three phase region. In: J. Chem. Eng. Data, Vol. 6 (1961) 2, 167-172
[216] Song, K.Y.; Kobayashi R.: The Water Content of $CO_2$-rich Fluids in Equilibrium with Liquid Water and / or Hydrates. Research Rep. #99, Project 775-85, GPA 1986
[217] Reamer, H.H. et al.: n-Butane-Water System in the Two-Phase Region. In: Ind. Eng. Chem., 44 (1952), 609
[218] Aoyagi, K. et al.: Improved measurements and correlation of the water content of methane gas in equilibrium with hydrate. In: GPA Annual convention 58 (1979) 25-27
[219] Sloan, E.D.; Khoury; F.M.; Kobayashi, R.: Water Content of Methane Gas in Equilibrium with Hydrates. In: Ind.Eng.Chem.Fundam., Vol.15 (1976) 4, 318-323
[220] Song, K.Y.; Kobayashi, R.: The water content of ethane, propane and their mixtures in equilibrium with liquid water or hydrates. In: Fluid Phase Equilibria, 95(1994),281-298
[221] Trebble, M.A.; Sigmund, P.M.: A Generalized Correlation for the Prediction of Phase Behaviour in Supercritical Systems. In: Can. J. Chem. Eng., 68 (1990), 1033-1039
[222] Nishiumi, H.; Arai, T.; Takeuchi, K.: Generalization of the Binary Interaction Parameter of the Peng-Robinson Equation of State by Component Family. In: Fluid Phase Equilibria, 42 (1988), 43-62
[223] Gao, G. et al.: A simple correlation to evaluate binary interaction parameters of the Peng Robinson eos: binary light hydrocarbon systems. In: Fluid Phase Equilibria 74 (1992), 85-93
[224] Avlonitis, G. et al.: A Generalized Correlation for the Interaction Coefficients of Nitrogen-Hydrocarbon Binary Mixtures. In: Fluid Phase Equilibria 101 (1994), p. 53-58
[225] Knapp, H., Döring, R., Oellrich, L., Plöcker, U., Prausnitz, J.M.: Vapour-Liquid Equilibria for Mixtures of Low Boiling Substances. Dechema Data Series Vol. VI, Part 1, Frankfurt 1982
[226] Kordas, A., Tsoutsouras, K., Stamataki, S., Tassios, D.: A Generalized Correlation for the Interaction Coefficients of $CO_2$-Hydrocarbon Binary Mixtures. In: Fluid Phase Equilibria 93 (1994), 141-166

[227] Kordas, A., Magoulas, K., Stamataki, S., Tassios, D.: Methane-Hydrocarbon Interaction Parameters Correlation for the Peng-Robinson and the t-mPR Equation of State. In: Fluid Phase Equilibria 112 (1995) 1, 33-44
[228] Knapp. H.; Oellrich, L.R. et al.: K-BP² — Karlsruhe-Berliner-Prozeß-Berechnungs-Paket. Institut für Technische Thermodynamik und Kältetechnik, Universität Karlsruhe
[229] Michelsen, M.L.: Calculation of Phase Envelopes and Critical Points for Multicomponent Mixtures. In: Fluid Phase Equilibria, 4 (1980), 1-10
[230] Pragnell, B.: Relying on humidity. Process engineering 74 (1993) No. 2, 41-42
[231] Forton, A.G.; Pragnell, R.F.: Development of the primary gravimetric hygrometer for the UK national humidity standard facility. In: [37], 79-89
[232] Siefering, K.; Berger, H.; Whitlock, W.: Quantitative analysis of contaminants in ultrapure gases at the parts-per-trillion level using atmospheric pressure ionization mass spectroscopy. In: J. Vac. Sci. Technol. A, Vol. 11 (1993) No.4, Jul/Aug, 1593-1597
[233] Mucha, J.A.; Barbalas, L.C.: Infrared Diode Laser Determination of Trace Moisture in Gases. In: [37], 691-697
[234] Keidel, F.A.: Determination of Water by Direct Amperometric Measurement. In: Analytical chemistry Vol. 31 (1959) No.12, 2043-2048
[235] Barendecht, E.: Determination of traces of water in gases by means of a modified Keidel elcetrolytic hygrometer. In: Analytica chimica acta 25 (1961), 402-404
[236] Baumann, F.: Application of Amperometric Hygrometers to the Determination of Water in Gases below 10 p.p.m.. In: Analytical chemistry, 34 (1962) 12, 1664-1665
[237] ISO 11541-1997(E): Natural Gas - Determination of water content at high pressure. Hrsg.: ISO, Internationale Organisation für Normung, Genf, 1997
[238] Chleck, D.: An aluminum oxide sensor with an integrated thin film heater. In: [37], 615-621
[239] Bryant, R.; Scelzo, M.: The impact of microprocessors on hygrometry. In: [37], 209-214
[240] Holloway, R.P.: Practical humidity measurement and control in gases at high pressures. In: [37], 1021-1025
[241] Harding, J.C.: Overcoming limitations inherent to aluminum oxide humidity sensors. In: [37], 367-378
[242] Mehrhoff, T.K.: Comparison of continous moisture monitors in the range of 1 to 15 ppm. In: Review of scientific instruments 56 (1985) No. 10, 1930-1933
[243] Teruko, I. et al.: A Dew-Point Hygrometer by Quartz Cristal. In: [37], p. 379
[244] Blakemoore, C.B.et al.: Continious trace moisture analysis. In: [45], p. 327-336
[245] Barrer, R.M.; Edge, A.V.J.: Proc, R. Soc. London, Ser. A, 300, 1 (1967) zitiert in : Marshall, D.R.; Saito, S.; Kobayashi, R.: Hydrates at High Pressures: Part I. In: AIChE J., March (1964), 202-205
[246] Jaeschke, M.; Schley, P.: Berechnung des Realgasfaktors von Erdgasen mit der AGA8-DC92 Zustandsgleichung. I. Aufbau der Gleichung. In: Gwf- Gas Erdgas, 137 (1996) No. 7, 339-345
[247] ISO CD 14532: Natural Gas: Terminology for Natural Gas. Hrsg.: ISO, Internationale Organisation für Normung, Genf, Mai 1996
[248] Althaus, K.; Oellrich, L.R. et al.: GERG model predictions and experimental verification of water dew points of natural gas. In: Proceedings of the 1998 International Gas Research Conference, 8-11 Nov. 1998, San Diego, California, USA, 541-550, Paper TSP-26
[249] Althaus, K.: Messung und Berechnung von Wassergehalten kohlenwasserstoffhaltiger Gasgemische; Dissertation University of Karlsruhe, 1999 As: VDI-Fortschrittsberichte, Reihe 3, No. 590, VDI-Verlag Duesseldorf, Germay